UNIVERSITÀ DEGLI STUDI FIRENZE

universität innsbruck

DOTTORATO DI RICERCA IN
SCIENZE AGRARIE E AMBIENTALI
CICLO XXX
Settore Scientifico Disciplinare AGR 13
Settore Concorsuale 07/E1

DOCTOR OF PHILOSOPHY
PROGRAMME BIOLOGY
FACULTY OF BIOLOGY

Coordinatore Prof. Pietramellara Giacomo

Carbon pools and microbiota along an alpine soil climosequence

Dottorando/PhD student

Bardelli Tommaso

Tutore/Supervisor

Prof. Pietramellara Giacomo

Univ. Prof. Dr. Insam Heribert

Coordinatore

Prof. Pietramellara Giacomo

The Dean of Studies

Univ. Prof. Dr. Illmer Paul

Anni/Period 2014-2017

Author

Bardelli Tommaso (PhD Cand.)

Dissertation submitted to the Department of Agrifood and Environmental Science of the University of Florence (Italy) and to the Institute of Microbiology of the Leopold-Franzens Universität Innsbruck (Austria) in fulfilment of the requirements for the degree Doctor of Philosophy (PhD).

Advisors

Prof. Pietramellara Giacomo
Department of Agrifood and Environmental Science,
University of Florence (Italy)

Univ. Prof. Dr. Insam Heribert
Institute of Microbiology, Universität Innsbruck (Austria)

Dr. Gómez Brandón María
Institute of Microbiology, Universität Innsbruck (Austria)

Dr. Ascher-Jenull Judith
Department of Agrifood and Environmental Science,
University of Florence (Italy)
Institute of Microbiology, Universität Innsbruck (Austria)

Cover Design & Layout

Bardelli Tommaso

This work was carried out at the **Department of Agrifood and Environmental Science (University of Florence, Italy)** and at the **Institut für Mikrobiologie (Leopold-Franzens Universität Innsbruck, Austria)**. This dissertation was funded by a PhD grant (DT16364) from the University of Florence (Italy).

Table of Contents

Abstract /Sommario /Zusammenfassung.…….....1

I. Introduction.…….....…13

II. Paper 1 - Effects of slope exposure on soil physico-chemical and microbiological properties along an altitudinal climosequence in the Italian Alps……...…39

III. Paper 2 - Ground cover and slope exposure effects on micro- and mesobiota in forest soils…….……...……..…….95

IV. Paper 3 - Physico-chemical and microbiological evidence of exposure effects on *Picea abies* – Coarse woody debris at different stages of decay……..…...…..139

V. Paper 4 - Impact of slope exposure on chemical and microbiological properties of Norway spruce deadwood and underlying soil during early stages of decomposition in the Italian Alps……..…….185

VI. Paper 5 - Chemical and microbiological changes in Norway spruce deadwood during the early stage of decomposition as a function of exposure in an Alpine setting.……...……...229

VII. Summary and conclusions……..…….....….263

VIII. Acknowledgments.……...…….……275

IX. Curriculum Vitae.……...…….....283

Abstract

Sommario

Zusammenfassung

Abstract

High mountain ecosystems offer ideal sequential scenarios for monitoring carbon (C) dynamics due to their sensitivity to changing environmental conditions. In this context, slope aspect and altitude are considered important topographical features affecting the local microclimate (i.e., temperature and precipitation patterns) and in consequence soil weathering and biogeochemical processes with implications for both ecosystem regulation and C feedbacks. Within forest ecosystems, deadwood is an essential structural and functional component as a reservoir for biological diversity and nutrient stocks (C–store). Therefore, the present work focuses on the influence of climate on soil features and deadwood decomposition dynamics as a function of different thermal conditions due to different slope exposure (north- *vs.* south-facing slopes) and altitude (from 1200 m to 2400 m above sea level) in (sub)alpine ecosystems in the Italian Alps.

This thesis offers a general introduction (*Chapter I*) and a compilation of papers in peer-reviewed journals. Following the intro, *Chapter II* deals with the main changes in composition, activity and diversity of the soil autochthonous microbiota in terms of slope exposure along the altitudinal climosequence in combination with a comprehensive overview of the soil physico-chemical properties. The findings show that the slope exposure largely influenced both edaphic properties and soil microbiota, even though such effects were altitude-dependent for most of the studied parameters. In particular, the three microbial domains (bacteria, fungi and archaea) responded differently to exposure in terms of abundance. Accordingly, enzyme type-specific reactions to slope exposure and altitude were also observed in this scenario.

In *Chapter III*, the influence of slope exposure was determined on both the autochthonous soil microbiota and mesofauna, with a special focus on

Enchytraeid community under different soil ground covers in subalpine forest ecosystems. The discriminatory assessment of the extracellular (eDNA) and intracellular (iDNA) fractions of the total soil DNA pool (soil metagenome) provided a new perspective on the exposure effects on soil microbiota, i.e., an index of soil microbial activity as well as information about the vertical distribution of eDNA through the soil layers. Overall, microannelids appeared to be sensitive, accurate and reliable biological indicators in these forested subalpine soils, showing a higher abundance at the north-facing slope on account of strong acidity indicator species. Furthermore, the exposure was found to be more determinant for shaping the composition of microannelid assemblages than the ground cover type.

In *Chapter IV*, the exposure-effects on the abundance and activity of the wood-inhabiting microbiota (bacteria, fungi and archaea) and selected microbial groups related to the nitrogen cycle (ammonia-oxidising bacteria (AOB) and nitrogen fixers' *nifH* gene) of *Picea abies* coarse woody debris were evaluated at different stages of natural decay (five-decay class study). All in all, higher microbial abundances were registered at the cooler, moister and more acidic north-facing slope and such exposure-effects (N>S) were in general more evident for the advanced decay stages. Accordingly, a more pronounced physical cell wood damage (by X-ray microtomography) together with a higher microbial activity (lower eDNA/iDNA ratio) was observed at the northern slope with respect to the southern slope. Furthermore, the impact of exposure was enzyme-specific and strongly dependent on the decay stage.

Finally, in *Chapters V* and *VI*, the physico-chemical and microbiological changes in both *P. abies* wood blocks and the underlying forest soil were monitored – in a field mesocosm experiment – as a function of slope exposure and time. This experiment attributed shifts in the wood- and soil-

inhabiting microbiota to different exposure-related thermal and moisture conditions. In particular, moisture conditions played a more prominent role at the subalpine sites, inducing shifts in the wood and soil microbial communities in terms of abundance and activity, while the influence of temperature was more dominant at the alpine sites.

Summarized, the findings of this work provide insights into the interrelation between soil micro- and mesofauna in the Alpine topography, as well as into the shifts in microbial communities during the dynamic process of deadwood decomposition, thus contributing to unravel the complex picture of forest ecosystem functioning under future climate scenarios.

Sommario

Gli ecosistemi montani sono scenari ideali per monitorare le dinamiche del carbonio (C) per via della loro sensibilità ai cambiamenti climatici. In questo contesto, l'esposizione e l'altitudine costituiscono importanti parametri topografici che influenzano il microclima (cioè i regimi termici e di precipitazione) e, di conseguenza, la formazione del suolo e i suoi processi biogeochemici con risvolto sia nel funzionamento che nella valutazione del C. Nell'ambito degli ecosistemi forestali, il legno morto è una componente strutturale e funzionale essenziale, sia come serbatoio per la diversità biologica che come stoccaggio di elementi nutritivi (sequestro di C). Il presente lavoro si focalizza pertanto sull'influenza del clima sulle caratteristiche del suolo e sulle dinamiche di decomposizione del legno morto in funzione delle diverse condizioni termiche dovute dalla diversa esposizione di pendenza (nord *vs.* sud) e altitudine (da 1200 a 2400 metri sopra il livello del mare) negli ecosistemi subalpini e alpini delle Alpi italiane.

Questa tesi propone un'introduzione generale all'argomento (*Capitolo I*) e una compilazione di articoli scientifici pubblicati e/o in oggetto di esame in *peer-reviewed* riviste scientifiche internazionali. A seguito dell'introduzione, il *Capitolo II* affronta i principali cambiamenti in composizione, attività e diversità delle comunità microbiche autoctone del suolo in funzione all'esposizione lungo la climosequenza altitudinale, in combinazione con una visione di insieme sulle proprietà fisico-chimiche del suolo. I risultati mostrano che l'esposizione ha ampiamente influenzato sia le proprietà edafiche che i microorganismi del suolo, anche se per la maggior parte dei parametri studiati l'effetto dell'esposizione era dipendente dall'altitudine. In particolare, i tre domini microbici (batteri, funghi e archaea) hanno risposto diversamente all'esposizione in termini di abbondanza. Di conseguenza,

sono state osservate anche reazioni enzimatiche specifiche a seconda dell'esposizione e altitudine.

Nel *Capitolo III*, l'influenza dell'esposizione è stata valutata sia sulle comunità microbiche autoctone del suolo che sulla mesofauna, con particolare attenzione alla comunità di Enchitreidi in diverse condizioni di copertura del suolo nell'ecosistema forestale subalpino. Le analisi quali-quantitative delle frazioni extracellulari (eDNA) e intracellulari (iDNA) del DNA totale del suolo (metagenoma del suolo) hanno fornito una nuova prospettiva sugli effetti dati dall'esposizione sui microorganismi del suolo; ovvero un indice di attività microbica del suolo così come informazioni in merito alla distribuzione verticale dell'eDNA lungo il profilo del suolo. Nel complesso, le comunità di microanellidi sembrano costituire accurati e affidabili indicatori biologici per questi suoli forestali subalpini, mostrando una forte abbondanza presso l'esposizione Nord, essendo specie indicatrice di suoli acidi. Inoltre, l'esposizione è risultata essere maggiormente determinante nella composizione dei microannelidi rispetto alla copertura del suolo.

Nel *Capitolo IV*, gli effetti dell'esposizione sull'abbondanza e attività delle comunità microbiche del legno (batteri, funghi e archaea) e di determinati gruppi microbici correlati al ciclo dell'azoto (batteri ammonio-ossidanti (AOB) e batteri fissanti l'azoto (gene *nifH*)) sono stati valutati nei diversi stadi di decomposizione del legno morto di *Picea abies* (studio delle cinque classi di decomposizione). Nel complesso, un'alta abbondanza microbica è stata registrata all'esposizione Nord essendo maggiormente fredda, umida e acida rispetto all'esposizione Sud e tale effetto (N>S) è stato generalmente evidenziato nelle fasi avanzate di decomposizione. Pertanto, anche una più pronunciata degradazione fisica del tessuto legnoso osservata mediante microtomografia ai raggi X, e accompagnata da una maggiore attività microbica (basso rapporto eDNA/iDNA) è emersa all'esposizione

settentrionale rispetto a quella meridionale. Inoltre, l'impatto dell'esposizione sulle attività enzimatiche è stata fortemente influenzata dallo stadio di decomposizione.

Infine, i *Capitoli V* e *VI* trattano di un esperimento in mesocosmo al fine di monitorare i cambiamenti fisico-chimici e microbiologici, sia nei cubetti di legno di *P. abies* che nel suolo forestale sottostante a essi, in funzione all'esposizione e lungo una determinata fascia temporale. Questo esperimento ha permesso di constatare che le diverse condizioni termiche e di umidità correlate in funzione all'esposizione hanno influenzato le comunità microbiche del legno e del suolo. In particolare, le condizioni di umidità hanno avuto un effetto marcato nei siti subalpini inducendo cambiamenti nelle comunità microbiche del legno e del suolo in termini di abbondanza e attività; mentre l'influenza della temperatura è stata maggiormente determinante nei siti alpini.

Riassumendo, i risultati di questo lavoro forniscono una approfondita visione sull'interrelazione tra i microorganismi e la mesofauna del suolo in ambiente alpino, nonché nei cambiamenti nelle comunità microbiche durante il processo della decomposizione del legno morto; contribuendo così ad illustrare meglio il quadro complesso del funzionamento dell'ecosistema forestale in un'ottica di futuri cambiamenti climatici.

Zusammenfassung

Alpine Gebirgswälder sind komplexe Ökosysteme die besonders sensitiv auf sich verändernde Umweltbedingungen wie globale Erwärmung reagieren. Sie bieten somit ideale Szenarien für Studien zur Kohlenstoff-Dynamik. In diesem Zusammenhang sind Hangexposition und Höhenstufen wichtige Faktoren welche das lokale Mikroklima bestimmen (i.e., Temperatur- und Niederschlagsverlauf), mit Auswirkung auf Verwitterung und biogeochemische Prozesse, und somit auf die gesamte Ökosystemdienstleistung und den Kohlenstoff-Kreislauf. Neben Boden spielt Totholz eine Schlüsselrolle in der Struktur und Funktion von Waldökosystemen, und trägt wesentlich zur Erhaltung der biologischen Vielfalt (Biodiversität) und der natürlichen Regeneration der Wälder bei, mit Einfluss auf die globalen Nährstoffkreisläufe und die Gesamtkohlenstoffspeicherung.

Der Forschungsschwerpunkt der vorgelegten Doktorarbeit liegt auf der Evaluierung von Klimaeinflüssen auf Bodencharakteristiken und Dynamiken im Totholzabbau infolge unterschiedlicher Hangexposition (Sonneneinstrahlung; Nord *vs.* Süd) und Höhenstufen (von 1200 bis 2400 Höhenmeter) entlang der ausgewählten Klimasequenz in (sub)alpinen italienischen Ökosystemen.

Diese Doktorarbeit besteht aus einer allgemeinen Einführung (*Kapitel I*) und einer Serie von Publikationen in internationalen, gutachtenbasierter Fachzeitschriften (*Kapitel II–VI*). *Kapitel II* befasst sich mit den Auswirkungen von Hangexposition-spezifischen klimatischen Bedingungen auf Komposition, Aktivität und Diversität der autochthonen mikrobiellen Gemeinschaften entlang der ausgewählten Klimasequenz, zusammen mit einer ausführlichen Charakterisierung der physikalisch-chemischen Bodeneigenschaften. Die Ergebnisse zeigen deutliche, meist Höhenstufen-

spezifische Auswirkungen der Hangexposition auf edaphische Eigenschaften und die Mikrobiota. Besonders bemerkenswert waren dabei die mikrobiellen Domänen-spezifischen Auswirkungen der Hangexposition auf die Abundanzen von Bakterien, Pilzen und Archaeen. Auch Enzym-spezifische Einflüsse der Hangexposition und Höhenstufen konnten entlang der ausgewählten Klimasequenz festgestellt werden.

Kapitel III widmet sich den Einflüssen der Hangexposition auf die autochthone Mikrobiota und Mesofauna in subalpinen Waldökosystemen, mit Schwerpunkt auf den Enchytraeiden-Gemeinschaften unter verschiedenen, repräsentativen Vegetationstypen. Die "komparativ-diskriminierende" Analyse der extrazellulären (eDNA) und intrazellulären (iDNA) Fraktionen des gesamten Boden-dann-Pools (soil metagenome) ermöglichte neue Einblicke in die Auswirkungen der Hangexposition auf die mikrobiellen Gemeinschaften; dieser innovative Versuchsansatz lieferte einen Index für die Bestimmung der mikrobiellen Aktivitäten, sowie Informationen über die vertikale Verteilung der eDNA entlang eines Bodenprofils. Die Studie der Mikroanneliden-Gemeinschaften bestätigte diese generell als sensitive und präzise biologische Indikatoren der subalpinen Waldböden; größere Abundanzen wurden auf den nordexponierten, im Vergleich zu südexponierten Versuchsflächen verzeichnet werden, mit der Präsenz von Indikator-Arten für stark saure Böden. Für die Mikroanneliden-Gemeinschaften zeigte sich die Hangexposition allgemein stärker prägend als der Vegetationstyp.

Kapitel IV befasst sich mit dem Einfluss der Hangexposition auf die Abundanz und Aktivität der Totholz-Mikrobiota (Bakterien, Pilze und Archaeen), sowie auf spezielle, am Stickstoffkreislauf beteiligte, mikrobielle Gruppen (Ammoniumoxidierende Bakterien, AOB; und Stickstofffixierende

Bakterien, *nifH*-Gen) in den fünf verschieden Stadien der natürlichen Holzzersetzung von *Picea abies* (5 Abbaustufen/Klassen-Studie).

Insgesamt wurden höhere mikrobielle Abundanzen für die nordexponierten Versuchsflächen gefunden, welche durch kühlere Temperaturen, feuchtere Böden und niedrigeren pH-Werten charakterisiert waren; dieser Expositions-Effekt (Nord>Süd) machte sich generell mit zunehmendem Zersetzungsgrad verstärkt bemerkbar. Dieses an den nordexponierten Hängen beobachtete Phänomen konnte durch die multidisziplinären Ergebnisse wie i) stärker ausgeprägte Zerstörung der Holz-Zellstruktur (Röntgen-Mikrotomographie), sowie ii) geringere mikrobielle Aktivität (engeres eDNA/iDNA Verhältnis) bestätigt werden. Der Expositionseffekt zeigte sich generell auch als enzymspezifisch und stark vom Holz-Zersetzungsgrad abhängig.

Kapitel V und *VI* beschreiben die Ergebnisse des Feld-Mesokosmen-Experimentes, welches durchgeführt wurde, um den Einfluss von Hangexposition und Zeit auf physikalisch-chemische und mikrobiologische Charakteristiken von Totholz (*P. abies*) und Waldböden (im direkten Kontakt mit den Holzblöcken) zu bestimmen. Dieser Versuchsansatz brachte die in Holz- und Boden-Mikrobiota beobachteten Veränderungen mit den unterschiedlichen Temperatur- und Feuchte-Verhältnissen (aufgrund unterschiedlicher Hangexposition) in Zusammenhang. Feuchte-Verhältnisse spielten auf den subalpinen Versuchsflächen eine dominante Rolle, während auf den alpinen Standorten der Faktor Temperatur ausschlaggebend für Veränderungen der Abundanz und Aktivität der mikrobiellen Gemeinschaften (Holz *vs.* Boden) war.

Die Forschungsergebnisse meiner Doktorarbeit geben Einblick i) in die komplexe Wechselbeziehung zwischen Mikro- und Mesobiota in (sub)alpinen Waldökosystemen, und ii) in die Veränderungen der

mikrobiellen Gemeinschaften während des dynamischen Prozesses des natürlichen Totholzabbaus, und tragen somit zum besseren Verständnis der komplexen Mechanismen bei, die einem funktionierendem Waldökosystem zu Grunde liegen, insbesondere mit Bezug auf Bodenkohlenstoffbilanz und somit auf die Produktivität der Wälder unter zukünftigen klimatischen Bedingungen.

I. Introduction

Climate impact in mountain ecosystems

It is well known that soil carbon (C) stocks are influenced by several environmental factors such as topography, slope exposure, elevation, climate, parent material and vegetation (Tsui et al., 2004; Sidari et al., 2008; Zhang et al., 2012); as well as by the quantity and quality of soil organic matter (SOM) (Balser and Firestone, 2005; Zhang et al., 2013; Xu et al., 2015); and the structure and function of soil microbial communities (Myers et al., 2001; Treseder, 2004; Wakelin et al., 2007; Wang et al., 2014). The latter play a key role in ecosystem services (i.e., decomposition/breakdown of OM) to guarantee soil health and fertility. However, the microbial response to changing climatic conditions still requires further research because to date, most studies have had a limited ability to differentiate between the complex climate effects on the soil ecosystem (Sun et al., 2013).

High-altitude ecosystems represent unique and ideal scenarios for the study of climate impact due to their sensitivity and responsiveness to environmental changes (Zhang et al., 2013; Yasir et al., 2015). In this context, soil climosequences that are also implicitly vegetation-sequences offer the possibility to evaluate the consequences of climatic gradients on a comparatively small scale owing to the rapid shifts in temperature and precipitation regimes ultimately affecting vegetation distribution and soil biodiversity (Zhang et al., 2013). This is of utmost importance considering that a drastic increase in the atmospheric concentrations of carbon dioxide (CO_2) and other anthropogenic greenhouse gasses (GHGs) such as methane (CH_4) and nitrous oxide (N_2O) has been observed during the last several decades, leading to temperature rises and significant changes in precipitation patterns (Davidson and Janssens, 2006; IPCC; 2007; Takahashi et al., 2010).

Indeed, a rise in soil temperature in response to projected climate warming could intensify soil microbial activities, thereby accelerating SOM turnover

rates and increasing C availability ultimately resulting in compositional and functional shifts in soil microbial communities (Ascher et al., 2012). These changes are more likely to occur in sensitive and extreme environments such as subalpine and alpine forest ecosystems. Some studies conducted at this type of ecosystems (Olympic Mountains of Washington state, USA: Prichard et al., 2000; Chelgerd Hilly area, Iran: Nahidan et al., 2015; Trentino area, Italy: Egli et al., 2006, 2009, 2016; Ascher et al., 2012) reported significant changes in SOM dynamics as a result of different thermal and moisture conditions represented by different slope exposure (north- *vs.* south-facing slopes). Altogether they pointed out that the SOM content was relatively higher in soils located at the northern than at the southern slopes due to the cooler and moister conditions at the north-facing slopes; thereby facilitating SOM accumulation instead of decomposition processes.

Slope exposure largely influences the local microclimate and the amount of solar irradiation intercepted by the slope orientation affecting the soil weathering and biogeochemical processes (Beniston, 2006; Barbosa et al., 2015; Egli et al., 2016). However, there is still a paucity of information about how the slope exposure and climate in general affect the activity and composition of micro- and mesobiota despite they are considered sensitive biological indicators in forest soils (Ascher et al., 2012). Soil heterotrophic microorganisms are responsible for the rate-limiting step in OM degradation via the production of hydrolytic and oxidative extracellular enzymes (Sinsabaugh et al., 2008; A'Bear et al., 2014); and they are further influenced by the activities of soil fauna that lives along them (Bardgett and Wardle, 2010). In this context, earthworms (epigeic, endogeic and anecic) and microannelids (Enchytraeids) as proxies of the macro- and mesofauna are considered keystones in the soil forest system thanks to their crucial role in the functioning and maintenance of detrital food webs (Didden, 1993;

Ascher et al., 2012; Karaban and Uvarov, 2014). Nevertheless, to date the interrelation of Alpine topography with the micro- and mesobiota is still poorly understood. This issue has been addressed in *Chapters II* and *III*.

Deadwood as an integral component in forest ecosystems

Deadwood is an essential component of forest ecosystems (Fig.1), as it serves as a reservoir for biological and functional diversity, sustains forest productivity, and provides shelter and nutrition to various organisms, primarily fungi and saproxylic insects (Harmon et al., 1986; Lombardi et al., 2013; Purahong et al., 2016). In natural forests, the deadwood input derives from tree mortality; large-dimensions residues such as logs, snags and coarse roots are known as coarse woody debris (CWD). In managed forests CWD input rate depends on logging and management activities including left-over stumps and/or branches (Petrillo et al., 2015). Other major disturbances (i.e., wind storms) could also occasionally influence CWD input (Harmon et al., 2013; Petrillo et al., 2015). A loss of deadwood has been linked to a loss of biodiversity and the dimension of decaying logs determines the distribution of wood-decomposing organisms. The larger the logs, the more ecological niches and microhabitats they provide (Hoppe et al., 2015).

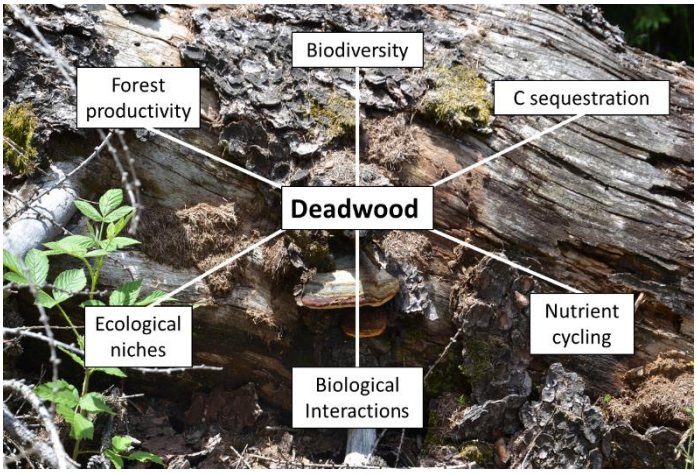

Fig.1. Roles of deadwood in forest ecosystem. Photo by T. Bardelli.

Moreover, deadwood represents a global C store estimated to be in the range of 73 ± 6 Pg (Pan et al., 2011), making its decomposition dynamics a determinant of the soil C balance and forest productivity (Fig. 1; Bradford et al., 2014). However, as pointed out by Lombardi et al. (2013), in European temperate and Mediterranean forest ecosystems deadwood decay mechanisms are still poorly described and there is a paucity of information on its contribution to nutrient pools and to long-term forest sustainability. One of the most common and useful approaches to determine and characterise the wood decay progression is to subdivide deadwood into five stages based on its visual and physical assessments (Maser et al., 1979; Hunter, 1990; Harmon et al., 2013; Petrillo et al., 2015, 2016; Gómez-Brandón et al., 2017; Tatti et al., 2017). The principal features of the five wood decay stages are shown in Table 1.

Table 1. Classification of deadwood at different stages of decay.

Decay stage	Characteristics
1 Recently dead	Recently dead tree, bark attached to stem; undecayed wood.
2 Weakly decayed	Bark loose or fallen off, decay penetrating less than 3 cm into wood from surface, initial mycelium under bark.
3 Medium decayed	Decay penetrating more than 3 cm into wood, core (or hollow tree surface) still hard.
4 Very decayed	Stem rotten throughout, no (few) hard parts, ellipsoid cross-section, fragmented outline of stem.
5 Almost decomposed	Stem outline heavily fragmented, completely decomposed in dome places; wood disintegrates when lifted; wood mold in tree cavities.

Adapted from Stokland, 2001.

As long as woody material decays, its physical and chemical quality gradually changes, and consequently a turnover of the microbial community takes place as species are replaced by those more suited to the substrate (Rajala et al., 2011, 2012). It has been reported that climate and/or biotic factors such as the abundance, composition and activity of the decomposer communities

along with the quality (i.e., chemical composition) of the substrate they decompose may largely influence wood decomposition rates (Liu et al., 2013; Purahong et al., 2016). Although climate is traditionally thought to be the predominant factor affecting deadwood decay at both global and regional scales, Bradford et al. (2014) demonstrated that other local-scale factors (i.e., fungal grazers, deadwood density, nitrogen availability) also had a large influence on the carbon dynamics of decomposing wood at regional scales. In line with this, Fravolini et al. (2016) underpinned that local-scale factors including not only soil properties but also topographic features, particularly the slope exposure, are important drivers affecting the deadwood decay process. Nevertheless, there is still a gap of knowledge about how the deadwood decay rate and the involved decomposer communities are affected by the slope exposure and, in general by climate in mountain forest ecosystems despite such information will contribute to broaden our understanding about the C-cycle dynamics in this type of ecosystems. In this regard, such gap is partially fulfilled with the findings of *Chapter IV*.

Over the decomposition process, deadwood is incorporated into the soil releasing nutrients and organic C that significantly influences the soil C balances (Magnusson et al., 2016). Stutz and Lang (2017) designated deadwood as a "pedogenic hot-spot" because it may induce changes in soil properties (soil porosity, available water capacity, total organic C and N) as long as it is decomposed. Particularly, soil- and wood-inhabiting microbiota especially fungi are affected by the wood decay dynamics; thereby directly influencing the nutrient cycling. Indeed, Mäkipää et al. (2017) observed that the wood-inhabiting fungi become increasingly species rich and more similar to the soil fungal communities as wood decay (Norway spruce logs) progresses. However, to date few studies have addressed the changes in both deadwood and the forest floor over time from a physico-chemical and

microbiological viewpoint (van der Wal et al., 2007; Risch et al., 2013; Gonzalez-Polo et al., 2013; Mäkipää et al., 2017) and especially under different thermal conditions like those observed in mountain forest ecosystems. Along these lines, the *Chapters V* and *VI* provide insight into the interfaces between deadwood and soil forest system in subalpine and alpine environments, respectively; and how the climate (different slope exposure and altitude) influence the microbiota involved in the wood decomposition processes. Overall, this underpins the importance of digging deeper into the wood-inhabiting microbiota in order to disentangle the biological mechanisms involved in the wood decay dynamics.

The role of fungi as wood decomposers

Fungi are close to the living, dying and dead wood through the presence of spores in the atmosphere or mycelial filaments in the surrounding soil (Hoppe, 2016). Under natural conditions, they are considered as the primary wood decomposers thanks to their ability to degrade lignin, which makes up to 40 % of the tissue dry weight in woody plants, via secretion of a battery of extracellular lignocellulolytic enzymes (Cornelissen et al., 2012; Purahong et al., 2014, 2016).

More specifically, there exist three types of fungal-caused wood rot: *brown*-rot, *white*-rot and *soft*-rot. Brown-rot is caused by fungi belonging to the phylum Basidiomycota (i.e., *Polyporaceae*), and only 6-7 % of wood-inhabiting fungi cause this type of rot (Hoppe, 2016). They are involved in cellulose and hemicellulose degradation through a mechanism that relies on the release and production of oxalic acids and hydroxyl radicals, respectively. On the contrary, white-rot fungi are capable of degrading all components of the cell wall (including lignin) by secreting a sophisticated battery of enzymes. Although brown-rot Basidiomycetes do not secrete these enzymes, they are also capable of oxidising lignin via a non-enzymatic

mechanism known as Fenton reaction (Martinez et al., 2005). Ultimately, soft-rot causing fungi that are mainly represented by members of the phylum Ascomycota are responsible for degrading celluloses and hemicelluloses of the secondary cell wall, thereby causing the spongy consistency of the wood (Hoppe, 2016).

Field surveys on wood-decaying fungi have mainly been confined to the observation of fruiting bodies at a specific time interval as pointed out by Hoppe et al. (2015). Nevertheless, over the last few years the application of high-throughput sequencing technologies has offered a more comprehensive picture of the fungal diversity patterns and community composition present in deadwood (Kubartova et al., 2012; Ovaskainen et al., 2013; Ottosson et al., 2014; Hoppe et al., 2015; Hiscox et al., 2015; van de Wal, 2015; Yamashita et al., 2015). It has been shown that the composition of wood-inhabiting fungal communities can be influenced by biotic and abiotic drivers. For instance, Purahong et al. (2016) identified several wood physico-chemical properties (i.e., decay stage, remaining mass, density, extractives, total lignin and pH) as the most important factors associated with the fungal community composition in forest ecosystems. This is consistent with previous findings from Rajala et al. (2011, 2012). There also exist biotic drivers like the priority effects that are the first arriving fungus can significantly influence the assembly of the following fungal communities and consequently the deadwood decomposition rate (Fukami et al., 2010). Furthermore, both antagonist and beneficial interactions between fungi and bacteria take place within the deadwood environment (Johnston et al., 2016), suggesting that bacteria might play a more important role in deadwood turnover than previously thought and ultimately, in nutrient cycling in forest ecosystems (Cornelissen et al., 2012; Hoppe et al., 2014, 2015; Kielav et al., 2016; Hervé et al., 2016; Johnston et al., 2016; Rinta-Kanto et al., 2016; Gómez-Brandón et al., 2017).

The role of bacteria as wood decomposers

Although bacteria have long been associated with decomposing wood as habitat, more attention has been paid to fungi within the same environment (Johnston et al., 2016). In functional terms, Greaves (1971) classified wood-inhabiting bacteria into four groups based on their role in decomposition: (i) bacteria that make wood more water-permeable without affecting its structural integrity; (ii) bacteria with the ability to attack wood structures; (iii) bacteria that establish a synergic interaction with wood-inhabiting microbiota; and (iv) bacteria that may act as antagonists to other bacteria and/or inhibit fungal decomposition. On the one hand, there is evidence of bacterial lysis in wood following fungal inoculation under starvation conditions (Johnston et al., 2016). Wood-inhabiting bacteria may also potentially have effects that are negative to fungi, as they may consume easily degradable substrates that are necessary for fungal colonisation and degradation activities (Folman et al., 2008; Johnston et al., 2016). On the other hand, wood-inhabiting fungi may also benefit from wood-colonising bacteria if they metabolise toxic intermediates and/or provide fungi with limiting nutrients like iron or nitrogen via nitrogen-fixation (De Boer and Van der Waal, 2008; Valášková et al., 2009; Hoppe et al., 2014; Johnston et al., 2016). It is known that nitrogen availability in deadwood is highly restricted, with a C to N ratio ranging from 350 to 800, which suggests that wood-degrading fungi may favour from associations with nitrogen-fixing bacteria to fulfil their nitrogen requirements for vegetative and generative growth (Merrill and Cowling, 1966; Larsen et al., 1978; Hoppe et al., 2014). For instance, Hoppe et al. (2015) found positive correlations between fungal sporocarps and the richness of *nifH* (dinitrogen reductase) genes in deadwood logs from *Fagus sylvatica* and *Picea abies*. Nitrogen is a very limited nutrient in early wood decay and can be accumulated over time (Baldrian et al., 2016). The role of nitrogen-fixing bacteria is to fix the atmospheric

dinitrogen (N_2) into a useful biological form (NH_3), being the *nifH* gene the most useful marker to study the distribution of this bacterial group in various environments including forest ecosystems (Levy-Booth et al., 2014).

The biological oxidation from ammonia (NH_3) to nitrite (NO_2^-) is also of great relevance in forest soils (Levy-Booth et al., 2014), as it is the rate-limiting step of the nitrification process. This reaction is carried out by both ammonia-oxidising bacteria (AOB) and archaea (AOA), which can be quantified by the ammonia-monooxygenase (*amoA*) gene (Rotthauwe et al., 1997; Francis et al., 2005; Leininger et al., 2006). Previous studies have shown that AOB and AOA respond differently to the environmental conditions, with one or the other being more competitive under given conditions, as they belong to separate phylogenetic domains with different cell biochemical and metabolic process (Erguder et al., 2009). However, with respect to soil, far less attention has been paid to these bacterial groups in the deadwood environment (see *Chapters IV* and *V*).

The application of high-throughput DNA sequencing approaches has opened new avenues for a more comprehensive understanding about the diversity patterns and community composition of saproxylic bacteria in the last few years. Several studies have shown the dominance of the phyla *Proteobacteria*, *Acidobacteria* and *Actinobacteria* in decaying wood from different tree species including *Picea abies*, *Fagus sylvatica* and *Pinus sylvestris* (Valášková et al., 2009; Sun et al., 2013; Hoppe et al., 2015; Kielav et al., 2016; Rinta-Kanto et al., 2016). This is in line with the fact that members from these phyla are known to possess enzymes involved in the breakdown of cellulolytic material (Lladó et al., 2016). Brown and Chang (2014) also found evidence of bacteria, i.e., Actinobacterium *Amycolatopsis* sp. 75iv2, with lignin-decomposing abilities. Moreover, diazotrophic *Alphaproteobacteria* (e.g. *Rhizobiales*) have also been reported to account up to 25% of the bacterial

community in *P. abies* logs during the intermediate and advanced stages of decay (Hoppe et al., 2015).

Different biotic and abiotic factors were found to govern the composition of wood-inhabiting bacteria including the host tree species and the forest management regime (Hoppe et al., 2015), and the physico-chemical properties of the wood particularly the remaining mass, density, water content and C:N ratio (Hoppe et al., 2015). Interestingly, Hoppe et al. (2016) found that the stage of wood decay was more determinant than pH for the shifts in wood-inhabiting bacterial communities. This is in disagreement with the soil environment, where pH is considered one of the most important predictors for bacterial community structure (Lauber et al., 2009). Moreover, it is believed that the composition of the primary wood-inhabiting bacterial communities may be a consequence of the composition of the surrounding soil bacterial communities, which suggests an edaphic origin of saproxylic bacteria or an indirect influence of the soil environment, for instance via alteration of the fungal community within deadwood (Johnston et al., 2016).

PhD thesis objectives and structure

The main objective of the present dissertation was to evaluate the climate effects (different thermal conditions due to differences in slope exposure and altitude) on soil properties and deadwood decomposition dynamics in (sub)alpine ecosystems in the Italian Alps, with a special focus on the composition and activity of micro- and mesobiota.

For this purpose, the following specific aims were addressed in chapters II to VI of this work in the research fields of forest ecology and microbiology:

1) to investigate the impact of the slope exposure (north- *vs.* south-facing slopes) on the physico-chemical and (micro)biological properties of (sub)alpine soils along an altitudinal gradient ranging from 1200 to 2400 m above sea level (**Chapter II**).

2) to determine the influence of the slope exposure and different soil ground cover types (grass, moss, litter and woody debris) on the soil autochthonous mesofauna (Enchytraeid community) and microbiota (bacteria, fungi, archaea) in subalpine forest ecosystems (**Chapter III**).

3) to evaluate the shifts in the wood-inhabiting microbiota (bacterial, fungal and archaeal communities) of *Picea abies* (L.) Karst coarse woody debris at different stages of natural decay (five-decay class study) as a function of slope exposure (**Chapter IV**).

4) to study the changes in the composition and activity of microbial communities in both *P. abies* wood blocks and the underlying soil – in immediate contact with the wood blocks – as a function of the slope exposure in subalpine and alpine scenarios during a 2- and 3-year mesocosm monitoring, respectively (**Chapters V** and **VI**).

This thesis is composed of three published scientific articles and two submitted manuscripts. The papers are listed below.

Bardelli, T., Gómez-Brandón, M., Ascher-Jenull, J., Fornasier, F., Arfaioli, P., Francioli, D., Egli, M., Sartori, G., Insam, H., Pietramellara, G., 2017. Effects of slope exposure on soil physico-chemical and microbiological properties along an altitudinal climosequence in the Italian Alps. Science of the Total Environment 575:1041-1055.

Gómez-Brandón, M., Ascher-Jenull, J., **Bardelli, T.**, Fornasier, F., Sartori, G., Pietramellara, G., Arfaioli, P., Egli, M., Beylich, A., Insam, H., 2017. Ground cover and slope exposure effects on micro- and mesobiota in forest soils. Ecological Indicators 80:174-185.

Gómez-Brandón, M., Ascher-Jenull, J., **Bardelli, T.**, Fornasier, F., Fravolini, G., Arfaioli, P., Ceccherini, M.T., Pietramellara, G., Lamorski, K., Slawiński, C., Bertoldi, D., Egli, M., Cherubini, P., Insam, H., 2017. Physico-chemical and microbiological evidence of exposure effects on *Picea abies* – coarse woody debris at different stages of decay. Forest Ecology and Management 391:376-389.

Bardelli, T., Ascher-Jenull, J., Burkia Stocker, E., Fornasier, F., Arfaioli, P., Fravolini, G., Roberta Alves Medeiros, L., Egli, M., Pietramellara, G., Insam, H., Gómez-Brandón, M. Impact of slope exposure on chemical and microbiological properties of Norway spruce deadwood and underlying soil during early stages of decomposition in the Italian Alps. *Submitted* to Catena.

Bardelli, T., Gómez-Brandón, M., Fornasier, F., Arfaioli, P., Egli, M., Pietramellara, G., Ceccherini, M.T., Insam, H., Ascher-Jenull, J. Chemical and microbiological changes in Norway spruce deadwood during the early stage of decomposition as a function of exposure in an Alpine setting. *Submitted* to Arctic, Antarctic, and Alpine Research.

The following additional scientific articles are not part of this dissertation but they resulted from the collaborations established during my PhD. Furthermore, their content is also related to the topics shown here and could be of full interest to the readers.

1. Fravolini, G., Egli, M., Derungs, C., Cherubini, P., Ascher-Jenull, J., Gómez-Brandón, M., **Bardelli, T.**, Tognetti, R., Lombardi, F., Marchetti, M. 2016. Soil attributes and microclimate are important drivers of initial deadwood decay in sub-alpine Norway spruce forests. Science of the Total Environment 569-570:1064-1076.

2. Egli, M., Hafner, S., Derungs, C., Ascher-Jenull, J., Camin, F., Sartori, G., Raab, G., Bontempo, L., Paolini, M., Ziller, L., **Bardelli, T.**, Petrillo, M., Abiven, S. 2016. Decomposition and stabilisation of Norway spruce needle-derived material in Alpine soils using 13C-labelling approach in the field. Biogeochemistry 131:321-338.

References

A'Bear, A.D., Jones, T.H., Kandeler, E., Boddy, L., 2014. Interactive effects of temperature and soil moisture on fungal- mediated wood decomposition and extracellular enzyme activity. Soil Biol. Biochem. 70, 151–158.

Ascher, J., Sartori, G., Graefe, U., Thornton, B., Ceccherini, M.T., Pietramellara, G., Egli, M., 2012. Are humus forms, mesofauna and microflora in subalpine forest soils sensitive to thermal conditions? Biol. Fertil. Soils. 48, 709–725.

Baldrian, P., Zrustova, P., Tláskal, V., Davidova, A., Merhautová, V., Vrška, T., 2016. Fungi associated with decomposing deadwood in a natural beech-dominated forest. Fungal Ecol. 23, 109–122.

Barbosa, C., García-Martínez, J., Pérez-Ortín, J.E., Mendes-Ferreira, A., 2015. Comparative transcriptomic analysis reveals similarities and dissimilarities in *Saccharomyces cerevisiae* wine strains response to nitrogen availability. PLoS ONE 10: e0122709.

Balser, T. C., Firestone, M. K., 2005. Linking microbial community composition and soil processes in a California annual grassland and mixed-conifer forest. Biogeochemistry, 73, 395–415.

Beniston, M., 2006. Mountain weather and climate: a general overview and a focus on climatic change in the Alps. Hydrobiologia 562, 3–16.

Bardgett, R., Wardle, D.A., 2010. Aboveground-Belowground Linkages. Biotic Interactions, Ecosystem Processes and Global Change. Oxford University Press, Oxford, UK.

Bradford, M.A., Warren , R.J. , Baldrian, P., Crowther, T.W., Maynard, D.S., Oldfield, E.E., Wieder, W.R., Wood, S.A., King, J.R., 2014. Climate fails to predict wood decomposition at regional scales. Nat. Clim. Chang. 4, 625–630.

Brown, M. E., Chang, M. C., 2014. Exploring bacterial lignin degradation. Curr. Opin. Chem. Biol. 19, 1–7.

Cornelissen, J.H.C., Sass-Klaassen, U., Poorter, L., Van Geffen, K., Van Logtestijn, R.S.P., Van Hal, J., Goudzwaard, L., Sterck, F.J., Klaassen, R.K.W.M., Freschet, G.T., Van der Wal, A., Eshuis, H., Zuo, J., De Boer, W., Lamers, T., Weemstra, M., Cretin, V., Martin, R., Den Ouden, J., Berg, M.P., Aerts, R., Mohren, G.M.J., Hefting, M.M., 2012. Controls on coarse wood decay in temperate tree species: birth of the LOGLIFE experiment. Ambio 41, 231–245.

Davidson, E.A., Janssens, I.A., 2006. Temperature sensitivity of soil carbon decomposition and feedbacks to climate change. Nature 440, 165–173.

De Boer, W., Van der Wal, A., 2008. Interactions between saprotrophic basidiomycetes and bacteria. In: Boddy, L., Frankland, J.C., Van West, P. (Eds.), Ecology of Saprotrophic Basidiomycetes. Accademic Press, Amsterdam, pp. 142–151.

Didden, W.A.M., 1993. Ecology of terrestrial Enchytraeidae. Pedobiologia 37, 2–29.

Egli, M., Mirabella, A., Sartori, G., Zanelli, R., Bischof, S., 2006. Effect of north and south exposure on weathering rates and clay mineral formation in Alpine soils. Catena 67, 155–174.

Egli, M., Sartori, G., Mirabella, A., Giaccai, D., Favilli, F., 2009. Effect of north and south exposure on organic matter in high Alpine soils. Geoderma 149, 124–136.

Egli, M., Hafner, S., Derungs, C., Ascher-Jenull, J. Camin, F., Sartori, G., Raab, G., Paolini, M., Bontempo, L., Ziller, L., Bardelli, T., Petrillo, M., Abiven, S., 2016. Decomposition and stabilisation of Norway spruce needle-derived material in Alpine soils using a 13C-labelling approach in the field. Biogeochemistry 13, 321–338.

Erguder, T.H., Boon, N., Wittebolle, L., Marzorati, M., Verstraete, W., 2009. Environmental factors shaping the ecological niches of ammonia-oxidizing archaea. FEMS Microbiol. Rev. 33, 855–869.

Folman, L.B., Klein Gunnewiek, P.J., Boddy, L., de Boer, W., 2008. Impact of white-rot fungi on numbers and community composition of bacteria colonizing beech wood from forest soil. FEMS Microbiol. Ecol. 63, 181–91.

Francis, C.A., Roberts, K.J., Beman, J.M., Santoro, A.E., Oakley, B.B., 2005. Ubiquity and diversity of ammonia-oxidizing archaea in water columns and sediments of the ocean. Proc. Natl. Acad. Sci. 102, 14683–14688.

Fravolini, G., Egli, M., Derungs, C., Cherubini, P., Ascher-Jenull, J., Gómez-Brandón, M., Bardelli, T., Tognetti, R., Lombardi, F., Marchetti, M., 2016. Soil attributes and microclimate are important drivers of initial deadwood decay in sub-alpine Norway spruce forests. Sci. Tot. Env. 569–570, 1064–1076.

Fukami, T., Dickie, I.A., Wilkie, J.P., Paulus, B.C., Park, D., Roberts, A., Buchanan, P.K., Allen, R.B., 2010. Assembly history dictates ecosystem functioning: evidence from wood decomposer communities. Ecol. Lett. 13, 675–684.

Gómez-Brandón, M., Ascher-Jenull, J., Bardelli, T., Fornasier, F., Fravolini, G., Arfaioli, P., Ceccherini, M.T., Pietramellara, G., Lamorski, K., Sławiński, C., Bertoldi, D., Egli, M., Cherubini, P., Insam, H., 2017. Physico-chemical and microbiological evidence of exposure effects on *Picea abies* – coarse woody debris at different stages of decay. For. Ecol. Manage. 391, 376–389.

Gonzalez-Polo, M., Fernández-Souto, A., Austin, A.T., 2013. Coarse woody debris stimulates soil enzymatic activity and litter decomposition in an old-growth temperate forest of Patagonia, Argentina. Ecosystems 16, 1025–1038.

Greaves, H., 1971. The bacterial factor in wood decay. Wood Sci. Technol. 5, 6–16.

Harmon, M.E., Franklin, J.F., Swanson, F.J., Sollins, P., Gregory, S.V., Lattin, J.D., Anderson, N.H., Cline, S.P., Aumen, N.G., Sedell, J.R., Lienkaemper, G.W., Cromack, K., Cummins, K.W., 1986. Ecology of coarse woody debris in temperate ecosystems. Adv. Ecol. Res. 15, 133–302.

Harmon, M.E., Fasth, B., Woodall, C.W., Sexton, J., 2013. Carbon concentration of standing and downed woody detritus: effects of tree taxa, decay class, position, and tissue type. Foreco 291, 259–267.

Hervé, V., Ketter, E., Pierrat, J.C., Gelhaye, E., Frey-Klett, P., 2016. Impact of *Phanerochaete chrysosporium* on the functional diversity of bacterial communities associated with decaying wood. PLoS ONE 11:e0147100.

Hiscox, J., Savoury, M., Müller, C.T., Lindahl, B.D., Rogers, H.J., Boddy, L., 2015. Priority effects during fungal community establishment in beech wood. ISME J. 9, 2246–2260.

Hoppe, B., Kahl, T., Karasch, P., Wubet, T., Bauhus, J., Buscot, F., Krüger, D., 2014. Network analysis reveals ecological links between N-fixing bacteria and wood-decaying fungi. PLos ONE 9:e88141.

Hoppe, B., Krüger, D., Kahl, T., Arnstadt, T., Buscot, F., Bauhus, F., Wubet, T., 2015. A pyrosequencing insight into sprawling bacterial diversity and community dynamics in decaying deadwood logs of *Fagus sylvatica* and *Picea abies*. Sci. Rep. 5, 9456. DOI 10.1038/srep09456

Hoppe, B., Purahong, W., Wubet, T., Kahl, T., Bauhus, J., Arnstadt, T., Hofrichter, M., Buscot, F., Krüger, D., 2016. Linking molecular deadwood-inhabiting fungal diversity and community dynamics to ecosystem functions and processes in Central European forests. Fungal Divers. 77, 367–379.

Hunter, M.L., 1990. Wildlife, forests and forestry: principles of managing forests for biological diversity, Prentice Hall, Englewood Cliffs, NJ, USA, pp 370.

IPCC, 2007. In: Solomon, S., Qin, D., Manning, M., Chen, Z., Marquis, M., Averyt, K.B., Tignor, M., Miller, H.L. (Eds.), Climate Change 2007: The Physical Science Basis Contribution of Working Group I to the Fourth Assessment Report of the Intergovernmental Panel on Climate Change. Cambridge University Press, Cambridge, United Kingdom and New York, NY, USA, 996 pp.

Johnston, S.R., Boddy, L, Weightman, A.J., 2016. Bacteria in decomposing wood and their interactions with wood-decaying fungi. FEMS Microbiol. Ecol. 92, 1–12.

Karaban, K., Uvarov, A.V., 2014. Non-trophic effects of earthworms on enchytraeids: An experimental investigation. Soil Biol. Biochem. 73, 84–92.

Kielav, A.M., Scheublin, T.R., Mendes, L.W., van Veen, J. A., Kuramae, E.E., 2016. Bacterial community succession in pine-wood decomposition. Front. Microbiol. 7, 1–12.

Kubartova, A., Ottosson, E., Dahlberg, A., Stenlid, J., 2012. Patterns of fungal communities among and with decaying logs, revealed by 454 sequencing. Mol. Ecol. 21, 4514–4532.

Laiho, R., Prescott, C.E., 2004. Decay and nutrient dynamics of coarse woody debris in northern coniferous forests: a synthesis. Can. J. For. Res. 34, 763–777.

Larsen, M.J., Jurgensen, M.F., Harvey, A.E., 1978. Nitrogen fixation associated with wood decay by some common fungi in western Montana. Can. J. For. Res. 8, 341–345.

Lauber, C.L., Hamady, M., Knight, R., Fierer, N., 2009. Pyrosequencing-based assessment of soil pH as a predictor of soil bacterial community structure at the continental scale. Appl. Environ. Microbiol. 75, 5111–5120.

Leininger, S., Urich, T., Schloter, M., Schwark, L., Qi, J., Nicol, G.W., Prosser, J.I., Schuster, S.C., Schleper, C., 2006. Archaea predominate among ammonia-oxidizing prokaryotes in soils. Nature 442, 806–809.

Levy-Booth, D.J., Prescott, C.E., Grayston, S.J., 2014. Microbial functional genes involved in nitrogen fixation, nitrification and denitrification in forest ecosystems. Soil. Biol. Biochem. 75, 11–25.

Liu, W., Schaefer, D., Qiao, L., Liu, X., 2013. What controls the variability of wood-decay rates? For. Ecol. Manag. 310, 623–631.

Lladó, S., Žifčáková, L., Větrovský, T., Eichlerová, I., Baldrian, P., 2016. Functional screening of abundant bacteria from acidic forest soil indicates the metabolic potential of Acidobacteria subdivision 1 for polysaccharide decomposition. Biol. Fertil. Soils 52, 251–260.

Lombardi, F., Cherubini, P., Tognetti, R., Cocozza, C., Lasserre, B., Marchetti, M., 2013. Investigating biochemical processes to assess deadwood decay of beech and silver fir in Mediterranean mountain forests. Ann. For. Sci. 70, 101–111.

Mäkipää, R., Rajala, T., Schigel, D., Rinne, K. T., Pennanen, T., Abrego, N., Ovaskainen, O., 2017. Interactions between soil-and dead wood-inhabiting fungal communities during the decay of Norway spruce logs. ISME J. 11, 1964–1974.

Magnússon, R.Í., Tietema, A., Cornelissen, J.H.C., Hefting, M.M., Kalbitz, K., 2016. Sequestration of carbon from coarse woody debris in forest soils. For. Ecol. Manag. 377, 1–15.

Guillén, F., Martínez, M. J., Gutiérrez, A., Del Rio, J. C., 2005. Biodegradation of lignocellulosics: microbial, chemical, and enzymatic aspects of the fungal attack of lignin. Int. Microb. 8, 195–204.

Maser, C., Anderson, R., Cromack, K., Williams, J.T., Martin, R.E., 1979. Dead and down woody material. In: Thomas, J.W. (Ed.), Wildlife Habitats in Managed Forests, the Blue Mountains of Oregon and Washington. USDA Forest Service Agriculture Handbook 553, pp. 79–85 (Portland).

Merrill, W., Cowling, E.B., 1966. Role of nitrogen in wood deterioration. IV. Relationship of natural variation in nitrogen content of wood to its susceptibility to decay. Phytopathology 56, 1324–1325.

Myers, R.T., Zak, D.R., White, D.C., Peacock, A., 2001. Landscape-level patterns of microbial community composition and substrate use in upland forest ecosystems. Soil Sci. Soc. Am. J. 65, 359–367.

Nahidan, S., Nourbakhsh, F., Mosaddeghi, M.R., 2015. Variation of soil microbial biomass C and hydrolytic enzyme activities in a rangeland ecosystem: are slope aspect and position effective? Arch. Agron. Soil. Sci. 61, 797–811.

Ottosson, E., Nordén, J., Dahlberg, A., Edman, M., Jönsson, M., Larsson, K. H., Ovaskainen, O., 2014. Species associations during the succession of wood-inhabiting fungal communities. Fungal Ecol. 11, 17–28.

Ovaskainen, O., Schigel, D., Ali-Kovero, H., Auvinen, P., Paulin, L., Nordén, B., Nordén, J., 2013. Combining high-throughput sequencing with fruit body surveys reveals contrasting life-history strategies in fungi. ISME J. 7, 1696–1709.

Pan, Y., Birdsey, R.A., Fang, J., Houghton, R., Kauppi, P.E., Kurz, W.A., Philips, O.L., Shvidenko, A., Lewis, S.L., Canadell, J.G., Ciais, P., Jacksom, R.B., Pacala, S.W., McGuire, A.D., Piao, S., Rautiainen, A., Sitch, S., Hayes, D., 2011. A large and persistent carbon sink in the world's forests. Science 333, 988–993.

Petrillo, M., Cherubini, P., Sartori, G., Abiven, S., Ascher, J., Bertoldi, D., Camin, F., Barbero, A., Larcher, R., Egli, M., 2015. Decomposition of Norway spruce and European larch coarse woody debris (CWD) in relation to different elevation and exposure in an Alpine setting. iForest 9, 154–164.

Petrillo, M., Cherubini, P., Fravolini, G., Marchetti, M., Ascher-Jenull, J., Schärer, M., Synal, H.A., Bertoldi, D., Camin, F., Larcher, R., Egli, M., 2016. Time since death and decay rate constants of Norway spruce and European larch deadwood in subalpine forests determined using dendrochronology and radiocarbon dating. Biogeosciences 13, 1537–1552.

Prichard, S. J., Peterson, D. L., Hammer, R. D., 2000. Carbon distribution in subalpine forests and meadows of the Olympic Mountains, Washington. Soil Sci. Soc. Am. J. 64, 1834–1845.

Purahong, W., Hoppe, B., Kahl, T., Schloter, M., Schulze, E.D., Bauhus, J., Buscot, F., Krüger, D., 2014. Changes within a single land-use category alter microbial diversity and community structure: molecular evidence from wood-inhabiting fungi in forest ecosystems. J. Environ. Manag. 139, 109–119.

Purahong, W., Arnstadt, T., Kahl, T., Bauhus, J., Kellner, H., Hofrichter, M., Krüger, D., Buscot, F., Hoppe, B., 2016. Are correlations between deadwood fungal community structure, wood physico-chemical properties and lignin-modifying enzymes stable across different geographical regions? Fungal. Ecol. 22, 98–105.

Rajala, T., Peltoniemi, M., Hantula, J., Mäkipää, R., Pennanen, T., 2011. RNA reveals a succession of active fungi during the decay of Norway spruce logs. Fungal. Ecol. 4, 437–448.

Rajala, T., Peltoniemi, M., Pennanen, T., Mäkipää, R., 2012. Fungal community dynamics in relation to substrate quality of decaying Norway spruce (*Picea abies* [L.] Karst.) logs in boreal forests. FEMS Microbiol. Ecol. 81, 494–505.

Rinta-Kanto, J.M., Sinkko, H., Rajala, T., Al-Soud, W.A., Sørensen, S.J., Tamminen, M.V., Timonen, S., 2016. Natural decay process affects the abundance and community structure of Bacteria and Archaea in *Picea abies* logs. FEMS Microbiol. Ecol. 1, 231.

Risch, A. C., Jurgensen, M. F., Page-Dumroese, D. S., Schütz, M., 2013. Initial turnover rates of two standard wood substrates following land-use change in subalpine ecosystems in the Swiss Alps. Can. J. For. Res. 43, 901–910.

Rotthauwe, J.H., Witzel, K.P., Liesack, W., 1997. The ammonia monooxygenase structural gene *amoA* as a functional marker: molecular fine-scale analysis of natural ammonia-oxidizing populations. Appl. Environ. Microbiol. 63, 4704–4712.

Sidari, M., Ronzello, G., Vecchio, G., Muscolo, A., 2008. Influence of slope aspects on soil chemical and biochemical properties in a *Pinus laricio* forest ecosystem of Aspromonte (Southern Italy). Eur. J. Soil Biol. 44, 364–372.

Sinsabaugh, R.L., Lauber, C.L.,Weintraub, M.N., Ahmed, B., Allison, S.D., Crenshaw, C., Contosta, A.R., Cusack, D., Frey, S., Gallo, M.E., Gartner, T.B., Hobbie, S.E., Holland, K., Keeler, B.L., Powers, J.S., Stursova, M., Takacs-Vesbach, C., Waldrop, M.P., Wallenstein, M.D., Zak, D.R., Zeglin, L.H., 2008. Stoichiometry of soil enzyme activity at global scale. Ecol. Lett. 11, 1252–1264.

Stokland, J.N., 2001. The coarse woody debris profile: an archive of recent forest history and an important biodiversity indicator. Ecol. Bull. 49, 71–83.

Stutz, K. P., Lang, F., 2017. Potentials and Unknowns in Managing Coarse Woody Debris for Soil Functioning. Forests 8, 37.

Sun, B., Wang, X.Y., Wang, F., Jiang, Y. J., Zhang, X. X., 2013. Assessing the relative effects of geographic location and soil type on microbial communities associated with straw decomposition. Appl. Environ. Microbiol. 79, 3327–3335.

Takahashi, M., Ishizuka, S., Ugawa, S., Sakai, Y., Sakai, H., Ono, K., Hashimoto, S., Matsuura, Y., Morisada, K., 2010. Carbon stock in litter, deadwood and soil in Japan's forest sector and its comparison with carbon stock in agricultural soils. Soil Sci. Plant. Nutr. 56, 19–30.

Tatti, D., Fatton, V., Sartori, L., Gobat, J. M., Le Bayon, R. C., 2017. What does 'lignoform'really mean? Appl. Soil Ecol. DOI 10.1016/j.apsoil.2017.06.037

Treseder, K. K., Mack, M. C., Cross, A., 2004. Relationships among fires, fungi, and soil dynamics in Alaskan boreal forests. Ecol. Appl. 14, 1826–1838.

Tsui, C. C., Chen, Z. S., Hsieh, C. F., 2004. Relationships between soil properties and slope position in a lowland rain forest of southern Taiwan. Geoderma 123, 131–142.

Valášková, V., De Boer, W., Gunnewiek, P.J.K., Popíšek, M., Baldrian, P., 2009. Phylogenetic composition and properties of bacteria coexisting with the fungus *Hypholoma fasciculare* in decaying wood. ISME J. 3, 1218–1221.

Van der Wal, A., De Boer, W., Smant, W., Van Veen, J.A., 2007. Initial decay of woody fragments in soil is influenced by size, vertical position, nitrogen availability and soil origin. Plant. Soil. 301, 189–201.

Van der Wal, A., Ottosson, E., de Boer, W., 2015. Neglected role of fungal community composition in explaining variation in wood decay rates. Ecology 96, 124–133.

Wakelin, S. A., Macdonald, L. M., Rogers, S. L., Gregg, A. L., Bolger, T. P., Baldock, J. A., 2008. Habitat selective factors influencing the structural composition and functional capacity of microbial communities in agricultural soils. Soil Biol. Biochem. 40, 803–813.

Wang, J. T., Cao, P., Hu, H. W., Li, J., Han, L. L., Zhang, L. M., He, J. Z., 2015. Altitudinal distribution patterns of soil bacterial and archaeal communities along Mt. Shegyla on the Tibetan Plateau. Microbial. Ecol. 69, 135–145.

Xu, Z., Yu, G., Zhang, X., Ge, J., He, N., Wang, Q., Wang, D., 2015. The variations in soil microbial communities, enzyme activities and their relationships with soil

organic matter decomposition along the northern slope of Changbai Mountain. Appl. Soil Ecol. 86, 19–29.

Zhang, S., Chen, D., Sun, D, Wang, X., Smith, J.L., Du, G., 2012. Impacts of altitude and position on the rates of soil nitrogen mineralization and nitrification in alpine meadows on the eastern Qinghai–Tibetan Plateau, China. Biol. Fertil. Soils. 48, 393–400.

Zhang, B., Liang, C., He, H., Zhang, X., 2013. Variations in soil microbial communities and residues along an altitude gradient on the northern slope of Changbai mountain, China. PLoS ONE 8:e66184.

Yasir, M., Azhar, E.I., Khan, I., Bibi, F., Baabdullah, R., Al-Zahrani, I.A., Al-Ghamdi, A.K. 2015. Composition of soil microbiome along elevation gradients in southwestern highlands of Saudi Arabia. BMC Microbiol. 15, 65.

Yamashita, S., Masuya, H., Abe, S., Masaki, T., Okabe, K., 2015. Relationship between the decomposition process of coarse woody debris and fungal community structure as detected by high-throughput sequencing in a deciduous broad-leaved forest in Japan. PLoS ONE 10:e0131510.

II. Paper 1

Effects of slope exposure on soil physico-chemical and microbiological properties along an altitudinal climosequence in the Italian Alps

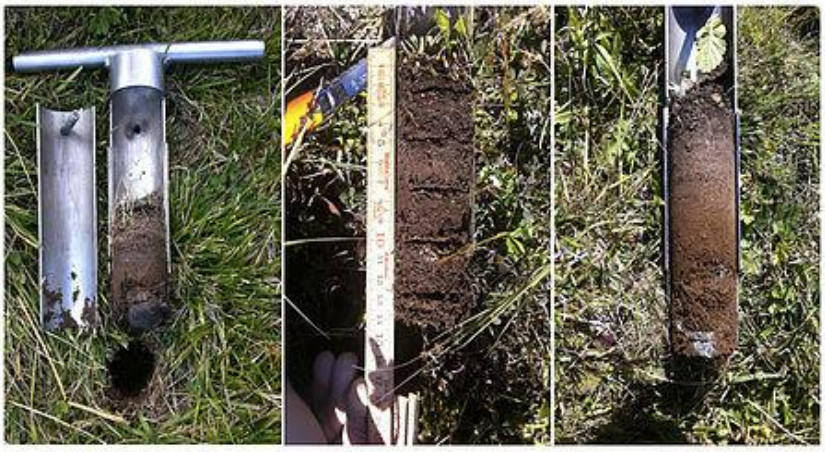

(photos by J. Ascher-Jenull)

Effects of slope exposure on soil physico-chemical and microbiological properties along an altitudinal climosequence in the Italian Alps

Tommaso Bardelli[a,b], María Gómez-Brandón[b,*], Judith Ascher-Jenull[a,b], Flavio Fornasier[c], Paola Arfaioli[a], Davide Francioli[d], Markus Egli[e], Giacomo Sartori[f], Heribert Insam[b], Giacomo Pietramellara[a]

[a]Department of Agrifood and Environmental Science, University of Florence, Piazzale delle Cascine 18, 50144 Florence, Italy

[b]Institute of Microbiology, University of Innsbruck, Technikerstraße 25d, 6020 Innsbruck, Austria

[c]Council for Research and Experimentation in Agriculture, Via Trieste 23, 34170 Gorizia, Italy

[d]Helmholtz Centre for Environmental Research-UFZ;06120; Halle (Saale), Germany

[e]Department of Geography, University of Zürich, Winterthurerstrasse 190, 8057 Zürich, Switzerland

[f]Museo delle Scienze (MUSE), Corso del Lavoro e della Scienza 3, 38122 Trento, Italy

*Corresponding author: Maria.Gomez-Brandon@uibk.ac.at

Science of the Total Environment, 1 January 2017, Volume 575, pp 1041-1055
DOI: 10.1016/j.scitotenv.2016.09.176

Contribution: T. Bardelli participated in the sampling campaign, in the experimental work including the statistical analyses, and in drafting the manuscript.

Abstract

Due to their sensitivity to changing environmental conditions sub- and alpine soils are often monitored in the context of climate change, usually, however, neglecting slope exposure. Therefore, we set up a climosequence-approach to study the effect of exposure and, in general, climate, on the microbial biomass and microbial composition and activity, comprising five pairs of north (N)- and south (S)-facing sites along an altitudinal gradient ranging from 1200 to 2400 m a.s.l. in the Italian Alps (Trentino Alto Adige, Italy). Soil physico-chemical properties were related to microbiological properties (microbial biomass: double strand DNA yield *vs.* substrate-induced respiration; community structure of bacteria, fungi and archaea: genetic fingerprinting DGGE *vs.* real-time PCR; microbial activity: basal respiration *vs.* multiple hydrolytic enzyme assays) to monitor shifts in the structure and activity of microbial communities as a function of climate and slope exposure and to evaluate the most determinant chemical parameters shaping the soil microbiota. The exposure-effect of slope exposure on several hydrolytic key-enzymes was enzyme-specific: e.g. β-glucosidase and acid phosphomonoesterase potential activities were more pronounced at the N-facing slope while the activities of alkaline phosphomonoesterase, pyrophosphate-phosphodiesterase and arylsulfatase were higher at the S-facing slope. Furthermore, the exposure-effect was domain-specific: bacteria (S > N, altitude-independent); fungi (N ~ S); and archaea (N > S; altitude-dependent). Additionally, the abiotic parameters shaping the community composition were in general depending on soil depth. Our multidisciplinary approach allowed us to survey the exposure and altitude effects on soil physico-chemical and microbiological properties and thus unravel the complex multiple edaphic factor-effects on soil biota in mountain ecosystem.

Keywords: Subalpine-alpine soils; soil texture; microbial communities; bacteria-fungi-archaea; multiple hydrolytic enzyme activities; soil depth

Highlights

- Slope aspect on microbial diversity and activity is often neglected.
- Slope exposure effect was enzyme-specific.
- Bacteria were more abundant on the south-facing slope irrespective of the altitude.
- Exposure did not significantly affect fungal abundance along the climosequence.
- Exposure effects on archaeal abundance were altitude-dependent.

Graphical Abstract

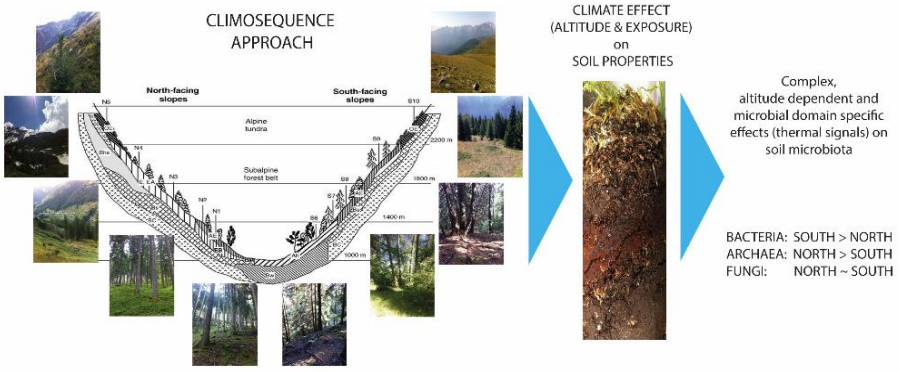

1. Introduction

The microbial response to changing climatic conditions requires further research because up to now, most studies have had a limited ability to differentiate between the complex climate effects on the soil ecosystem (Sun et al., 2013). This is partly due to its heterogeneity and discontinuity (micro-, meso-, macroscale), which makes soil a cryptic (micro)habitat even when considering the new knowledge gained from molecular screening approaches, including recent high-throughput next generation DNA sequencing (Insam et al., 2001; Nannipieri et al., 2003; Orgiazzi et al., 2015). It has been shown that thermal conditions at high altitudes and unfavourable soil conditions (e.g. very low pH in strongly leached soils) affect the structure and function of soil microbial communities (Margesin et al., 2009; Ascher et al., 2012; Zhang et al., 2013; Siles and Margesin, 2016; Siles et al., 2016). To date, however, contradictory findings have been reported on soil microbial biomass and microbial diversity along altitudinal gradients in mountain ecosystems. A decrease in bacterial and fungal biomass (assessed by phospholipid fatty acid biomarkers) with increasing altitude was observed in the Austrian Central Alps (1500 – 2530 m above sea level, a.s.l.; Margesin et al., 2009). On the contrary, Siles and Margesin (2016) found a greater bacterial and fungal biomass, using quantitative real-time PCR, as well as an increased microbial activity, assessed by basal respiration and enzymatic activities, at higher altitudes along an altitudinal gradient from 545 to 2000 m a.s.l. in the Italian Alps. Accordingly, these latter authors observed that the higher microbial abundances were significantly and positively related to an increase in the levels of soil organic matter and nutrients with altitude. This fact could be explained by the greater recalcitrance of coniferous litter, resulting in a higher C sequestration and lower nutrient immobilization rates at higher altitudes (Berger et al., 2015). Nevertheless, any clear pattern in bacterial and fungal

diversity/richness was recorded along the above-mentioned altitudinal gradient. Interestingly, Siles and Margesin (2016) observed that environmental and soil chemical properties, primarily soil pH and C/N ratio, explained the variations in microbial communities' properties better than altitude itself.

Slope aspect is considered an important topographic factor affecting local microclimate (Egli et al., 2006, 2009; Carletti et al., 2009; Barbosa et al., 2015). The amount of solar irradiation influences soil temperature, soil water retention and availability, nutrient dynamics (Carletti et al., 2009; Egli et al., 2009), composition and activity of soil microbial communities (Carletti et al., 2009; Margesin et al., 2009; Ascher et al., 2012) and soil mesofauna (Ascher et al., 2012). Therefore, we set up a climosequence approach comprising five pairs of north- and south-facing sites along an altitudinal gradient from 1200 to 2400 m a.s.l., so as to evaluate potential effects of the state factor climate (thermal conditions due to differences in exposure and altitude) on (i) microbial biomass (dsDNA content; substrate-induced respiration); (ii) microbial abundance (bacteria, fungi and archaea; real-time PCR); (iii) microbial activity (basal respiration); (iv) microbial community in terms of diversity and phylotype richness of the three microbial domains (denaturing gradient gel electrophoresis-DGGE genetic fingerprinting); and (v) multiple hydrolytic enzyme activities involved in the C, N, P and S cycles. We also assessed how these microbial properties vary within the topsoil (0 – 5, 5 – 10 and 10 – 15 cm) and, in addition, which physico-chemical factors are the most important drivers for soil microbial diversity along the climosequence scenario.

We hypothesised that: (1) soils at lower elevations and south exposure provide favourable climatic conditions for the autochthonous soil microbiota (higher biomass and activity); (2) the abundance, richness and

diversity of the three microbial domains – bacteria, fungi and archaea – will be affected by the slope exposure, and this exposure-effect will be dependent on the altitude; (3) the climate effects will be more pronounced in the uppermost topsoil-layer due to its direct exposure.

2. Material and Methods

2.1. Study area and soil sampling

The study area is located in Val di Rabbi (Trentino) in the south Alpine belt in northern Italy. The area was chosen due to (i) its situation in-between a rather warm Insubrien and a cold Alpine climate; (ii) the general suitability of the sites (accessibility of north- and south-facing sites at different altitudes); and (iii) the comprehensive database about soils and GIS data. A detailed map of the study area is given in Egli et al. (2006). The ten selected sites were located between 1200 and 2400 m a.s.l., five sites at north- (N_{1-5}) and five sites at south-facing (S_{6-10}) slopes (Fig. 1, Table 1), and were sampled in August 2012. To allow the comparison among soils collected on N- and S-facing slopes, the altitudes of the sites on both slopes were selected to be as similar as possible. We selected old-growth forest sites and natural grasslands to minimise the influence of human activities and the grazing by livestock. Overall, all the sites were located in catchments with acidic paragneiss or morainic material consisting of acidic paragneiss (Egli et al., 2006; Table 1), and the soils were classified as Cambisols to Umbrisols or Podzols (WRB, 2014; Table 1). In Val di Rabbi the mean annual temperature ranges from 8.2 (valley floor) to around 0 °C (at 2400 m a.s.l.), whereas the mean annual precipitation ranges from 800 to 1300 mm/year (Sboarina and Cescatti, 2004; Table 1). Three independent plots (5 × 5 m) placed at ± 50 m a.s.l. from each other were selected in each of the 10 main study sites and five soil sub-samples were randomly taken in each plot in 5 cm depth intervals starting at the top of the organic layer (0 – 5, 5 – 10 and

10 – 15 cm), using a corer device (ø 5 cm; 5 cm correspond to 100 cm^3). The soil horizon profile description for each soil depth (0 – 5 cm, OL + OF + OH; 5 – 10 cm, OH + A + Bs; 10 – 15 cm, Bs) was performed directly in the field according to the classification key proposed by Zanella et al. (2011), the Guidelines for Soil Description (FAO, 2006) and the German soil classification system (Ad-hoc-AG Boden, 2005). A total of 450 soil samples (10 sites × 3 plots × 5 sub-samples × 3 soil depths) were placed in polyethylene bags and transported on ice to the laboratory. They were sieved (< 2 mm), carefully separated from root fragments and stones, and kept at 4 °C for physico-chemical analyses and at -20 °C for molecular analyses, respectively.

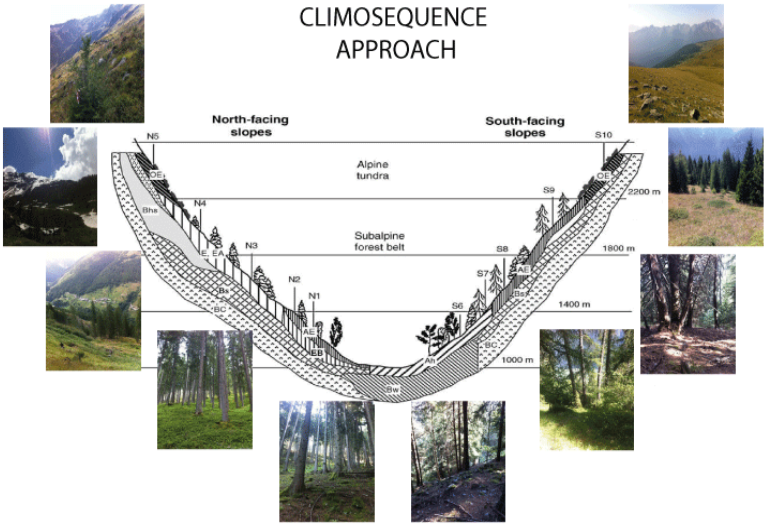

Fig. 1. Overview of the study area comprising five pairs of north (N_1-N_5) and south (S_6-S_{10})-facing sites along an altitudinal gradient from 1200 to 2400 m a.s.l. in the Italian Alps (Trentino Alto Adige, Italy). The photos (J. Ascher-Jenull) were assembled by T. Bardelli on the modified scheme of Egli et al. (2006).

Table 1.

Characteristics of the ten study sites at north-and south-facing slopes (N_{1-5} and S_{6-10}, respectively) in Val di Rabbi (Egli et al., 2006; Petrillo et al., 2015).

Sites	Altitude (m a.s.l.)	Aspect (°N)	Slope (°)	MAP (nmy^{-1})	MAAT (° C)	MAST (° C)	Parent material	Dominating tree species	Land use	Soil classification (WRB)
N_1	1180	340	31	950	5.6	7.3	Paragneiss debris	*Picea abies*	Natural forest (ecological forestry)	Chromi-Episkeletic Cambisol (Dystric)
S_6	1185	160	31	950	7.6	8.1	Paragneiss debris	*Picea abies*	Ex-coppice, natural forest (ecological forestry)	Episkeleti-Endoleptic Cambisol (Chromi-Dystric)
N_2	1390	0	28	1000	4.6	6.3	Paragneiss debris	*Picea abies*	Natural forest (ecological forestry)	Chromi-Episkeletic Cambisol (Dystric)
S_7	1400	145	33	1000	6.6	8.7	Paragneiss debris	*Larix decidua*	Natural forest (ecological forestry)	Dystri-Endoskeletic Cambisol
N_3	1620	0	29	1060	3.5	5.8	Paragneiss debris	*Picea abies*	Natural forest (ecological forestry)	Chromi-Endoskeletic Cambisol (Dystric)
S_8	1660	210	33	1060	5.5	6.0	Paragneiss debris	*Picea abies*	Natural forest (ecological forestry)	Skeletic Umbrisol
N_4	1930	20	12	1180	1.4	5.0	Paragneiss debris, Moraine material	*Larix decidua*	Originally used as pasture	Episkeletic Podzol
S_9	1995	160	25	1180	3.4	6.4	Paragneiss debris	*Larix decidua*	Ex-pasture, natural forest (ecological forestry)	Skeletic Umbrisol
N_5	2390	30	25	1300	-1.0	2.2	Paragneiss debris	*Rhododendro-vaccinietum*	Natural grassland and shrubs	Enti-Umbric Podzol (Episkeletic)
S_{10}	2420	190	28	1300	1.0	4.5	Paragneiss debris	*Festuca spp.*	Natural grassland	Dystri-Epileptic Cambisol

MAP = mean annual precipitation; MAAT = mean annual air temperature (Sboarina and Cescatti, 2004); MAST = mean annual soil temperature.

2.2. Physico-chemical analyses

The volatile solids content was determined from the weight loss following ignition in a muffle furnace (Carbolite, CWF 1000) at 550 °C for 5 h. Total C and N contents were analysed in dried samples, using a CN analyser (TruSpec CHN; LECO, Michigan, U.S.A.). Particle-size analysis was assessed following the pipette procedure according to Indorante et al. (1990). Soil bulk density was determined according to Grossman and Reinsch (2002). Electrical conductivity (EC) and pH were determined in soil:distilled water extracts (1:10, w/v) by using a conductivity Meter LF 330 WTW (Weilheim, Germany) and a pH Meter Metrohm 744, respectively. Inorganic nitrogen (NH_4^+ and NO_3^-) was measured in 0.0125 M $CaCl_2$ extracts, as described by Kandeler (1993a,b).

2.3. Soil enzymes activities

Eight hydrolytic enzymes involved in the principal nutrient cycles were determined, namely: (i) C-cycle: β-glucosidase (*gluc*), acetate esterase (*ester*); (ii) N-cycle: chitinase (*chit*), leucine-aminopeptidase (*leu*), (iii) P-cycle: acid (*acP*)- and alkaline phosphomonoesterases (*alkP*), pyrophosphate-phosphodiesterase (*piroP*); (iv) S-cycle: arylsulphatase (*arylS*). All of the potential enzymatic activities were measured in duplicate from all the soil samples by a heteromolecular exchange procedure (Fornasier and Margon, 2007), using a 3% solution of lysozyme as desorbant and bead-beating to disrupt soil aggregates and microbial cells. Briefly, 0.4 g of soil (fw) were placed into 2-mL microcentrifuge tubes, together with 1.4 mL of a solution containing 3% lysozyme and glass beads. The tubes were then subjected to bead-beating using a Retsch 400 beating mill at 30 strokes s^{-1} for 3 min, followed by centrifugation at 20,000 g for 5 min. The supernatant containing desorbed enzymes was dispensed into 384-well white microplates with the appropriate buffer to fluorometrically quantify the enzymatic

activities using fluorescent, 4-methyl-umbelliferyl- (MUF) and 4-amido-7-methyl-coumarine (AMC) substrates. All measurements were done in duplicate and the activities were expressed as nanomoles of MUF (or AMC) min^{-1} g^{-1} dry soil.

2.4. MicroResp

Basal respiration (BR) and substrate-induced respiration (SIR) were assessed as CO_2 evolution by using the micro-respiration technique (MicroRespTM) (Campbell et al., 2003). Briefly, soil samples were placed into a deep-well microplate, the moisture content was adjusted to 60% of their water holding capacity. BR was measured in wells with only deionised water added (25 µL); whilst SIR was determined by adding glucose (1% dry matter basis), applied in a volume of 25 µL. Two technical replicates were run for each field replicate. The absorbance was measured twice at 590 nm (Zenyth 3100, Anthos, Eugendorf, Austria), one immediately prior to sealing the soil microplate, and the other one at the end of 6 h incubation at 25 °C. Absorbance values were converted to CO_2 concentration, using a standard calibration curve as described by Campbell et al. (2003) and Lalor et al. (2007) and CO_2 evolution from individual wells was determined.

2.5. Molecular analyses

2.5.1. Soil microbial biomass index (dsDNA)

Whole community DNA was extracted from soil samples (0.5 g, fw) by mechanical cell disruption (bead-beating) in presence of a sodium phosphate buffer (0.12 M, pH 8 Na_2HPO_4), and *crude* (not purified) double strand DNA (dsDNA) was directly quantified by using PicoGreen fluorescent dye (Life Technologies) as described in Fornasier et al. (2014).

2.5.2. DNA extraction

Whole-community DNA was extracted from soil samples (0.5 g, fw) and purified by using a commercial kit (FastDNA Kit for Soil, MP-Biomedicals) as described in Ascher et al. (2009). DNA was qualitatively characterised by agarose gel electrophoresis (1X Tris Acetate-EDTA buffer; 1:10000 EtBr; 0.8% w/v; 100V 60 min) to assess the molecular weight and fragment length distribution in comparison to a DNA Mass Ladder Mix (Fermentas, 80-20,000 bp). The concentration of DNA was assessed using two quantification methods, namely via fluorometric (Quant-iT PicoGreen; specific for dsDNA) and spectrophotometric (Picodrop; DNA absorbance at 260 nm) measurements.

2.5.3. Denaturing gradient gel electrophoresis (PCR-DGGE)

Microbial community level endpoint PCR was performed with 1 μL DNA in 25 μL solution containing a final concentration of 2X MyTaq reaction buffer (Bioline GmbH, Germany); 0.2 μM of each primer to target bacteria (968f-GC/UNI1401r; Nübel et al., 1996), fungi (FF390/FR1-GC; Vainio and Hantula, 2000) and archaea (Parch519f-GC/Arc915r; Coolen et al., 2004); 0.4 mg mL^{-1} bovine serum albumin (BSA; Sigma, Austria); 10 mM TMAC (tetramethylammonium chloride); 1X Enhancer (VWR Internation GmbH, Germany); 0.035 U MyTaq DNA polymerase (Bioline GmbH, Germany), and distilled water (RNase/DNase free, Gibco™, UK). The PCR amplification of SSU rDNA targets of the three domains — bacteria, fungi and archaea — was performed following the cycling conditions described by Ascher et al. (2012), Shemekite et al. (2014), and Coolen et al. (2004), respectively. Proper sizes of amplification products were verified by electrophoresis on 1% agarose gels. The gel electrophoresis was performed by loading 60 ng of PCR products in an 8% (w/v) polyacrylamide gel as described by Shemekite et al. (2014). A denaturing gradient of 40 – 70% and

30 – 65% was used for bacteria and for fungi and archaea, respectively. GeneRuler 1 kb DNA ladder (Fermentas, Life Technology) served as marker. Gels were run in an INGENYphorU System (Ingeny International BV, The Netherlands) at a constant temperature (60 °C) and voltage (100 V) for 16 h. Gels were stained with silver nitrate using the Hoefer Automated Gel Stainer (Amersham Pharmacia Biotech, Germany), air dried and scanned for subsequent image analysis. Similarities among microbial communities as a function of exposure and soil depth were assessed by UPGMA (unweighted pair group method with arithmetic mean) cluster analyses based on Dice similarity coefficients (Dice, 1945) using the Quantity One 4.5.1 software (Bio-Rad) according to Ascher et al. (2012). Pairwise comparisons of prominent microbial community members/populations based on absence or presence of unique and shared DGGE bands were assessed and the resulting similarities (%) in microbial community structures among the studied soils were visualized by dendrograms. The phylotype richness of the bacterial, fungal and archaeal communities was determined as the number of bands within the DGGE gels. The Shannon's diversity index (H') was calculated as formulated by Eichner et al. (1999), using the following equation:

$$H' = -\sum p_i \ln p_i$$

where p_i expresses the proportional number in a specific group relative to the total number.

2.5.4. Quantitative real-time PCR

Quantitative real-time PCR (qPCR) analysis was performed to determine the 16S rRNA gene copy number of bacteria and archaea, and the 18S rRNA gene copy number of fungi. Real-time PCR was performed with the 1X Sensimix™ SYBR® Hi-rox (Bioline, USA) based on the DNA-intercalating dye SYBR Green I. The Rotorgene 6000 Real Time Thermal Cycler

(Corbett Research, Sydney, Australia) was used in combination with the Rotor-Gene Series Software 1.7. Standard curves were constructed with PCR amplified 16S rDNA (bacteria and archaea) and PCR amplified 18S rDNA (fungi) according to the cycling conditions from the section 2.5.3, and by using the following pure cultures as templates: *Nitrosomonas europaea* (DSMZ 21879) as bacteria, *Methanobacterium formicicum* (DSMZ 1535) as archaea and *Fusarium solani* (DSMZ 10696) as fungi. The primer sets used for qPCR were as follows: 1055f/1392r (bacteria, Ferris et al., 1996), FF390/FR1 (fungi, Prévost-Bouré et al., 2011), Parch519f/Arc915r (archaea, Coolen et al., 2004). Stock concentration [gene copies μL^{-1}] was determined via PicoGreen measurement and freshly prepared for each run. Ten-fold dilutions were used for standard curve construction. The reactions were performed in 20 µL assays with each reaction mix containing 1X Sensimix™ SYBR® Hi-rox (Bioline, USA), forward and reverse primers (200 nM each primer), 0.4 mg mL^{-1} BSA, distilled water (RNase/DNase free, Gibco™, UK) and 2 µL of either 1:10 diluted DNA-extract, and ten-fold diluted standard DNA. All the standards and samples were run in duplicate. After an initial denaturation at 94 °C (bacteria and archaea) and 95 °C (fungi) for 10 min, thermal cycling comprised 40 cycles of 20 s at 95 °C, 15 s at 58 °C and 30 s at 72 °C for bacteria; 15 s at 95 °C, 30 s at 50 °C and 30 s at 72 °C for fungi; and 30 s at 94 °C, 40 s at 57 °C and 30 s at 72 °C for archaea. To check for product specificity and potential primer dimer formation, runs were completed with a melting analysis starting from 60 °C to 95 °C with temperature increments of 0.25 °C and a transition rate of 5 s. The purity of the amplified products was further checked by the presence of a single band of the expected length on a 1% agarose gel stained with the DNA stain Midori Green (Nippon Genetics, Germany) via UV-transillumination (Vilber Lourmat Deutschland GmbH).

2.6. Statistical analyses

Statistical analyses were performed with Statistica 9 (StatSoft, USA). A factorial analysis of variance (ANOVA) was done to evaluate the effects of exposure (north *vs.* south) and soil depth (0 – 5, 5 – 10 and 10 – 15 cm) on the physico-chemical and microbiological parameters along the climosequence. Normality and variance homogeneity of the dataset were tested prior to ANOVA by using the Shapiro–Wilk and Levene´s tests, respectively. Before analysis, data were log- or square root-transformed to meet the assumptions for ANOVA. Significant differences ($p < 0.05$) in the main effects were further analysed by paired comparisons with the Tukey HSD test. This post hoc test also allowed us to determine whether the exposure effects were more pronounced in the uppermost topsoil-layer by comparing the three different soil layers (i.e., 0 – 5, 5 – 10, 10 – 15 cm) from the north-facing slopes with those from the corresponding south-facing slope. Associations between the potential enzymatic activities and the principal chemical and microbiological variables were explored using Pearson's correlation. Non-metric multidimensional scaling (NMDS) based on Bray-Curtis distance was carried out using the software PAST to visualize the patterns of bacterial, fungal and archaeal communities along the climosequence. A model of multivariate analysis of variance was constructed using distance-based redundancy analysis (dbRDA) based on the Bray-Curtis distance to determine the environmental variables that were most influential on the bacterial, fungal and archaeal community compositions. Marginal tests were performed to determine the amounts of variation explained by the selected variables. Significance tests were performed through nonparametric permutation, which does not rely on the assumption of multivariate normality (Taylor et al., 2009).

3. Results

To assess the exposure effects (N *vs.* S), the results obtained from the climosequence approach were principally evaluated by pairwise comparison of the sites located at similar altitudes (Figure 1, Table 1).

3.1 Physico-chemical analyses

An overview of the physico-chemical parameters as a function of the slope exposure and soil depth along the climosequence is given in Table 2. The output of factorial ANOVA with regard to the different experimental factors is shown in Table 4. Slope exposure had a significant impact on the percentage of volatile solids assessed as an estimation of the soil organic matter (SOM) content (Table 4), with higher values on north- than south-facing sites along the altitudinal gradient. This trend is in line with previous studies in the Trentino area (Egli et al., 2006, 2009; Ascher et al., 2012; Nahidan et al., 2015). This parameter decreased significantly with increasing soil depth (Table 4), with the highest OM content in the 0 – 5 cm soil layer in both slope exposures. Accordingly, we observed that the soil bulk density was significantly higher on the south- than on the north-facing sites between 1200 and 1600 m a.s.l. (Table 4), reflecting the SOM content (assessed as volatile solids; N > S; Table 2); whilst at the highest altitudes no differences were found, resulting in a significant interaction between exposure and altitude (Table 4). The ten study sites were silty-sandy or sandy-silty soils according to the particle-size analysis. As described by Egli et al. (2006, 2010), the cooler and more acidic conditions gave rise to more pronounced weathering processes and increased clay minerals formation at the north-facing sites. Moreover, the clays were found to be negatively correlated to soil pH which indicates that N-facing slopes are often related to more acidic environments (Carletti et al., 2009; Begum et al., 2010). Additionally, due to the accumulation of often weakly-degraded OM on N slopes, more –

COOH and –OH functional groups or phenolic compounds are present (Egli et al., 2009). As such, we found that soil acidity (pH) varied significantly with slope exposure (Table 4), with lower values in north- than in south-facing sites. In accordance with previous studies (Nahidan et al., 2015), the north-facing slopes were characterised by greater EC levels (Table 4), with two times higher values in soils from the north-facing sites between 1600 and 2000 m a.s.l. A plausible explanation could be that the higher OM content results in a higher soil cation exchange capacity and hence increased EC values. Moreover, as shown by Smith et al. (2002) nitrate content could also contribute to increase the EC levels. In fact, the greatest differences in the NO_3^- content with respect to exposure (12 times higher on the N- than on the S-slope) were recorded for the altitude of 2000 m a.s.l. This was also supported by a positive correlation between EC and NO_3^- content ($R = 0.821$, $p < 0.001$). In both slopes, a significant diminution of EC was found with the soil depth (Table 4), with greater levels in the 0 – 5 cm soil layer, being three and four times higher than in the 5 – 10 and 10 – 15 cm layers, respectively. The total C content was statistically higher (2 – 3 times) on north- than on south-facing sites between 1200 and 1600 m a.s.l. (Table 4). However, no exposure effects were found for the higher altitudes (2000 and 2400 m a.s.l.), leading to a significant interaction between exposure and altitude (Table 4). Similar trends regarding the slope exposure were found for total N and C:N ratio (Table 4). A significant decrease in this ratio was found with soil depth in both slopes (Table 4). Previous works reported a higher inorganic N pool at the south-facing slopes (Zhang et al., 2012 and Nahidan et al., 2015). Nonetheless, in our study higher NH_4^+ concentrations were recorded in soils on north-facing sites (1 – 4 times higher) between 1200 and 2000 m a.s.l. (Table 2), while on the highest sites the NH_4^+ levels were greater on south exposure resulting in a significant interaction between both exposure and altitude (Table 4). A similar pattern was observed for

NO_3^- content (Table 4), and 12 times higher NO_3^- levels were registered on the north-than on the south-facing soils at 2000 m a.s.l. (Table 2). Overall, both NH_4^+ and NO_3^- levels were significantly higher in the top 5 cm (Table 4).

Table 2.

Physico-chemical properties of the soils collected at the ten study sites at north-and south-facing areas ($N_{1\text{-}5}$ and $S_{6\text{-}10}$, respectively). The results are shown pairwise, i.e., the couples of north- and south-facing sites at the same elevation (N_1-S_6; N_2-S_7; N_3-S_8; N_4-S_9; N_5-S_{10}), so as to evaluate the exposure-effect. Values are means (n=3) with the standard deviations in brackets. Data are expressed on a dry weight basis. Different font of letters discriminate among the three soil depths (0-5 cm, bold type; 5-10 cm, gray; 10-15 cm, italics) and different letters, in each of the soil depths, indicate significant differences ($p < 0.05$; ANOVA followed by Tukey post-hoc test) in function of the exposure-effect.

Sites	Soil depth (cm)	Volatile solids (%)	Bulk density (g/cm³)	Soil moisture (%)	Sand (%)	Silt (%)	Clay (%)	pH	Electrical Conductivity (µS cm⁻¹)	Total C (%)	Total N (%)	C/N	NH_4^+ (mg kg⁻¹ dw)	NO_3^- (mg kg⁻¹ dw)
N_1	0-5	47.7 (5.7) **bc**	0.25 (0.1) **bc**	33.6 (8.6) **de**	59 (5.9) **ab**	26 (5.0) **a**	15 (1.1) **bcd**	4.8 (0.4) **ab**	81.3 (22.3) **bc**	24.6 (2.4) **b**	0.9 (0.2) **bc**	26.9 (3.9) **a**	45.3 (12.7) **bc**	24.3 (4.3) **bc**
	5-10	22.2 (11.5) bc	0.91 (0.2) b	13.7 (4.9) c	45 (3.5) ab	34 (1.2) ab	20 (3.5) ab	4.8 (0.4) bcd	39.2 (5.2) bcd	10.6 (6.2) bc	0.5 (0.3) cd	20.6 (2.2) ab	29.4 (5.0) bcd	11.7 (7.5) b
	10-15	11.0 (2.1) *b*	0.97 (0.1) *bc*	14.5 (1.5) *c*	51 (7.2) *abc*	35 (3.9) *abc*	14 (5.1) *ab*	4.8 (0.3) *bcd*	27.8 (4.5) *bc*	4.4 (1.9) *b*	0.3 (0.1) *b*	18.1 (3.7) *abc*	17.0 (6.8) *b*	2.2 (0.8) *b*
S_6	0-5	21.4 (7.2) **d**	0.70 (0.1) **a**	22.0 (4.1) **e**	56 (4.2) **ab**	30 (2.1) **a**	14 (2.1) **bcd**	6.0 (0.5) **a**	84.1 (2.5) **bc**	10.2 (3.7) **c**	0.5 (0.1) **c**	19.9 (3.3) **abc**	25.3 (5.2) **c**	7.3 (1.0) **c**
	5-10	9.3 (1.3) c	1.37 (0.1) a	10.9 (1.0) c	56 (5.1) ab	30 (3.3) ab	13 (1.8) ab	5.7 (0.6) a	40.5 (27.5) bcd	4.0 (0.5) c	0.2 (0.04) d	17.4 (2.8) bc	13.7 (7.0) d	3.2 (0.8) b
	10-15	6.5 (1.7) *b*	1.52 (0.1) *a*	11.5 (1.4) *c*	57 (6.5) *ab*	30 (4.9) *bc*	13 (1.6) *ab*	5.6 (0.5) *ab*	19.8 (11.6) *bc*	2.6 (0.8) *b*	0.2 (0.03) *b*	15.4 (1.9) *abc*	6.7 (1.6) *b*	3.1 (0.2) *b*
N_2	0-5	86.8 (5.2) **a**	0.15 (0.04) **c**	70.4 (6.2) **a**	46 (12.3) **ab**	33 (9.0) **a**	21 (4.4) **abc**	4.7 (0.8) **b**	169.3 (10.8) **ab**	42.8 (9.8) **a**	1.8 (0.2) **ab**	23.8 (4.2) **ab**	49.5 (8.2) **bc**	51.5 (19.7) **ab**
	5-10	58.2 (16.7) a	0.78 (0.3) bc	39.4 (10.0) ab	45 (6.5) ab	33 (8.7) ab	22 (3.1) ab	4.3 (0.6) cd	87.9 (15.5) a	33.1 (13.5) a	1.3 (0.4) ab	24.8 (4.0) a	61.5 (31.7) bc	12.1 (8.6) b
	10-15	25.5 (17.3) *ab*	0.93 (0.2) *bc*	28.1 (7.1) *b*	38 (1.6) *d*	43 (0.6) *ab*	19 (1.6) *ab*	4.5 (0.6) *cd*	45.3 (26.5) *ab*	11.3 (8.4) *ab*	0.5 (0.4) *ab*	20.0 (1.8) *ab*	24.1 (5.9) *ab*	4.4 (0.8) *b*
S_7	0-5	51.0 (0.1) **bc**	0.31 (0.2) **bc**	19.5 (3.4) **e**	57 (10.0) **ab**	34 (10.7) **a**	13 (0.7) **cd**	5.7 (0.2) **ab**	178.0 (110.0) **a**	23.1 (1.0) **b**	1.3 (0.1) **abc**	18.1 (2.0) **bc**	65.5 (33.6) **bc**	26.9 (15.3) **bc**
	5-10	21.0 (1.9) bc	0.61 (0.05) cd	14.7 (1.4) c	58 (3.9) ab	29 (4.8) ab	13 (0.9) ab	5.8 (0.2) a	46.9 (21.2) b	9.0 (2.3) bc	0.6 (0.2) cd	15.9 (1.5) bc	17.4 (2.8) cd	5.9 (4.2) b
	10-15	14.6 (4.3) *ab*	1.18 (0.05) *ab*	15.7 (2.0) *c*	59 (1.7) *a*	32 (5.6) *abc*	8 (4.6) *b*	5.8 (0.3) *a*	28.8 (8.1) *bc*	5.6 (1.6) *b*	0.4 (0.1) *ab*	14.9 (2.0) *abc*	9.5 (1.2) *b*	3.4 (0.2) *b*
N_3	0-5	83.8 (3.9) **a**	0.17 (0.1) **c**	71.5 (5.8) **a**	51 (13.8) **ab**	31 (4.8) **a**	18 (14.8) **abcd**	4.6 (0.3) **b**	184.9 (36.4) **a**	46.3 (2.3) **a**	2.1 (0.2) **a**	22.5 (2.2) **abc**	170.1 (22.3) **a**	38.5 (13.1) **bc**
	5-10	69.7 (22.1) a	0.33 (0.2) d	60.7 (20.4) a	37 (13.2) b	45 (12.7) a	18 (7.3) ab	4.2 (0.2) d	90.3 (26.8) a	38.7 (12.9) a	1.8 (0.7) a	22.0 (2.3) ab	113.9 (21.5) a	7.1 (4.6) b
	10-15	33.5 (7.4) *a*	0.84 (0.07) *bc*	30.2 (6.4) *b*	41 (11.2) *cd*	46 (15.0) *a*	13 (4.2) *ab*	4.2 (0.3) *d*	64.7 (12.9) *a*	18.8 (8.1) *a*	0.9 (0.4) *a*	21.1 (1.8) *a*	53.1 (17.5) *a*	1.5 (0.05) *b*
S_8	0-5	60.5 (16.6) **b**	0.41 (0.1) **abc**	30.2 (1.2) **de**	60 (3.9) **ab**	21 (11.1) **a**	19 (8.5) **abcd**	5.4 (0.4) **ab**	164.1 (108.3) **ab**	24.0 (11.4) **b**	1.1 (0.5) **bc**	21.0 (0.8) **abc**	53.9 (29.3) **bc**	20.2 (5.7) **bc**
	5-10	19.8 (6.7) bc	0.69 (0.1) bc	19.3 (5.7) bc	48 (8.9) ab	36 (6.4) ab	16 (3.1) ab	5.4 (0.2) ab	31.3 (15.3) bcd	10.1 (5.9) bc	0.6 (0.4) cd	16.7 (2.0) bc	23.2 (11.3) cd	2.2 (2.3) b
	10-15	17.3 (4.7) *ab*	0.89 (0.2) *bc*	17.5 (6.2) *c*	35 (10.4) *d*	46 (12.0) *ab*	20 (1.6) *ab*	5.4 (0.3) *abc*	25.5 (8.5) *bc*	6.1 (0.5) *b*	0.4 (0.1) *ab*	14.2 (1.7) *abc*	10.1 (1.0) *b*	1.1 (0.05) *b*

Table 2.

Continued

Sites	Soil depth (cm)	Volatile solids (%)	Bulk density (g/cm³)	Soil moisture (%)	Sand (%)	Silt (%)	Clay (%)	pH	Electrical Conductivity (µS cm⁻¹)	Total C (%)	Total N (%)	C/N	NH_4^+ (mg kg⁻¹ dw)	NO_3^- (mg kg⁻¹ dw)
N_4	0-5	44.9 (19.3) **bc**	0.39 (0.09) **bc**	58.3 (2.5) **ab**	68 (7.2) **a**	22 (3.2) **a**	10 (4.4) **d**	5.2 (0.4) **ab**	110.4 (33.8) **abc**	20.7 (9.4) **bc**	1.3 (0.6) **abc**	15.9 (4.4) **bc**	142.4 (53.7) **a**	79.4 (23.3) **a**
	5-10	22.7 (11.1) bc	0.91 (0.07) b	38.5 (4.4) ab	67 (12.7) a	23 (6.8) b	10 (6.4) b	4.8 (0.2) bcd	43.0 (2.8) bc	11.6 (7.1) bc	0.9 (0.5) bc	12.4 (1.8) c	71.2 (11.6) ab	42.6 (14.9) a
	10-15	15.5 (5.6) *ab*	0.92 (0.09) *bc*	35.2 (3.7) *ab*	61 (9.6) *a*	25 (2.7) *c*	14 (11.7) *ab*	4.8 (0.2) *bcd*	34.9 (6.6) *abc*	6.9 (3.1) *b*	0.5 (0.2) *ab*	12.7 (2.8) *c*	25.6 (11.3) *ab*	36.0 (9.6) *a*
S_9	0-5	36.6 (1.3) **cd**	0.48 (0.05) **ab**	40.3 (3.0) **cd**	37 (8.7) **b**	37 (6.7) **a**	26 (2.0) **a**	5.4 (0.1) **ab**	51.2 (8.1) **c**	19.2 (1.0) **bc**	1.3 (0.1) **abc**	14.8 (0.7) **c**	36.9 (4.9) **c**	9.5 (2.2) **c**
	5-10	21.3 (1.6) bc	0.60 (0.05) cd	38.0 (2.9) ab	39 (7.5) b	36 (6.7) ab	24 (1.8) a	5.1 (0.1) abc	20.1 (1.2) bcd	10.7 (1.2) bc	0.8 (0.1) bcd	14.0 (0.4) c	39.0 (19.2) bcd	2.5 (0.8) b
	10-15	16.0 (2.3) *ab*	0.84 (0.04) *bc*	36.6 (1.1) *ab*	45 (6.5) *bcd*	26 (16.6) *c*	29 (12.1) *a*	5.3 (0.1) *abc*	14.4 (1.7) *bc*	7.1 (0.8) *ab*	0.5 (0.1) *ab*	13.7 (1.4) *bc*	32.0 (9.4) *ab*	1.6 (0.03) *b*
N_5	0-5	49.8 (13.1) **bc**	0.35 (0.1) **bc**	54.1 (5.8) **bc**	50 (10.7) **ab**	28 (8.8) **a**	21 (2.3) **abc**	4.9 (0.2) **ab**	37.2 (8.8) **c**	27.3 (8.0) **b**	1.5 (0.3) **ab**	18.4 (1.8) **bc**	50.5 (19.6) **bc**	12.6 (6.4) **c**
	5-10	29.9 (8.3) b	0.74 (0.2) bc	42.4 (5.5) a	53 (2.4) ab	29 (1.6) ab	18 (1.3) ab	4.9 (0.1) abcd	15.3 (6.6) d	16.3 (5.6) b	0.8 (0.2) bcd	20.7 (1.4) ab	32.3 (20.1) bcd	4.2 (1.6) b
	10-15	19.7 (3.0) *ab*	0.65 (0.2) *c*	40.2 (11.9) *a*	57 (6.6) *ab*	26 (4.1) *c*	17 (3.2) *ab*	4.9 (0.1) *abcd*	9.2 (1.2) *c*	10.8 (1.5) *ab*	0.5 (0.04) *ab*	20.0 (2.4) *ab*	13.6 (5.3) *b*	3.3 (0.1) *b*
S_{10}	0-5	36.5 (5.1) **cd**	0.40 (0.1) **abc**	53.5 (5.2) **bc**	49 (11.6) **ab**	28 (3.9) **a**	24 (7.7) **ab**	5.1 (0.2) **ab**	45.5 (7.3) **c**	20.7 (2.3) **bc**	1.3 (0.2) **abc**	16.3 (0.4) **bc**	80.5 (17.7) **b**	15.3 (1.0) **c**
	5-10	23.4 (0.4) bc	0.52 (0.08) cd	43.8 (1.8) a	51 (5.6) ab	27 (1.4) ab	21 (4.9) ab	5.0 (0.1) abcd	19.4 (7.5) cd	11.7 (0.4) bc	0.7 (0.03) bcd	16.0 (0.7) bc	33.1 (8.2) bcd	5.5 (1.8) b
	10-15	15.4 (0.1) *ab*	0.68 (0.04) *c*	37.2 (1.5) *ab*	54 (2.1) *ab*	27 (0.7) *c*	19 (2.5) *ab*	5.1 (0.1) *abcd*	12.0 (1.2) *bc*	6.5 (0.6) *b*	0.4 (0.1) *ab*	15.7 (1.6) *abc*	23.8 (9.2) *ab*	4.8 (0.8) *b*

3.2. Enzymatic activities

An overview of the potential hydrolytic enzyme activities as a function of the slope exposure and soil depth along the climosequence is given in Figures 2 and 3. The output of factorial ANOVA with regard to the different experimental factors is shown in Table 4. The exposure-effect on β-glucosidase activity was dependent on the altitude and soil depth (Table 4). A two times higher activity was recorded for soils from the north-facing sites at an altitude of 1600 m a.s.l. and for the 5-10 and 10-15-cm soil layers (Fig. 2A); while no significant differences with exposure were found for the remaining altitudes (Fig. 2A). Moreover, a higher potential activity was found in the uppermost soil layer (0 – 5 cm), followed by the 5 – 10 cm layer, where the β-glucosidase potential activity was two times greater than in the 10 – 15 cm layer (Fig. 2A). Acetate esterase activity was not significantly affected by the slope exposure (Table 4); whereas a decrease was found with increasing soil depth, being two times higher in the 0 – 5 cm soil layer compared to 10 – 15 cm layer (Fig. 2B). Likewise, slope exposure did not significantly influence the chitinase activity (Table 4). A significant decrease with soil depth was however measured (Fig. 2C). The effect of slope exposure on the leucine-aminopeptidase activity was altitude-dependent (Table 4), thereby giving significant differences only at 1400 m a.s.l. (Fig. 2D). A significant decrease was found with soil depth on both slopes (Fig. 2D; Table 4). The acid phosphomonoesterase potential activity was significantly higher on north-facing sites, irrespective of the altitudinal gradient (Fig. 3A; Table 4). On both slopes, the three soil depths were different from each other with the highest activity in the uppermost soil layer (0 – 5 cm; Fig. 3A). Slope exposure also affected significantly the alkaline phosphomonoesterase activity (Table 4); however, this activity was two-times higher on south-facing sites along the altitudinal gradient (Fig. 3B). The highest potential activities were recorded in the uppermost soil

layer (Figs. 3A, B). The pyrophosphate-phosphodiesterase potential activity followed the same trend as that shown for the alkaline phosphomonoesterase (Table 4), with higher values on the south- than on the north-facing sites (Fig. 3C). A significant decrease was observed with soil depth on both slopes (Fig. 3C). Significant changes with exposure were recorded for arylsulphatase activity (Table 4), being one to two times higher on south-facing sites along the altitudinal gradient (Fig. 3D). Also here, a significant decrease with increasing soil depth was found on both slopes (Fig. 3D).

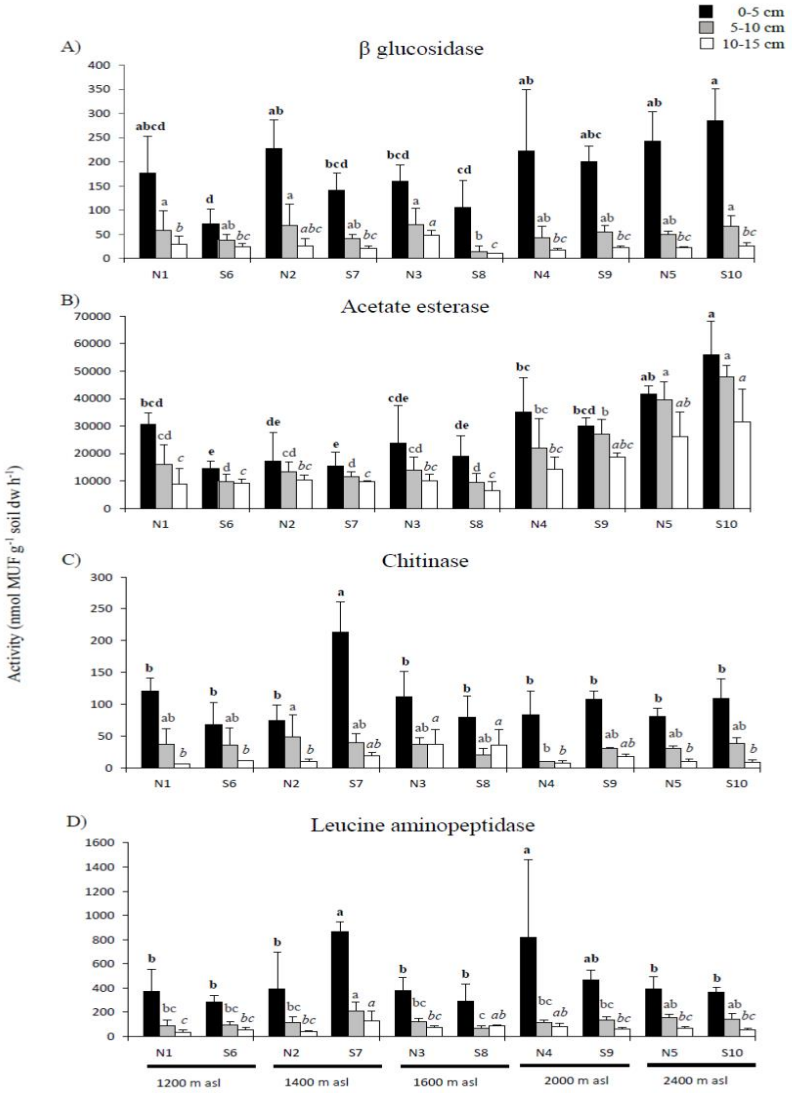

Fig. 2. Potential activities of β-glucosidase (A), acetate esterase (B), chitinase (C), leucine aminopeptidase (D) in the soils from the ten study sites at north- and south-facing areas ($N_{1\text{-}5}$ and $S_{6\text{-}10}$, respectively). The results are shown pairwise, i.e. the couples of north- and south-facing sites (N_1-S_6; N_2-S_7; N_3-S_8; N_4-S_9; N_5-S_{10}) at the same elevation (1200 m; 1400 m; 1600 m; 2000 m; 2400 m a.s.l.). Values are mean values ± standard deviation. Different font of letters discriminates among the three soil depths (0 – 5 cm, bold type; 5 – 10 cm, gray; 10 – 15 cm, italics) and different letters, in each of the soil depths, indicate significant differences ($p < 0.05$; ANOVA followed by Tukey post-hoc test) as a function of slope exposure.

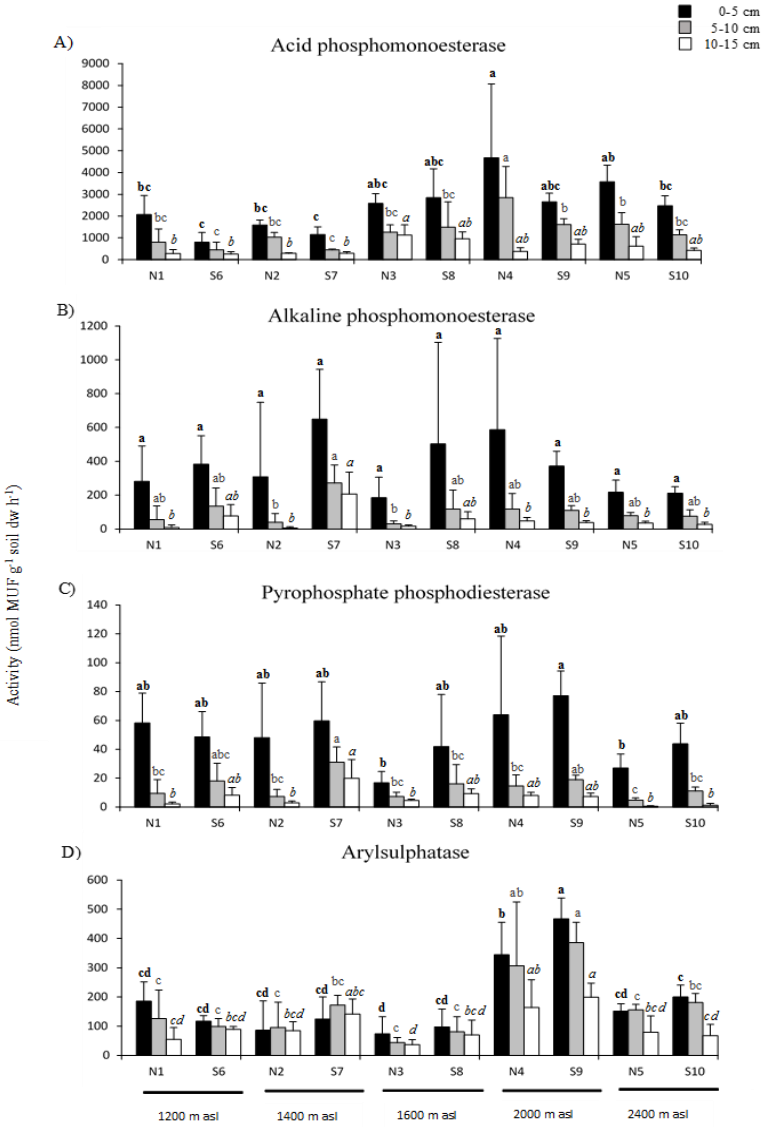

Fig. 3. Potential activities of acid-phosphomonoesterase (A), alkaline phosphomonoesterase (B), pyrophosphate phosphodiesterase (C), arylsulphatase (D) in the soils collected at the ten study sites at north- and south-facing areas ($N_{1\text{-}5}$ and $S_{6\text{-}10}$, respectively). The results are shown pairwise, i.e. the couples of north- and south-facing sites (N_1-S_6; N_2-S_7; N_3-S_8; N_4-S_9; N_5-S_{10}) at the same elevation (1200 m; 1400 m; 1600 m; 2000 m; 2400 m a.s.l.). Values are mean values ± standard deviation. Different font of letters discriminates among the three soil depths (0 – 5 cm, bold type; 5 – 10 cm, gray; 10 – 15 cm, italics) and different letters, in each of the soil depths, indicate significant differences ($p < 0.05$; ANOVA followed by Tukey post-hoc test) as a function of slope exposure.

3.3. Microbial community abundance, activity and composition

An overview of the microbial biomass, activity and abundance of the three domains (bacteria, fungi and archaea) as a function of the slope exposure and soil depth along the climosequence is given in Table 3. The output of factorial ANOVA with regard to the different experimental factors is shown in Table 4. Soil microbial biomass assessed as double-strand DNA (dsDNA) was not significantly affected by the slope exposure (Table 4). However, a significant reduction in dsDNA was observed with soil depth (Table 4), being two to three times higher in the 0 – 5 cm soil layer compared to the 10 – 15 cm layer (Table 3). In contrast, a higher amount of microbial biomass (determined by SIR) was detected on the north-facing slopes (two times higher; Tables 3 and 4) regardless of the altitude. Moreover, the highest SIR values were found in the 0 – 5 cm soil layer (Tables 3 and 4), being two to four times greater than in the 5 – 10 and 10 – 15 cm layers, respectively (Table 3). Although both methods (dsDNA *vs.* SIR) are culture-independent, the latter method probably stimulates the activity/reactivity of predominant and fast growing soil microorganisms (Lin and Brookes, 1999); whereas the dsDNA-approach proposed by Fornasier et al. (2014) directly measures the extractable DNA of the overall autochthonous soil microbiota, independent of their growth strategy (r- *vs.* k-strategists). Furthermore, the aforementioned dsDNA-method, based on the direct quantification of crude (not purified) DNA, bypasses an unavoidable DNA loss when PCR-compatible DNA is required for downstream analyses and thus, the method yields a reliable quantitative estimator of the soil microbial biomass.

Exposure also affected significantly soil microbial activity assessed as BR (Table 4) and, in general, higher values were recorded on north- than on south-facing sites along the altitudinal gradient (Tables 3). A significant

decrease in BR was observed with soil depth (Tables 3 and 4). The bacterial 16S rRNA gene copy number was significantly influenced by the slope exposure (Table 4), with higher levels at south exposure (Table 3). A decrease in bacterial abundance was found with soil depth on both slopes (Tables 3 and 4). In addition, the NMDS ordination plots and the cluster analyses based on DGGE fingerprints revealed shifts in the bacterial community diversity as a function of the slope exposure (Fig. 4A; Fig. S1). Specifically, a clear separation between north- and south-facing sites was observed along the NMDS axis 1 for the three soil depths (Fig. 4A; Table 5). Moreover, for each soil depth the ten study sites grouped distinctly along the NMDS axis 2, which indicates changes in bacterial community diversity in response to the altitude (Fig. 4A; Table 5). Among the studied physico-chemical parameters, total C content appeared to be among the most determinant factors for structuring bacterial communities in all of the three soil depths (Table 5). Soil pH and NO_3^- content also influenced bacterial communities in both the 5 – 10 and 10 – 15 cm layers (Table 5). No significant differences were found in the bacterial phylotype richness and diversity with slope exposure, irrespective of the altitudinal gradient (Table S1). However, these two indexes significantly decreased with increasing soil depth ($F_{2,60} = 11.56$, $p \leq 0.0001$; $F_{2,60} = 8.88$, $p \leq 0.0001$ respectively).

A low pH is considered physiologically disadvantageous to bacteria leading to a reduced bacterial competition and thus favouring fungal growth (Rousk et al., 2010). Bearing this in mind we could expect that the more acidic conditions at north exposure could have promoted the fungal growth leading to a higher abundance of this group in comparison to the south-facing slopes. However, exposure did not seem to have a significant impact on the fungal 18S rRNA gene copy number for any of the study sites as revealed by the qPCR approach (Tables 3 and 4).

Table 3.
Microbiological properties of the soils collected at the ten study sites at north-and south-facing areas ($N_{1\text{-}5}$ and $S_{6\text{-}10}$, respectively). The results are shown pairwise, i.e., the couples of north- and south-facing sites at the same elevation (N_1-S_6; N_2-S_7; N_3-S_8; N_4-S_9; N_5-S_{10}), so as to evaluate the exposure-effect. Values are means (n=3) with the standard deviations in brackets. Data are expressed on a dry weight basis. Different font of letters discriminate among the three soil depths (0-5 cm, bold type; 5-10 cm, gray; 10-15 cm, italics) and different letters, in each of the soil depths, indicate significant differences ($p < 0.05$; ANOVA followed by Tukey post-hoc test) in function of the exposure-effect.

Sites	Soil depth (cm)	Microbial biomass index (µg dsDNA g^{-1} soil)	Substrate-induced respiration (µg C g^{-1} h^{-1})	Basal respiration (µg C g^{-1} h^{-1})	Bacteria (gene copy number g^{-1} soil)	Fungi (gene copy number g^{-1} soil)	Archaea (gene copy number g^{-1} soil)
N_1	0-5	170.45 (23.8) **ab**	46.78 (6.5) **ab**	26.69 (3.3) **ab**	1.23E+09 (7.22E+08) **b**	3.39E+09 (4.60E+09) **a**	1.40E+08 (7.54E+07) **ab**
	5-10	90.03 (33.1) bc	27.74 (5.6) a	16.45 (3.6) ab	6.64E+08 (8.35E+07) b	2.78E+08 (1.56E+08) b	1.25E+08 (5.79E+07) abcd
	10-15	64.65 (19.0) *bcd*	18.89 (3.6) *a*	8.04 (2.7) *a*	4.44E+08 (6.10E+07) *a*	4.03E+08 (1.19E+08) *bc*	2.69E+08 (4.47E+07) *ab*
S_6	0-5	104.43 (8.2) **b**	49.56 (18.5) **a**	10.86 (7.8) **ab**	3.38E+09 (1.38E+09) **ab**	5.13E+08 (6.27E+08) **b**	1.25E+08 (9.32E+07) **abc**
	5-10	63.94 (16.8) c	15.26 (4.7) bc	13.33 (10.2) abcd	3.32E+09 (1.92E+07) ab	3.76E+08 (3.23E+08) b	1.71E+08 (5.13E+07) abc
	10-15	50.79 (10.9) *d*	6.98 (1.9) *bc*	7.74 (5.6) *a*	1.15E+09 (7.28E+08) *a*	1.09E+08 (2.62E+07) *c*	1.27E+08 (2.60E+07) *ab*
N_2	0-5	194.46 (73.5) **ab**	33.15 (5.9) **abc**	30.88 (9.9) **a**	6.17E+09 (4.92E+09) **a**	5.92E+08 (4.23E+08) **b**	7.16E+07 (5.80E+07) **abc**
	5-10	148.75 (44.9) a	20.08 (2.1) ab	17.54 (3.3) ab	4.39E+09 (3.74E+09) a	3.62E+09 (5.30E+09) a	1.47E+08 (1.03E+08) abcd
	10-15	85.55 (19.4) *ab*	8.52 (4.5) *bc*	8.39 (3.0) *a*	2.72E+09 (4.00E+09) *a*	1.49E+09 (1.03E+09) *ab*	2.20E+08 (3.76E+07) *ab*
S_7	0-5	178.27 (99.3) **ab**	15.20 (0.8) **bc**	7.32 (4.7) **b**	7.92E+09 (5.46E+09) **a**	3.62E+08 (3.07E+08) **b**	1.66E+07 (1.22E+07) **c**
	5-10	108.42 (41.5) abc	5.52 (0.6) c	7.22 (5.9) cd	3.47E+09 (2.15E+09) ab	3.13E+09 (2.12E+09) ab	4.64E+07 (3.74E+07) d
	10-15	97.92 (21.2) *a*	4.00 (1.4) *c*	6.71 (4.2) *a*	1.74E+09 (1.99E+09) *a*	2.50E+09 (7.23E+08) *a*	9.69E+07 (3.74E+07) *b*
N_3	0-5	144.46 (44.5) **ab**	46.62 (10.0) **ab**	31.10 (1.0) **a**	3.46E+09 (2.50E+09) **ab**	2.67E+08 (2.22E+08) **b**	9.18E+07 (8.62E+07) **abc**
	5-10	101.68 (14.9) abc	22.50 (11.2) ab	18.60 (8.2) a	2.75E+09 (2.01E+09) ab	3.25E+08 (1.57E+08) b	1.04E+08 (5.21E+07) bcd
	10-15	63.28 (25.4) *bcd*	8.75 (1.8) *bc*	7.41 (2.4) *a*	1.76E+09 (1.94E+09) *a*	3.67E+08 (1.84E+08) *bc*	1.49E+08 (9.04E+07) *ab*
S_8	0-5	161.37 (86.9) **ab**	26.18 (6.4) **abc**	22.49 (5.6) **ab**	4.33E+09 (7.75E+08) **ab**	2.96E+08 (2.00E+08) **b**	1.34E+08 (9.45E+07) **ab**
	5-10	93.67 (57.3) abc	6.29 (2.5) c	5.44 (1.8) cd	4.01E+09 (7.75E+08) a	5.49E+08 (1.64E+08) ab	2.11E+08 (2.51E+07) ab
	10-15	56.09 (23.0) *cd*	4.49 (0.6) *bc*	4.31 (0.5) *a*	2.45E+09 (2.28E+09) *a*	4.41E+08 (1.08E+08) *bc*	1.69E+08 (6.93E+07) *ab*

Table 3.

Continued

Sites	Soil depth (cm)	Microbial biomass index (µg dsDNA g^{-1} soil)	Substrate-induced respiration (µg C g^{-1} h^{-1})	Basal respiration (µg C g^{-1} h^{-1})	Bacteria (gene copy number g^{-1} soil)	Fungi (gene copy number g^{-1} soil)	Archaea (gene copy number g^{-1} soil)
N_4	0-5	222.32 (107.5) **a**	39.25 (21.1) **abc**	31.49 (18.2) **a**	4.65E+09 (1.32E+09) **ab**	3.48E+08 (3.18E+08) **b**	1.61E+08 (6.51E+07) **a**
	5-10	104.49 (49.1) abc	13.90 (7.8) bc	10.92 (5.3) abcd	3.39E+09 (2.13E+09) ab	1.76E+08 (8.94E+07) b	2.29E+08 (1.77E+08) a
	10-15	76.41 (27.9) *abcd*	7.75 (1.8) *bc*	6.96 (1.5) *a*	3.72E+09 (2.24E+09) *a*	7.53E+07 (5.98E+07) *c*	2.33E+08 (1.47E+08) *ab*
S_9	0-5	167.91 (6.9) **ab**	12.91 (4.6) **c**	8.93 (1.6) **ab**	5.39E+09 (2.25E+09) **ab**	1.94E+08 (2.05E+08) **b**	3.76E+07 (2.34E+07) **bc**
	5-10	123.34 (22.1) ab	5.73 (0.9) c	4.68 (0.5) d	5.04E+09 (3.68E+08) a	2.93E+08 (1.57E+08) b	6.47E+07 (2.53E+07) cd
	10-15	78.94 (11.2) *abc*	6.63 (1.3) *bc*	4.53 (0.5) *a*	4.93E+09 (5.03E+08) *a*	4.02E+08 (2.24E+08) *bc*	1.42E+08 (3.27E+07) *ab*
N_5	0-5	109.22 (11.1) **b**	39.27 (10.9) **abc**	25.70 (7.0) **ab**	5.44E+09 (1.30E+09) **ab**	4.15E+08 (1.37E+08) **b**	1.28E+08 (8.85E+07) **abc**
	5-10	80.01 (5.4) bc	20.34 (9.6) ab	13.86 (4.0) abc	4.40E+09 (1.03E+09) a	1.68E+08 (5.49E+07) b	1.20E+08 (6.82E+06) abcd
	10-15	67.84 (15.1) *bcd*	13.75 (5.9) *ab*	9.28 (2.8) *a*	2.78E+09 (1.90E+09) *a*	1.93E+08 (6.67E+07) *c*	3.09E+08 (1.17E+07) *a*
S_{10}	0-5	164.84 (48.8) **ab**	19.34 (7.4) **abc**	15.53 (5.6) **ab**	4.73E+09 (1.21E+09) **ab**	1.53E+08 (5.27E+07) **b**	6.73E+07 (2.03E+07) **abc**
	5-10	103.82 (16.1) abc	13.12 (2.4) bc	9.13 (2.6) bcd	2.66E+09 (1.31E+09) ab	9.57E+07 (5.60E+07) b	6.72E+07 (1.39E+07) cd
	10-15	75.61 (21.9) *abcd*	9.06 (2.1) *bc*	7.41 (0.9) *a*	3.84E+09 (7.55E+08) *a*	1.06E+08 (3.85E+07) *c*	2.80E+08 (8.36E+07) *ab*

The range of standards (gene copies μL^{-1}) used for quantifying each group (bacteria, fungi, archaea) by quantitative real-time PCR, along with the details of the calibration curves were the following:
Bacteria: range = 10^2-10^7; R^2= 0.99756; slope = -3.365; Intercept = 31.890; Efficiency = 0.98
Fungi: range = 10^2-10^7; R^2 = 0.99802; slope = -3.382; Intercept = 32.707; Efficiency = 0.85
Archaea: range = 10^2-10^7; R^2 = 0.99739; slope = -4.010; Intercept = 35.192; Efficiency = 0.78

Table 4.

Statistical output of the physico-chemical and microbiological parameters.

Parameters	Exposure		Altitude		Soil depth		Exposure × Altitude		Exposure × Soil depth		Altitude × Soil depth	
	F	p	F	p	F	p	F	p	F	p	F	p
Volatile solids	**125.05**	***	**58.15**	***	**29.55**	***	**3.74**	**	1.66	ns	**2.42**	*
Bulk density	**19.04**	***	**24.90**	***	**135.35**	***	**12.70**	***	**3.27**	*	**5.40**	***
Soil moisture	**129.02**	***	**71.12**	***	**71.65**	***	**25.39**	***	**10.90**	***	**2.46**	*
Sand	0.23	ns	**3.22**	**	0.85	ns	**13.82**	***	0.24	ns	**2.28**	*
Silt	0.23	ns	**5.04**	***	1.77	ns	**2.79**	*	0.49	ns	**2.38**	*
Clay	2.04	ns	**3.15**	*	0.73	ns	**13.15**	***	0.11	ns	0.88	ns
pH	**107.30**	***	**3.63**	*	1.70	ns	**8.24**	***	0.26	ns	0.26	ns
EC	**26.29**	***	**43.28**	***	**124.61**	***	**7.02**	***	2.20	ns	0.52	ns
Total C	**51.37**	***	**17.96**	***	**78.38**	***	**6.22**	***	1.03	ns	0.75	ns
Total N	**30.57**	***	**17.55**	***	**66.28**	***	**4.52**	**	1.47	ns	0.43	ns
C/N	**46.86**	***	**22.81**	***	**13.42**	***	**5.74**	***	0.26	ns	1.79	ns
NH_4^+	**54.13**	***	**16.30**	***	**73.61**	***	**12.88**	***	1.83	ns	0.40	ns
NO_3^-	**66.39**	***	**11.83**	***	**123.26**	***	**22.73**	***	**3.57**	*	**4.29**	***
gluc	**12.16**	***	**3.61**	**	**161.67**	***	**8.25**	***	0.08	ns	1.58	ns
ester	1.26	ns	**40.64**	***	**31.06**	***	**2.85**	*	0.46	ns	0.89	ns
chit	1.81	ns	2.10	ns	**71.03**	***	0.43	ns	0.68	ns	1.09	ns
leu	1.82	ns	**5.25**	**	**153.71**	***	**5.75**	***	0.84	ns	1.43	ns
acP	**7.79**	**	**19.87**	***	**82.70**	***	1.01	ns	2.45	ns	1.67	ns
alkP	**4.02**	*	1.44	ns	**23.45**	***	0.39	ns	0.13	ns	0.45	ns
piroP	**30.18**	***	**9.50**	***	**115.06**	***	1.85	ns	1.28	ns	**2.80**	**
arylS	**7.04**	**	**16.91**	***	**7.68**	***	0.88	ns	0.11	ns	1.47	ns
ds tDNA	0.66	ns	**4.41**	**	**38.88**	***	1.83	ns	0.08	ns	0.35	ns
SIR	**94.58**	***	**14.99**	***	**117.62**	***	1.36	ns	1.48	ns	1.70	ns
BR	**55.18**	***	2.05	ns	**40.18**	***	1.26	ns	**4.02**	*	1.51	ns
Bacteria	**4.33**	*	**5.39**	***	**7.66**	***	1.00	ns	0.01	ns	0.72	ns
Fungi	0.60	ns	**7.42**	***	0.33	ns	1.73	ns	2.69	ns	**2.15**	*
Archaea	**11.24**	***	**3.26**	**	**17.88**	***	**4.93**	***	0.21	ns	1.52	ns

pH (pH H_2O), EC (Electrical conductivity); NH_4^+ (Ammonium content); NO_3^- (Nitrate content); *gluc* (β glucosidase), *ester* (acetate-esterase), *chit* (chitinase), *leu* (leucine-aminopeptidase), *acP* (acid phosphomonoesterase), *alkP* (alkaline phosphomonoesterase), *piroP* (pirophosphate phosphodiesterase), *arylS* (arylsulphatase); ds tDNA (Soil microbial biomass index), SIR (Substrate Induced Respiration), BR (Basal Respiration), Bacteria (16S rRNA gene copy number); Fungi (18S rRNA gene copy number), Archaea (16S rRNA gene copy number).

ns (no significant); * p <0.05; ** p <0.01; *** p <0.001

This could indicate that fungi were less sensitive than bacteria to variations in pH between the two slope exposures. Pietikäinen et al. (2005) also showed that fungal populations of a forest and an agricultural soil appeared to be less negatively affected by low temperatures than bacteria. This could also explain why no differences in the fungal abundance were found. Fungal NMDS ordination plots and the dbRDA model analysis (Figure 4B; Table 5) also revealed that only the fungal community inhabiting the 5 – 10 cm soil layer was significantly affected by slope exposure. This is in agreement with the fungal DGGE patterns (Fig. S2). Total C significantly shaped the fungal communities in the upper-soil layer (Table 5), while the NH_4^+ content, the C/N ratio and pH were identified as the abiotic factors responsible for the fungal community changes in the 5 – 10 and 10 – 15 cm soil layers (Table 5). Neither the fungal phylotype richness nor the fungal diversity were significantly influenced by the slope exposure (Table S1). A significant increase of both parameters was, however, recorded with soil depth ($F_{2,60}$ = 100.46, $p \leq 0.0001$; $F_{1,60} = 32.61$; $p \leq 0.0001$, respectively).

Exposure had a significant impact on the archaeal 16S rRNA gene copy number, although this effect varied along the altitudinal gradient (Table 4). The abundance of archaea was three times greater in soils of north-facing sites located at an altitude of 1400 m a.s.l. and 2000 m a.s.l., while no differences in this parameter with exposure were found in the remaining sites (Table 3). Indeed, at these specific altitudes, the archaeal abundance was negatively correlated with soil pH (N_2-S_7: $R = -0.559$, $p \leq 0.05$; N_4-S_9: $R = -0.718$, $p \leq 0.01$). Accordingly, Bengston et al. (2012) observed a reduction in the archaeal abundance, assessed by real-time PCR, with increasing soil pH (pH range 4.0 to 5.1) in an arable soil. This and other previous studies (Nicol et al., 2008; Lehtovirta et al., 2009; Bates et al., 2011) underpinned that soil pH together with C/N ratio are important parameters affecting the archaeal populations. Archaeal community diversity was also

significantly affected by slope exposure (Fig. 4C; Fig. S3C). The discrimination between the north- and the south-facing sites along the NMDS axis 1 was more pronounced for the 0–5 cm soil layer (Fig. 4C). Moreover, for the top 5 cm a clear shift in archaeal community with the altitude was recorded along the NMDS axis 2 (Fig. 4C). In accordance with Bates et al. (2011), the C/N ratio was the main factor shaping the archaeal community composition in the top 5 cm (Table 5). Additionally, no significant exposure effects were found for the archaeal phylotype richness and diversity along the studied climosequence, except for the altitude of 1200 m a.s.l. (Table S1), where we measured a higher phylotype richness at north exposure ($F_{4,60} = 4.68$, $p = 0.002$). Furthermore, both the phylotype richness and diversity increased with increasing soil depth ($F_{2,60} = 43.65$, $p \leq 0.0001$; $F_{2,60} = 12.57$, $p \leq 0.0001$, respectively).

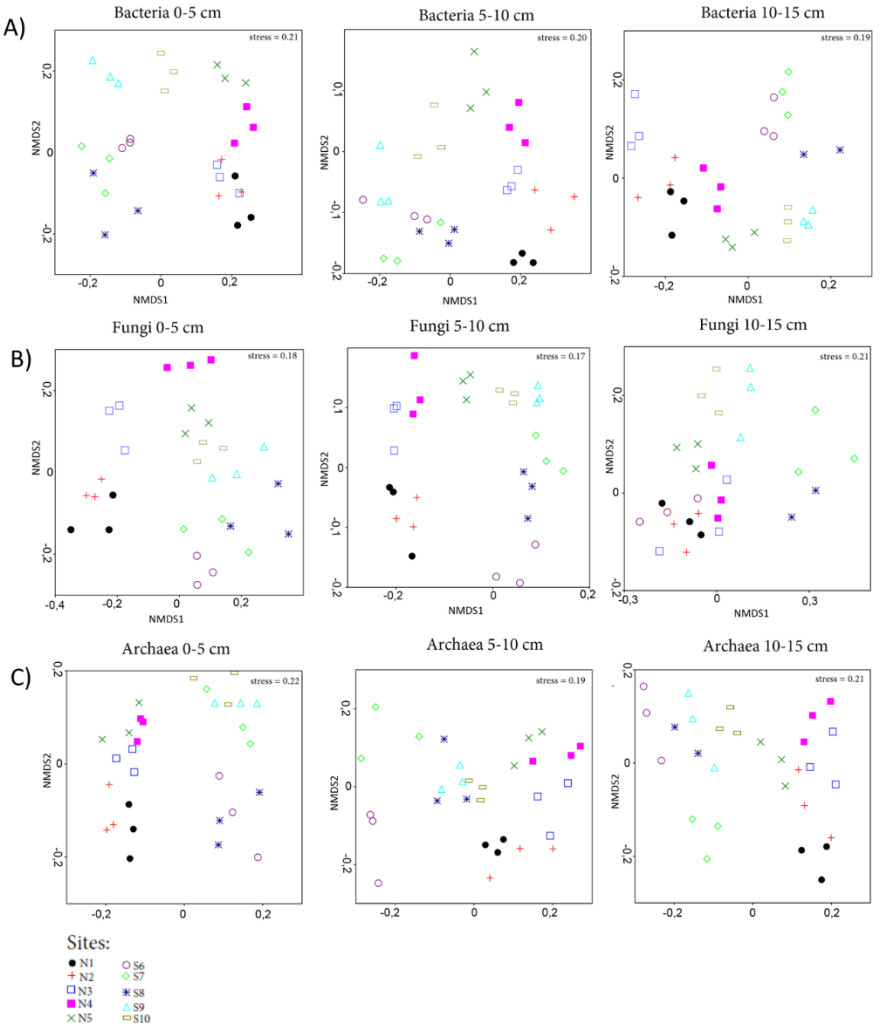

Fig. 4. Non-metric multidimensional scaling (NMDS) ordination describing (A) bacterial, (B) fungal and (C) archaeal communities at different soil depths (0 – 5 cm, 5 – 10 cm, 10 – 15 cm) for the ten sites located at north- ($N_{1\text{-}5}$) and south-facing ($S_{6\text{-}10}$) slopes.

Table 5.
Relationships between the predictor variables and the microbial community structure of the three domains at different soil depths (0-5, 5-10, 10-15 cm).

	Soil depth (cm)	Altitude			Exposure			Soil moisture			pH			%C			NO_3^-			NH_4^+			C/N ratio		
		var	F	p	var	F	p	var	F	p	var	F	p	var	F	p	var	F	p	var	F	p	var	F	p
Bacteria	0-5	3.38	3.61	***	2.42	2.59	***	—	—	—	—	—	—	2.77	2.96	**	—	—	—	—	—	—	—	—	—
Bacteria	5-10	17.79	6.53	***	8.00	2.94	***	—	—	—	6.34	2.33	**	4.56	1.68	*	5.09	1.87	*	—	—	—	—	—	—
Bacteria	10-15	2.92	1.91	*	5.77	3.76	***	3.45	2.25	*	3.91	2.55	**	4.09	2.67	*	3.83	2.50	**	—	—	—	—	—	—
Fungi	0-5	7.41	3.75	**	—	—	—	—	—	—	—	—	—	4.75	2.40	*	—	—	—	—	—	—	—	—	—
Fungi	5-10	29.02	7.12	***	23.07	5.66	**	—	—	—	—	—	—	—	—	—	—	—	—	16.82	4.13	**	15.01	3.68	**
Fungi	10-15	11.87	2.96	**	—	—	—	—	—	—	11.97	2.99	**	—	—	—	—	—	—	—	—	—	—	—	—
Archaea	0-5	6.60	2.43	***	11.35	4.18	***	—	—	—	—	—	—	—	—	—	—	—	—	—	—	—	13.42	2.05	**
Archaea	5-10	—	—	—	—	—	—	—	—	—	—	—	—	—	—	—	—	—	—	—	—	—	—	—	—
Archaea	10-15	—	—	—	—	—	—	—	—	—	—	—	—	—	—	—	—	—	—	—	—	—	—	—	—

Results show marginal tests using the dbRDA model, where var indicates the proportion of microbial community variation (Var) explained by the predictor variable.

* p <0.05; ** p <0.01; *** p <0.001

4. Discussion

4.1 Changes of the soil physico-chemical and microbiological properties along the climosequence

As occurred in the present study, altitudinal-defined climate conditions provide specific vegetation types and soil environments thereby influencing the diversity, abundance and activity of soil microbial communities (Djukic et al., 2010; Zhang et al., 2013). On the one hand, we found that both microbial biomass and activity assessed by SIR and basal respiration were more expressed at the north- than at the south-facing sites. Along these lines, Ascher et al. (2012) reported higher levels of microbial biomass, determined by the total amount of phospholipid fatty acids (PLFAs) and the yields of intracellular DNA, on northern slopes in the Trentino area, in the vicinity of the study sites of the present work. Nahidan et al. (2015) also detected higher values of microbial biomass carbon at north-facing slopes (using the fumigation–incubation method). Additionally, Kang et al. (2003) measured an increased soil respiration, determined by infrared gas analyser, at north-facing sites when compared to the south-facing slope irrespective of the altitude (220 – 1100 m a.s.l.) in three mountain forests in Korea. However, an opposite trend was observed by Carletti et al. (2009), who found higher levels of soil microbial biomass carbon at the south-facing sites. The disparity between our results and those reported by Carletti et al. (2009) must also be interpreted in the light of the 'method-result effect' (Nannipieri et al., 2003). Indeed, within our study we also observed a different effect of exposure on microbial biomass depending on the methodology used (dsDNA *vs.* SIR).

Furthermore, altitude- and enzyme-specific exposure effects were detected along our climosequence. This supports the importance of performing a multiple enzyme assay to avoid misinterpretation of environmental changes

induced effects by considering single enzyme activities as indicators of specific nutrient cycles (Nannipieri et al., 2012). Two enzyme activities involved in the C cycle were checked in the present study, namely the β-glucosidase and the acetate esterase. The first one has a relevant role in soils because it catalyses the hydrolysis of cellulose, one of the main components in the plant debris (Nannipieri et al., 2012). Its potential activity was greater in soils from the north- than those from the south-facing slopes primarily at the altitude of 1600 m a.s.l., which is in accordance with the positive correlation found between the OM levels (assessed as volatile solids) and β-glucosidase activity at this study site (N_3-S_8, $R = 0.850$, $p \leq 0.001$). Nonetheless, no exposure effect was observed for β-glucosidase activity at the higher sites (2000 and 2400 m a.s.l.). This might be due to the higher proportion of grassland and a colder climate compared to the other sites surveyed, thus influencing the enzymatic processes involved in the plant debris decomposition, and hence the β-glucosidase activity (Blagodatskaya et al., 2016). It is also known that fungi are the predominant source of certain enzymes like glucosidases in soil (Hayano and Tubaki, 1985). No significant differences in the fungal abundance were, however, recorded between north- and south-facing slopes.

Moreover, no-exposure effect was detected for both acetate esterase and chitinase potential activities regardless of the altitude. This could be due the fact that these two latter enzymes are involved in the degradation of SOM components with slower turnover times (acetic acid esters and chitin respectively) than those degraded by β-glucosidase. The differences in the SOM content with respect to slope exposure might have affected to a lesser extent the potential activities of these two enzymes. Additionally, this could indicate that the turnover of high molecular compounds (like chitin) is less sensitive to the temperature differences between both slope exposures (Table 1). Significant differences in the leucine-aminopeptidase potential

activity with slope exposure were only recorded for the altitude of 1400 m a.s.l., registering a higher activity at south exposure. Previous studies (Sinsabaugh et al., 2005; Ramirez et al., 2012) suggested that higher N concentrations could limit the related enzyme activities in soil, which could partly explain why a greater activity was measured at the south-facing site that are characterised by a lower inorganic N pool. Sinsabaugh et al. (2008) also observed a higher leucine-aminopeptidase activity responsible for the release of amino acids from polypeptides with increasing soil pH levels (pH 4 to 8.5). Although both slope exposures were generally acidic, we found an increase in pH on south-facing sites. Moreover, it has been reported that bacteria play an important role in the production of leucine-aminopeptidases (Burke et al., 2011) and, accordingly, we detected higher bacterial gene copy numbers at the south-facing slope.

Acid and alkaline phosphomonoesterases are responsible for the mineralisation of organic P into phosphate by hydrolysing phosphoric (mono) ester bonds under acid and alkaline conditions, respectively (Nannipieri et al., 2012). They have an important role for the P cycling in forest ecosystems, particularly where P availability may limit plant productivity (Nanniperi et al., 2003). In our study, we found a greater acid phosphomonoesterase activity at the north-facing slopes. Although plants exude acid phosphomonoesterases, especially under P deficiency, the majority of phosphatase enzymes in soil probably originate from microorganisms (Bünemann, 2015). Indeed, we found a positive correlation between acid phosphomonoesterase activity and soil microbial biomass (dsDNA) for each pairs of sites (N_1-S_6, $R = 0.848$, $p \leq 0.001$; N_2-S_7, $R = 0.721$, $p \leq 0.001$; N_3-S_8, $R = 0.871$, $p \leq 0.001$; N_4-S_9, $R = 0.754$, $p \leq 0.001$; N_5-S_{10}, $R = 0.567$, $p \leq 0.05$).

Tabatabai (1994) stated that bacterial phosphatases have a higher pH optimum than fungal phosphatases and as such, soils dominated by alkaline phosphatases are expected to have larger bacterial populations. Accordingly, a greater alkaline phosphomonoesterase activity was recorded at the south-facing slopes characterised by less acidic conditions. Arylsulphatase activity, which is involved in the hydrolysis of organic sulfate esters into inorganic S (Turner, 2010), was also more pronounced at the south-facing slopes, where we found a higher bacterial abundance. According to Makoi and Ndakidemi (2008) bacteria secrete arylsulphatases into the environment as a response to S limitation. In disagreement with our findings, Nahidan et al. (2015) observed higher alkaline phosphomonoesterase and arysulphatase activities at the north-facing slopes in a rangeland ecosystem of west central Iran.

Although microbial biomass and activity were more pronounced at the north-facing slopes, the higher bacterial abundance was recorded at the south-facing slope along the altitudinal gradient. It has been shown that bacterial growth is more favoured at neutral or slightly alkaline conditions (Rousk et al., 2010). Even small variations in the soil pH range (Penannen et al., 1998; Siles and Margesin, 2016) such as those observed in the present study, in which soil pH values only differed by 1 unit between both slope exposures, may induce changes in the bacterial abundance and diversity. Soil acidity was also one of the most important driving factors for the community structure of bacteria inhabiting in the 5 – 10 and 10 – 15 cm soil layers as indicated by the dbRDA model analysis (Table 5). This was not the case for the bacterial DGGE profiles from the uppermost topsoil (0 – 5 cm); indicating that other abiotic factors like total C affected the bacterial community diversity to a larger extent than soil pH. However, fungi were not affected by exposure indicating that they were less affected than bacteria to variations in soil pH with exposure. It should also be mentioned that we found a high variation among replicates with regard to qPCR quantification

probably due to the variation inherent to the field campaign. Compared to fungi and bacteria, archaea are not among the primary decomposers of SOM (Singh et al., 2012a,b). They are nonetheless expected to have an important role in alpine settings as they are known to be well adapted to the harsh conditions of these environments (Singh et al., 2012b; Xu et al., 2014). We found that the impact of exposure on the archaeal abundance was altitude-dependent, registering a higher copy number at the north- than at the south-facing slopes for the altitudes of 1400 and 2000 m a.s.l. Both soil pH and the C/N ratio were the main drivers affecting the abundance and diversity of archaeal communities in these study sites.

4.2 Shifts in the soil physico-chemical and microbiological properties with soil depth

We hypothesised that exposure and altitudinal effects on the studied microbiological parameters would be more evident in the uppermost topsoil layer (0 – 5 cm), because this soil layer is more exposed to the changing environmental conditions such as shifts in temperature and/or OM input. This hypothesis seems to be confirmed for microbial activity (BR). Furthermore, a reduced microbial biomass and activity was measured in the soil layer 10 – 15 cm. Similarly, Fierer et al. (2003) detected a reduced soil microbial biomass with increasing soil depth using different approaches such as SIR, total PLFA content and chloroform fumigation-extraction. Accordingly, we found that the hydrolytic enzyme activities were also reduced with soil depth. Such a reduction occurred in concert with a decline in soil moisture, total C and N, and inorganic N contents. It is known that the availability of substrate for enzymatic breakdown decreases with depth, which may result in a spatial disconnection of enzyme and substrate (Holden and Fierer, 2005). No changes in soil pH, one of the factors often

associated with enzyme activities, were recorded within the three topsoil layers.

The organic matter in the deeper layers is due to decomposition products from aboveground or rhizo-deposition (Lejon et al., 2005; Schmidt et al., 2011). The decreasing availability of fresh organic material and the reduced soil moisture with increasing depth is likely to affect the autochthonous microbiota in terms of abundance, richness and diversity (Schnecker et al., 2015; Xu et al., 2015). Accordingly, a reduced bacterial abundance and diversity was found in the 10 – 15 cm soil layer in comparison with the top 5 cm. Although no changes were observed for fungi in terms of abundance we measured an increase in fungal richness and diversity with soil depth. This could be attributed to mycorrhizal associations and rooting distribution in these deeper layers (Lejon et al., 2005). Furthermore, the higher archaeal abundance, richness and diversity with increasing soil depth underline the capacity of this microbial group to adapt to less favourable environmental conditions (i.e., reduced OM content). In accordance with our findings, Kemnitz et al. (2007) found an increase in archaeal abundance (gene copy numbers) along a 20 cm soil profile in an acidic forest soil in Marburg (Germany).

A clear discrimination between north- and south-facing slopes was detectable for bacterial communities (DGGE-genetic fingerprinting) for each of the three soil depths; whereas it was soil layer-dependent for fungal and archaeal communities. These specific microbial responses could be due to the different soil physico-chemical characteristics ascribed to each soil depth (Egli et al. 2009, 2010; Ascher et al., 2012).

5. Conclusions

Our complex climosequence approach provided evidences that thermal conditions (exposure and altitude) and consequently the state factor climate,

shape edaphic properties and soil microbiota in terms of biomass, activity and composition, supporting and deepening previous findings from the Trentino area (Ascher et al., 2012). Our results showed (1) a higher microbial biomass (SIR) and activity (BR) in the north-facing slopes irrespective of the altitude, contradicting our initial hypothesis. The discrepancy to findings in literature with respect to the microbial biomass results might be ascribed to the different methodology used (dsDNA *vs.* SIR). (2) Altitude- and enzyme-specific exposure effects were detected along the climosequence. (3) The three microbial domains responded differently to exposure in terms of abundance: bacteria (S > N; altitude-independent), fungi (N ~ S), archaea (N > S; altitude-dependent). (3) The NMDS ordination plots enabled a new view on the exposure effects on the microbial community structures, whereas changes in both phylotype richness and diversity in function of the slope exposure were only detected for the archaeal community (N > S; dependent on the altitude). (4) The effect of climate was most pronounced in the uppermost topsoil-layer, however only for the microbial activity. On the whole, our findings encourage the application of a similar climosequence approach in different Alpine environments, so as to further discriminate among the complex multiple-factors shaping soil biota in the context of global warming.

Acknowledgments

This research is part of the DecAlp D.A.CH. project (Project I989-B16). T. Bardelli has been funded by a PhD grant from the University of Florence (Italy). J. Ascher-Jenull and M. Gómez-Brandón have been supported by the Fonds zur Förderung der wissenschaftlichen Forschung (FWF) Austria (Project I989-B16). We would like to thank Layzza Roberta Alves Medeiros, Sebastian Waldhuber and Ljubica Begovic for their help in the laboratory. We also acknowledge Paul Fraiz for his highly valuable help in language

editing. We are also indebted to Dr. Fabio Angeli of the Ufficio distrettuale forestale – Malé (Trento, Italy) and his team for their support in the field.

References

Ad-hoc-AG Boden, 2005. Bodenkundliche Kartieranleitung, 5. Auflage. Hannover (438 pp).

Ascher, J., Ceccherini, M.T., Pantani, O.L., Agnelli, A., Borgogni, F., Guerri, G., Nannipieri, P., Pietramellara, G., 2009. Sequential extraction and genetic fingerprinting of a forest soil metagenome. Applied Soil Ecology 42, 176–181.

Ascher, J., Sartori, G., Graefe, U., Thornton, B., Ceccherini, M.T., Pietramellara, G., Egli, M., 2012. Are humus forms, mesofauna and microflora in subalpine forest soils sensitive to thermal conditions? Biology and Fertility of Soils 48, 709–725.

Barbosa, W.R., Romero, R.E., de Souza Junior, V.S., Cooper, M., Sartor, L.R., de Moya Partiti, C.S., de Oliveira Jorge, F., Cohen, R., de Jesus, S.L., Ferreira, T.O., 2015. Effects of slope orientation on pedogenesis of altimontane soils from the Brazilian semi-arid region (Baturité massif, Ceará). Environmental Earth Sciences 73, 3731–3743.

Bates, S.T., Berg-Lyons, D., Caporaso, J.G., Walters, W.A., Knight, R., Fierer, N., 2011. Examining the global distribution of dominant archaeal populations in soil. The ISME Journal 5, 908–917.

Begum, F., Bajracharya, R.M., Sharma, S., Sitaula, B.K., 2010. Influence of slope aspect on soil physico-chemical and biological properties in the mid hills of central Nepal. International Journal of Sustainable Development and World Ecology 17, 438–443.

Bengtson, P., Sterngren, A.E., Rousk, J., 2012. Archaeal abundance across a pH gradient in an arable soil and its relationship to bacterial and fungal growth rates. Applied and Environmental Microbiology 78, 5906–5911.

Berger, T.W., Duboc, O., Djukic, I., Tatzber, M., Gerzabek, M.H., Zehetner, F., 2015. Decomposition of beech (*Fagus sylvatica*) and pine (*Pinus nigra*) litter along an Alpine elevation gradient: decay and nutrient release. Geoderma 251–252, 92–104.

Blagodatskaya, E., Blagodatsky, S., Khomyakov, N., Myachina, O., Kuzyakov, Y., 2016. Temperature sensitivity and enzymatic mechanisms of soil organic matter decomposition along an altitudinal gradient on Mount Kilimanjaro. Scientific Report 6, doi:10.1038/srep22240.

Bünemann, E.K., 2015. Assessment of gross and net mineralization rates of soil organic phosphorus - A review. Soil Biology and Biochemistry 89, 82–98.

Burke, D.J., Weintraub, M.N., Hewins, C.R., Kalisz, S., 2011. Relationship between soil enzyme activities, nutrient cycling and soil fungal communities in a northern hardwood forest. Soil Biology and Biochemistry 43, 795–803.

Campbell, C.D., Chapman, S.J., Cameron, C.M., Davidson, M.S., Potts, J.M., 2003. A rapid microtiter plate method to measure carbon dioxide evolved from carbon substrate amendments so as to determine the physiological profiles of soil microbial communities by using whole soil. Applied and Environmental Microbiology 69, 3593–3599.

Carletti, P., Vendramin, E., Pizzeghello, D., Concheri G., Zanella, A., Nardi, S., Squartini, A., 2009. Soil humic compounds and microbial communities in six spruce forests as function of parent material, slope aspect and stand age. Plant and Soil 315, 47–65.

Coolen M.J.L., Hopmans E.C., Rijpstra, W.I.C., Muyzer, G., Schouten, S., Volkman, J.K., Damste, J.S.S., 2004. Evolution of the methane cycle in Ace Lake (Antarctica) during the Holocene: response of methanogens and methanotrophs to environmental change. Organic Geochemistry 35, 1151–1167.

Dice, L.R., 1945. Measures of the amount of ecologic association between species. Ecology 26, 297–302.

Djukic, I., Zehetner, F., Tatzber, M., Gerzabek, M.H., 2010. Soil organic-matter stocks and characteristics along an Alpine elevation gradient. Journal of Plant Nutrition and Soil Science 173, 30–38.

Egli, M., Mirabella, A., Sartori, G., Zanelli, R., Bischof, S., 2006. Effect of north and south exposure on weathering rates and clay mineral formation in Alpine soils. Catena 67, 155–174.

Egli, M., Sartori, G., Mirabella, A., Favilli, F. 2009. Effect of north and south exposure on organic matter in high Alpine soils. Geoderma 149, 124–136.

Egli, M., Sartori, G., Mirabella, A., Giaccai, D., Favilli, F., Scherrer, D., Krebs, R., Delbos, E. 2010. The influence of weathering and organic matter on heavy metals lability in silicatic Alpine soils. Science of The Total Environment 408, 931–946.

Eichner, C.A., Erb, R.W., Timmis, K.N., Wagner-Döbler, I., 1999. Thermal Gradient Gel Electrophoresis Analysis of Bioprotection from Pollutant Shocks in the Activated Sludge Microbial Community. Applied and Environmental Microbiology 65, 102–109.

FAO, 2006. Guidelines for Soil Description. 4th edition. FAO, Rome.

Ferris, M.J., Muyzer, G., Ward, D.M., 1996. Denaturing gradient gel electrophoresis profiles of 16S rRNA-defined populations inhabiting a hot spring microbial mat community. Applied and Environmental Microbiology 62, 340–346.

Fierer, N., Schimel, J.P., Holden, P.A., 2003. Variations in microbial community composition through two soil depth profiles. Soil Biology and Biochemistry 35, 167–176.

Fornasier, F., Margon, A., 2007. Bovine serum albumin and Triton X-100 greatly increase phosphomonoesterases and arylsulphatase extraction yield from soil. Soil Biology and Biochemistry 39, 2682–2684.

Fornasier, F., Ascher, J., Ceccherini, M.T., Tomat, E., Pietramellara, G., 2014. A simplified rapid, low-cost and versatile DNA-based assessmentof soil microbial biomass. Ecological indicators 45, 75–82.

Grossman, R.B., Reinsch, T.G., 2002. Bulk density and linear extensibility. In: Dane, J.H., Topp, G.C., (Eds.), Methods of soil analysis. Part 4. SSSA Book Ser. 5. SSSA, Madison, WI, p. 201–205.

Hayano, K., Tubaki, K., 1985. Origin and properties of β-glucosidase activity of tomato-field soil. Soil Biology and Biochemistry 17, 553–557.

Holden, P.A., Fierer, N., 2005. Microbial processes in the Valdose Zone. Valdose Zone Journal 4, 1–21.

Indorante, S. J., Hammer, R. D., Koenig, P. G., Follmer, L. R., 1990. Particle-size analysis by a modified pipette procedure. Soil Science Society of America Journal, 54, 560–563.

Insam, H., 2001. Developments in soil microbiology since the mid 1960s. Geoderma 100, 389–402.

Kandeler, E., 1993a. Bestimmung von Ammonium. In: Schinner, F., Öhlinger, R., Kandeler, E., Margesin, R. (Eds.), Bodenbiologische Arbeitsmethoden. Springer, Berlin, Heidelberg, pp. 366–368.

Kandeler, E., 1993b. Bestimmung von Nitrat. In: Schinner, F., Öhlinger, R., Kandeler, E., Margesin, R. (Eds.), Bodenbiologische Arbeitsmethoden. Springer, Berlin, Heidelberg, pp. 369–371.

Kang, S., Doh, S., Lee, D., Lee, D., Jin, V.L., Kimball, J.S., 2003. Topographic and climatic controls on soil respiration in six temperate mixed-hardwood forest slopes, Korea. Global Change Biology 9, 1427–1437.

Kemnitz, D., Kolb, S., Conrad, R., 2007. High abundance of Crenarchaeota in a temperate acidic forest soil. FEMS Microbiology Ecology 60, 442–448.

Lalor, B.M., Cookson, W.R., Murphy, D.V., 2007. Comparison of two methods that assess soil community level physiological profiles in a forest ecosystem. Soil Biology and Biochemistry 39, 454–462.

Lehtovirta, L.E., Prosser, J.I., Nicol, G.W., 2009. Soil pH regulates the abundance and diversity of Group1.1c Crenarchaeota. FEMS Microbiology Ecology 70, 367–376.

Lejon, D.P.H., Chaussod, R., Ranger, J., Ranjard, L., 2005. Microbial community structure and density under different tree species in an acid forest soil (Morvan, France). Microbial Ecology 50, 614–625.

Lin, Q., Brookes, P.C., 1999. An evaluation of the substrate-induced respiration method. Soil Biology and Biochemistry 31, 1969–1983.

Makoi, J.H.R., Ndakidemi, P.A., 2008. Selected soil enzymes: examples of their potential roles in the ecosystem. African Journal of Biotechnology 7, 181–191.

Margesin, R., Jud, M., Tscherko, D., Schinner, F., 2009. Microbial communities and activities in alpine and subalpine soils. FEMS Microbiology Ecology 67, 208–218.

Nahidan, S., Nourbakhsh, F., Mosaddeghi, M.R., 2015. Variation of soil microbial biomass C and hydrolytic enzyme activities in a rangeland ecosystem: are slope aspect and position effective? Archives of Agronomy and Soil Science 61, 797–811.

Nannipieri, P., Ascher, J., Ceccherini, M.T., Landi, L., Pietramellara, G., Renella, G., 2003. Microbial diversity and soil functions, European Journal of Soil Science 54, 655–670.

Nannipieri, P., Giagnoni, L., Renella, G., Puglisi, E., Ceccanti, B., Masciandaro, G., Fornasier, F., Moscatelli, M.C., Marinari, S., 2012. Soil enzymology: classical and molecular approaches. Biology and Fertility of Soils 48, 743–762.

Nicol, G.W., Leininger, S., Schleper, C., Prosser, J.I., 2008. The influence of soil pH on the diversity, abundance and transcriptional activity of ammonia oxidizing archaea and bacteria. Environmental Microbiology 10, 2966–2978.

Nübel, U., Engelen, B., Felske, A., Snaidr, J., Wieshuber, A., Amann, RI., Ludwig, W., Backhaus, H., 1996. Sequence heterogeneities of genes encoding 16S rRNAs in Paenibacillus polymyxa detected by temperature gradient gel electrophoresis. Journal of Bacteriology 178, 5636–5643.

Orgiazzi, A., Dunbar, M.B., Panagos, P., de Groot, G.A., Lemanceau, P., 2015. Soil biodiversity and DNA barcodes: opportunities and challenges. Soil Biology and Biochemistry 80, 244–250.

Pennanen, T., Fritze, H., Vanhala, P., Kiikkilä, O., Neuvonen, S., Bååth, E., 1998. Structure of a microbial community in soil after prolonged addition of low levels of simulated acid rain. Applied and Environmental Microbiology 64, 2173–2180.

Petrillo, M., Cherubini, P., Sartori, G., Abiven, S., Ascher, J., Bertoldi, D., Camin, F., Barbero, A., Larcher, R., Egli, M., 2015. Decomposition of Norway spruce and European larch coarse woody debris (CWD) in relation to different elevation and exposure in an Alpine setting. iForest 9, 154–164.

Pietikäinen, J., Pettersson, M., Bååth, E., 2005. Comparison of temperature effects on soil respiration and bacterial and fungal growth rates. FEMS Microbiology Ecology 52, 49–58.

Prévost-Bouré, N.C., Christen, R., Dequiedt, S., Mougel, C., Lelièvre, M., Jolivet, C., Shahbazkia, H.R., Guillou, L., Arrouays, D., Ranjard, L., 2011. Validation and application of a PCR primer set to quantify fungal communities in the soil environment by real-time PCR. Plos One 6, e24166.

Ramirez, K.S., Craine, J.M., Fierer, N., 2012. Consistent effects of nitrogen amendments on soil microbial communities and processes across biomes. Global Change Biology 18, 1918–1927.

Rousk, J., Baath, E., Brookes, P.C., Lauber, C.L., Lozupone, C., Caporaso, J.G., Knight, R., Fierer, N., 2010. Soil bacterial and fungal communities across a pH gradient in an arable soil. The ISME Journal 4, 1340–1351.

Sboarina, C., Cescatti, A., 2004. Il clima del Trentino – distribuzione spaziale delle principali variabili climatiche [The climate of Trentino – spatial distribution of the principal climatic variables]. Report 33, Centro di Ecologia Alpina Monte Bondone, Trento, Italy, pp. 20.

Schmidt, M. W. I., Torn, M. S., Abiven, S., Dittmar, T., Guggenberger, G., Janssens, I. A., Kleber, M., Kögel-Knabner, I., Lehmann, J., Manning, D. A. C., Nannipieri, P., Rasse, D. P., Weiner, S., and Trumbore, S. E., 2011. Persistence of soil organic matter as an ecosystem property. Nature 478, 49–56.

Schnecker, J., Wild, B., Takriti, M., Alves, R.J.E., Gentsch, N., Gittel, A., Hofer, A., Klaus, K., Knoltsch, A., Lashchinskiy, N., Mikutta, R., Richter, A., 2015. Microbial community composition shapes enzyme patterns in topsoil and subsoil horizons

along a latitudinal transect in Western Siberia. Soil Biology and Biochemistry 83, 106–115.

Shemekite, F., Gómez-Brandón, M., Franke-Whittle, I.H., Insam, H., Assefa, F., 2014. Coffee husk composting: An investigation of the process using molecular and non-molecular tools. Waste Management 34, 642–652.

Siles, J.A., Cajthaml, T., Minerbi S., Margesin, R., 2016. Effect of altitude and season on microbial activity, abundance and community structure in Alpine forest soils. FEMS Microbiology Ecology 92, 1–12.

Siles, J.A., Margesin, R., 2016. Abundance and Diversity of Bacterial, Archaeal, and Fungal Communities Along an Altitudinal Gradient in Alpine Forest Soils: What are the Driving Factors? Microbial Ecology 72, 207–220.

Singh, D., Takahashi, K., Kim, M., Chun, L., Adams, J.M., 2012a. A hump-backed trend in bacterial diversity with elevation on Mount Fuji, Japan. Microbial Ecology 63, 429–437.

Singh, D., Takahashi, K., Adams, J.M., 2012b. Elevational patterns in archaeal diversity on Mt. Fuji, PLoS One 7, e44494.

Sinsabaugh, R.L., Gallo, M.E., Lauber, C., Waldrop, M.P., Zak, D.R., 2005. Extracellular enzyme activities and soil organic matter dynamics for northern hardwood forests receiving simulated nitrogen deposition. Biogeochemistry 75, 201–215.

Sinsabaugh, R.L., Lauber, C.L.,Weintraub, M.N., Ahmed, B., Allison, S.D., Crenshaw, C., Contosta, A.R., Cusack, D., Frey, S., Gallo, M.E., Gartner, T.B., Hobbie, S.E., Holland, K., Keeler, B.L., Powers, J.S., Stursova, M., Takacs-Vesbach, C., Waldrop, M.P., Wallenstein, M.D., Zak, D.R., Zeglin, L.H., 2008. Stoichiometry of soil enzyme activity at global scale. Ecology Letters 11, 1252–1264.

Smith, J.L., Halvorson, J.J., Bolton Jr, H., 2002. Soil properties and microbial activity across a 500 m elevation gradient in a semi-arid environment. Soil Biology and Biochemistry 34, 1749–1757.

Sun, B., Wang, X.Y., Wang, F., Jiang, Y. J., Zhang, X. X., 2013. Assessing the relative effects of geographic location and soil type on microbial communities associated with straw decomposition. Applied and Environmental Microbiology 79, 3327–3335.

Tabatabai, M.A., 1994. Soil enzymes. In: Weaver R.W., Angle S., Bottomley P., Bezdicek D., Smith S., Tabatabai A., Wollum E. (eds) Methods in soil analysis. Part 2. Microbiological and biochemical properties. Soil Science Society of America, Madison, pp. 775–833.

Taylor, L.L., Leake, J.R., Quirk, J., Hardy, K., Banwart, S.A., Beerling, D.J., 2009. Biological weathering and the long-term carbon cycle: integrating mycorrhizal evolution and function into the current paradigm. Geobiology 7, 171–191.

Turner, B.L., 2010. Variation in pH optima of hydrolytic enzyme activities in tropical rain forest soils. Applied and Environmental Microbiology 76, 6485–6493.

Vainio, E.J., Hantula, J., 2000. Direct analysis of wood-inhabiting fungi using denaturing gradient gel electrophoresis of amplified ribosomal DNA. Mycological Research 104, 927–936.

Xu, M., Li, X., Cai, X., Gai, J., Li, X., Christie, P., Zhang, J., 2014. Soil microbial community structure and activity along a montane elevational gradient on the Tibetan Plateau. European Journal of Soil Biology 64, 6–14.

Xu, Z., Yu, G., Zhang, X., Ge, J., He, N., Wang, Q., Wang, D., 2015. The variations in soil microbial communities, enzyme activities and their relationships with soil organic matter decomposition along the northern slope of Changbai Mountain. Applied Soil Ecology 86, 19–29.

Zanella A., Jabiol B., Ponge J.F., Sartori G., De Waal R., Van Delft B., Graefe U., Cools N., Katzensteiner K., Hager H., Englisch M., 2011. A European morpho-functional classification of humus forms. Geoderma 164, 138–145.

Zhang, S., Chen, D., Sun, D., Wang, X., Smith, J.L., Du, G., 2012. Impacts of altitude and position on the rates of soil nitrogen mineralization and nitrification in alpine

meadows on the eastern Qinghai-Tibetan Plateau, China. Biology and Fertility of Soils 48, 393–400.

Zhang, B., Liang, C., He, H., Zhang, X., 2013. Variations in Soil Microbial Communities and Residues Along an Altitude Gradient on the Northern Slope of Changbai Mountain, China. PLoS ONE 8, e66184.

Supplementary Material

Effects of slope exposure on soil physico-chemical and microbiological properties along an altitudinal climosequence in the Italian Alps

Tommaso Bardelli[a,b], María Gómez-Brandón[b,*], Judith Ascher-Jenull[a,b], Flavio Fornasier[c], Paola Arfaioli[a], Davide Francioli[d], Markus Egli[e], Giacomo Sartori[f], Heribert Insam[b], Giacomo Pietramellara[a]

[a]Department of Agriffod and Environmental Science, University of Florence, Piazzale delle Cascine 18, 50144 Florence, Italy

[b]Institute of Microbiology, University of Innsbruck, Technikerstraße 25d, 6020 Innsbruck, Austria

[c]Council for Research and Experimentation in Agriculture, Via Trieste 23, 34170 Gorizia, Italy

[d]Helmholtz Centre for Environmental Research-UFZ;06120; Halle (Saale), Germany

[e]Department of Geography, University of Zürich, Winterthurerstrasse 190, 8057 Zürich, Switzerland

[f]Museo delle Scienze (MUSE), Corso del Lavoro e della Scienza 3, 38122 Trento, Italy

* Corresponding author: Maria.Gomez-Brandon@uibk.ac.at

Table S1.

Phylotype richness and Shannon's diversity index of the bacterial, fungal and archaeal communities recorded at the ten study sites at north-and south-facing areas ($N_{1\text{-}5}$ and $S_{6\text{-}10}$, respectively). The results are shown pairwise, i.e., the couples of north- and south-facing sites at the same elevation (N_1-S_6; N_2-S_7; N_3-S_8; N_4-S_9; N_5-S_{10}), so as to evaluate the exposure-effect. Values are means (n=3) with the standard deviations in brackets.

Sites	Soil depth (cm)	Bacterial richness (OTU numbers)	Bacterial diversity (Shannon index)	Fungal richness (OTU numbers)	Fungal diversity (Shannon index)	Archaeal richness (OTU numbers)	Archaeal diversity (Shannon index)
N_1	0-5	57 (5)	3.7 (0.1)	29 (4)	2.5 (0.1)	22 (5)	2.6 (0.3)
	5-10	35 (7)	2.8 (0.2)	41 (3)	2.7 (0.3)	31 (7)	2.5 (0.3)
	10-15	41 (4)	3.4 (0.1)	52 (14)	3.1 (0.3)	39 (3)	3.1 (0.1)
S_6	0-5	49 (9)	3.5 (0.2)	21 (2)	2.0 (0.3)	16 (7)	2.2 (0.5)
	5-10	47 (3)	3.5 (0.2)	48 (5)	3.1 (0.4)	23 (7)	2.3 (0.6)
	10-15	45 (1)	3.5 (0.2)	49 (6)	2.9 (0.4)	27 (2)	2.7 (0.4)
N_2	0-5	51 (9)	3.5 (0.2)	35 (6)	2.8 (0.4)	16 (7)	2.1 (0.6)
	5-10	39 (12)	3.1 (0.3)	42 (6)	2.8 (0.2)	28 (2)	2.8 (0.2)
	10-15	46 (11)	3.5 (0.3)	52 (6)	3.1 (0.2)	35 (5)	2.8 (0.5)
S_7	0-5	45 (4)	3.4 (0.1)	28 (7)	2.4 (0.2)	30 (3)	2.9 (0.1)
	5-10	39 (7)	3.3 (0.2)	45 (3)	2.7 (0.2)	29 (9)	2.3 (0.6)
	10-15	36 (2)	3.2 (0.01)	30 (7)	2.8 (0.3)	36 (7)	2.8 (0.1)
N_3	0-5	54 (7)	3.5 (0.1)	28 (6)	2.6 (0.3)	27 (2)	2.7 (0.2)
	5-10	47 (1)	3.5 (0.1)	32 (7)	2.4 (0.1)	30 (5)	2.6 (0.1)
	10-15	30 (13)	2.9 (0.2)	49 (8)	3.0 (0.3)	33 (5)	2.8 (0.1)
S_8	0-5	53 (5)	3.6 (0.1)	23 (4)	2.5 (0.2)	17 (5)	1.9 (0.5)
	5-10	39 (1)	3.1 (0.1)	41 (3)	2.8 (0.3)	30 (5)	2.8 (0.2)
	10-15	43 (5)	3.3 (0.2)	35 (11)	2.7 (0.4)	35 (4)	3.0 (0.2)

Table S1. Continued.

Sites	Soil depth (cm)	Bacterial richness (OTU numbers)	Bacterial diversity (Shannon index)	Fungal richness (OTU numbers)	Fungal diversity (Shannon index)	Archaeal richness (OTU numbers)	Archaeal diversity (Shannon index)
N_4	0-5	49 (4)	3.6 (0.1)	18 (6)	1.8 (0.7)	28 (3)	2.8 (0.01)
	5-10	45 (12)	3.4 (0.2)	42 (5)	2.6 (0.2)	32 (9)	2.7 (0.3)
	10-15	49 (11)	3.5 (0.3)	41 (2)	3.0 (0.2)	37 (6)	2.9 (0.2)
S_9	0-5	31 (16)	2.8 (1.0)	19 (4)	2.0 (0.3)	24 (5)	2.8 (0.3)
	5-10	40 (3)	3.3 (0.01)	39 (3)	2.6 (0.1)	34 (3)	2.7 (0.2)
	10-15	47 (4)	3.5 (0.01)	41 (8)	2.7 (0.2)	43 (4)	3.2 (0.1)
N_5	0-5	55 (13)	3.7 (0.2)	17 (2)	2.1 (0.3)	29 (3)	2.7 (0.2)
	5-10	44 (3)	3.4 (0.03)	44 (3)	2.8 (0.03)	29 (3)	2.8 (0.1)
	10-15	48 (3)	3.5 (0.04)	44 (4)	2.9 (0.2)	35 (3)	2.8 (0.1)
S_{10}	0-5	62 (2)	3.8 (0.02)	22 (5)	2.3 (0.5)	24 (7)	2.5 (0.3)
	5-10	40 (8)	3.3 (0.1)	40 (9)	2.6 (0.3)	36 (5)	2.8 (0.3)
	10-15	49 (1)	3.5 (0.1)	49 (7)	2.9 (0.3)	41 (5)	3.1 (0.3)

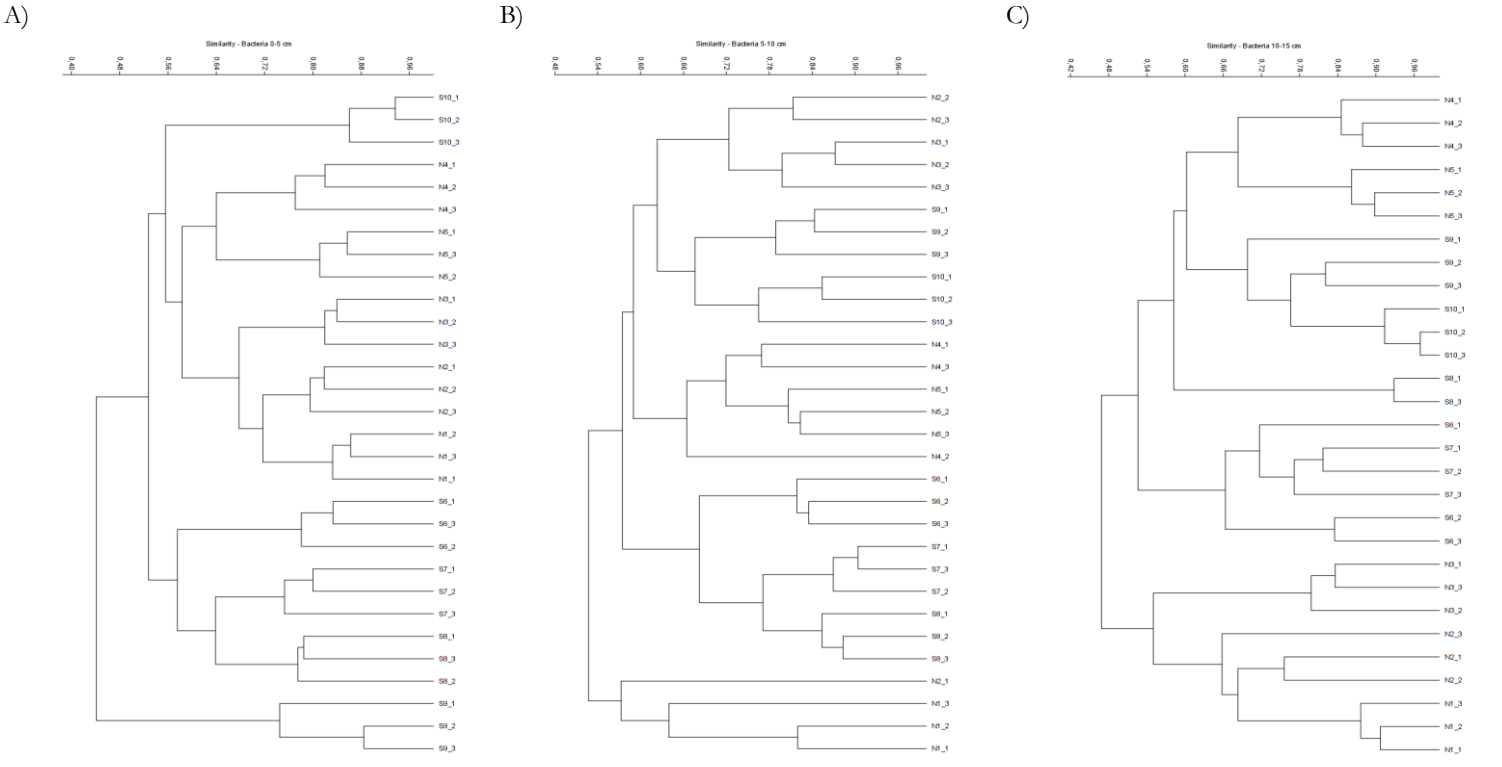

Fig. S1. Cluster analyses based on 16S rRNA gene for bacterial fingerprints (A, B, C) obtained from the ten study sites at north- and south-facing areas ($N_{1\text{-}5}$ and $S_{6\text{-}10}$, respectively) for each of the three soil depths (0-5 cm, 5-10 cm and 10-15 cm). The results are shown pairwise, i.e. the couples of north- and south-facing sites (N_1-S_6; N_2-S_7; N_3-S_8; N_4-S_9; N_5-S_{10}) at the same elevation (1200 m; 1400 m; 1600 m; 2000 m; 2400 m a.s.l.). Values at the axis correspond to the percentage of similarity, based on the Dice correlation coefficient.

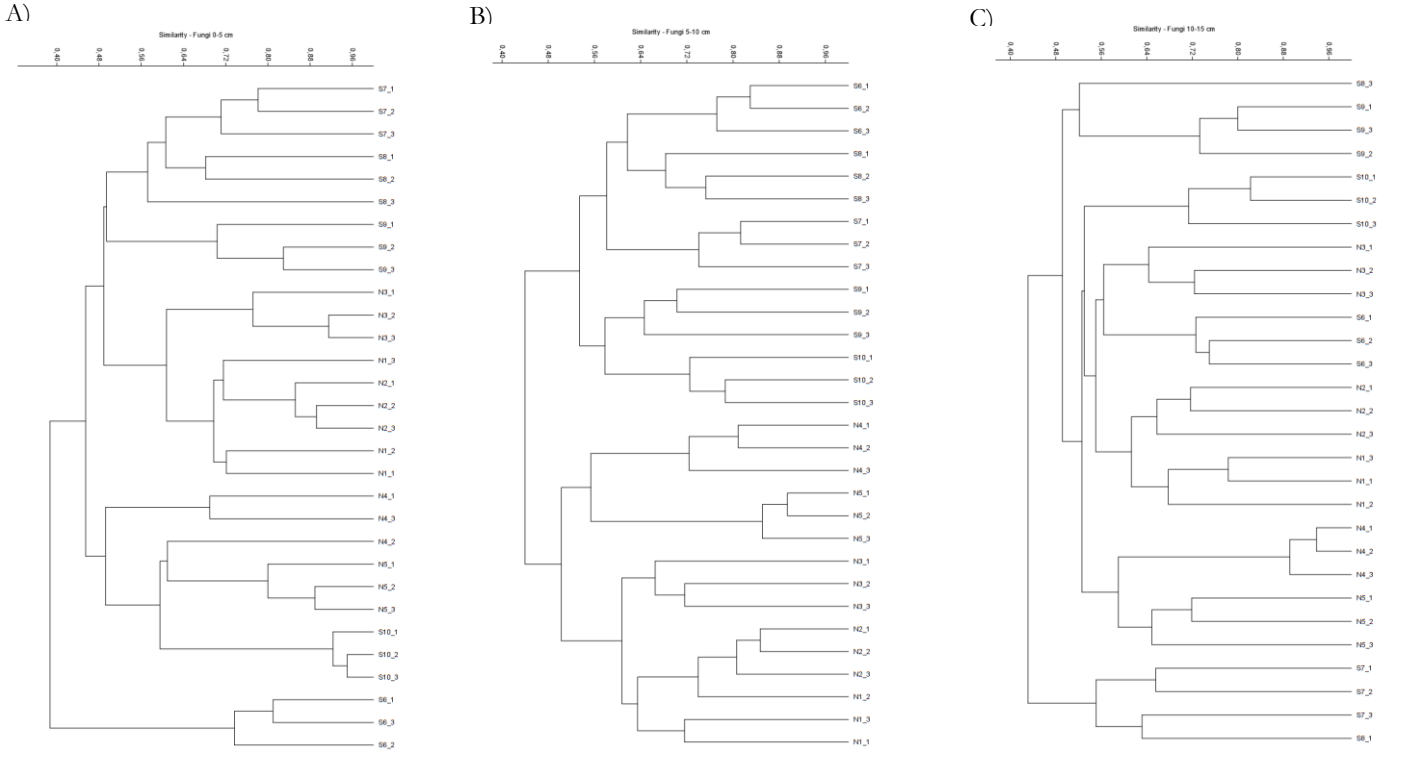

Fig. S2. Cluster analyses based on 18S rRNA gene for fungal fingerprints (A, B, C) obtained from the ten study sites at north- and south-facing areas ($N_{1\text{-}5}$ and $S_{6\text{-}10}$, respectively) for each of the three soil depths (0-5 cm, 5-10 cm and 10-15 cm). The results are shown pairwise, i.e. the couples of north- and south-facing sites (N_1-S_6; N_2-S_7; N_3-S_8; N_4-S_9; N_5-S_{10}) at the same elevation (1200 m; 1400 m; 1600 m; 2000 m; 2400 m a.s.l.). Values at the axis correspond to the percentage of similarity, based on the Dice correlation coefficient.

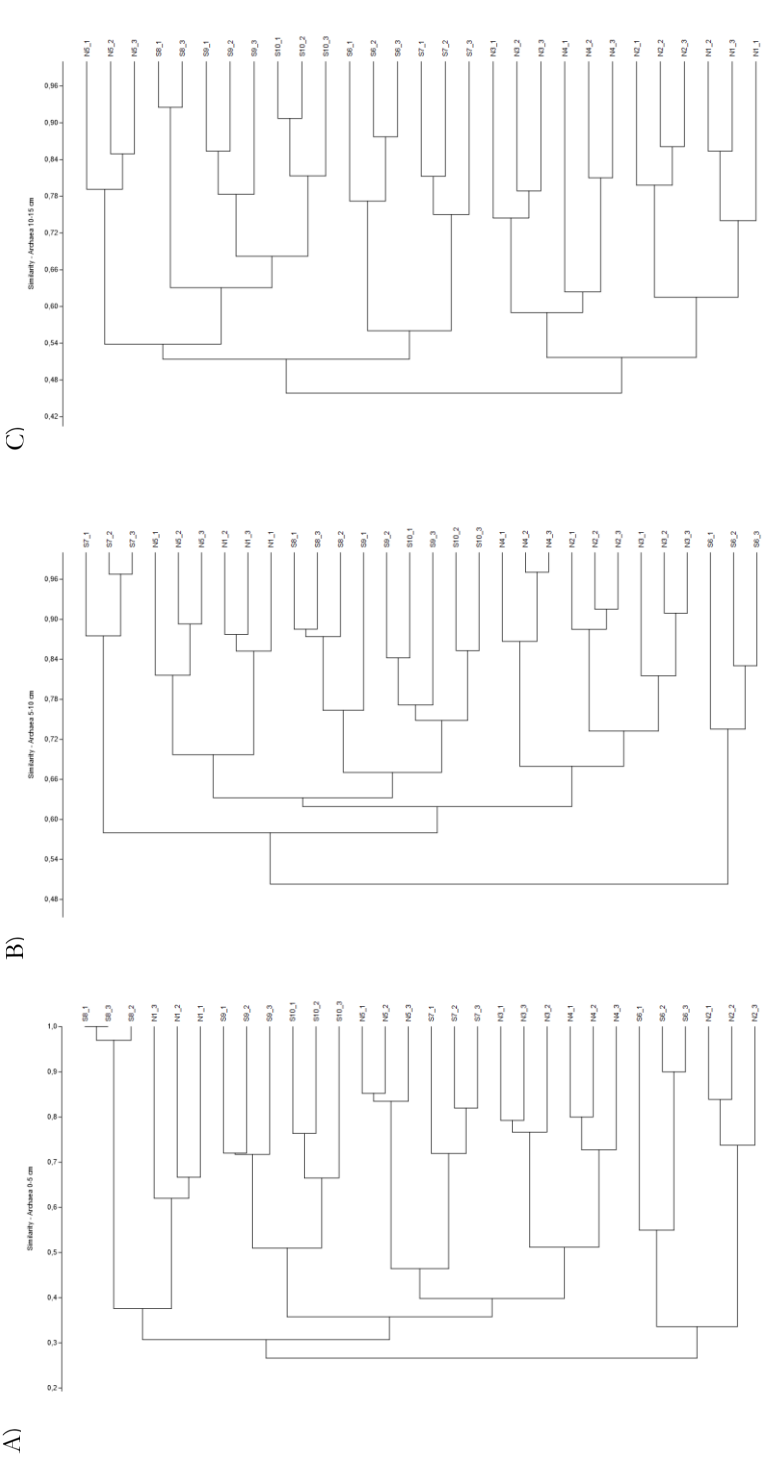

Fig. S3. Cluster analyses based on 16S rRNA gene for archaeal fingerprints (A, B, C) obtained from the ten study sites at north- and south-facing areas ($N_{1\text{-}5}$ and $S_{6\text{-}10}$, respectively) for each of the three soil depths (0-5 cm, 5-10 cm and 10-15 cm). The results are shown pairwise, i.e. the couples of north- and south-facing sites (N_1-S_6; N_2-S_7; N_3-S_8; N_4-S_9; N_5-S_{10}) at the same elevation (1200 m; 1400 m; 1600 m; 2000 m; 2400 m a.s.l.). Values at the axis correspond to the percentage of similarity, based on the Dice correlation coefficient.

III. Paper 2

Ground cover and slope exposure effects on micro- and mesobiota in forest soils

(photo by T. Bardelli)

(photo by D. Tatti)

Ground cover and slope exposure effects on micro- and mesobiota in forest soils

María Gómez-Brandón[a,1,*], Judith Ascher-Jenull[a,b,1], **Tommaso Bardelli[a,b]**, Flavio Fornasier[c], Giacomo Sartori[d], Giacomo Pietramellara[b], Paola Arfaioli[b], Markus Egli[e], Anneke Beylich[f], Heribert Insam[b] , Ulfert Graefe[f]

[a]Institute of Microbiology, University of Innsbruck, Technikerstraße 25d, 6020 Innsbruck, Austria
[b]Department of Agrifood and Environmental Science, University of Florence, Piazzale delle Cascine 18, 50144 Florence, Italy
[c]Council for Research and Experimentation in Agriculture, Via Trieste 23, 34170 Gorizia, Italy
[d]Museo delle Scienze (MUSE), Corso del Lavoro e della Scienza 3, 38122 Trento, Italy
[e]Department of Geography, University of Zürich, Winterthurerstrasse 190, 8057 Zürich, Switzerland
[f]IFAB Institut für Angewandte Bodenbiologie GmbH, Tornberg 24a, 22337 Hamburg, Germany

[*]Corresponding author: Maria.Gomez-Brandon@uibk.ac.at
[1]Both authors contributed equally to this paper

Ecological Indicators, September 2017, Volume 80, pp 174-185
DOI: 10.1016/j.ecolind.2017.05.032

Contribution: T. Bardelli participated in defining the field experimental design and sampling campaign, and in performing part of the laboratory work.

Abstract

The interrelation of Alpine topography with the micro – and mesobiota is still poorly understood. We investigated the effects of ground cover type and slope exposure on the soil microbial biomass (double-stranded DNA, dsDNA) and abundances (real time PCR, qPCR); hydrolytic enzyme activities; and enchytraeid community structure in top soils (2.5-cm increments depth) in subalpine forests in the Italian Alps. Dominant ground covers were grass, moss, litter and woody debris at the north- and the south-facing slopes. The autochthonous soil microbiota (bacteria, fungi and archaea) was quantified by qPCR in the extracellular (eDNA) and intracellular fraction (iDNA) of the total soil DNA pool. A higher eDNA/iDNA ratio indicative of lower microbial activity was recorded in the deepest layer of the grass plots at the north-facing slope. This can be related to a lower degradation of eDNA and/or to an accumulation of eDNA with increasing depth as a result of leaching. The exposure effect was enzyme-specific and higher activities occurred under woody debris primarily at the south-facing slope. These plots also showed a higher nutrient content and a greater microbial biomass assessed as dsDNA yields. Total microannelid abundance was elevated on north-facing slopes on account of strong acidity indicator species. This was related to soil pH being one unit lower compared to the south-facing slope. The thickness of the organic layer (OL+OF+OH) was elevated at the north-facing slope due to a considerably thicker OH-horizon. The vast majority of microannelids at this slope occurred in the organic layer, while at south exposure they were almost evenly distributed between the organic layer and the mineral soil (A-horizon). Exposure was found to be more determinative for the composition of microannelid assemblages than the ground cover type.

Keywords: microbial communities; microannelids; extracellular DNA; hydrolytic enzyme activities; humus forms

Highlights

- Discrimination between extra- and intracellular DNA in subalpine environments.
- Enzyme type-specific reactions to ground cover and slope exposure.
- Thermal effect due to exposure largely affected enchytraeid community composition.
- Exposure rather than ground cover had a higher influence on humus profile properties.

1. Introduction

Mountain ecosystems are predicted to experience a rapid warming in the future with distinct consequences for soil organic matter (SOM) quality and quantity (Mountain Research Initiative EDW Working Group, 2015). According to Beniston et al. (1997), an increase of approximately 2 °C of the annual minimum temperature has been observed in the European Alps during the 20th century. Changes in the abiotic environment due to rising temperatures may affect the microbial community structure, its activity and diversity, as well as vegetation composition (A'Bear et al., 2014), with implications for both ecosystem regulation and carbon feedbacks (Allison et al., 2010).

Soil microorganisms and in turn their enzymatic capabilities are further influenced by the activities of soil fauna that lives along them (Bardgett and Wardle, 2010). Enchytraeidae (Clitellata: Oligochaeta) are considered a keystone group responsible for the maintenance of decomposition processes and the functioning of detrital food webs (Didden, 1993; Karaban and Uvarov, 2014). The response of enchytraeids to abiotic factors was

found to be species-dependent (Graefe and Beylich, 2003; Beylich and Graefe, 2009). Species assemblages of soil microannelids can exhibit site-specific differences as shown by Beylich et al. (1995); Jänsch et al. (2005); and Ascher et al. (2012). These latter authors observed that both the slope exposure and the altitude - and consequently the thermal conditions - exerted an interactive effect on the microannelid population in a forested Alpine ecosystem. They found that the species richness of microannelid assemblages was higher under warmer conditions (south-exposure and lower altitudes).

Slope aspect determines the amount of solar irradiation, and thus energy received. This does not only influence the soil temperature, but also the soil water retention and availability, nutrient dynamics (Egli et al., 2006, 2009), composition and activity of soil microbial communities (Kang et al., 2003; Ascher et al., 2012) and soil fauna (Ascher et al., 2012). However, to date the interrelation of Alpine topography with the micro – and mesobiota is still poorly understood. We assume that humus forms represent these interactions in a generic way. Humus form thickness and horizontation were studied to detect relations with depth distribution of soil biota.

We hypothesise that the influence of slope aspect is modified by factors being effective on a smaller scale, such as shadowing by trees or higher water retention under woody debris. Therefore, we tested the effects of ground cover type and slope exposure on the soil microbial biomass and abundances; hydrolytic enzyme activities; and enchytraeid community structure in top soils of subalpine forests in the Italian Alps. The autochthonous soil microbiota (bacteria, fungi and archaea) was quantified in the extracellular (eDNA) and intracellular fraction (iDNA) of the total soil DNA pool. The eDNA/iDNA ratio was also calculated as a proxy of microbial activity.

2. Material and Methods

2.1. Study area and soil sampling

We studied two sites located at a subalpine altitude of 1600 m a.s.l. in Val di Rabbi (Trentino, Italy) on a north- and south-facing slope, respectively (N_3: 46° 24' 08" N; 10° 48' 46.2" E; and S_8: 46° 22' 41.4" N; 10° 55' 19.3" E). Both subalpine sites are on acidic paragneiss or morainic material consisting of paragneiss, predominated by Norway spruce (*Picea abies* (L.) Karst) (Petrillo et al., 2015). The soils are classified as Cambisols to Umbrisols according to Egli et al. (2006). The sampling was performed in June 2013, where the annual air temperature at site N_3 was 3.5 °C and at site S_8 5.5 °C (Fravolini et al., 2016).

The dominant ground covers were i) grass, moss and accumulation of branches at the north-, and ii) grass, organic litter and accumulation of branches at the south-facing sites. At each study site and for each ground cover three adjacent plots (5 x 5 m) were set up at 5 m distance from each other in a total area of 25 x 25 m. For the chemical and microbiological analyses five soil samples were randomly taken in each plot with a sampling depth of 15 cm wherever possible, using a corer device (ø 5 cm). Due to a high stone content, sampling depth was in some cases reduced to 10 or 12.5 cm. Samples were divided using a knife into sub-samples of 2.5 cm depth intervals starting at the top of the organic layer (2.5 cm depth correspond to ~50 cm^3). For the soil fauna and description of the humus profile one soil sample was collected from each plot in the immediate vicinity of the sample taken for the pH measurement by using the corer device as described above. The humus profile description was performed directly in the field using the open soil corer. Afterwards, soil samples for microbiological and physico-chemical analyses were kept in cooling boxes and transferred to the laboratory. They were sieved (< 2 mm), carefully separated from root

fragments and stones, and stored at 4 °C for physico-chemical and biological analyses and at -20 °C for molecular analyses, respectively. Soil samples for microannelid determination were kept in plastic bags, transported to the laboratory at ambient temperature and stored at 10 ± 2 °C until extraction.

2.2. Physico-chemical analyses

Soil samples were oven-dried (105 °C) for at least 24 h to determine their dry weight. The volatile solids (VS) content was determined by loss on ignition (LOI) in a muffle furnace (Carbolite, CWF 1000) at 550 °C for 5 h. Total C and N contents were analysed in dried samples, using a CN analyzer (TruSpec CHN; LECO, Michigan, U.S.A.). Electrical conductivity (EC) and pH were determined in soil:water extracts (1:10, w/v) by using a conductivity Meter LF 330 WTW (Weilheim, Germany) and a pH Meter Metrohm 744, respectively. Inorganic nitrogen (NH_4^+ and NO_3^-) was determined in 0.0125 M $CaCl_2$ extracts, as described by Kandeler (1993a, b). Total P was determined by H_2SO_4-H_2O_2-HF digestion as described by Bowman (1988). Available P was assessed following the Bray and Kurtz method based on NH_4F extraction recommended for acid soils (Bray and Kurtz, 1945). Both the total and available P concentrations were determined according to the ascorbic acid method as described by Kuo (1996).

2.3. Potential enzymatic activities

A heteromolecular exchange procedure as described by Fornasier and Margon (2007) by using a 4% solution of lysozyme as desorbant and bead-beating agent was used for the assessment of the following hydrolases: i) C-cycle: cellulase (*cell*); xylanase (*xyl*); α- and β-glucosidases (*alfagluc* and *betagluc*); ii) P-cycle: acid and alkaline phosphomonoesterase (*acP* and *alkP*); phosphodiesterase (*bisP*); pyrophosphate-phosphodiesterase (*piroP*); iii) N-cycle: leucine- and lysine-aminopeptidase (*leu* and *lys*); iv) S-cycle:

arylsulfatase (*arylS*);. All the measurements were performed in duplicate for each field replicate and the activities were expressed as nanomoles of 4-methyl-umbelliferyl (MUF) min^{-1} g^{-1} dry soil.

2.4. Microbial biomass assessed as double-stranded DNA (dsDNA)

Direct extraction of total soil DNA (tDNA) followed by PicoGreen-based quantification of *crude* (not purified) double-stranded DNA (dsDNA) was performed to estimate soil microbial biomass (Fornasier et al., 2014).

2.5. Sequential DNA extraction (eDNA *vs.* iDNA)

The sequential extraction of the extracellular (eDNA) and intracellular fraction (iDNA) of the soil metagenome was performed according to Ascher et al. (2009a) by applying a combined mechanical-chemical cell lysis using the Fast DNA Kit for soil and FastPrep instrument (MP Biomedicals). DNA extracts were purified using the GeneClean® procedure (MP Biomedicals) and quantitatively and qualitatively characterised by PicoGreen based fluorometry (dsDNA; Qubit, LifeTechnologies), µL-spectrophotometry (PicoDrop) and agarose-gel electrophoresis (Ascher et al., 2012).

2.6. Quantitative real-time PCR

Quantitative real-time PCR (qPCR) analysis was chosen to determine the 16S rRNA gene copy number of bacteria and archaea, and the 18S rRNA gene copy number of fungi from both the intracellular and extracellular fractions of the total soil DNA pool. Real-time PCR was conducted using the 1X Sensimix™ SYBR® Hi-rox (Bioline, USA) and performed in a Rotor-Gene™ 6000 (Corbett Research, Sydney, Australia) in 20-µl volumes. Each standard reaction mix contained 1X Sensimix™ SYBR® Hi-rox (Bioline, USA), forward and reverse primers (200 nM each primer), 0.4 mg mL^{-1} BSA, distilled water (RNase/DNase free, Gibco™, UK) and 2 µL of

1:10 diluted DNA-extracts, and ten-fold diluted standard DNA. To build the standards we used purified PCR products of known concentrations of the following pure cultures as template: *Nitrosomonas europaea* (DSMZ 21879) – bacteria; *Methanobacterium formicicum* (DSMZ 1535) – archaea; and *Fusarium solani* – fungi. The primer pairs used were: 1055f/1392r (bacteria; Ferris et al., 1996); FF390/FR1 (fungi; Prévost- Bouré et al., 2011); and Parch 519f/Arc915r (archaea; Coolen et al., 2004). Stock concentration [gene copies μL^{-1}] was determined via PicoGreen measurement and freshly prepared for the standard curve construction with ten-fold dilutions ranging from 109 to 102 copies μL^{-1}. All standards and samples were run in duplicate following the cycling conditions shown in Bardelli et al. (2017). To check for product specificity and potential primer dimer formation, runs were completed with a melting analysis starting from 60 °C to 95 °C with temperature increments of 0.25 °C and a transition rate of 5 s. The purity of the amplified products was also checked by the presence of a single band of the expected length on a 1% agarose gel stained with the DNA stain Midori Green (Nippon Genetics, Germany) and visualised by UV-transillumination (Vilber Lourmat Deutschland GmbH).

2.7. Humus forms and soil fauna

2.7.1. Humus forms

The designation of the humus forms and organic horizons followed Zanella et al. (2011). The mineral horizon designation was done according to the Guidelines for Soil Description (FAO, 2006) and the German soil classification system (Ad-hoc-AG-Boden, 2005).

2.7.2. Microannelid sample treatment

Microannelid extraction from soil samples was performed over 48 h by a wet-funnel technique without heating (Dunger and Fiedler, 1989; ISO

23611-3, 2007). The extracted animals were counted and then identified alive according to the key of Schmelz and Collado (2010). Knowledge-based acidity indicator values and humus form preferences according to Graefe and Schmelz (1999) are referred to. The following acidity indicator groups are distinguished: 'indicators of strong acidity' (species with indicator values 1–3), 'indicators of moderate acidity' (species with indicator values 4–6) and 'indicators of slight acidity' (species with indicator value 7). During preliminary investigations in the precedent year, microannelid assemblages were found that did not match the visible humus form. In order to disentangle this inconsistency a sampling design was chosen that allowed physico-chemical measurements like pH in the direct vicinity of the microannelid assemblage.

2.8. Statistical analyses

One-factor ANOVA was carried out for each soil depth separately to evaluate the effects of ground cover on the soil physico-chemical and microbiological parameters at both north-and south-facing sites. Significant differences ($p < 0.05$) were further analysed by paired comparisons with the Tukey HSD test. The vertical gradient of each variable was tested by repeated measurements ANOVA (ANOVAR) considering the sequentially sampled soil horizons in 2.5-cm intervals. The normality and the variance homogeneity of the data were tested prior to ANOVA by using the Kolmogorov-Smirnov and Levene´s tests, respectively. Before analysis, data were log- or square root-transformed to meet the assumptions for ANOVA (when it was required). The software package Statistica 9 (StatSoft, USA) was used to perform these analyses.

Statistical analyses for microannelid parameters were performed using the software package Systat 13.1 (Systat Software inc., USA). The normality and the variance homogeneity of the data were tested prior to ANOVA or Two-

sample t-test. Before analysis, microannelid abundance data were square root-transformed to meet the assumptions for ANOVA (Post-Hoc: Tukey HSD-test) or Two-sample t-test. A nonparametric Mann-Whitney U-Test was carried out to evaluate the effects of exposure and ground cover on the dominance of microannelid acidity indicator groups as well as on the thickness of organic horizons (L, OF, OH), as transformations (ln, log, square-root) did not produce satisfactory results. Data for the total thickness of the humus layer were normally distributed, thus a t-test was used, checking for differences between N_3 and S_8. Pearson correlations to evaluate the potential use of eDNA as a nutrient source for microannelids were also assessed with the Systat 13.1 software program.

3. Results

3.1. Soil physico-chemical and microbiological parameters

An overview of the soil physico-chemical and microbiological parameters of the topsoil (0-15 cm: 2.5 cm intervals) at the north- and the south-facing sites (N_3 and S_8) under the different ground covers is given in Tables 1-4. For each of the soil depths, those parameters that led to significant differences among the ground cover types according to one-factor ANOVA are reported below.

In the uppermost soil layer (0-2.5 cm) at N_3 the electrical conductivity was 2-fold lower in the moss plots than in the branch and grass plots (ANOVA $F_{2,6} = 5.3$, $p = 0.047$). Likewise, leucine- and lysine-aminopeptidase potential activities were also around 3-times lower in the moss plots than in the other two ground covers (*leu*: ANOVA $F_{2,6} = 9.5$, $p = 0.014$; *lys*: ANOVA $F_{2,6} = 9.4$, $p = 0.014$). The same trend was recorded for the alkaline phosphomonoesterase activity (*alkP*: ANOVA $F_{2,6} = 5.5$, $p = 0.044$). Furthermore, the highest total P content was recorded in the moss plots (ANOVA $F_{2,6} = 8.5$, $p = 0.018$). For both iDNA and eDNA fractions the

bacterial and fungal abundance assessed by qPCR were significantly higher in the moss plots followed by grass and branch plots (bacteria, iDNA: ANOVA $F_{2,6}$ = 18.4, p = 0.003; eDNA: ANOVA $F_{2,6}$ = 12.1, p = 0.008; fungi, iDNA: ANOVA $F_{2,6}$ = 41.1, p = 0.0003; eDNA: ANOVA $F_{2,6}$ = 15.8, p = 0.004). In addition, the archaeal abundance in the iDNA fraction was around 3-times higher in the moss plots than in those covered with grass and branches (ANOVA $F_{2,6}$ = 5.7, p = 0.04).

In the soil layers ranging from 2.5 to 7.5 cm at N_3 the highest total P content was also found in the moss plots (ANOVA $F_{2,6}$ = 6.1, p = 0.035; ANOVA $F_{2,6}$ = 82.8, p = 0.00004, respectively). Moreover, for the 2.5-5 cm soil layer the lowest alkaline phosphomonoesterase, leucine- and lysine-aminopeptidase activities were registered in the moss plots (*alkP*: ANOVA $F_{2,6}$ = 5.4, p = 0.045; *leu*: ANOVA $F_{2,6}$ = 5.6, p = 0.042; *lys*: ANOVA $F_{2,6}$ = 6.4, p = 0.032). Likewise, in the 5-7.5 cm layer the alkaline phosphomonoestarase, together with pyrophosphate-phosphodiesterase and cellulase activities were between 3-6 times lower in the moss plots than in the other ground cover types (*alkP*: ANOVA $F_{2,6}$ = 7.3, p = 0.024; *piroP*: ANOVA $F_{2,6}$ = 11.2, p = 0.009; *cell*: ANOVA $F_{2,6}$ = 5.4, p = 0.045). In contrast to the top 7.5 cm, in the 7.5-10 cm layer total P was 2-fold higher in the grass plots compared to moss and branch plots (ANOVA $F_{2,6}$ = 14.8, p = 0.005).

Table 1
Overview of soil physico-chemical parameters at the north- and the south-facing sites (N_3 and S_8, respectively) and as a function of the different ground covers (branches, grass, moss and litter). Values are means with SD in brackets. Data are expressed on a dry weight basis. Different letters in bold, for each of the soil depths, indicate significant differences ($p < 0.05$; ANOVA followed by Tukey post-hoc test) with regard to the ground cover type. Due to a high stone content, sampling depth was in some cases reduced to 10 or 12.5 cm.

Soil depth	**0-2.5 cm**			**2.5-5 cm**			**5-7.5 cm**			**7.5-10 cm**			**10-12.5 cm**		
Site N_3	**Branches**	**Grass**	**Moss**	**Branches**	**Grass**	**Moss**	**Branches**	**Grass**	**Moss**	**Branches**	**Grass**	**Moss**	**Branches**	**Grass**	**Moss**
Moisture (%)	48**a** (6.4)	50**a** (13.1)	53**a** (4.4)	42**a** (2.8)	55**a** (2.1)	57**a** (5.8)	44**a** (5.8)	42**a** (7.6)	47**a** (12)	36**a** (7.9)	25**a** (3.6)	36**a** (8.3)	n.a.	33 (7.1)	n.a.
LOI (%)	83**a** (4.6)	87**a** (1.2)	81**a** (17)	64**a** (12.8)	77**a** (18.2)	80**a** (19)	34**a** (6.3)	52**a** (5.8)	83**a** (10)	22**a** (2.7)	16**a** (4.3)	35**a** (9.2)	n.a.	13 (4.7)	n.a.
pH	5.2**a** (0.5)	5.4**a** (0.3)	4.6**a** (0.1)	4.8**a** (0.5)	4.7**a** (0.4)	4.0**a** (0.2)	4.6**a** (0.5)	4.3**a** (0.4)	3.9**a** (0.2)	4.4**a** (0.3)	4.4**a** (0.3)	4.0**a** (0.4)	n.a.	4.3 (0.6)	n.a.
EC ($\mu S\ cm^{-1}$)	160**a** (21)	166**a** (31)	84**b** (22)	74**a** (11)	67**a** (22)	60**a** (19)	45**a** (14)	50**a** (13)	55**a** (18)	29**a** (7.0)	34**a** (13)	37**a** (12)	n.a.	41 (3.0)	n.a.
Total C (%)	47**a** (1.4)	49**a** (1.5)	47**a** (6.7)	33**a** (6.4)	44**a** (8.4)	41**a** (11)	27**a** (9.4)	49**a** (1.7)	45**a** (7.0)	5.8**a** (1.7)	6.5**a** (1.8)	4.7**a** (3.0)	n.a.	18.5 (7.9)	n.a.
Total N (%)	1.7**a** (0.2)	1.6**a** (0.1)	1.6**a** (0.3)	1.4**a** (0.3)	1.5**a** (0.5)	1.4**a** (0.1)	0.9**a** (0.2)	1.5**a** (0.4)	1.1**a** (0.3)	0.4**a** (0.02)	0.3**a** (0.05)	0.2**a** (0.01)	n.a.	0.6 (0.1)	n.a.
NH_4^+ ($mg\ kg^{-1}$ dw)	145**a** (35)	123**a** (37)	116**a** (20)	118**a** (37)	104**a** (14)	62**b** (16)	49**ab** (17)	35**a** (11)	56**b** (11)	24**a** (9.0)	15**a** (4.0)	12**a** (2.0)	n.a.	26 (9.0)	n.a.
NO_3^- ($mg\ kg^{-1}$ dw)	64**a** (12)	44**a** (13)	142**a** (35)	39**a** (8.0)	23**a** (3.0)	34**a** (11)	6.0**a** (2.0)	11**a** (2.0)	8.0**a** (2.0)	3.0**a** (0.3)	0.8**a** (0.03)	1.0**a** (0.03)	n.a.	1.3 (0.3)	n.a.
Total P ($mg\ kg^{-1}$)	542**a** (72)	657**ab** (135)	926**b** (119)	333**a** (96)	734**ab** (152)	1033**b** (338)	534**a** (178)	391**a** (93)	628**b** (110)	266**a** (62)	591**b** (184)	221**a** (21)	n.a.	469 (28)	n.a.
Available P ($mg\ kg^{-1}$)	291**a** (43)	216**a** (42)	358**a** (17)	105**a** (55)	193**a** (91)	139**a** (47)	66**a** (23)	87**a** (28)	55**a** (19)	13**a** (2.0)	14**a** (7.0)	25**a** (3.0)	n.a.	12 (3.0)	n.a.

LOI: loss on ignition
EC: electrical conductivity
n.a.: not available

Table 1. To be continued

Soil depth	0-2.5 cm			2.5-5 cm			5-7.5 cm			7.5-10 cm			10-12.5 cm			12.5- 15 cm		
Site S_8	**Branches**	**Grass**	**Litter**	**Branches**	**Grass**	**Litter**	**Branches**	**Grass**	**Litter**	**Branches**	**Grass**	**Litter**	**Branches**	**Grass**	**Litter**	**Branches**	**Grass**	**Litter**
Moisture (%)	58**a** (5.3)	43**a** (6.5)	50**a** (8.7)	52**a** (8.3)	41**a** (9.5)	35**a** (8.8)	43**a** (9.1)	34**a** (4.7)	26**a** (8.2)	39**a** (3.4)	33**a** (9.7)	19**a** (4.3)	n.a.	25**a** (7.3)	18**a** (4.4)	n.a.	n.a.	19 (4.9)
LOI (%)	79**a** (10.6)	74**a** (13)	63**a** (10)	79**a** (11.3)	29**b** (8.0)	20**b** (19)	72**a** (11)	27**b** (3.5)	20**b** (4.3)	57**a** (5.4)	14**b** (3.2)	14**b** (1.6)	n.a.	14**a** (1.1)	13**a** (1.9)	n.a.	n.a.	12 (2.5)
pH	5.3**a** (0.3)	5.3**a** (0.1)	5.3**a** (0.7)	5.6**a** (0.6)	5.0**a** (0.4)	5.3**a** (0.9)	5.2**a** (0.9)	4.7**a** (0.6)	5.2**a** (0.8)	5.0**a** (0.8)	4.8**a** (0.5)	5.0**a** (0.2)	n.a.	5.0**a** (0.3)	5.2**a** (0.1)	n.a.	n.a.	5.1 (0.2)
EC ($\mu S\ cm^{-1}$)	208**a** (41)	64**b** (16)	62**b** (15)	129**a** (30)	37**b** (9.0)	40**b** (4.0)	105**a** (11)	29**b** (6.8)	35**b** (5.0)	92**a** (21)	24**b** (7.0)	42**b** (11)	n.a.	15**a** (5.0)	22**a** (6.0)	n.a.	n.a.	24 (2.0)
Total C (%)	43**a** (3.6)	39**a** (7.4)	35**a** (10)	41**a** (6.6)	15**b** (4.1)	18**b** (7.3)	44**a** (0.2)	14**b** (1.7)	9.1**b** (2.6)	27**a** (7.1)	6.7**b** (2.4)	5.9**b** (0.5)	n.a.	6.0**a** (1.1)	7.2**a** (2.1)	n.a.	n.a.	5.4 (1.8)
Total N (%)	1.6**a** (0.1)	1.2**a** (0.1)	1.3**a** (0.5)	1.4**a** (0.1)	0.7**a** (0.1)	0.8**a** (0.06)	1.4**a** (0.1)	0.5**b** (0.2)	0.4**b** (0.01)	1.1**a** (0.2)	0.3**b** (0.06)	0.3**b** (0.01)	n.a.	0.3**a** (0.01)	0.3**a** (0.07)	n.a.	n.a.	0.3 (0.08)
NH_4^+ (mg kg^{-1} dw)	160**a** (44)	69**b** (9.0)	60**b** (9.0)	96**a** (14)	29**b** (11)	24**b** (5.0)	77**a** (16)	23**b** (5.0)	17**b** (7.0)	68**a** (18)	12**b** (3.0)	13**b** (0.5)	n.a.	12**a** (4.0)	14**a** (5.0)	n.a.	n.a.	9.0 (2.0)
NO_3^- (mg kg^{-1} dw)	154**a** (33)	33**b** (9.0)	32**b** (6.0)	66**a** (17)	15**b** (2.0)	15**b** (3.0)	19**a** (8.0)	3.0**b** (0.9)	3.0**b** (1.0)	26**a** (9.0)	2.0**b** (0.8)	1.0**b** (0.09)	n.a.	1.0**a** (0.08)	1.0**a** (0.03)	n.a.	n.a.	0.8 (0.02)
Total P (mg kg^{-1})	687**a** (189)	663**a** (199)	592**a** (144)	537**a** (190)	635**a** (176)	582**a** (40)	496**a** (95)	321**a** (84)	407**a** (72)	566**a** (103)	344**a** (34)	549**a** (149)	n.a.	328**a** (21)	483**a** (157)	n.a.	n.a.	456 (167)
Available P (mg kg^{-1})	196**a** (20)	116**a** (41)	161**a** (35)	161**a** (25)	74**ab** (18)	35**b** (9.0)	73**a** (11)	22**b** (6.0)	20**b** (6.0)	65**a** (16)	8.0**b** (0.5)	12**b** (1.5)	n.a.	8.0**a** (0.5)	8.0**a** (0.9)	n.a.	n.a.	8.0 (1.5)

LOI: loss on ignition
EC: electrical conductivity
n.a.: not available

In the top 2.5 cm at S_8 the branch ground cover had a higher EC level (3-fold higher) compared to grass and litter plots (ANOVA $F_{2,6}$ = 15.8, p = 0.004). The same trend was observed for inorganic N (NH_4^+: ANOVA $F_{2,6}$ = 10.4, p = 0.011; NO_3^-: ANOVA $F_{2,6}$ = 28.8, p = 0.0008). Accordingly, in the subsequent layers from 2.5 to 10 cm, the branch plots showed the highest EC, loss on ignition, total C and N, as well as the highest inorganic N and available P content. Moreover, certain enzyme activities involved in the C cycle (*betaglu*: ANOVA $F_{2,6}$ = 5.6, p = 0.042; and *cell*: ANOVA $F_{2,6}$ = 8.3, p = 0.019), together with those related to the N- and P-cycles (*leu*: ANOVA $F_{2,6}$ = 8.7, p = 0.017; *lys*: ANOVA $F_{2,6}$ = 11.52, p = 0.009; *alkP*: ANOVA $F_{2,6}$ = 10.2, p = 0.012) were also significantly higher (between 2-5 times) in the branch plots compared to the grass and litter ones in the 2.5-5-cm soil layer. These three latter enzyme activities followed the same trend with respect to the ground covers in the 5-7.5-cm and 7.5-10-cm layers. Additionally, the highest phosphodiesterase and pyrophosphate-phosphodiesterase activities were registered in the branch plots in the 5-7.5-cm soil layer (*bisP*: ANOVA $F_{2,6}$ = 17.4, p = 0.003; *piroP*: ANOVA $F_{2,6}$ = 5.9, p = 0.038). The branch plots also showed the highest xylanase and phosphodiesterase activities in the 7.5-10-cm layer (*xyl*: ANOVA $F_{2,6}$ = 5.2, p = 0.04; *bisP*: ANOVA $F_{2,6}$ = 22.6, p = 0.002). Accordingly, soil microbial biomass assessed as dsDNA content was also significantly higher in the branch plots than in the grass and litter ones for the soil layers ranging from 5 to 10 cm (ANOVA $F_{2,6}$ = 12.9, p = 0.006; ANOVA $F_{2,6}$ = 7.4, p = 0.023 for 5-7.5 and 7.5-10-cm layers, respectively).

Table 2.
Overview of soil potential enzymatic activities at the north- and the south-facing sites (N_3 and S_8, respectively) and as a function of the different ground covers (branches, grass, moss and litter). Values are means with SD in brackets. Data are expressed as nanomoles of MUF min^{-1} g^{-1} wood dry weight. Different letters in bold, for each of the soil depths, indicate significant differences ($p < 0.05$; ANOVA followed by Tukey post-hoc test) with regard to the ground cover type. Due to a high stone content, sampling depth was in some cases reduced to 10 or 12.5 cm.

Soil depth	**0-2.5 cm**			**2.5-5 cm**			**5-7.5 cm**			**7.5-10 cm**			**10-12.5 cm**		
Site N_3	**Branches**	**Grass**	**Moss**	**Branches**	**Grass**	**Moss**	**Branches**	**Grass**	**Moss**	**Branches**	**Grass**	**Moss**	**Branches**	**Grass**	**Moss**
Cellulase	59**a** (12)	36**a** (12)	21**a** (5.1)	12**a** (6.3)	16**a** (3.3)	9.0**a** (3.7)	5.8**a** (2.2)	5.2**a** (4.0)	1.6**b** (0.4)	1.4**a** (0.7)	2.4**a** (1.1)	1.2**a** (0.9)	n.a.	1.1 (0.3)	n.a.
Xylanase	48**a** (7.2)	37**a** (2.8)	28**a** (7.3)	29**a** (8.8)	36**a** (13)	22**a** (4.4)	20**a** (3.7)	20**a** (9.3)	9.6**a** (2.5)	8.2**a** (3.9)	9.2**a** (2.0)	5.2**a** (1.4)	n.a.	5.4 (1.4)	n.a.
α- glucosidase	42**a** (7.9)	29**a** (7.0)	29**a** (7.8)	30**a** (13.7)	24**a** (6.1)	24**a** (1.3)	22**a** (3.0)	19**a** (9.0)	12**a** (4.5)	8.7**a** (1.8)	16**a** (7.1)	7.4**a** (1.4)	n.a.	10 (3.3)	n.a.
β-glucosidase	349**a** (70)	223**a** (64)	139**a** (30.5)	106**a** (25)	126**a** (41)	68**a** (20)	63**a** (7.0)	59**a** (10)	24**a** (9.5)	25**a** (3.4)	28**a** (8.8)	15**a** (5.1)	n.a.	21 (2.6)	n.a.
Acid phosphomonoesterase	520**a** (134)	516**a** (194)	641**a** (93)	626**a** (188)	733**a** (182)	554**a** (125)	366**a** (41)	533**a** (95)	198**a** (52)	210**a** (69)	432**a** (98)	160**a** (40)	n.a.	157 (24)	n.a.
Alkaline phosphomonoesterase	342**a** (88)	286**a** (32)	79**b** (19)	215**a** (69)	84**ab** (16)	50**b** (11)	55**a** (28)	42**a** (14)	18**b** (8.0)	16**a** (3.2)	29**a** (8.0)	11**a** (1.2)	n.a.	20 (9.0)	n.a.
Phosphodiesterase	37**a** (8.0)	29**a** (2.9)	16**a** (0.6)	32**a** (0.9)	21**a** (9.0)	16**a** (2.1)	11**a** (0.4)	10**a** (1.9)	4.1**a** (1.4)	5.1**a** (0.9)	10**a** (1.7)	3.7**a** (0.6)	n.a.	5.3 (0.8)	n.a.
Pyrophosphate-phospodiesterase	35**a** (6.0)	25**a** (4.0)	6.1**b** (1.4)	38**a** (5.0)	6.4**ab** (0.6)	2.9**b** (1.4)	6.0**a** (0.5)	3.1**ab** (0.09)	0.9**b** (0.1)	1.9**a** (0.3)	3.7**a** (0.4)	1.0**a** (0.06)	n.a.	1.9 (0.05)	n.a.
Leucine-aminopeptidase	487**a** (72)	469**a** (143)	177**b** (22)	338**a** (96)	187**ab** (51)	107**b** (25)	121**a** (8.0)	98**a** (15)	59**a** (11)	47**a** (12)	97**a** (34)	44**a** (10)	n.a.	48 (13)	n.a.
Lysine-aminopeptidase	307**a** (35)	340**a** (42)	103**b** (14)	209**a** (55)	115**ab** (32)	65**b** (17)	88**a** (6.0)	61**a** (18)	40**a** (8.0)	32**a** (8.0)	50**a** (15)	32**a** (3.0)	n.a.	30 (13)	n.a.
Arylsulphatase	7.0**a** (1.6)	6.3**a** (1.7)	2.7**a** (0.8)	12**a** (5.6)	4.9**a** (0.9)	3.6**a** (0.8)	10**a** (0.7)	13**a** (1.9)	2.3**a** (1.4)	5.9**a** (0.05)	6.0**a** (6.2)	2.0**a** (0.09)	n.a.	7.1 (1.7)	n.a.

n.a.: not available

Table 2. To be continued

Soil depth	0-2.5 cm			2.5-5 cm			5-7.5 cm			7.5-10 cm			10-12.5 cm			12.5- 15 cm		
Site S_8	**Branches**	**Grass**	**Litter**	**Branches**	**Grass**	**Litter**	**Branches**	**Grass**	**Litter**	**Branches**	**Grass**	**Litter**	**Branches**	**Grass**	**Litter**	**Branches**	**Grass**	**Litter**
Cellulase	29**a** (10)	23**a** (14)	26**a** (12)	15**a** (2.1)	4.4**b** (1.5)	2.6**b** (0.7)	5.4**a** (2.7)	1.3**a** (0.5)	1.6**a** (0.8)	6.7**a** (3.5)	1.3**b** (0.1)	1.8**b** (0.4)	n.a.	0.6**a** (0.2)	0.9**a** (0.1)	n.a.	n.a.	0.9 (0.2)
Xylanase	23**a** (9.6)	28**a** (12.3)	21**a** (10.1)	21**a** (4.6)	17**a** (4.9)	14**a** (5.2)	14**a** (3.7)	8.9**a** (2.6)	7.9**a** (1.4)	18**a** (1.1)	5.9**b** (1.2)	6.7**b** (1.2)	n.a.	4.2**a** (0.7)	5.0**a** (1.4)	n.a.	n.a.	4.5 (0.9)
α- glucosidase	18**a** (3.3)	25**a** (3.5)	17**a** (2.7)	18**a** (3.6)	16**a** (9.9)	8.3**a** (1.9)	16**a** (2.9)	8.5**a** (1.6)	6.3**a** (1.8)	14**a** (5.2)	6.4**a** (1.5)	5.2**a** (0.5)	n.a.	3.2**a** (0.8)	3.6**a** (0.5)	n.a.	n.a.	2.8 (0.4)
β-glucosidase	140**a** (41)	141**a** (35)	126**a** (35)	129**a** (5.3)	56**b** (14)	37**b** (9.0)	62**a** (11)	26**a** (6.5)	25**a** (5.0)	52**a** (19)	20**a** (8.5)	29**a** (11)	n.a.	9.3**a** (1.4)	17**a** (1.6)	n.a.	n.a.	13 (2.7)
Acid phosphomonoesterase	670**a** (188)	763**a** (170)	739**a** (107)	639**a** (187)	659**a** (95)	594**a** (152)	538**a** (89)	714**a** (147)	662**a** (156)	1031**a** (260)	660**a** (190)	878**a** (157)	n.a.	264**a** (25)	805**a** (217)	n.a.	n.a.	647 (85)
Alkaline phosphomonoesterase	135**a** (12)	168**a** (29)	137**a** (18)	183**a** (22)	62**b** (17)	35**b** (6.1)	177**a** (29)	27**b** (1.0)	15**b** (1.8)	106**a** (27)	29**b** (8.0)	13**b** (2.5)	n.a.	18**a** (1.5)	12**a** (1.1)	n.a.	n.a.	14 (0.8)
Phosphodiesterase	29**a** (9.5)	35**a** (12)	29**a** (5.1)	26**a** (3.6)	19**a** (1.1)	10**a** (1.0)	33**a** (1.2)	11**b** (3.0)	7.0**b** (0.9)	29**a** (7.5)	10**b** (3.0)	6.2**b** (0.5)	n.a.	8.2**a** (1.4)	6.7**a** (1.3)	n.a.	n.a.	5.5 (1.4)
Pyrophosphate-phospodiesterase	28**a** (3.6)	40**a** (15)	47**a** (12)	49**a** (17)	12**a** (6.0)	11**a** (0.7)	44**a** (8.0)	6.4**b** (0.9)	6.4**b** (1.0)	26**a** (2.0)	8.2**b** (0.8)	8.3**b** (0.09)	n.a.	5.8**a** (0.6)	7.2**a** (0.03)	n.a.	n.a.	5.6 (1.2)
Leucine-aminopeptidase	200**a** (23)	226**a** (65)	124**a** (31)	205**a** (41)	106**ab** (20)	52**b** (4.0)	187**a** (28)	58**b** (9.0)	31**b** (10)	152**a** (34)	50**b** (14)	31**b** (5.0)	n.a.	39**a** (4.0)	27**a** (2.0)	n.a.	n.a.	25 (8.0)
Lysine-aminopeptidase	133**a** (22)	143**a** (41)	80**a** (23)	126**a** (18)	59**b** (13)	29**b** (9.0)	105**a** (22)	37**b** (6.0)	17**b** (0.7)	96**a** (15)	33**b** (11)	18**b** (1.5)	n.a.	22**a** (2.0)	13**a** (1.0)	n.a.	n.a.	12 (1.5)
Arylsulphatase	2.4**a** (0.1)	3.0**a** (0.8)	3.3**a** (0.9)	5.6**a** (0.7)	4.9**a** (0.7)	2.2**a** (0.3)	14**a** (0.6)	7.5**a** (1.4)	3.8**a** (1.2)	8.0**a** (1.7)	8.0**a** (1.9)	6.7**a** (3.4)	n.a.	9.3**a** (1.3)	6.1**a** (1.9)	n.a.	n.a.	4.7 (0.5)

n.a.: not available

The vertical gradient (0-15 cm) of each parameter was also evaluated for each of the ground cover types at N_3 and S_8 (Tables 1-4). A reduction in moisture content with soil depth was only recorded for the litter ground cover, being around 2-fold lower in the last three soil layers (from 7.5 to 15 cm) than in the uppermost 2.5-cm soil fraction (ANOVAR $F_{5,20} = 26.6$, $p < 0.0001$). A reduced loss on ignition as a function of soil depth was detected for both the branch and the grass plots (ANOVAR $F_{3,12} = 18.5$, $p = 0.02$; ANOVAR $F_{4,16} = 66.2$, $p < 0.0001$). Likewise, the uppermost layer from the moss and litter ground covers showed a higher loss on ignition (3-4 times higher) compared to the deeper layers (moss: ANOVAR $F_{3,12} = 30.1$, $p < 0.0001$; litter: ANOVAR $F_{5,20} = 40.02$, $p < 0.0001$). At N_3 soil pH was significantly higher in the top 2.5 cm regardless of the ground cover (branches: ANOVAR $F_{3,12} = 3.8$, $p = 0.04$; grass: ANOVAR $F_{4,16} = 5.9$, $p = 0.004$; moss: ANOVAR $F_{3,12} = 12.8$, $p = 0.0004$). A significant reduction in EC with depth was recorded for all of the ground covers at N_3 and S_8 (branches: ANOVAR $F_{3,12} = 24.9$, $p < 0.0001$; grass: ANOVAR $F_{4,16} = 16.1$, $p < 0.0001$; moss: ANOVAR $F_{3,12} = 7.9$, $p = 0.003$; litter: ANOVAR $F_{5,20} = 11.4$, $p < 0.0001$). For the branch ground cover the lowest total C content was found in the deepest layer ranging from 7.5 to 10 cm, being 8 and 1.5-fold lower than in the top 2.5 cm at N_3 and S_8, respectively (ANOVAR $F_{3,12} = 23.1$, $p < 0.0001$). A similar trend with increasing depth was found for total N (ANOVAR $F_{3,12} = 24.6$, $p = 0.009$) and inorganic N (NH_4^+: ANOVAR $F_{3,12} = 14.07$, $p = 0.003$ and NO_3: ANOVAR $F_{3,12} = 19.5$, $p < 0.0001$). The abovementioned parameters were also significantly reduced with depth in the moss and litter plots. The same occurred in the grass plots, even though at N_3 there was an increase in the deepest layer (10-12.5 cm) in comparison with the 7.5-10-cm soil layer. Total P significantly varied with soil depth only for the moss plots where its content was between 2 and 5 times lower in the 7.5-10-cm layer than in the other soil layers (ANOVAR

$F_{3,12}$ = 8.1, p = 0.003). Overall, a decrease in available P with increasing soil depth was detected for all the ground covers at both study sites (branches: ANOVAR $F_{3,12}$ = 26.4, p < 0.0001; grass: ANOVAR $F_{4,16}$ = 15.8, p < 0.0001; moss: ANOVAR $F_{3,12}$ = 15.3, p = 0.0002; litter: ANOVAR $F_{5,20}$ = 44.6, p < 0.0001).

The branch plots at N_3 showed the highest cellulase, xylanase and β-glucosidase activities in the uppermost 2.5-cm soil layer (*cell*: ANOVAR $F_{3,12}$ = 10.5, p = 0.001; *xyl*: ANOVAR $F_{3,12}$ = 19.1, p < 0.0001; *betagluc*: ANOVAR $F_{3,12}$ = 14.3, p = 0.008). The same trend as a function of depth was observed for the alkaline phosphomonoesterase (ANOVAR $F_{3,12}$ = 5.2, p = 0.01), and the N-related enzyme activities (*leu*: ANOVAR $F_{3,12}$ = 5.5, p = 0.013; *lys*: ANOVAR $F_{3,12}$ = 7.1, p = 0.005). These changes with depth were, however, less evident in the branch plots located at S_8. For the grass ground cover all the enzymes related to the C cycle (*cell*: ANOVAR $F_{4,16}$ = 13.1, p < 0.0001; *xyl*: ANOVAR $F_{4,16}$ = 23.4, p < 0.0001; *alfagluc*: ANOVAR $F_{4,16}$ = 10.4, p = 0.0002; *betagluc*: ANOVAR $F_{4,16}$ = 23.8, p < 0.0001) and those involved in the P cycle (*acP*: ANOVAR $F_{4,16}$ = 3.3, p = 0.04; *alkP*: ANOVAR $F_{4,16}$ = 13.4, p < 0.0001; *bisP*: ANOVAR $F_{4,16}$ = 16.1, p < 0.0001; *piroP*: ANOVAR $F_{4,16}$ = 13.9, p < 0.0001) were significantly higher in the first top 2.5 cm at both slopes. This trend was also found for leucine- and lysine-aminopeptidase activities at N_3 (*leu*: ANOVAR $F_{4,16}$ = 21.5, p < 0.0001; *lys*: ANOVAR $F_{4,16}$ = 11.4, p = 0.0001). Likewise, the highest enzyme activities in moss and litter plots (except for arylsulphatase activity) were also recorded in the uppermost soil layer.

Table 3

Overview of the microbial biomass index determined by dsDNA along with the yields of intracellular (iDNA) and extracellular DNA (eDNA) and the eDNA/iDNA ratio at the north- and the south-facing sites (N_3 and S_8, respectively) and as a function of the different ground covers (branches, grass, moss and litter). Values are means with SD in brackets. Data are expressed on a dry weight basis. Different letters in bold, for each of the soil depths, indicate significant differences ($p < 0.05$; ANOVA followed by Tukey post-hoc test) with regard to the ground cover type. Due to a high stone content, sampling depth was in some cases reduced to 10 or 12.5 cm.

Soil depth	**0-2.5 cm**			**2.5-5 cm**			**5-7.5 cm**			**7.5-10 cm**			**10-12.5 cm**			**12.5-15 cm**		
Site N_3	**Branch**	**Grass**	**Moss**	**Branch**	**Grass**	**Moss**	**Branch**	**Grass**	**Moss**	**Branch**	**Grass**	**Moss**	**Branch**	**Grass**	**Moss**	**Branch**	**Grass**	**Moss**
dsDNA yields (µg g^{-1} soil)	452**a** (79)	354**a** (98)	308**a** (31)	349**a** (145)	346**a** (45)	282**a** (15)	281**a** (76)	276**a** (67)	120**a** (32)	153**a** (84)	119**a** (55)	87**a** (15)	n.a.	84 (12)	n.a.	n.a	n.a	n.a.
iDNA yields (µg g^{-1} soil)	197**a** (41)	97**a** (20)	69**a** (24)	91**a** (10)	83**a** (22)	48**a** (7.0)	71**a** (15)	83**a** (28)	60**a** (17)	31**a** (0.3)	73**b** (2.0)	29**a** (15)	n.a.	25 (2.0)	n.a.	n.a	n.a	n.a.
eDNA yields (µg g^{-1} soil)	17**a** (5.0)	45**a** (10)	36**a** (5.0)	27**a** (15)	55**a** (15)	27**a** (4.0)	18**a** (3.0)	27**a** (6.0)	15**a** (3.0)	12**a** (7.0)	13**a** (7.0)	9.0**a** (3.0)	n.a.	24 (4.0)	n.a.	n.a	n.a	n.a.
eDNA/iDNA ratio	0.13**a** (0.02)	0.46**a** (0.18)	0.56**a** (0.19)	0.38**a** (0.06)	0.65**a** (0.15)	0.60**a**(0.19)	0.32**a** (0.15)	0.45**a** (0.11)	0.23**a** (0.04)	0.38**a** (0.13)	0.18**a** (0.06)	0.34**a** (0.16)	n.a.	0.96 (0.08)	n.a.	n.a	n.a	n.a.
Site S_8	**Branch**	**Grass**	**Litter**	**Branch**	**Grass**	**Litter**	**Branch**	**Grass**	**Litter**	**Branch**	**Grass**	**Litter**	**Branch**	**Grass**	**Litter**	**Branch**	**Grass**	**Litter**
dsDNA yields (µg g^{-1} soil)	237**a** (40)	241**a** (73)	247**a** (63)	325**a** (164)	272**a** (85)	155**a** (45)	322**a** (68)	150**b** (41)	91**b** (47)	390**a** (97)	160**b** (39)	65**b** (15)	n.a.	82**a** (24)	51**a** (9.0)	n.a.	n.a.	41 (9.0)
iDNA yields (µg g^{-1} soil)	83**a** (14)	92**a** (30)	119**a** (5.0)	97**a** (32)	68**a** (21)	29**a** (8.0)	84**a** (26)	55**a** (16)	57**a** (19)	99**a** (32)	61**a** (18)	58**a** (14)	n.a.	34**a** (6.0)	53**a** (15)	n.a.	n.a.	28 (10)
eDNA yields (µg g^{-1} soil)	12**a** (5.0)	9.0**a** (1.0)	12**a** (4.0)	13**a** (7.0)	17**a** (8.0)	9.0**a** (2.0)	12**a** (3.0)	15**a** (5.0)	8.0**a** (2.0)	27**a** (3.0)	13**a** (6.0)	7.0**a** (1.0)	n.a.	7.0**a** (2.0)	7.0**a** (0.6)	n.a.	n.a.	6.0 (0.2)
eDNA/iDNA ratio	0.15**a** (0.05)	0.11**a** (0.05)	0.10**a** (0.04)	0.13**a** (0.07)	0.23**a** (0.09)	0.29**a** (0.07)	0.16**a** (0.05)	0.31**a** (0.08)	0.17**a** (0.09)	0.25**a** (0.09)	0.23**a** (0.10)	0.13**a** (0.05)	n.a.	0.21**a** (0.02)	0.18**a** (0.09)	n.a	n.a (0.11)	0.28

n.a.: not available

The eDNA yields, and consequently the eDNA/iDNA ratio, were significantly lower in the 7.5-10-cm soil layer than in the uppermost layer in the grass plots at N_3 (eDNA: ANOVAR $F_{4,16} = 5.6$, $p = 0.005$; ratio: ANOVAR $F_{4,16} = 3.5$, $p = 0.03$). Moreover, there was a significant decrease in the dsDNA content with increasing depth in both grass and moss plots (ANOVAR $F_{4,16} = 5.7$, $p = 0.005$; ANOVAR $F_{3,12} = 67.9$, $p < 0.0001$, respectively). The lowest iDNA yields were also recorded in the deepest layer (7.5-10 cm) of the moss plots (ANOVAR $F_{3,12} = 4.8$, $p = 0.02$). The same occurred for the abundance of the different microbial groups assessed by qPCR in the extracellular (bacteria: ANOVAR $F_{3,12} = 36.7$, $p < 0.0001$; fungi: ANOVAR $F_{3,12} = 8.9$, $p = 0.02$; archaea: ANOVAR $F_{3,12} = 5.2$, $p = 0.015$) and intracellular DNA fractions (bacteria: ANOVAR $F_{3,12} = 6.1$, $p = 0.009$; fungi: ANOVAR $F_{3,12} = 4.9$, $p = 0.01$; archaea: ANOVAR $F_{3,12} = 8.0$, $p = 0.003$). In the litter plots the highest dsDNA, iDNA and eDNA yields were also found in the top 2.5 cm (dsDNA: ANOVAR $F_{5,20} = 44.6$, $p < 0.0001$; eDNA: ANOVAR $F_{5,20} = 6.1$, $p = 0.002$; iDNA: ANOVAR $F_{5,20} = 11.2$, $p < 0.0001$), being around 2-fold higher than in the other soil layers.

Table 4

Abundance of bacteria, fungi and archaea determined by quantitative real-time PCR in both the intra- and extracellular DNA fractions at the north- and the south-facing sites (N_3 and S_8, respectively) and as a function of the different ground covers (branches, grass, moss and litter). Values are means with SD in brackets. Data are expressed on a dry weight basis. Different letters in bold, for each of the soil depths, indicate significant differences ($p < 0.05$; ANOVA followed by Tukey post-hoc test) with regard to the ground cover type.

Soil depth	**0-2.5 cm**			**2.5-5 cm**			**5-7.5cm**		
Site N_3	**Branch**	**Grass**	**Moss**	**Branch**	**Grass**	**Moss**	**Branch**	**Grass**	**Moss**
Bacteria iDNA	1.3 x 10^8**b** (6.8 x10^7)	1.3 x 10^9**a** (3.1 x10^7)	1.6 x 10^9**a** (2.1 x10^7)	4.9 x 10^8**a** (5.4 x10^7)	9.6 x 10^8**a** (5.9 x10^7)	3.6 x 10^8**a** (2.8 x10^7)	3.3 x 10^8**a** (3.1 x10^7)	1.2 x 10^9**a** (7.3 x10^8)	1.3 x 10^9**a** (7.7 x10^7)
Bacteria eDNA	9.2 x 10^6**b** (3.4 x10^5)	1.7 x 10^8**a** (9.7 x10^6)	2.4 x 10^8**a** (9.7 x10^7)	2.0 x 10^8**a** (7.7 x10^7)	1.1 x 10^8**a** (3.6 x10^6)	1.1 x 10^8**a** (7.5 x10^6)	3.8 x 10^7**a** (1.6 x10^6)	9.6 x 10^7**a** (3.0 x10^6)	2.8 x 10^7**a** (1.9 x10^6)
Fungi iDNA	3.2 x 10^7**b** (3.5 x10^6)	2.1 x 10^8**a** (8.3 x10^6)	3.6 x 10^8**a** (1.6 x10^7)	1.6 x 10^8**a** (1.7 x10^7)	2.7 x 10^8**a** (2.1 x10^6)	1.9 x 10^8**a** (1.5 x10^7)	1.8 x 10^8**a** (2.2 x10^6)	1.7 x 10^8**a** (6.5 x10^6)	1.4 x 10^8**a** (9.1 x10^6)
Fungi eDNA	1.3 x 10^6**b** (6.6 x10^4)	3.3 x 10^7**a** (8.7 x10^5)	4.3 x 10^7**a** (3.8 x10^5)	1.0 x 10^7**a** (9.8 x10^5)	3.4 x 10^7**a** (4.4 x10^5)	6.5 x 10^7**a** (3.5 x10^6)	4.1 x 10^7**a** (9.5 x10^5)	9.7 x 10^6**a** (4.1 x10^5)	4.6 x 10^6**a** (1.5 x10^4)
Archaea iDNA	5.7 x 10^7**b** (4.2 x10^5)	7.8 x 10^7**b** (5.1 x 10^6)	2.6 x 10^8**a** (5.8 x10^6)	1.2 x 10^8**a** (7.5 x10^6)	8.7 x 10^7**a** (4.6 x10^5)	6.8 x 10^7**a** (2.8 x10^6)	1.0 x 10^8**a** (9.4 x10^6)	1.1 x 10^8**a** (3.3 x10^7)	2.7 x 10^8**a** (8.0 x10^6)
Archaea eDNA	4.5 x 10^5**a** (3.9 x10^3)	8.9 x 10^5**a** (4.1 x10^4)	1.1 x 10^6**a** (6.5 x10^3)	8.2 x 10^5**a** (1.3 x10^5)	7.5 x 10^5**a** (2.0 x10^4)	8.7 x 10^5**a** (1.3 x10^4)	1.4 x 10^6**a** (1.1 x10^3)	4.5 x 10^5**a** (1.1 x10^4)	1.0 x 10^5**a** (8.2 x10^3)
Site S_8	**Branch**	**Grass**	**Litter**	**Branch**	**Grass**	**Litter**	**Branch**	**Grass**	**Litter**
Bacteria iDNA	3.9 x 10^8**a** (1.2 x10^7)	1.3 x 10^8**a** (8.0 x10^6)	2.3 x 10^8**a** (7.7 x10^6)	2.3 x 10^8**a** (1.2 x10^6)	4.5 x 10^8**a** (3.8 x10^6)	1.4 x 10^8**a** (9.9 x10^6)	3.6 x 10^8**a** (2.7 x10^6)	3.7 x 10^8**a** (2.5 x10^7)	1.5 x 10^8**a** (9.8 x10^6)
Bacteria eDNA	1.4 x 10^7**a** (8.9 x10^5)	7.9 x 10^6**a** (1.5 x10^5)	1.1 x 10^7**a** (9.7 x10^4)	1.1 x 10^7**a** (6.5 x10^5)	2.7 x 10^7**a** (1.3 x10^5)	9.1 x 10^6**a** (9.7 x10^4)	6.1 x 10^6**a** (4.6 x10^4)	2.3 x 10^7**a** (1.6 x10^5)	5.3 x 10^6**a** (1.6 x10^4)
Fungi iDNA	6.5 x 10^7**a** (1.5 x10^5)	3.5 x 10^7**a** (6.6 x10^5)	3.3 x 10^7**a** (8.7 x10^5)	2.8 x 10^7**a** (9.5 x10^5)	6.8 x 10^7**a** (2.5 x10^5)	2.7 x 10^7**a** (1.5 x10^7)	4.1 x 10^7**a** (4.0 x10^6)	4.9 x 10^7**a** (8.5 x10^5)	4.7 x 10^7**a** (3.4 x10^6)
Fungi eDNA	3.9 x 10^6**a** (2.2 x10^5)	1.8 x 10^6**a** (9.3 x10^4)	1.3 x 10^6**a** (6.4 x10^4)	1.2 x 10^6**a** (8.5 x10^4)	2.6 x 10^6**a** (1.4 x10^5)	1.7 x 10^6**a** (2.0 x10^4)	5.0 x 10^5**a** (3.7 x10^3)	3.4 x 10^6**a** (2.3 x10^4)	2.4 x 10^6**a** (2.5 x10^4)
Archaea iDNA	7.4 x 10^7**a** (3.5 x10^5)	3.8 x 10^7**a** (1.7 x10^5)	3.3 x 10^7**a** (8.3 x10^5)	5.3 x 10^7**a** (1.4 x10^6)	8.4 x 10^7**a** (5.4 x10^6)	2.3 x 10^7**a** (9.5 x10^5)	6.0 x 10^7**a** (1.4 x10^6)	6.8 x 10^7**a** (2.0 x10^6)	3.4 x 10^7**a** (7.7 x10^4)
Archaea eDNA	1.7 x 10^5**a** (7.9 x10^3)	4.9 x 10^5**a** (2.3 x10^4)	5.4 x 10^5**a** (6.9 x10^2)	8.8 x 10^5**a** (1.1 x10^2)	7.3 x 10^5**a** (4.8 x10^3)	1.7 x 10^6**a** (4.8 x10^3)	1.6 x 10^5**a** (8.9 x10^4)	1.1 x 10^6**a** (5.3 x10^3)	9.0 x 10^5**a** (9.5 x10^3)

n.a.: not available

Table 4. To be continued

Soil depth	7.5-10 cm			10-12.5 cm			12.5-15 cm		
Site N_3	**Branch**	**Grass**	**Moss**	**Branch**	**Grass**	**Moss**	**Branch**	**Grass**	**Moss**
Bacteria iDNA	2.3×10^{8}**a** (3.1×10^{7})	1.1×10^{9}**a** (1.3×10^{8})	7.3×10^{8}**a** (6.3×10^{6})	n.a.	7.2×10^{8} (2.5×10^{7})	n.a.	n.a.	n.a.	n.a.
Bacteria eDNA	3.7×10^{7}**a** (9.2×10^{5})	5.4×10^{7}**a** (3.6×10^{6})	1.7×10^{7}**a** (1.3×10^{6})	n.a.	3.9×10^{7} (8.5×10^{6})	n.a.	n.a.	n.a.	n.a.
Fungi iDNA	5.2×10^{7}**a** (4.8×10^{5})	1.4×10^{8}**a** (9.2×10^{6})	7.6×10^{7}**a** (6.2×10^{5})	n.a.	4.0×10^{7} (8.0×10^{5})	n.a.	n.a.	n.a.	n.a.
Fungi eDNA	2.1×10^{6}**a** (6.2×10^{4})	5.7×10^{6}**a** (4.3×10^{4})	2.4×10^{6}**a** (2.0×10^{4})	n.a.	9.6×10^{6} (1.1×10^{5})	n.a.	n.a.	n.a.	n.a.
Archaea iDNA	4.5×10^{7}**a** (7.7×10^{5})	8.9×10^{7}**a** (8.3×10^{5})	8.4×10^{7}**a** (7.9×10^{5})	n.a.	5.3×10^{7} (4.0×10^{5})	n.a.	n.a.	n.a.	n.a.
Archaea eDNA	1.4×10^{6}**a** (3.0×10^{4})	7.4×10^{5}**a** (9.5×10^{3})	5.4×10^{5}**a** (4.9×10^{3})	n.a.	2.2×10^{6} (8.2×10^{3})	n.a.	n.a.	n.a.	n.a.
Site S_8	**Branch**	**Grass**	**Litter**	**Branch**	**Grass**	**Litter**	**Branch**	**Grass**	**Litter**
Bacteria iDNA	3.2×10^{8}**a** (2.9×10^{6})	2.1×10^{8}**a** (1.2×10^{6})	1.8×10^{8}**a** (7.6×10^{6})	n.a.	1.5×10^{8}**a** (5.1×10^{6})	6.5×10^{7}**a** (7.9×10^{5})	n.a.	n.a.	2.8×10^{7} (1.5×10^{5})
Bacteria eDNA	1.6×10^{7}**a** (7.1×10^{5})	1.3×10^{7}**a** (7.7×10^{5})	7.0×10^{6}**a** (3.9×10^{5})	n.a.	6.4×10^{6}**a** (5.1×10^{4})	4.6×10^{6}**a** (2.3×10^{4})	n.a.	n.a.	2.8×10^{6} (1.1×10^{4})
Fungi iDNA	2.5×10^{7}**a** (1.3×10^{6})	2.7×10^{7}**a** (3.0×10^{5})	2.3×10^{7}**a** (9.8×10^{4})	n.a.	1.7×10^{7}**a** (7.0×10^{5})	1.3×10^{7}**a** (5.7×10^{4})	n.a.	n.a.	2.4×10^{7} (7.3×10^{4})
Fungi eDNA	1.3×10^{6}**a** (4.4×10^{3})	1.3×10^{6}**a** (3.9×10^{3})	2.7×10^{6}**a** (5.7×10^{4})	n.a.	2.0×10^{6}**a** (1.5×10^{3})	4.3×10^{6}**a** (4.2×10^{3})	n.a.	n.a.	1.6×10^{6} (1.3×10^{5})
Archaea iDNA	5.0×10^{7}**a** (3.8×10^{5})	6.0×10^{7}**a** (2.2×10^{6})	2.4×10^{7}**a** (2.1×10^{3})	n.a.	3.9×10^{7}**a** (3.5×10^{5})	1.9×10^{7}**a** (8.8×10^{4})	n.a.	n.a.	6.7×10^{6} (2.6×10^{6})
Archaea eDNA	6.4×10^{5}**a** (6.8×10^{4})	3.5×10^{5}**a** (8.3×10^{3})	2.4×10^{6}**a** (2.6×10^{3})	n.a.	8.5×10^{5}**a** (5.0×10^{2})	2.2×10^{6}**a** (8.8×10^{4})	n.a.	n.a.	2.2×10^{6} (1.7×10^{5})

n.a.: not available

3.2. Soil mesofauna (microannelids) and humus forms

The list of microannelid species extracted from soil samples at N_3 and S_8 plots is compiled in Table 5. All species belong to the family Enchytraeidae. Species are arranged according to their allocation to acidity indicator groups. These coincide, in general, with the preferred occurrence of the species in Moder or Mull humus profiles.

Table 5. Microannelid species extracted from soil samples at N_3 (north-facing) and S_8 (south-facing) at different ground covers (G = grass, B = branches, M = moss, L = litter) and their ecological classification with respect to soil acidity and humus form preference. n=3 for each ground-cover type. sd: standard deviation.

	N_3G	N_3B	N_3M	S_8G	S_8B	S_8L	Acidity indicator group	Humus form preference
Bryodrilus ehlersi	12	10	-	-	-	-	strong	Moder
Cognettia sphagnetorum	103	114	116	6	26	6	strong	Moder
Euenchytraeus bisetosus	-	2	4	-	-	-	strong	Moder
Marionina clavata	58	161	30	-	-	-	strong	Moder
Mesenchytraeus pelicensis	-	4	1	2	-	-	strong	Moder
Enchytraeus norvegicus	1	-	-	14	-	6	moderate	Intermed
Enchytronia parva	10	1	-	8	5	17	moderate	Intermed
Mesenchytraeus glandulosus	7	2	11	-	5	-	moderate	Intermed
Achaeta sp. (dzwi)1	-	-	-	-	-	1	slight	Mull
Buchholzia appendiculata	19	55	-	1	-	21	slight	Mull
Fridericia bisetosa	-	-	-	-	2	3	slight	Mull
Fridericia bulboides	4	9	-	17	3	5	slight	Mull
Fridericia connata	-	-	-	-	36	1	slight	Mull
Fridericia stephensoni	-	-	-	3	-	-	slight	Mull
Fridericia waldenstroemi	-	-	-	-	1	-	slight	Mull
Fridericia sp. juv.2	3	1	-	7	3	17	slight	Mull
Hemifridericia parva	18	24	-	-	-	-	slight	Mull
Henlea perpusilla	7	10	-	4	2	3	slight	Mull
Total of extracted animals	242	393	162	62	83	80		
Number of species	11	12	5	9	9	10		
Abundance (Ind.m^{-2}) mean	41081	66718	27502	10525	14091	13581		
sd	21130	34508	7345	4894	10442	2984		
Indicators of strong acidity	72%	74%	93%	13%	31%	7%		
Indicators of moderate acidity	7%	1%	7%	35%	12%	29%		
Indicators of slight acidity	21%	25%	0%	52%	57%	64%		

1 Species not yet formally described
2 Juvenile specimens not determinable to species level

Total microannelid abundance was significantly affected by slope exposure, being higher at N_3 ($p = 0.001$, SQR transformation, t-test). This was mainly due to a considerably higher number of strong acidity indicators, while the number of indicators of moderate as well as slight acidity was similar at N_3 and S_8 (Fig. 1). The comparison of plots with the same exposure but different ground covers revealed no significant difference in total abundance. In terms of dominance (relative abundance) indicators of strong acidity reached an average of > 70% at N_3, whereas at S_8 indicators of slight acidity amounted to > 50% at each ground-cover type (Table 5). The dominance of indicators of strong acidity was thus significantly higher at N_3 ($p = 0.001$), while the dominance of indicators of moderate and slight acidity was significantly higher at S_8 ($p = 0.041$ and $p = 0.009$, respectively, U-test).

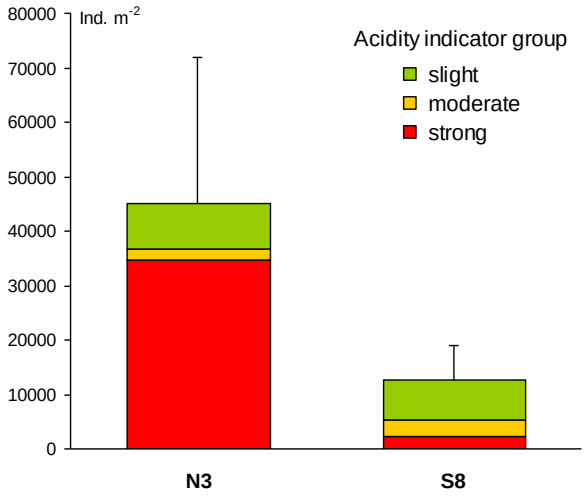

Fig. 1. Total microannelid abundance (mean) at the two study sites N_3 and S_8. Microannelid species are divided into three acidity indicator groups: indicators of slight, moderate and strong acidity. Error bar: standard deviation.

The average thickness of the organic layers OL+OF+OH amounted to 8 cm at N_3 and to 5 cm at S_8 (Fig. 2). Most discriminating between both sites was the thickness of the OH-horizon, being significantly ($p = 0.001$) thicker north-facing (5.0 cm) than south-facing (1.9 cm). The comparison of the morphological humus profile with the vertical distribution of microannelids revealed that > 80% of the animals at N_3 lived in the organic horizons above the mineral soil, whereas at S_8 the animals were almost evenly distributed between the organic layer and the A-horizon. Total microannelid abundance showed no relation to soil depth in the uppermost 10 cm neither at N_3 nor at S_8. However, by the distinction of indicator groups the tendency to higher proportions of indicators of slight acidity in the upper layers became visible (Fig. 2). This was in agreement with the pH values that tended to decrease with increasing soil depth. For each single sample, the relation between the occurrence of acidity indicators and the pH value showed a recurring pattern: in layers with a pH < 5 indicators of strong acidity were by far predominant, whereas indicators of slight acidity prevailed above that threshold. This was found in spite of the fact that the humus profile in all the three field replicates includes a thick OH-horizon, which characterises the humus form as Moder (Fig. S1). This finding is partly blurred when pH as well as dominance of indicator groups is displayed as mean values of several replicates (comp. Fig 2 with Figs. S1-S3).

Regarding the relation between microbial DNA and microannelids, the eDNA yields were positively correlated with the abundances of microannelids at the N_3 grass plot (total enchytraeids: $p = 0.003$; $R = 0.727$; and *Cognettia sphagnetorum*: $p = 0.026$; $R = 0.591$). Likewise, positive correlations were found between eDNA yields and the total enchytraeid abundances at the N_3 moss plot ($p = 0.024$; $R = 0.642$); even though in this

case enchytraeid abundance was also correlated with iDNA and total dsDNA (data not shown).

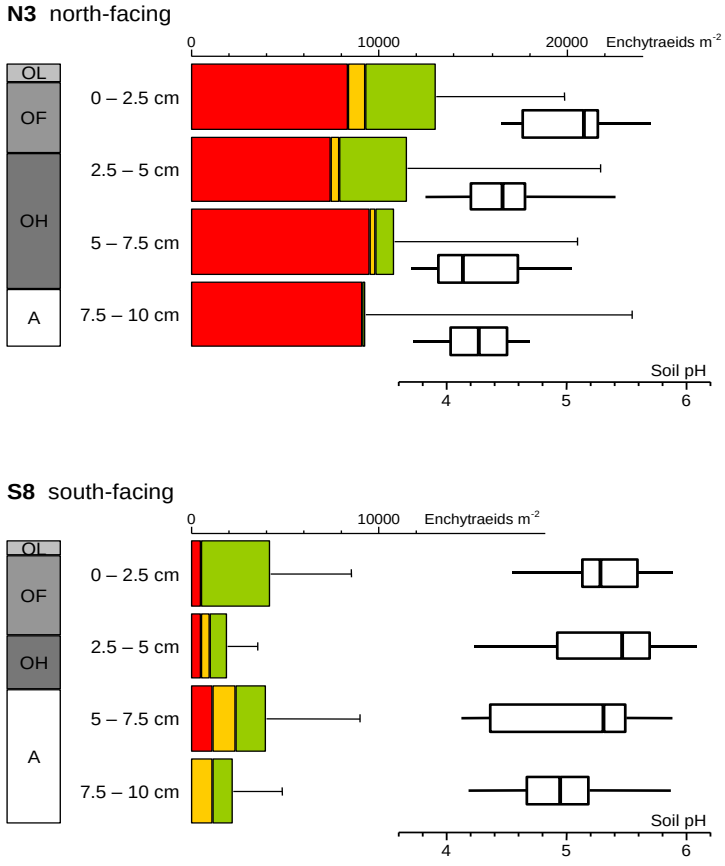

Fig. 2. Comparison between the morphological humus profile (column), the vertical distribution of microannelids (bars) and the pH (box-plots) at study sites N_3 and S_8. Thickness of organic horizons and abundance of microannelids are arithmetic means (all parameters n=9). Microannelid species are summarized according to acidity indicator groups (green: slight acidity; yellow: moderate acidity; red: strong acidity). Designation of humus horizons according to Zanella et al. (2011).

4. Discussion

4.1. Changes in soil physico-chemical and microbiological parameters as a function of ground cover and slope exposure

Understanding how the ground cover type affects the composition and activity of soil microbial communities enables a better comprehension of forest ecosystem functioning and sustainability (Uroz et al., 2016). In particular, at the N-facing slope the moss ground cover was characterised by a lower alkaline phosphomonoesterase activity in comparison with both grass and branch ground covers and irrespective of the soil depth. This could be due to the fact that the highest total P content was also recorded in the moss plots. Indeed, an increase in P-acquiring enzyme activities would be expected in case of P deficiency (Fraser et al., 2015). This enzyme activity is responsible for the mineralisation of organic P into phosphate by hydrolysing phosphoric (mono) ester bonds under alkaline conditions. Although plants exude phosphomonoesterases, especially under P deficiency, the majority of phosphatase enzymes in soil probably originate from microorganisms (Nannipieri et al., 2012).

In our study, the three representative ground covers at N_3 (branch, grass and moss) significantly differed in terms of microbial abundance only in the first top 2.5 cm, where the highest abundance for the three microbial domains was registered in the moss plots regardless of the DNA fraction. Despite this fact the moss ground cover showed the lowest value of both leucine- and lysine-aminopeptidase activities in the top 5 cm, even though it has been reported that bacteria play an important role in the production of leucine-aminopeptidases (Burke et al., 2011). Sinsabaugh et al. (2008) also found a higher leucine-aminopeptidase activity with increasing soil pH levels (pH 4 to 8.5). Although the three predominant ground covers were generally acidic at N_3, a slightly lower pH was recorded in the moss plots.

Nevertheless, at the S-facing slope most of the enzymes related to C and N cycles showed a higher potential activity in the branch plots within the 10-cm soil depth. Soil moisture and soil organic matter (SOM) content have been shown as major determinants of the level and activity of soil enzymes (Makoi and Ndakidemi, 2008; Štursová and Baldrian, 2011). Indeed, in our study SOM determined by loss on ignition, along with the total C and the inorganic N content (NH_4^+ and NO_3^-) were also higher under the branch ground cover at S_8. Accordingly, soil microbial biomass assessed as dsDNA yields followed the same trend as SOM within the 5 to 10-cm soil depth. On the other hand, the fact that at S_8 alkaline phosphomonoesterase and phosphodiesterase activities showed a higher activity in the branch plots, which were characterised by a higher content of available P, might indicate that the soil microbial community in these plots has a P demand greater than in the other ground covers. Consequently, a higher metabolic effort via secretion of these enzymes is made to access organic P.

Overall, most of the enzymatic activities decreased with increasing soil depth at both slope exposures. This occurred in concert with a decline in microbial biomass as well as in inorganic N, total C and N content. In fact, the availability of substrate for enzymatic breakdown decreases with depth, which increases the probability of a spatial disconnection of enzyme and substrate (Holden and Fierer, 2005). In addition, in deeper layers SOM can be bound to minerals or occluded in aggregates therefore limiting the access for microorganisms (Schnecker et al., 2015).

The eDNA/iDNA ratio was calculated to obtain i) an index of microbial activity as a function of the ground cover, and ii) information about the movement (vertical distribution) of DNA along the topsoil profile (0-15 cm). Lower eDNA/iDNA ratios could be indicative of a higher microbial activity and be related to an increase in iDNA yields (higher potentially

living microbial biomass under favorable conditions, i.e., in the upper layers of the topsoil), and/or to a higher eDNA degradation. Contrarily, an increase in this ratio indicative of lower microbial activity might be related to a lower degradation of eDNA and/or to an accumulation of eDNA in deeper soil layers as a result of leaching (Potè et al., 2003; Ceccherini et al., 2007, 2009). In our case, only the grass plots at the north-facing slope showed a significantly higher eDNA/iDNA ratio in the 10-12.5 cm topsoil layer. Due to its vertical distribution along the topsoil there is also the possibility for eDNA to reach a microbial cell far from the donor cell (structural/functional flexibility). This fact together with the possibility of eDNA to persist in soil (Nielsen et al., 2007; Agnelli et al., 2007) has to be considered within the context of genetic exchange via natural transformation with evolutionary implications (Ascher et al., 2009b; Pietramellara et al., 2009).

4.2. Changes in enchytraeid community as a function of ground cover and slope exposure

Exposure and, in general, climate seems to have a significant influence on the thickness of the organic layer being thicker at the north-facing slope as shown in Ascher et al. (2012). This is related to a striking difference between the north-facing and south-facing site concerning the partitioning of total C between the organic layers (OL+OF+OH) and the mineral soil (A, E) in the uppermost 10 cm of the humus profile. However, there is only a gradual difference in terms of humus form classification, as at every sample point at both sites an OH horizon was present, which characterises the humus form as Moder according to the European (Zanella et al., 2011) as well as to the German classification system (Ad-hoc-AG Boden, 2005). The south-facing grass and litter plots included an only shallow OH of 0.5 cm thickness. Such a profile may be classified as Mullartiger Moder (German system) or

Hemimoder (Zanella et al., 2011). This relates well to the much lower dominance of Moder-preferring species at S_8 compared to N_3.

Certainly, the presence of Mull-preferring microannelid species in a Moder is a rather unexpected phenomenon. One could argue the preference classes were based on observations from central Europe and cannot be applied to other geographic regions. However, the phenomenon is consistent with the measured pH values in the soil. Species with preference for mull are at the same time indicators of slight acidity (Table 5), occurring mainly in soils above pH(water) 5.0 as known from investigations at soil monitoring sites in Germany (Graefe and Beylich, 2003). The change of dominance of indicator species along the pH-gradient is less a gradual shift than a switch into another community that often occurs between the exchanger and the aluminium buffer range (Graefe and Beylich, 2006). This is most obvious when pH and the occurrence of species are compared at the microscale of single plots.

What are the reasons for the observed discontinuities in the humus profile? First of all, it has to be considered that the studied sites are located at relatively steep slopes (N_3: 29°; S_8: 33°), where erosion and accumulation processes cannot be excluded. Deadwood branches often accumulate uphill close to tree trunks catching there also other material transported under the influence of gravity and water. Some results (i.e., higher moisture content, microannelid density increasing with depth) can be explained by such slope related accumulation processes. Melt-water run-off during snowmelt may be another key factor. Snow in Alpine regions can accumulate eolian dust containing carbonates and other weatherable minerals. This leads to the release of base cations during the melting period and contributes to the relative high base saturation in organic layers in high mountains (Küfmann, 2003). The interaction of melt-water and soil during surface and subsurface

run-off modifies both the chemistry of the percolate and the pH of the forest floor (Seip, 1980; Stottlemyer and Toczydlowski, 1996). Moreover, melt-water and/or eolian dust as potential carrier of eDNA (Wackernagel et al., 2006; Pietramellara et al., 2009) may have impact on the discontinuities in the humus profile and the correlated discontinuity in the mesofauna, as the observed site-specific correlations between microbial DNA and microannelids indicate. These site-specific correlations indicate that eDNA (N_3 grass plots) and microbes (DNA in general, independent of its presence as extracellular or intracellular DNA; N_3 moss plots) could act as a potential nutrient source for the mesofauna. Indeed, DNA can be present in the gut of the mesofauna as a part of the undigested soil and therefore be indirectly used to satisfy their nutrient demands.

It turns out that the thermal effect due to exposure determines large-scale differences in morphological, chemical and biological properties of the topsoil (Ascher et al., 2012). The small scale heterogeneity of the humus profile properties seems to be, however, more influenced by slope related processes such as microerosion, accumulation and melt-water run-off than by the type of ground cover (grass, moss, branches, litter).

Conclusions

The enzyme type-specific reactions to ground cover and slope exposure indicate the importance of performing multiple enzyme assays in order to avoid misinterpretation of nutrient cycles. Moreover, testing the soils in 2.5-cm increments to a depth of up to 15 cm revealed depth gradients on the soil chemical properties (e.g. the NH_4^+ content) but also the enzymes and micro- (e.g. eDNA) and macrobiological properties (enchytraeid community). Microannelids appeared to be sensitive, accurate and reliable biological indicators in the forested subalpine soils. Indicators of slight acidity clearly dominate on south-facing soils. It furthermore seems that

eDNA might act as a nutrient source for the mesofauna. All in all, our findings encourage the use of the discriminatory assessment of both DNA fractions (eDNA *vs.* iDNA) as a sort of 'low cost alternative' for a generic screening of microbial communities and their response to changing environmental conditions.

Acknowledgements

M. Gómez-Brandón and J. Ascher-Jenull have been funded by the Fonds zur Förderung der wissenschaftlichen Forschung (FWF) Austria (Project I989-B16) and partially by the Ente Cassa Risparmio di Firenze. T. Bardelli has been funded by a PhD grant from the University of Florence (Italy). We would like to thank Guy Rochat and Rebecca Mayer for their help in the field sampling and in the laboratory. Moreover, we are grateful to Prof. Gabriele Broll and Prof. Jean-Michel Gobat for having selected the ground covers in the study sites. We are also indebted to Dr. Fabio Angeli of the Ufficio distrettuale forestale – Malé (Trento, Italy) and his team for their support in the field. We also want to thank the three anonymous reviewers for their suggestions and constructive comments on the present manuscript.

References

A'Bear, A.D., Jones, T.H., Kandeler, E., Boddy, L., 2014. Interactive effects of temperature and soil moisture on fungal- mediated wood decomposition and extracellular enzyme activity. Soil Biol. Biochem. 70, 151–158.

Ad-hoc-AG Boden, 2005. Bodenkundliche Kartieranleitung, 5. Auflage. Hannover (438 pp).

Agnelli, A., Ascher, J., Corti, G., Ceccherini, M.T., Pietramellara, G., Nannipieri, P., 2007. Purification and isotopic signatures (δ13C, δ15N, Δ14C) of soil extracellular DNA. Biol. Fertil. Soils 44: 353–361.

Allison, S.D., Wallenstein, M.D., Bradford, M.A., 2010. Soil-carbon response to warming dependent on microbial physiology. Nat. Geosci. 3, 336–340.

Ascher, J., Ceccherini, M.T., Pantani, O.L., Agnelli, A., Borgogni, F., Guerri, G., Nannipieri, P., Pietramellara, G., 2009a. Sequential extraction and genetic fingerprinting of a forest soil metagenome. Appl. Soil Ecol. 42:176–181.

Ascher, J., Ceccherini, M.T., Guerri, G., Pietramellara, G., 2009b. "e-motion" of extracellular DNA (e-DNA) in soil. Fresen. Environ. Bull. 18: 1764–1767.

Ascher, J., Sartori, G., Graefe, U., Thornton, B., Ceccherini, M.T., Pietramellara, G., Egli, M., 2012. Are humus forms, mesofauna and microflora in subalpine forest soils sensitive to thermal conditions? Biol. Fertil. Soils 48, 709–725.

Bardelli, T., Gómez-Brandón, M., Ascher-Jenull, J., Fornasier, F., Arfaioli, P., Francioli, D., Egli, M., Sartori, G., Insam, H., Pietramellara, G., 2017. Effects of slope exposure on soil physico-chemical and microbiological properties along an altitudinal climosequence in the Italian Alps. Sci. Total Environ. 575, 1041–1055.

Bardgett, R., Wardle, D.A., 2010. Aboveground-Belowground Linkages. Biotic Interactions, Ecosystem Processes and Global Change. Oxford University Press, Oxford, UK.

Beniston, M., Díaz, H.F., Bradley, R.S., 1997. Climatic change at high elevation sites: an overview. Clim. Chang. 36, 233–251.

Beylich, A., Fründ, H.-C., Graefe, U., 1995. Environmental monitoring of ecosystems and bioindication by means of decomposer communities. Newsl. Enchytr. 4, 25–34.

Beylich, A., Graefe, U., 2009. Investigations of annelids at soil monitoring sites in Northern Germany: reference ranges and time-series data. Soil organisms 81, 175–196.

Bowman, R.A., 1988. A rapid method to determine total phosphorus in soil. Soil Sci. Soc. Am. J. 52, 1301–1304.

Bray, R., Kurtz, L.T., 1945. Determination of total, organic and available forms of phosphorus in soils. Soil Sci. 59, 39–46.

Burke, D.J., Weintraub, M.N., Hewins, C.R., Kalisz, S., 2011. Relationship between soil enzyme activities, nutrient cycling and soil fungal communities in a northern hardwood forest. Soil Biol. Biochem. 43, 795–803.

Ceccherini, M.T., Ascher, J., Pietramellara, G., Nannipieri, P., 2007. Vertical advection of extracellular DNA by water capillarity in soil columns. Soil Biol. Biochem. 39, 158–163.

Ceccherini, M.T., Ascher, J., Agnelli, A., Borgogni, F., Pantani, O.L., Pietramellara, G., 2009. Experimental discrimination and molecular characterization of the extracellular soil DNA fraction. Anton Leeuw. Int J. G. 96, 653–657.

Coolen M.J.L., Hopmans E.C., Rijpstra, W.I.C., Muyzer, G., Schouten, S., Volkman, J.K., Damste, J.S.S., 2004. Evolution of the methane cycle in Ace Lake (Antarctica) during the Holocene: response of methanogens and methanotrophs to environmental change. Org. Geochem. 35, 1151–1167.

Didden, W.A.M, 1993. Ecology of terrestrial Enchytraeidae. Pedobiologia 37, 2–29.

Dunger, W., Fiedler, H.J., 1989. Methoden der Bodenbiologie. Gustav Fischer, Stuttgart.

Egli, M., Mirabella, A., Sartori, G., Zanelli, R., Bischof, S., 2006. Effect of north and south exposure on weathering rates and clay mineral formation in Alpine soils. Catena 67, 155–174.

Egli, M., Sartori, G., Mirabella, A., Favilli, F., Giaccai, D., Delbos, E., 2009. Effect of north and south exposure on organic matter in high Alpine soils. Geoderma 149, 124–136.

FAO, 2006. Guidelines for Soil Description. 4th edition. FAO, Rome.

Ferris, M.J., Muyzer, G., Ward, D.M., 1996. Denaturing gradient gel electrophoresis profiles of 16S rRNA-defined populations inhabiting a hot spring microbial mat community. Appl. Environ. Microbiol. 62, 340–346.

Fornasier, F., Margon, A., 2007. Bovine serum albumin and Triton X-100 greatly increase phosphomonoesterases and arylsulphatase extraction yield from soil. Soil Biol. Biochem. 39, 2682–2684.

Fornasier, F., Ascher, J., Ceccherini, M.T., Tomat, E., Pietramellara, G., 2014. A simplified rapid, low-cost and versatile DNA-based assessmentof soil microbial biomass. Ecol. indic. 45, 75–82.

Fraser, T. D., Lynch, D.H., Bent, E., Entz, M.H., Dunfield, K.E., 2015. Soil bacterial *phoD* gene abundance and expression in response to applied phosphorus and long-term management. Soil Biol. Biochem. 88, 137–147.

Fravolini, G., Egli, M., Derungs, C., Cherubini, P., Ascher-Jenull, J., Gómez Brandón, M., Bardelli, T., Tognetti, R., Lombardi, F., Marchetti, M., 2016. Soil attributes and microclimate are important drivers of initial deadwood decay in sub-alpine Norway spruce forests Sci. Tot. Environ. 569–570, 1064–1076.

Graefe, U., Schmelz, R.M., 1999. Indicator values, strategy types and life forms of terrestrial Enchytraeidae and other microannelids. Newsl. Enchytr. 6, 59–67.

Graefe, U., Beylich, A., 2003. Critical values of soil acidification for annelid species and the decomposer community. Newsl. Enchytr. 8, 51–55.

Graefe, U., Beylich, A., 2006. Humus forms as tool for upscaling soil biodiversity data to landscape level? Mitteilungen der Deutschen Bodenkundlichen Gesellschaft 108, 6–7.

Holden, P.A., Fierer, N., 2005. Microbial processes in the Valdose Zone. Valdose Zone J. 4, 1–21.

ISO 23611-3. Soil quality—sampling of soil invertebrates—Part3: Sampling and soil extraction of enchytraeids. International Organization for Standardization; ISO 23611–3:2007, Geneva.

Jänsch, S., Römbke, J., Didden, W., 2005. The use of enchytraeids in ecological soil classification and assessment concepts. Ecotox. Environ. Safe. 62, 266–277.

Kandeler, E., 1993a. Bestimmung von Ammonium, in: Schinner, F., Öhlinger, R., Kandeler, E., Margesin, R. (Eds.), Bodenbiologische Arbeitsmethoden. Springer, Berlin, Heidelberg, pp. 366–368.

Kandeler, E., 1993b. Bestimmung von Nitrat, in: Schinner, F., Öhlinger, R., Kandeler, E., Margesin, R. (Eds.), Bodenbiologische Arbeitsmethoden. Springer, Berlin, Heidelberg, pp. 369–371.

Kang, S., Doh, S., Lee, D., Lee, D., Jin, V.L., Kimball, J.S., 2003. Topographic and climatic controls on soil respiration in six temperate mixed-hardwood forest slopes, Korea. Glob. Chang. Biol. 9, 1427–1437.

Karaban, K., Uvarov, A.V., 2014. Non-trophic effects of earthworms on enchytraeids: An experimental investigation. Soil Biol. Biochem. 73, 84–92.

Küfmann, C., 2003. Soil types and eolian dust in high-mountainous karst of the Northern Calcareous Alps (Zugspitzplatt, Wetterstein Mountains, Germany). Catena 53, 211–227.

Kuo, S., 1996. Phosphorus, in: Sparks, D.L. (Ed.), Methods of Soil Analysis. Part 3. Chemical Methods. SSSA Book Series, Vol. 5. Soil Science Society of America, Madison, WI, pp. 869–919.

Makoi, J.H.R., Ndakidemi, P.A., 2008. Selected soil enzymes: examples of their potential roles in the ecosystem. Afr. J. Biotechnol. 7, 181–191.

Mountain Research Initiative EDW Working Group, 2015. Elevation-dependent warming in mountain regions of the world. Nat. Clim. Change 5, 424–430.

Nannipieri, P., Giagnoni, L., Renella, G., Puglisi, E., Ceccanti, B., Masciandaro, G., Fornasier, F., Moscatelli, M.C., Marinari, S., 2012. Soil enzymology: classical and molecular approaches. Biol. Fertil. Soils 48, 743–762.

Nielsen, K.M., Johnsen, P.J., Bensasson, D., Daffonchio, D., 2007. Release and persistence of extracellular DNA in the environment. Environ. Biosafety Res. 6, 37–53.

Petrillo, M., Cherubini, P., Sartori, G., Abiven, S., Ascher, J., Bertoldi, D., Camin, F., Barbero, A., Larcher, R., Egli, M., 2015. Decomposition of Norway spruce and European larch coarse woody debris (CWD) in relation to different elevation and exposure in an Alpine setting. iForest 15, 154–164.

Pietramellara, G., Ascher, J., Borgogni, F., Ceccherini, M.T., Guerri, G., Nannipieri, P., 2009. Extracellular DNA in soil and sediment: fate and ecological relevance. Biol. Fertil. Soils 45, 219–235.

Poté, J., Ceccherini, M.T., Van Tran,V., Rosselli, W., Wildi, W., Simonet, P., Vogel, T., 2003. Fate and transfer of antibiotic resistance genes in saturated soil columns. Eur. J. Soil Biol. 39, 65–71.

Prévost-Bouré, N.C., Christen, R., Dequiedt, S., Mougel, C., Lelièvre, M., Jolivet, C., Shahbazkia, H.R., Guillou, L., Arrouays, D., Ranjard, L., 2011. Validation and application of a PCR primer set to quantify fungal communities in the soil environment by real-time PCR. Plos One 6, e24166.

Schmelz, R.M., Collado, R., 2010. A guide to European terrestrial and freshwater species of Enchytraeidae (Oligochaeta). Soil Organisms 82, 1–176.

Schnecker, J., Wild, B., Takriti, M., Eloy Alves, R.J., Gentsch, N., Gittel, A., Hofer, A., Klaus, K., Knoltsch, A., Lashchinskiy, N., Mikutta, R., Richter, A., 2015. Microbial community composition shapes enzyme patterns in topsoil and subsoil horizons along a latitudinal transect in Western Siberia. Soil Biol. Biochem. 83, 106–115.

Seip, H.M., 1980. Acid snow - snowpack chemistry and snowmelt, in: Hutchinson, T.C., Havas, M. (Eds.). Effects of Acid Precipitation on Terrestrial Ecosystems. Plenum Publishing Co., pp. 77–94.

Sinsabaugh, R.L., Lauber, C.L.,Weintraub, M.N., Ahmed, B., Allison, S.D., Crenshaw, C., Contosta, A.R., Cusack, D., Frey, S., Gallo, M.E., Gartner, T.B., Hobbie, S.E., Holland, K., Keeler, B.L., Powers, J.S., Stursova, M., Takacs-Vesbach, C., Waldrop, M.P., Wallenstein, M.D., Zak, D.R., Zeglin, L.H., 2008. Stoichiometry of soil enzyme activity at global scale. Ecol. Lett. 11, 1252–1264.

Stottlemyer, R., Toczydlowski, D., 1996. Modification of snowmelt chemistry by forest floor and mineral soil, Northern Michigan. J. Environ. Qual. 25, 828–836.

Štursová, M., Baldrian, P., 2011. Effects of soil properties and management on the activity of soil organic matter transforming enzymes and the quantification of soil-bound and free activity. Plant Soil 338, 99–110.

Uroz, S., Oger, P., Tisserand, E., Cébrond, A., Turpault, M.-P., Buée, M., De Boer, W., Leveau, J.H.J., Frey-Klett, P., 2016. Specific impacts of beech and Norway spruce on the structure and diversity of the rhizosphere and soil microbial communities. Sci. Rep. 6:27756.

Wackernagel, W., 2006.The various sources and the fate of DNA in soil, in: Nannipieri, P., Smalla, K. (Eds.). Soil Biology. Springer-Verlag, Berlin, Heidelberg, pp. 117–139.

Zanella A, Jabiol B, Ponge JF, Sartori G, De Waal R, Van Delft B, Graefe U, Cools N, Katzensteiner K, Hager H, Englisch M., 2011. A European morpho-functional classification of humus forms. Geoderma 164, 138–145.

Supplementary Material

Ground cover and slope exposure effects on micro- and mesobiota in forest soils

María Gómez-Brandón[a,1,*], Judith Ascher-Jenull[a,b,1], **Tommaso Bardelli[a,b]**, Flavio Fornasier[c], Giacomo Sartori[d], Giacomo Pietramellara[b], Paola Arfaioli[b], Markus Egli[e], Anneke Beylich[f], Heribert Insam[b] , Ulfert Graefe[f]

[a]Institute of Microbiology, University of Innsbruck, Technikerstraße 25d, 6020 Innsbruck, Austria
[b]Department of Agrifood and Environmental Science, University of Florence, Piazzale delle Cascine 18, 50144 Florence, Italy
[c]Council for Research and Experimentation in Agriculture, Via Trieste 23, 34170 Gorizia, Italy
[d]Museo delle Scienze (MUSE), Corso del Lavoro e della Scienza 3, 38122 Trento, Italy
[e]Department of Geography, University of Zürich, Winterthurerstrasse 190, 8057 Zürich, Switzerland
[f]IFAB Institut für Angewandte Bodenbiologie GmbH, Tornberg 24a, 22337 Hamburg, Germany

*Corresponding author: María Gómez-Brandón,
E-mail address: maria.gomez-brandon@uibk.ac.at

[1]Both authors contributed equally to this paper

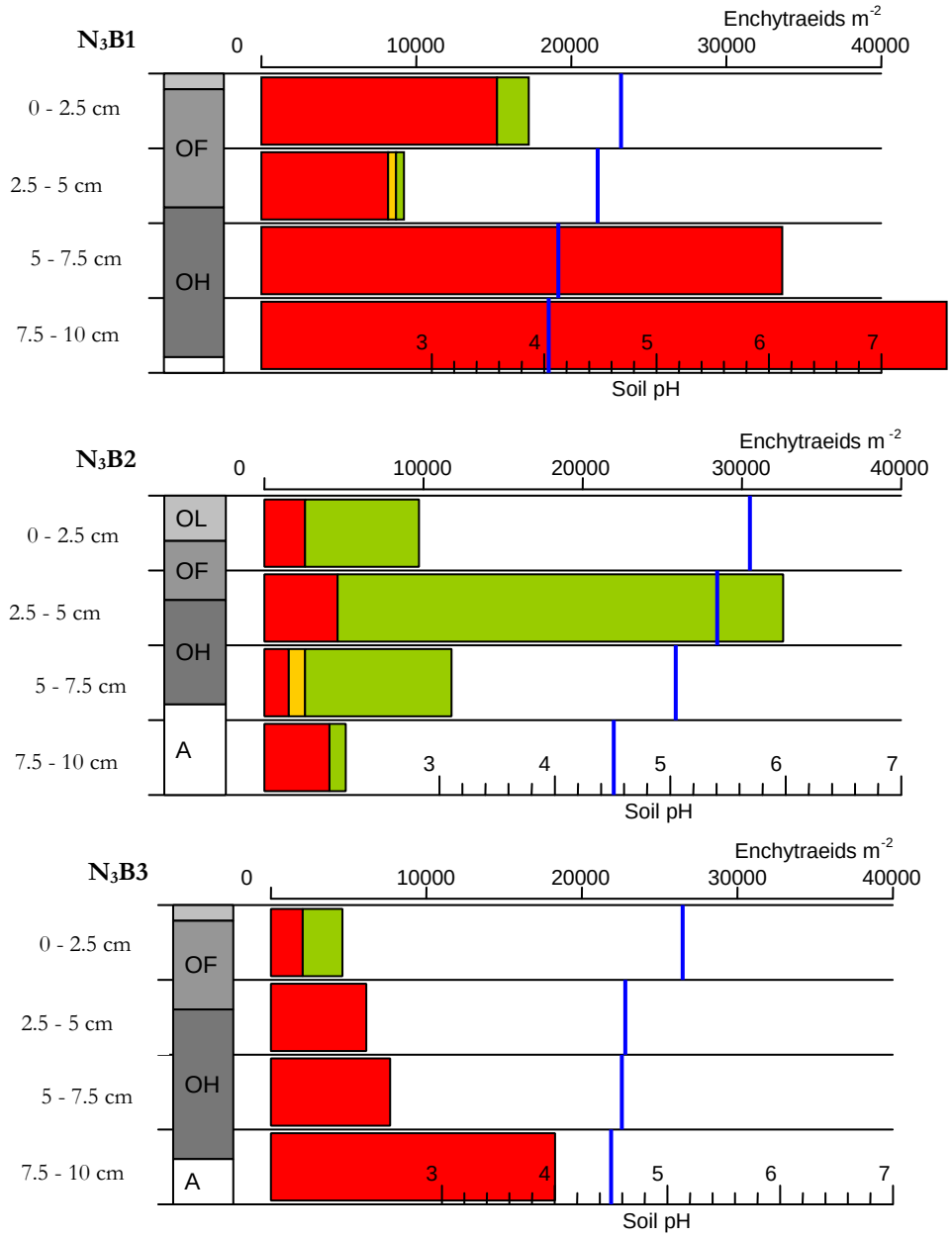

Fig. S1. Comparison between the morphological humus profile (column), the activity profile of microannelids (bars) and the pH-profile (blue lines) for the three plots of the soil cover "branches" at site N_3, showing the pH dependent distribution of acidity indicators in different soil depths (green: slight acidity; yellow: moderate acidity; red: strong acidity).

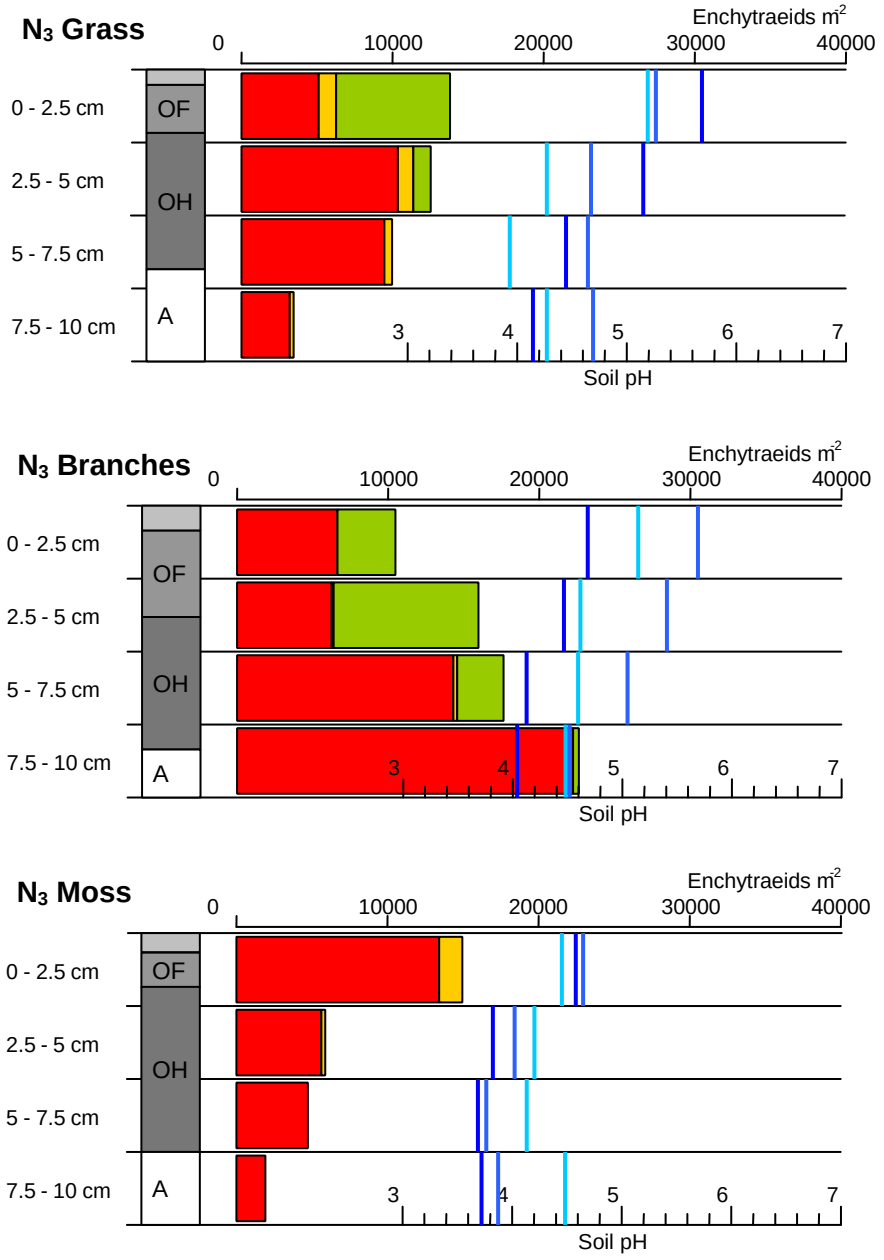

Fig. S2. Comparison between the morphological humus profile (column), the activity profile of microannelids (bars) and the pH-profile (blue lines) for the three soil cover types at site N_3 (mean values of microannelid abundance, n=3; colour coding of acidity indicator groups as in Fig. S1).

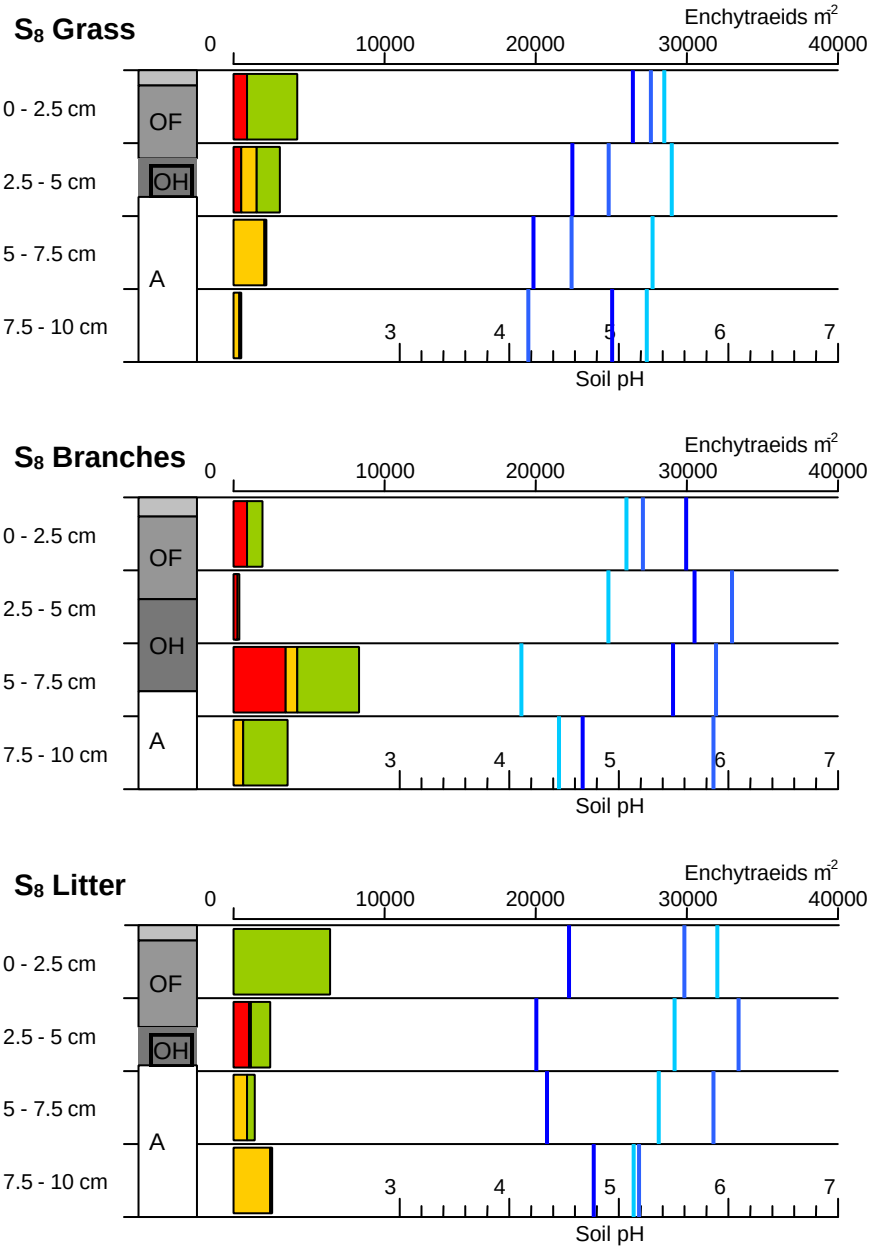

Fig. S3. Comparison between the morphological humus profile (column), the activity profile of microannelids (bars) and the pH-profile (blue lines) for the three soil cover types at site S_8 (mean values of microannelid abundance, n=3; colour coding of acidity indicator groups as in Fig. S1).

IV. Paper 3

Physico-chemical and microbiological evidence of exposure effects on *Picea abies* – Coarse woody debris at different stages of decay

(photos by J. Ascher-Jenull)

Physico-chemical and microbiological evidence of exposure effects on *Picea abies* – coarse woody debris at different stages of decay

María Gómez-Brandón[a,*], Judith Ascher-Jenull[a,b,*], **Tommaso Bardelli[a,b]**, Flavio Fornasier[c], Giulia Fravolini[d], Paola Arfaioli[b], Maria Teresa Ceccherini[b], Giacomo Pietramellara[b], Krzysztof Lamorski[e], Cezary Sławiński[e], Daniela Bertoldi[f], Markus Egli[g], Paolo Cherubini[h], Heribert Insam[a]

[a]Institute of Microbiology, University of Innsbruck, Technikerstraβe 25d, A-6020 Innsbruck, Austria
[b]Department of Agrifood and Environmental Science, University of Florence, Piazzale delle Cascine 18, 50144 Florence, Italy
[c]Consiglio per la Ricerca e la Sperimentazione in Agricoltura, Centro di Ricerca per lo Studio delle Relazioni tra Pianta e Suolo (C.R.A.-R.P.S.), Via Trieste 23, I- 34170 Gorizia, Italy
[d]Department of Bioscience and Territory, University of Molise, 86090 Pesche, Italy
[e]Institute of Agrophysics, Polish Academy of Sciences, Doświadczalna 4, 20-290 Lublin, Poland
[f]IASMA, Fondazione Edmund Mach, 38010 San Michele all'Adige, Italy
[g]Department of Geography, University of Zürich, Winterthurerstrasse 190, 8057 Zürich, Switzerland
[h]WSL Swiss Federal Institute for Forest, Snow and Landscape Research, 8903 Birmensdorf, Switzerland

*Both authors contributed equally to this paper
Corresponding autor: Maria.Gomez-Brandon@uibk.ac.at

Forest Ecology and Management, May 2017, Volume 391, pp 376-389

DOI:10.1016/j.foreco.2017.02.033

Contribution: T. Bardelli participated in the field experimental design and sampling campaign, as well as in performing part of the laboratory work.

Abstract

Although slope aspect determines the amount of solar irradiation, with implications on the functioning of forest ecosystems, little is known yet about how this affects the aboveground deadwood decomposition dynamics. Therefore, we set up a climosequence case study to evaluate the impact of slope exposure (north- *vs.* south-facing sites) on the physico-chemical and microbiological properties of *Picea abies* coarse woody debris (CWD) at different stages of natural decay (decay classes, DCls 1-5) in an Italian Alpine setting. Variations in bacterial, fungal and archaeal abundances were assessed by real-time PCR in the extra- and intracellular DNA fractions (eDNA *vs.* iDNA) of the total deadwood DNA pool. Physico-chemical wood properties (macro- and micronutrients; lignin and cellulose content; 3D structure via X-ray microtomography) were also performed along with the determination of key enzymatic activities involved in the main nutrient cycles. Overall, higher microbial abundances were registered in *Picea abies* CWD samples at the cooler, more acidic and moister north-facing site, which are favourable conditions especially for fungal wood decomposers. This thermal signal (N>S) was more evident for the advanced decay stages (DCls 4 and 5), being wood pH the most determinant factor for discriminating between both slopes. We also found that the impact of exposure was enzyme-specific and strongly dependent on the decay class, except for those enzymes involved in the P cycle. In addition, the eDNA/iDNA ratio provided a simple yet powerful index of microbial activity in terms of exposure, with lower values at the north-facing slope indicative of a higher microbial activity. This is in line with the more pronounced physical wood damage detected at this slope by the X-ray microtomography. A higher microbial activity at the cooler north-facing site rather seems surprising – a circumstance that probably is not due to temperature itself but due to increased moisture availability at this slope.

Keywords: climosequence; wood decay; extracellular DNA; quantitative PCR; hydrolytic enzymes; X-ray microtomography

1. Introduction

Deadwood is an important structural and functional component of forest ecosystems, acting as a temporal store of plant nutrients and water, and providing shelter and nutrition to various organisms, primarily fungi and saproxylic insects (Harmon et al., 1986; Floudas et al., 2012; Zuo et al., 2016). Moreover, deadwood represents a global carbon store estimated to be in the range of 73 ± 6 Pg (Pan et al., 2011), making its decomposition dynamics a determinant of the soil carbon balance and forest productivity (Bradford et al., 2014). However, as pointed out by Lombardi et al. (2013), in European cool to temperate and Mediterranean forest ecosystems deadwood is still poorly described and there is a paucity of information on its contribution to soil carbon and nutrient pools and to long-term forest sustainability.

Microorganisms, particularly fungi, are key determinants of lignocellulose decomposition thanks to the secretion of a battery of oxidoreductases and hydrolases (Purahong et al., 2016) and, therefore, of deadwood decomposition in forest ecosystems (Fischer et al., 2012). Through their presence as spores in the atmosphere or even as mycelial filaments in the surrounding soil, fungi are always in the vicinity of living, dying and dead wood (Hoppe et al., 2015a). It has also been shown that wood-inhabiting fungi may benefit from wood-colonising bacteria if they metabolise toxic intermediates and/or provide fungi with limiting nutrients like iron or nitrogen via nitrogen-fixation (de Boer and Van der Wal, 2008; Hoppe et al., 2014; Valášková et al., 2009). It is known that N availability in deadwood is highly restricted, with a C to N ratio ranging from 350 to 800, which suggests that wood-inhabiting fungi may benefit from associations with N-

fixing bacteria to fulfil their N requirements for vegetative and generative growth (Hoppe et al., 2014). On the other hand, wood-inhabiting bacteria may potentially confer negative effects to fungi, as they compete for easily degradable substrates that are necessary for fungal colonization and degradation activities (Folman et al., 2008). Although the direct contribution of bacteria to wood decomposition rate and dynamics seems to be smaller than that exerted by fungi, bacterial communities might play a more important role in deadwood turnover than previously thought and ultimately, in nutrient cycling in forest ecosystems (Hoppe et al., 2014, 2015b; Hervé et al., 2016; Johnston et al., 2016).

The so-called five-decay class system has commonly been used to describe the wood decay progression in the field (Hunter, 1990; Harmon et al., 2013; Lombardi et al., 2013; Petrillo et al., 2015, 2016). As woody material decays, its physical and chemical quality gradually changes and consequently a microbial community succession takes place as species are replaced by those more suited to the substrate (Rajala et al., 2012). In this regard, a climosequence approach may provide insight into deadwood decay dynamics in response to thermal conditions represented by different altitudes and exposure (Fravolini et al., 2016; Petrillo et al., 2015, 2016).

The aim of the present study was to evaluate the shifts in the wood-inhabiting microbiota of *Picea abies* (L.) Karst at different stages of decay at two subalpine sites located at north and south exposure in the Italian Alps (Val di Rabbi, Trentino) to account for different thermal conditions. Variations in bacterial, fungal and archaeal abundances with exposure were assessed in the extra- and intracellular DNA fractions (eDNA *vs.* iDNA) of the total deadwood DNA pool and related to specific physico-chemical properties of wood (i.e., pH, macro-micronutrients, lignin and cellulose content); as well as to the potential activities of key enzymes involved in the

main nutrient cycles. In addition, we were interested in better characterising the structural organisation of the deadwood because it may distinctly affect the decay processes (Mayo et al., 2010; Sedighi Gilani et al., 2014).

We hypothesised that: (1) warmer climatic conditions at south exposure will favour the deadwood decomposition in terms of microbial biomass and activity; (2) the exposure-effects on deadwood physico-chemical and microbiological properties will be more evident for the advanced decay stages; (3) the eDNA/iDNA ratio will provide a simple yet powerful index of microbial activity (the lower the ratio, the higher the activity) as a function of exposure and progressing wood decay.

2. Material and methods

2.1. Study sites and sampling strategy

The investigation area was located in Val di Rabbi (Trentino) in the south Alpine belt in northern Italy. The two study sites were located at an altitude of 1930 and 1995 m a.s.l. at north (N) and south (S)-facing slopes, respectively (Egli et al., 2006). The main characteristics of the N-facing slope were: aspect 20°N; slope 12°; mean annual air temperature (MAAT) 1.4 °C; mean annual precipitation (MAP) 1180 mm yr^{-1}; while the S-facing slope was characterised by: aspect 160°N; slope 25°; MAAT 4.4 °C; MAP 1180 mm yr^{-1} (Petrillo et al., 2015). Both study sites were on acidic paragneiss or morainic parent material consisting of paragneiss (Egli et al., 2006; Petrillo et al., 2015).

Coarse woody debris (CWD) samples from decaying Norway spruce (*Picea abies* (L.) Karst) were collected in August 2013 as described by Petrillo et al. (2015). Norway spruce constitutes the dominant tree species in these study sites together with the co-occurring European larch (*Larix decidua* Mill.) (Petrillo et al., 2015, 2016). CWD samples were classified in-situ using the

five decay class system based on visual, geometric and tactile features according to Hunter (1990): (1) hard wood, penetrable with a knife to only a few mm, bark and twigs (diameter <1 cm) intact; (2) rather hard wood, penetrable with a knife to less than 1 cm, bark and twigs begin to shed away, branches (diameter 1–4 cm) intact; (3) distinctly softened wood, penetrable with a knife to approximately 1–4 cm, bark and branches partially lost, original log circumference intact; (4) considerably decayed wood, penetrable with a knife to approximately 5–10 cm, bark lost in most places, original log circumference begins to disintegrate; (5) wood that disintegrates either to a very soft crumbly texture or is flaky and fragile, penetrable with a knife to more than 10 cm, original log circumference barely recognizable or not discernable.

Briefly, at each site five replicates for each decay class were collected, resulting in a total of 50 samples (2 study sites x 5 decay classes x 5 field replicates). Each field replicate was a composite sample deriving from 5 sub-samples that were pooled together in the field. The CWD volume assessment of each decay class was done as shown by Petrillo et al. (2015). All CWD samples were placed in a coolbox until they were taken to the laboratory, where before analyses they were pulverized using a cutting-mill (Fritsch-Pulverisette; 4 mm). After each sample, drill bits were cleaned by air-brushing and rinsed with distilled water between samples. All drill dust samples from each decay class were placed in a single sterilised vinyl bag and stored at 4 ºC and -20 ºC for physico-chemical and (micro)biological characterisation, respectively. For X-ray microtomography analyses, untreated (not cut-milled) wood samples were stored at -20 ºC (as described in section 2.7).

2.2. Physico-chemical analyses

Cut-milled CWD samples (5 g, fresh weight) were placed into a Petri dish and oven-dried (105 °C) for at least 24 h in order to determine the dry mass of the different decay classes. The volatile solids (VS) content was determined from the mass loss following ignition in a muffle furnace (Carbolite, CWF 1000) at 550 °C for 5 h. Electrical conductivity (EC) and pH were determined in wood:water extracts (1:5, w/v) by using a conductivity Meter LF 330 WTW (Weilheim, Germany) and a pH Meter Metrohm 744, respectively. Ammonium content was measured in 0.0125 M $CaCl_2$ extracts as described by Kandeler (1993). Total C and N were determined using a CN analyser (Vario Macro CN, Elementar, Hanau, Germany– combustion analysis). The concentration of P, K, Ca, Mg, Fe and Mn was assessed by using ICP-OES (Optima 8300, Perkin Elmer, Waltham, USA) after acid digestion of 0.5 g of powdered wood with 4 mL of HNO_3 in a closed vessel (UltraWAVE Milestone, Shelton, CT, USA – maximum temperature 230 °C). The α-cellulose content was assessed following the protocol of Leavitt and Danzer (1993) and Boettger et al. (2007). The Klason lignin, which is insoluble in strong acid, was determined according to Dence and Lin (1992) in a sequential extraction where first the water-soluble compounds were extracted. Ultrapure water (80 °C) was then added to each sample (1 g fw) and stirred 3 times for 15 min. Afterwards, the samples were centrifuged, dried and washed with ethanol as described by Fravolini et al. (2016). The supernatants were then discarded before adding ethanol again and filtering the samples. The filters were dried overnight at 60 °C followed by the addition of 3 mL of sulphuric acid (72 %) to 300 mg of the filter cake. After autoclaving for 1 h at 120 °C, the resulting solution was filtered into ceramic crucibles and the liquid evaporated at 110 °C, before weighing the lignin in the crucibles (Klason lignin). The acid-soluble lignin (ASL; Klason, 1893) in the filtrate was measured photometrically at 250 nm (Cary 50 conc UV-Visible Spectrophotometer). The total lignin is

the sum of the ASL + the Klason lignin; this lignin fraction also includes other recalcitrant compounds, such as tannins, cutin and suberin.

2.3. Sequential extraction of extra- and intracellular DNA

The sequential DNA extraction approach proposed by Ascher et al. (2009) for the soil metagenome was adopted to discriminate the extracellular (eDNA) and the intracellular (iDNA) fraction of the total deadwood DNA pool. Two technical replicates were included per each sample. Briefly, eDNA was extracted by gentle washings of 0.1 g cut-milled wood (fw) with 500 µL of 0.12 M Na_2HPO_4 at pH 8 in microcentrifuge tubes (2 mL) and horizontally shaken for 30 min (100 movements/min). The slurry was then centrifuged (4 °C, 30 min at 7500 g) and the supernatant collected. The wood pellet was subjected to the same procedure for two more cycles; the supernatants were pooled resulting in a final volume of 1.5 mL containing crude eDNA. Intracellular DNA was extracted from the residual pellet after the extraction of eDNA. The pellet was resuspended in 978 µL of 0.12 M Na_2HPO_4 at pH 8 and 122 µL MT buffer, transferred to tubes containing a lysing matrix (Lysing Matrix E; Fast DNA Kit for Soil; MP-Biomedicals) and one 1/4" Ceramic sphere (MPI biochemical cat. # 6540-424) to guarantee a complete disruption of the wood tissue. The samples were then processed by a combined mechanical-chemical cell lysis using the FastPrep instrument in combination with the reagents included in the Fast DNA Kit for soil. Bead beating conditions were 40 s at a speed equal to 5.5 m/min. The DNA extracts (eDNA; iDNA) were purified using the GeneClean procedure (MP-Biomedical) in order to reach PCR compatibility. DNA extracts were quantitatively and qualitatively characterised by PicoGreen based fluorimetry (dsDNA; Qubit, LifeTechnologies), µL-spectrophotometry (PicoDrop) and agarose-gel electrophoresis (Ascher et al., 2012). DNA yields (eDNA *vs.* iDNA) were expressed as µg DNA g^{-1}

wood (dry weight). Furthermore, the eDNA/iDNA ratio – as a function of proceeding decay status and exposure – was calculated as an estimator of microbial activity.

2.4. Quantitative real-time PCR (qPCR)

Real-time PCR was performed to quantify the microbial groups shown in Table 1 from both the eDNA and iDNA fractions of the total deadwood DNA pool with the 1X Sensimix™ SYBR® Hi-rox (Bioline, USA) based on the DNA-intercalating dye SYBR Green I. The Rotorgene 6000 Real Time Thermal Cycler (Corbett Research, Sydney, Australia) was used in combination with the Rotor-Gene Series Software 1.7. To build the standards we used purified PCR products of known concentrations from the pure cultures shown in Table 1. Stock concentration [gene copies μL^{-1}] was determined via PicoGreen measurement and freshly prepared. Ten-fold dilutions ranging from 108 to 102 copies μL^{-1} were applied for the standard curve construction. Quantitative PCR was performed in 20-µL assays with each reaction mix containing 1X Sensimix™ SYBR® Hi-rox, forward and reverse primers (200 nM each primer), 0.4 mg mL^{-1} BSA, distilled water (RNase/DNase free, Gibco™, UK) and 2 µL of either 1:10 diluted DNA-extract (for bacteria, archaea, fungi, AOB16S, *Nitrobacter* sp.); or undiluted DNA (for the 5 genera of methanogens, and N-cycle related functional genes); and ten-fold diluted standard DNA. For the primers used see Table 1. All standards and samples were run in duplicate following the cycling conditions in Table 1. To check for product specificity and potential primer dimer formation, runs were completed with a melting analysis starting from 60 °C to 95 °C with temperature increments of 0.25 °C and a transition rate of 5 s. The purity of the amplified products was also checked by the presence of a single band of the expected length on a 1% agarose gel stained with the DNA stain Midori Green (Nippon Genetics, Germany).

Table 1. Thermal profiles and primer pairs used for real-time PCR quantification of the different microbial groups assessed in the five deadwood decay classes.

Target group	Source of standard	Thermal profile	Primer	Annealing position	Amplicon length (bp)	References
Bacteria	*Nitrosomonas europaea* DSMZ 21879	95ºC-20 s/58ºC-15s/72ºC-30s	1055f, 1392r	16rDNA	352	Ferris et al. (1996)
Ammonia-oxidising bacteria (AOB)	*N. europaea* DSMZ 21879	95ºC-20 s/64ºC-15s/72ºC-15s	CTO189fA/B CTO 189fC, RT1r	16rDNA	116	Kowalchuk et al. (1997) Hermansson and Lindgren (2001)
Nitrobacter sp.	*Nitrobacter winogradsky* DSMZ 10237	94ºC-20 s/58ºC-15s/72ºC-20s	1198f, 1423r	16rDNA	227	Graham et al. (2007)
Ammonia-oxidising bacteria (AOB)	plasmid containing an *amoA* sequence	95ºC-25 s/57ºC-25s/72ºC-40s	amoA1F, amoA2R	*amoA* gene	491	Rothauwe et al. (1997)
Ammonia-oxidising archaea (AOA)	plasmid containing an *amoA* sequence	95ºC-25 s/53ºC-25s/72ºC-40s	Arch-amoAF, Arch-amoAR	*amoA* gene	635	Francis et al. (2005)
Nitrogen-fixing bacteria	*Azospirillum irakense*	95ºC-45 s/55ºC-45s/72ºC-45s	nifHf, nifHR	*nif*H gene	432	Rosch et al. (2002) Töwe et al. (2010)
Archaea	*M:formicicum* DSMZ1535	94ºC-30 s/57ºC-40s/72ºC-30s	Parch519f, Arc915r	16rDNA	420	Øvreås et al. (1997) Coolen et al. (2004)
Genus *Methanosaeta*	*M. concilii* DSMZ 2139	95ºC-20 s/60ºC-20s/72ºC-20s	MS1b, SAE835r	16rDNA	266	Shigematsu et al. (2003) Goberna et al. (2010)
Genus *Methanosarcina*	*M. barkeri* DSMZ 800	95ºC-20 s/64ºC-20s/72ºC-20s	240f, 589r	16rDNA	366	Franke-Whittle et al. (2009)
Genus *Methanobacterium*	*M. formicicum* DSMZ 1535	95ºC-20 s/58ºC-20s/72ºC-20s	fMbium, 748r	16rDNA	191	Goberna et al. (2010)
Genus *Methanosphaera*	*M. stadtmanae* DSMZ 3091	95ºC-20 s/61ºC-20s/72ºC-20s	594f, 747r	16rDNA	170	Goberna et al. (2010)
Genus *Methanoculleus*	*M. thermophilus* DSMZ 2640	95ºC-20 s/65ºC-20s/72ºC-20s	298f, 586r	16rDNA	308	Franke-Whittle et al. (2009)
Fungi	*Fusarium solani*	95ºC-15 s/50ºC-30s/72ºC-30s	FF390, FR1	18rDNA	390	Vainio and Hantula (2000) Prévost-Bouré et al. (2011)

In all real-time PCR runs an initial denaturing step of 10 min at 95 ºC was applied. Cycle repetitions were 40 for all the runs.
f= forward, r= reverse
Primer CTO189f A/B and primer CTO189C were used in a ratio 2:1.

2. 5. Double-stranded DNA content quantitation as estimator of microbial biomass

Determination of dsDNA content was carried out according to Fornasier et al. (2014) with the following modifications: an amount of 60-180 mg of cut-milled wood was weighed in duplicate in 2-mL Eppendorf tubes, by adding 1.20 mL of 0.12 M, pH 7.8, Na-phosphate buffer (Ascher et al., 2009), together with two 1/4" ceramic spheres (MPI biochemical cat. # 6540-424). Tubes were then subjected to bead-beating using a Retsch MM400 beating mill set at 30 Hz for 120 s, followed by centrifugation at 20000 g. Twenty μL of supernatant containing crude total DNA were taken and diluted in TE (TRIS 10mM; EDTA 1mM; pH 7.5) buffer as necessary (111-221 times). Afterwards, 25 μL of diluted extract were pipetted in duplicate into 384-well black microplates for determination of dsDNA content using Pico-Green reagent (Life Technologies) and a fluorimeter (Synergy HT microplate reader; BIO-TEK).

2.6. Potential enzymatic activities

Seventeen hydrolytic enzymatic activities involved in C, N, P and S biogeochemical cycles (Table 2) were measured in wood extracts by applying a heteromolecular exchange process (Fornasier and Margon, 2007). The procedure was similar to that used for dsDNA extraction-quantification with the following modifications: extraction buffer consisted in a 3% lysozyme solution in 0.1 M NaCl, pH 6.7; and the bead-beating lasted 180 s. After centrifugation, 750 μL of supernatant were taken and diluted with 250 μL of TRIS 50 mM, pH 7.0 buffer. Twenty μL of diluted extracts were pipetted in duplicate on 384-well microplates with 40 μL of appropriate buffer in order to determine fluorometrically the different potential enzyme activities by using the substrates listed in Table 2. Each microplate was read 4 times at time intervals of 5-180 minutes, according to the intensity of each

enzyme using a Synergy HT microplate reader (BIO-TEK). All the measurements were performed in duplicate for each field replicate and the activities were expressed as nanomoles of 4-methyl-umbelliferyl (MUF) min-1 g^{-1} dry wood.

Table 2. Overview of the potential enzymatic activities and their corresponding buffers and substrates evaluated in the present study.

Abbreviation	Enzyme	Buffer	Substrate	Biogeochemical cycle
arylS	arylsulfatase	MES 200mM pH 6	4- methylumbelliferyl sulfate	S
chit	chitinase	MES 200mM pH 6	4- methylumbelliferyl- N- acetyl- beta- D- glucosaminide	N
leu	leucine-aminopeptidase	THAM 200mM pH 7.5	L- Leucine 7- amido- 4methyl-coumarine hydrochloride	N
trip	tripsin- and papain-like protease	THAM 200mM pH 7.5	N-alpha-CBZ-L-Arginine 7-amido-4-methylcoumarin hydrochloride	N
alfaG	alfa-glucosidase	MES 200mM pH 6	4- methylumbelliferyl- alpha- D-glucopyranoside	C
betaG	beta- glucosidase	MES 200mM pH 6	4- methylumbelliferyl- beta- D-glucopyranoside	C
cell	cellulase	MES 200mM pH 6	4- methylumbelliferyl- beta- D-cellobioside	C
xil	xilosidase	MES 200mM pH 6	4- methylumbelliferyl- beta- D-xilopyranoside	C
uroni	glucuronidase	MES 200mM pH 6	4- methylumbelliferyl- beta- D-glucuronide	C
ester_ac	acetate-esterase	MES 200mM pH 6	4- methylumbelliferyl acetate	C
ester_nona	nonanoate-esterase	THAM 200mM pH 7.5	4- methylumbelliferyl nonanoate	C
ester_palm	palmitate-esterase	THAM 200mM pH 7.5	4- methylumbelliferyl palmitate	C
acP	acid phosphomonoesterase	MES 200mM pH 6	4- methylumbelliferyl phosphate	P
alkP	alkaline phosphomonoesterase	THAM 200mM pH 9	4- methylumbelliferyl phosphate	P
bisP	phosphodiesterase	THAM 200mM pH 7.5	bis(4- methylumbelliferyl) phosphoric acid	P
piroP	pirophosphate-phosphodiesterase	THAM 200mM pH 7.5	bis(4- methylumbelliferyl) pyrophosphoric acid	P
inosit	inositol-phosphatase	MES 200mM pH 6	4- methylumbelliferyl myo-inositol-1-phosphate	P

2.7. X-ray microtomography analyses

CWD samples were firstly dried 24 h at 50 °C and then cut into dimensions of 3 x 3 x 10 mm in order to achieve the best contrast for computational X-ray microtomography (μCT) analyses, which were carried out using the GE Nanotom S device at the IA PAS microtomography facility. During the μCT scanning the sample was rotated to register 2D-images of the scanned

samples. Based on these 2D-images a 3D-sample structure was recovered using reconstruction software. In order to reduce the potential noise, a 2D-image was acquired for each angular position of the different samples, resulting in an average value of 25 images recorded with slight (few pixels), random, perpendicular to X-ray beam detector movements. The resolution of the registered 2D images was 2284 x 2304 pixels and they were 14-bit depth grey level. The spatial resolution of 3D reconstructed volume – voxel size – was 1 μm. The X-ray source parameters were the following: accelerating voltage of 45 kV, cathode current of 350 μA and tungsten exit window. Although the temperature in μCT chamber remains stable during the scan, the sample itself is heated by X-rays, which can cause slight thermal sample dimension changes. This could interfere for the 1-μm resolution scans during the reconstruction phase. To avoid this, a 0.5 h pre-scan was conducted prior to the main scan. For the 3D volume reconstruction the DatosX 2.0 software was chosen, which resulted in 2284 x 2284 x 2304 16 bit gray level volume. For image analysis, processing and visualization VG Studio 2.0, Avizo 9 and Fiji software were used. The basic procedure for image processing involved the selection of the region of interest (ROI), along with the application of 3D median filtering with the kernel diameter equal to 3 px. The following nomenclature for ortho-views was used in this study: tangential view/cross section –cross section by the plane normal to tangential direction; radial view/cross section –cross section by the plane normal to radial direction; and longitudinal view/cross section –cross section by the plane normal to longitudinal direction.

2.8. Statistical analyses

The effect of exposure (north *vs.* south exposure) and wood decay stage (decay classes 1 to 5) on the chemical parameters and the potential enzymatic activities (except for tripsin-and-papain like protease and

palmitate-esterase) was evaluated by a two-factorial analysis of variance (ANOVA). For analysis of the qPCR data, a factorial ANOVA was also carried out in which three factors were fixed: exposure (north *vs.* south); wood decay stage (decay classes 1 to 5) and DNA fraction (extracellular DNA *vs.* intracellular DNA). The normality and the variance homogeneity of the data were tested prior to ANOVA by using the Shapiro-Wilks and Levene´s tests, respectively. Before analysis, data were log- or square root-transformed to meet the assumptions for ANOVA (when it was required). When data did not meet the normality condition, non-parametric tests (Kruskal-Wallis test) were performed to test for differences in wood nutrient content and in the two above-mentioned enzymatic activities (trip and esterpalm) as a function of exposure and wood decay stage. All the aforementioned analyses were performed with the Statistica software (version 9). Non-metric multidimensional scaling (NM-MDS) on log-normalized data was used to map the physico-chemical parameters to the shifts in microbial abundances (qPCR for both DNA fractions) and enzyme activities at the different wood decay stages as a function of slope exposure. The NM-MDS was calculated based on Bray-Curtis distance indices. The lengths of the arrows indicate the significance of the physico-chemical parameters for sample differentiation. This multivariate analysis was conducted with the PAST software (Version 2.17).

3. Results

3.1. Physico-chemical parameters

An overview of the wood physico-chemical parameters as a function of decay stage (decay classes, DCls 1-5) and exposure (N- *vs.* S-facing slope) is given in Table 3.

Exposure had a significant effect on the moisture content of CWD samples ($F_{1,20}$ = 17.2, p = 0.0005), with 1.5 times higher values at the N- than at the

S-facing slope. An increased moisture level was observed with increasing decay stage ($F_{4,20}$ = 31.5, $p \leq 0.0001$), being between 2 – 4 times greater in DCls 4 and 5 than in DCls 1-3 at both slopes. The percentage of volatile solids (VS) was in average 99 % for all the decay classes at both slopes, except for DCl 5 at the N-facing slope, where VS were 68 %, resulting in a significant interaction between decay class and exposure ($F_{4,100}$ = 6.2, p = 0.002). Wood pH was significantly affected by the slope exposure ($F_{1,20}$ = 40.5, $p \leq 0.0001$), with an average value of 4.0 at the N- and 4.6 at the S-facing site. However, no significant differences were found with respect to the decay stage. At the S-facing site DCls 1, 3 and 4 had 1.5-times higher EC values than at the N-facing site. However, no exposure-effect was found for DCl 2; whilst for DCl 5 EC was 1.5-fold greater at north- than at south exposure (interaction decay class x slope exposure $F_{4,20}$= 3.3, p = 0.03). Moreover, two-fold lower EC values were recorded in the DCls 3-5 than in DCls 1-2 at the N-facing slope; a decrease in EC with increasing decay stage was also reported at the S-facing site. Although no exposure-effect was detected for the total N content, it differed significantly with the wood decay stage (p = 0.0001), with higher values in the DCls 4 and 5 (2-6 times higher) than in the DCls 1-3 at both slopes. In addition, even though the effect of exposure on NH_4^+ content was dependent on the decay class ($F_{4,20}$ = 24.9, $p \leq 0.0001$), no clear trend between the N- and the S-facing slopes was detectable. The exposure-effect on the total C content was only evident for the DCl 5 (p = 0.02), with a lower amount at the N- than at the S-facing slope. Exposure did not affect the percentage of cellulose ($F_{1,20}$ = 0.2, p = 0.7); while significant differences were recorded depending on the stage of decay ($F_{4,20}$ = 40.4, $p \leq 0.0001$), registering 2- and 4-fold higher values in the DCls 1-3 than in the DCls 4-5. Exposure, however, had a significant impact on the lignin content ($F_{1,20}$ = 9.5, p = 0.006) being 1.2 times higher at the S- than at the N-facing site, and with greater values for the DCls 4-5 ($F_{4,20}$=

6.9, p = 0.001). Ca, K and Mg concentrations were between 2-4 times higher at the N-facing slope with respect to the comparable south-facing one (p = 0.0004, p = 0.004 and p = 0.002, respectively). Except for Ca, the concentrations of K and Mg were around 7 times greater in DCl 5 than in DCls 1-4 at north exposure (K: p = 0.04; Mg: p= 0.03). Exposure did not have a significant effect on P and Fe concentrations; however, both nutrients varied significantly with the stage of decay (p = 0.0009 and p = 0.0003, respectively), registering the highest P concentration in DCl 5 at both slopes. This decay class was also characterised by a remarkably higher Fe concentration at the N-facing slope, being 52-fold greater than in DCl 4, and between 180-360 times higher than in DCls 1-3. Mn concentration was also significantly higher in DCl5 (between 2-5 times higher) than in the other decay classes (p = 0.005).

Table 3. Physico-chemical properties and elemental concentrations in the decay classes 1 to 5 from the north- and south-facing slopes. Values are means ± standard deviation. Data are given on a dry weight basis.

	North-facing slope					South-facing slope				
Decay classes	**1**	**2**	**3**	**4**	**5**	**1**	**2**	**3**	**4**	**5**
Moisture (%)	26 ± 6	31 ± 7	47 ± 17	69 ± 5	64 ± 8	14 ± 1	14 ± 3	18 ± 6	44 ± 18	74 ± 1
VS (%)	99 ± 0.6	99 ± 0.3	100 ± 0.3	99 ± 0.7	68 ± 11	99 ± 0.4	99 ± 0.4	100 ± 0.1	100 ± 0.3	99 ± 0.5
pH	4.1 ± 0.1	4.0 ± 0.1	3.8 ± 0.2	3.9 ± 0.1	4.2 ± 0.1	5.0 ± 0.2	4.3 ± 0.5	4.8 ± 0.5	4.7 ± 0.1	4.6 ± 0.3
EC (µS cm^{-1})	145 ± 4	160 ± 26	67 ± 14	66 ± 16	63 ± 14	173 ± 11	160 ± 28	111 ± 14	86 ± 12	45 ± 1.5
Total N (g kg^{-1})	2.2 ± 0.5	1.3 ± 0.1	1.0 ± 0.1	4.3 ± 0.3	6.2 ± 1.0	1.8 ± 0.6	1.2 ± 0.2	1.3 ± 0.2	2.3 ± 0.2	3.3 ± 0.4
NH_4^+ (mg kg^{-1})	6.5 ± 0.5	1.4 ± 0.08	1.5 ± 0.1	2.5 ± 0.5	13.8 ± 4.2	6.3 ± 2.5	4.2 ± 0.6	6.3 ± 2.8	6.1 ± 1.8	6.2 ± 2.7
Total C (%)	47 ± 0.9	47 ± 0.7	47 ± 0.3	48 ± 0.3	32 ± 8.7	47 ± 0.4	47 ± 0.4	47 ± 0.4	50 ± 0.4	50 ± 0.5
Cellulose (%)	30.9 ± 2.7	18.7 ± 3.6	29.9 ± 4.9	13.2 ± 1.6	7.0 ± 1.8	24.8 ± 8.6	30.8 ± 1.8	28.6 ± 2.5	4.8 ± 1.7	7.7 ± 2.5
Klason lignin (%)	33.7 ± 1.8	39.2 ± 3.8	25.7 ± 5.7	45.8 ± 1.1	39.8 ± 8.7	42.7 ± 4.2	36.1 ± 1.4	36.4 ± 2.6	55.7 ± 1.3	55.7 ± 0.3
Ca (g kg^{-1})	3.2 ± 2.0	2.1 ± 0.4	1.9 ± 0.6	3.2 ± 0.8	2.2 ± 0.5	1.3 ± 0.3	0.6 ± 0.1	0.7 ± 0.1	1.4 ± 0.2	2.5 ± 1.0
K (g kg^{-1})	0.6 ± 0.3	0.5 ± 0.1	< 0.3	0.7 ± 0.1	4.5 ± 1.0	0.4 ± 0.1	0.6 ± 0.4	< 0.3	0.3 ± 0.0	0.4 ± 0.1
Mg (g kg^{-1})	0.6 ± 0.4	0.5 ± 0.2	0.3 ± 0.1	0.6 ± 0.1	4.1 ± 1.3	0.4 ± 0.2	0.2 ± 0.0	0.2± 0.0	0.2 ± 0.1	0.5 ± 0.2
P (mg kg^{-1})	123 ± 29	83 ± 6	<50	243 ± 15	437 ± 95	87 ± 40	133± 85	53 ± 6	100 ± 17	137 ± 21
Fe (mg kg^{-1})	97 ± 68	58 ± 22	114 ± 84	408 ± 104	21295 ± 8835	124 ± 66	70 ± 15	94 ± 23	243 ± 67	572 ± 409
Mn (mg kg^{-1})	85 ± 78	93 ± 35	36 ± 9	93 ± 49	166 ± 107	107 ± 27	55 ± 17	36 ± 3	60 ± 13	113 ± 35

VS: volatile solids
EC: electrical conductivity

3.2. Extra- and intracellular DNA yields

The sequential extraction of the extracellular (eDNA) and intracellular (iDNA) fraction of the total deadwood DNA pool yielded amounts ranging from 1 to 20 μg eDNA g^{-1} wood and from 1 to 40 μg iDNA g^{-1} wood (Fig. 1A, B). Slope exposure significantly influenced the eDNA content only in the case of DCl 4, giving rise to 3-fold higher yields at the N- than at the S-facing slope ($F_{4,20}$ = 2.8, p = 0.04; Fig. 1A). The stage of decay also had a significant impact on this parameter ($F_{4,20}$ = 36.1, p ≤ 0.0001). At north exposure eDNA content was 17-and 13-times higher in DCls 4 and 5 compared to DCls 1-3; and at south exposure the amount of eDNA was about 6- and 13-fold higher in the last two decay classes, respectively. The exposure-effect on the yields of iDNA was only significant for DCls 4 and 5 ($F_{4,20}$ = 2.8, p = 0.04; Fig. 1B). The amount of iDNA was 11- and 4-times higher at the N-facing site for these two decay classes (Fig. 1B). In addition, iDNA yields varied significantly with the stage of decay at both slopes ($F_{4,20}$ = 21.7, p ≤ 0.0001), being around 20-times higher in DCls 4 and 5 than in DCls 1-3 at north exposure, while at south exposure it was about 5-fold higher in DCl 5 than in the remaining decay classes (Fig. 1B). A higher eDNA/iDNA ratio was in general found for the CWD samples collected at the S-facing site irrespective of the decay class ($F_{4,20}$= 29.0, p ≤ 0.0001; Fig. 1C). An exposure-effect on dsDNA yields was only recorded for DCl 4, being 2-times higher at the N- than at the S-facing site ($F_{4,20}$= 3.1, p = 0.04; Fig. 1D). At both slopes, DCls 4 and 5 had a higher dsDNA content (Fig. 1D) in comparison with DCls 1-3 ($F_{4,20}$= 23.9, p ≤ 0.0001), and these differences were more obvious at north exposure where dsDNA yields were around 6-fold higher in the last two decay classes (Fig. 1D).

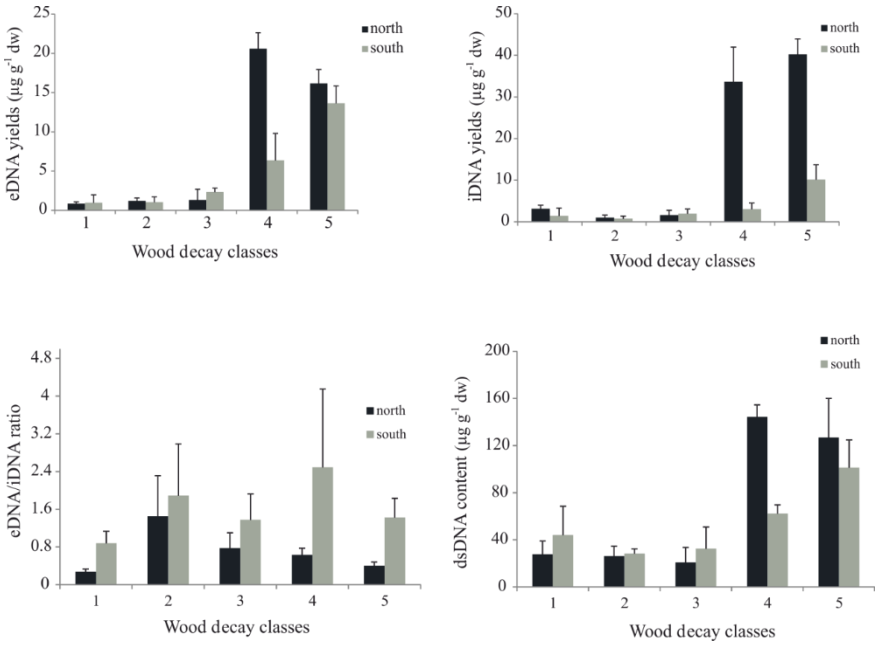

Fig. 1. Yields of extracellular DNA (eDNA; A) and intracellular DNA (iDNA; B); eDNA/iDNA ratio (C); and dsDNA content (D) as a function of proceeding decay of *Picea abies* CWD (decay classes 1-5) and slope exposure (north- *vs.* south-facing slope).

3.3. Community- and functional gene-level real-time PCR of the extra- and intracellular DNA fractions from *P. abies* CWD samples

Bacterial abundance was 17- and 3-times higher in CWD samples at the N- than at the S-facing site ($F_{1,100}$ = 106.1, $p \leq 0.0001$) for iDNA and eDNA fractions, respectively (Tables 4 and 5). The same trend was observed for fungi ($F_{1,100}$ = 44.7, $p \leq 0.0001$) and archaea ($F_{1,100}$ = 39.7, $p \leq 0.0001$). Moreover, these three microbial groups were more abundant at the advanced decay stages, i.e., in the DCls 4 and 5 for both DNA fractions, and these differences were more evident at the N-facing slope (bacteria: $F_{4,100}$= 6.9, $p \leq 0.0001$; fungi: $F_{4,100}$= 8.4, $p \leq 0.0001$; archaea: $F_{4,100}$= 4.8, p = 0.001). For instance, for the iDNA fraction, the bacterial abundance was 18- and 60-fold higher in the DCls 4 and 5 compared to the DCls 1-3 (Table 5).

The same trend was observed for the eDNA fraction in which the abundance of bacteria was 20-times higher in the last two decay classes (Table 4).

CWD samples at the N-facing slope were also characterised by a greater abundance of ammonia-oxidising bacteria (AOB 16S) than those at the S-facing slope irrespective of the decay stage ($F_{1,100}$ = 158.6, $p \leq 0.0001$). Moreover, DCls 4 and 5 had the highest AOB 16S abundance with regard to both DNA fractions ($F_{4,100}$= 15. 4, $p \leq 0.0001$; Tables 4 and 5). The abundance of *Nitrobacter* sp. followed a similar trend than that shown for AOB 16S (Tables 4 and 5). Exposure also had a significant effect on the *nif*H gene abundance ($F_{1,100}$ = 131.6, $p \leq 0.0001$), being 10-fold higher in CWD samples at the N- than at the S-facing slope. Moreover, at north exposure, *nif*H abundance was around 5-fold higher in the advanced decay stages (DCls 4 and 5) than in DCls 1-3 in the eDNA fraction (Table 4); and between 10- and 30-times higher in the iDNA fraction (Table 5). The ammonia-oxidation marker gene *amo*A was studied for targeting both ammonia-oxidising bacteria (AOB) and archaea (AOA). The *amo*A AOB gene was only detected in the iDNA fraction of DCls 4 and 5 at north exposure, reaching values of 4.6×10^5 and 2.3×10^6 copies per gram wood dw, respectively (Table 5). Likewise, at the same slope the *amo*A AOA gene was only detected in the iDNA fraction of DCl 5, having a value of 5.5×10^6 copies per gram wood dw (Table 5). Among the five genera of methanogens, we found that the abundance of *Methanosarcina*, *Methanosphaera* and *Methanoculleus* was below the detection limit (Tables 4 and 5). Nevertheless, the genus *Methanobacterium* was detected in the iDNA fraction of the DCls 3-5 (Table 5), and in the eDNA fraction of the DCl 3 at the N-facing site (Table 4). In addition, at both slopes the genus *Methanosaeta* was present in both DNA fractions of the DCls 4 and 5 (Tables 4 and 5).

Table 4. Real-time PCR analysis from the extracellular DNA fraction of the decay classes 1 to 5 from the north- and south-facing slopes. Values are means with standard deviation in brackets. Units are expressed as gene copy number per g wood dw.

	North-facing slope					South-facing slope				
Decay classes	**1**	**2**	**3**	**4**	**5**	**1**	**2**	**3**	**4**	**5**
Bacteria	2.5×10^8 (2.1×10^7)	1.5×10^8 (9.8×10^6)	1.7×10^8 (1.3×10^6)	3.5×10^9 (1.2×10^7)	3.9×10^9 (8.8×10^7)	8.9×10^7 (1.3×10^6)	8.3×10^7 (6.1×10^5)	2.6×10^8 (1.4×10^6)	5.8×10^8 (2.8×10^6)	1.5×10^9 (4.9×10^6)
Fungi	1.7×10^9 (1.5×10^8)	5.8×10^8 (5.8×10^5)	9.2×10^8 (5.7×10^7)	6.3×10^9 (3.6×10^7)	7.3×10^9 (1.9×10^7)	4.4×10^8 (4.8×10^6)	3.9×10^8 (3.4×10^6)	5.9×10^8 (4.6×10^5)	3.9×10^8 (2.1×10^5)	9.5×10^8 (4.7×10^6)
Archaea	1.3×10^8 (1.0×10^6)	9.4×10^7 (4.9×10^6)	1.9×10^8 (1.1×10^7)	1.7×10^9 (1.2×10^7)	8.4×10^8 (3.3×10^6)	1.3×10^8 (1.5×10^6)	6.3×10^7 (6.6×10^5)	6.1×10^7 (3.0×10^5)	6.3×10^7 (2.5×10^5)	2.2×10^8 (1.5×10^5)
AOB16S	7.8×10^6 (7.2×10^4)	1.3×10^7 (1.0×10^5)	1.9×10^7 (1.8×10^5)	3.6×10^7 (3.2×10^5)	2.9×10^7 (2.4×10^5)	6.1×10^6 (1.1×10^4)	5.7×10^6 (1.8×10^5)	6.3×10^6 (1.2×10^5)	8.2×10^6 (5.9×10^4)	2.4×10^7 (3.6×10^5)
***Nitrobacter* sp.**	1.1×10^7 (1.0×10^6)	7.9×10^6 (4.9×10^4)	1.3×10^7 (1.1×10^6)	3.6×10^8 (9.1×10^6)	3.6×10^8 (8.9×10^6)	1.5×10^6 (1.0×10^5)	2.7×10^6 (1.4×10^4)	1.2×10^7 (2.5×10^5)	3.3×10^7 (9.9×10^4)	1.6×10^8 (7.2×10^6)
***nif*H gene**	6.3×10^6 (1.2×10^4)	4.8×10^6 (9.8×10^4)	7.0×10^6 (8.3×10^4)	4.2×10^7 (6.4×10^5)	2.9×10^7 (7.9×10^5)	1.4×10^6 (7.9×10^4)	1.1×10^6 (6.8×10^3)	3.9×10^6 (1.4×10^4)	7.5×10^6 (1.0×10^4)	2.3×10^7 (8.4×10^4)
***amo*A-AOB gene**	b.d.l.	b.d.l.	b.d.l.	b.d.l.	b.d.l.	b.d.l.	b.d.l.	b.d.l.	b.d.l.	b.d.l.
***amo*A-AOA gene**	b.d.l.	b.d.l.	b.d.l.	b.d.l.	b.d.l.	b.d.l.	b.d.l.	b.d.l.	b.d.l.	b.d.l.
Genus *Methanobacterium*	b.d.l.	b.d.l.	1.8×10^6 (8.3×10^5)	b.d.l.	b.d.l.	b.d.l.	b.d.l.	b.d.l.	b.d.l.	b.d.l.
Genus *Methanosaeta*	b.d.l.	b.d.l.	b.d.l.	3.9×10^5 (8.3×10^3)	2.8×10^5 (9.1×10^3)	b.d.l.	b.d.l.	1.3×10^5 (7.2×10^3)	1.8×10^5 (7.6×10^3)	5.3×10^5 (8.2×10^3)

b.d.l. = below detection limit
AOB = ammonia-oxidising bacteria
AOA = ammonia-oxidising archaea

Table 5. Real-time PCR analysis from the intracellular DNA fraction of the decay classes 1 to 5 from the north- and south-facing slopes. Values are means with standard deviation in brackets. Units are expressed as gene copy number per g wood dw.

	North-facing slope					South-facing slope				
Decay classes	**1**	**2**	**3**	**4**	**5**	**1**	**2**	**3**	**4**	**5**
Bacteria	9.6×10^8 (2.2×10^7)	3.7×10^8 (2.1×10^6)	8.4×10^8 (6.5×10^5)	1.1×10^{10} (2.8×10^6)	3.7×10^{10} (3.6×10^6)	3.1×10^8 (3.1×10^6)	1.3×10^8 (1.2×10^6)	2.4×10^8 (1.3×10^6)	6.2×10^8 (4.8×10^5)	1.7×10^9 (4.3×10^6)
Fungi	1.9×10^9 (1.6×10^6)	2.2×10^9 (1.5×10^6)	1.5×10^9 (1.4×10^3)	1.4×10^{10} (7.6×10^6)	1.0×10^{10} (2.2×10^6)	7.9×10^8 (5.2×10^5)	2.4×10^9 (7.2×10^6)	2.4×10^9 (9.8×10^6)	2.6×10^9 (7.8×10^6)	6.1×10^9 (1.0×10^6)
Archaea	1.3×10^8 (1.0×10^6)	9.4×10^7 (4.9×10^5)	2.0×10^8 (1.1×10^4)	1.7×10^9 (1.2×10^6)	8.4×10^8 (3.3×10^6)	1.3×10^8 (1.8×10^5)	6.3×10^7 (1.1×10^4)	6.1×10^7 (3.0×10^4)	6.3×10^7 (2.5×10^4)	2.2×10^8 (9.8×10^5)
AOB16S	9.1×10^6 (1.4×10^3)	1.8×10^7 (6.3×10^4)	1.9×10^7 (1.1×10^4)	4.4×10^7 (4.9×10^4)	9.7×10^7 (7.2×10^5)	7.2×10^6 (3.4×10^3)	6.9×10^6 (9.4×10^4)	6.3×10^6 (8.8×10^3)	8.8×10^6 (2.4×10^3)	2.5×10^7 (5.9×10^4)
***Nitrobacter* sp.**	4.3×10^7 (4.2×10^4)	9.0×10^6 (6.7×10^4)	4.9×10^7 (4.8×10^5)	7.9×10^8 (2.3×10^5)	1.9×10^9 (1.1×10^5)	1.8×10^7 (2.1×10^4)	8.7×10^6 (6.1×10^3)	1.5×10^7 (4.1×10^3)	5.4×10^7 (4.4×10^3)	1.8×10^8 (5.5×10^4)
***nif*H gene**	7.5×10^6 (9.3×10^3)	1.1×10^7 (7.3×10^5)	2.7×10^7 (9.5×10^4)	2.3×10^8 (1.1×10^5)	2.6×10^8 (7.6×10^5)	7.1×10^6 (1.3×10^3)	1.5×10^6 (8.8×10^3)	3.9×10^6 (9.9×10^3)	1.1×10^7 (6.8×10^3)	2.7×10^7 (1.1×10^4)
***amo*A-AOB gene**	b.d.l.	b.d.l.	b.d.l.	4.6×10^5 (1.3×10^5)	2.3×10^6 (7.3×10^3)	b.d.l.	b.d.l.	b.d.l.	b.d.l.	b.d.l.
***amo*A-AOA gene**	b.d.l.	b.d.l.	b.d.l.	b.d.l.	5.5×10^6 (8.1×10^3)	b.d.l.	b.d.l.	b.d.l.	b.d.l.	b.d.l.
Genus *Methanobacterium*	b.d.l.	b.d.l.	7.1×10^6 (9.3×10^3)	2.6×10^5 (1.0×10^5)	1.9×10^5 (9.3×10^3)	b.d.l.	b.d.l.	b.d.l.	b.d.l.	b.d.l.
Genus *Methanosaeta*	b.d.l.	b.d.l.	b.d.l.	1.9×10^6 (5.3×10^3)	3.4×10^6 (8.2×10^3)	b.d.l.	b.d.l.	2.6×10^5 (9.3×10^2)	4.0×10^5 (1.3×10^2)	2.7×10^6 (7.8×10^3)

b.d.l. = below detection limit
AOB = ammonia-oxidising bacteria
AOA = ammonia-oxidising archaea

3.4. Potential enzymatic activities

An overview of the potential hydrolytic enzyme activities from CWD samples at the different decay stages and exposure is given in Table 6. DCls 4 and 5 showed a higher arylsulphatase activity at the N- than at the S-facing slope (9 and 3-times higher, respectively); however, no significant exposure-effects were found for DCls 1-3 (exposure x decay class $F_{4,20} = 3.34$, $p = 0.03$). The exposure-effect on chitinase activity was also dependent on the decay class ($F_{4,20} = 2.95$, $p = 0.04$), with greater values (2 and 4 times) at the N-facing slope for DCls 1 and 4. However, a higher leucine-aminopeptidase activity was recorded at the S-facing slope, except for DCl 4 which showed a higher activity (3 times) at the N-facing site ($F_{4,20} = 2.89$, $p= 0.04$). In contrast, exposure did not have a significant impact on the tripsin-and papain-like protease activity. The stage of wood decay affected significantly these two latter enzyme activities (*leu*: ANOVA $F_{4,20} = 4.3$; $p = 0.01$; *trip*: Kruskal-Wallis test $H_{4,30} = 21.6$; $p = 0.0002$). At north exposure the highest activities were registered for DCl 4; while at south exposure the highest levels were detected in DCls 3 and 5 for leucine-aminopeptidase and tripsin-and papain-like protease activities, respectively. The potential activities of α-and β-glucosidases, cellulase and xylanase also varied significantly with exposure and decay stage (*alfaG*: $F_{4,20} = 4.3$, $p = 0.002$; *betaG*: $F_{4,20} = 4.8$, $p = 0.007$; *cell*: $F_{4,20} = 4.9$, $p = 0.006$; *xil*: $F_{4,20} = 4.6$, $p = 0.009$). The same trend was observed for glucuronidase, acetate esterase and palmitate esterase activities (*uroni*: $F_{4,20} = 12.3$, $p \leq 0.0001$; *esterac*: $F_{4,20} = 8.6$, $p = 0.0003$; *esterpalm*: Kruskal-Wallis test $H_{4,30} = 10.8$; $p = 0.03$). In addition, at the N-facing slope the highest activities were in general recorded for the DCl4.

Table 6. Potential enzymatic activities in the decay classes 1 to 5 from the north- and south-facing slopes. The full name of the enzymatic activities is given in Table 2. Values are means ± standard deviation. Data are expressed as nanomoles of MUF min^{-1} g^{-1} dry soil.

	North-facing slope					South-facing slope				
Decay classes	**1**	**2**	**3**	**4**	**5**	**1**	**2**	**3**	**4**	**5**
aryS	1.9 ± 1.1	1.7 ± 0.2	1.8 ± 0.9	20.5 ± 7.1	38.5 ± 13.4	1.3 ± 0.9	1.5 ± 0.4	1.4 ± 0.1	2.2 ± 1.4	13.3 ± 5.3
chit	93.3 ± 53.1	46.4 ± 10.8	31.4 ± 14.3	51.1 ± 24.3	16.2 ± 8.3	38.1 ± 13.5	41.3 ± 9.8	42.2 ± 14.4	11.6 ± 8.7	15.5 ± 5.4
leu	31.3 ± 14.9	25.3 ± 10.7	44.2 ± 19.5	248.6 ± 39.4	67.6 ± 28.0	54.7 ± 39.6	75.1 ± 32.1	204.6 ± 74.7	88.0 ± 10.8	119.6 ± 40
trip	0.0 ± 0.0	0.3 ± 0.02	0.2 ± 0.01	3.2 ± 0.4	0.8 ± 0.1	0.0 ± 0.0	0.0 ± 0.0	0.0 ± 0.0	0.5 ± 0.08	1.1 ± 0.4
alfa_G	3.3 ± 1.3	0.8 ± 0.05	2.0 ± 0.9	9.0 ± 2.3	2.4 ± 0.9	1.6 ± 0.9	1.5 ± 0.4	2.0 ± 0.6	2.6 ± 0.9	2.1 ± 1.0
beta_G	202.5 ± 91.6	41.3 ± 3.7	42.9 ± 13.0	381.1 ± 72.8	93.7 ± 9.9	89.5 ± 35.4	83.5 ± 36.3	114.3 ± 25.6	159.0 ± 36.7	118.6 ± 57.3
cell	34.9 ± 14.2	3.8 ± 1.1	3.5 ± 1.9	73.3 ± 29.3	11.2 ± 1.0	16.5 ± 12.6	14.3 ± 6.3	18.0 ± 8.0	18.0 ± 2.9	14.2 ± 8.2
xil	16.9 ± 9.1	5.0 ± 1.0	9.2 ± 3.1	66.7 ± 10.3	19.3 ± 5.7	10.6 ± 2.3	15.7 ± 7.0	20.8 ± 4.5	28.3 ± 5.3	22.7 ± 9.5
uroni	1.3 ± 0.7	0.8 ± 0.1	0.7 ± 0.3	7.7 ± 2.1	3.9 ± 1.3	1.3 ± 0.5	1.8 ± 0.8	2.5 ± 1.3	3.4 ± 0.6	4.8 ± 2.3
ester_ac	1956 ± 943	1354 ± 243	1026 ± 333	5224 ± 1639	2958 ± 1629	1483 ± 699	1528 ± 448	1969 ± 349	2933 ± 714	2788 ± 416
ester_nona	144.1 ± 24.7	36.2 ± 10.0	53.8 ± 17.9	1465 ± 761	294 ± 87	131.8 ± 43.3	91.7 ± 38.0	131.9 ± 55.1	244.4 ± 53.4	214.0 ± 64.1
ester_palm	1.4 ± 0.9	0.2 ± 0.01	0.2 ± 0.05	4.8 ± 1.9	1.3 ± 0.3	0.2 ± 0.05	0.1 ± 0.02	0.3 ± 0.03	0.4 ± 0.01	0.7 ± 0.09
acP	160.8 ± 43.1	35.2 ± 12.3	282.4 ± 97.2	1339 ± 337.5	1514 ± 517	134.9 ± 25.3	185.6 ± 30.9	467.4 ± 95.4	960.1 ± 312	1476 ± 515
bisP	11.2 ± 5.9	2.4 ± 0.9	19.8 ± 13.3	33.4 ± 6.8	18.5 ± 6.1	10.0 ± 3.7	6.4 ± 1.8	12.1 ± 3.8	15.9 ± 5.9	28.7 ±6.9
piroP	1.1 ± 0.2	0.4 ± 0.05	4.9 ± 1.7	4.2 ± 1.5	2.3 ±0.8	0.6 ± 0.07	0.5 ± 0.04	0.5 ± 0.1	1.3 ± 0.08	2.9 ± 0.9
inosit	7.0 ± 1.1	1.6 ± 0.6	7.5 ± 3.3	16.5 ±1.6	11.3 ± 4.6	3.2 ± 1.2	4.6 ± 1.8	9.4 ± 3.1	13.8 ± 4.9	13.7 ± 4.7
alkP	35.0 ± 14.4	0.7 ± 0.1	22.5 ± 6.6	119.3 ± 59.2	45.4 ± 27.7	13.2 ± 2.9	11.2 ± 4.0	23.3 ± 13.7	50.4 ± 14.4	90.6 ± 20.7

No exposure-effect was found for any of the enzymes involved in the P-cycle. Nonetheless, they were significantly influenced by the stage of wood decay (*acP*: $F_{4,20} = 35.3$, $p \leq 0.0001$; *alkP*: $F_{4,20} = 7.1$, $p = 0.001$; *bisP*: $F_{4,20} = 7.7$, $p = 0.0006$; *inosit*: $F_{4,20} = 8.1$, $p = 0.0005$), with the exception of pirophostate-phosphodiesterase. Higher activities were in general recorded in DCls 4 and 5 than in DCls 1-3.

3.5. Non-metric multidimensional scaling (NM-MDS) analysis

Exposure effects and the physico-chemical parameters shaping the microbiological properties (microbial abundances and enzyme activities) from *Picea abies* CWD at different decay stages were visualised in the NM-MDS plot (Fig. 2). Overall, DCls 1-3 (negative side) grouped differently from DCls 4 and 5, which were found to cluster on the positive side of the first ordination axis, indicating that each decay class, independently of the slope exposure, represents a special matrix and thus, a specific microhabitat. Moisture ($r = 0.77$) along with N, P and Fe contents ($r = 0.87$, 0.72 and 0.73) were the major determinants for the clustering of the CWD samples along this axis, with higher values with increasing stage of decay. The opposite trend was observed for EC, that it was negatively correlated with axis 1 ($r = -0.72$). Moreover, CWD samples were differentiated along the second axis as a function of exposure, with N-facing samples at the positive side and S-facing ones at the negative side, being pH the most important parameter ($r = 0.44$) for this differentiation.

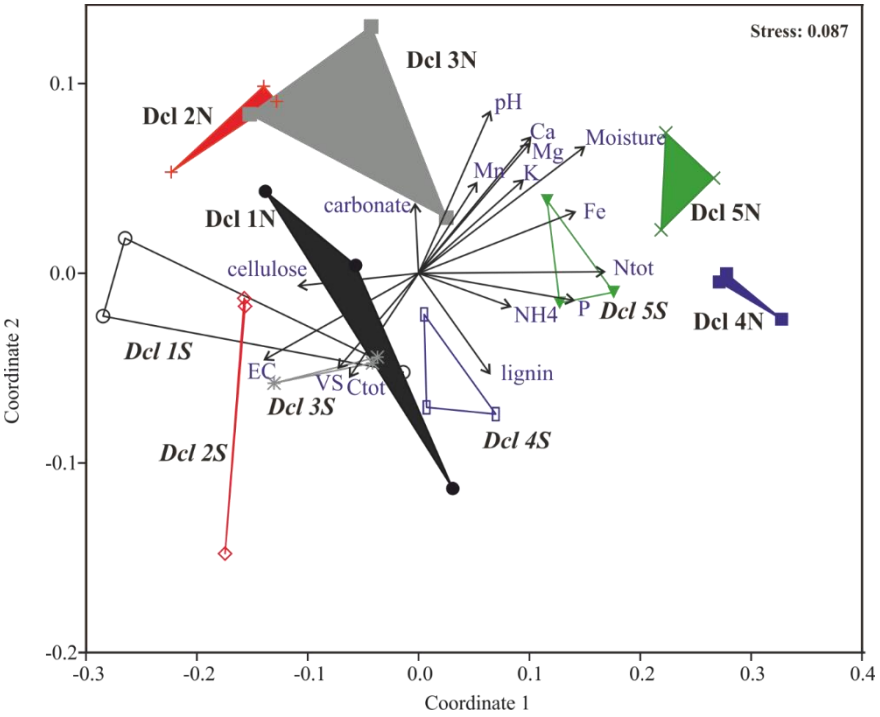

Fig. 2. Non-metric multidimensional scaling (NM-MDS) on log-normalized data was used to map the physico-chemical parameters to the shifts in microbial abundances for both DNA fractions (eDNA and iDNA) assessed by real-time PCR and enzyme activities at the different wood decay stages as a function of slope exposure. The NM-MDS was calculated based on Bray-Curtis distance indices. The lengths of the arrows indicate the significance of the physico-chemical parameters for sample differentiation. The different colored triangles refer to the different decay classes (DCl 1: black; DCl 2: red; DCl3: grey; DCl4: blue; and DCl5: green). Full and empty symbols refer to the north- and the south-facing slope respectively.

3.6. X-ray tomography

X-ray microtomography (μCT) analyses enabled the differentiation of the wood cell types, including tracheids, vessels, xylem rays and bordered pits, as a function of slope exposure and decay stage (Figs. 3-6). Generally, no substantial differences were detected among the first three decay classes (DCls 1-3). On the one hand, no sign of degradation was in general observed for the tracheid cell walls of the DCl 1 (Figs. 3 and 4). Nonetheless, the degradation of the wood cell wall was evident for the DCl

4, being this fact more pronounced at the N-facing slope (data not shown); indeed, the structure of the xylem rays showed signs of degradation only for the CWD samples collected at this slope. The DCl 5 was even more degraded than DCl4 showing cracks along the radial direction (Figs. 5 and 6). Furthermore, if we consider the tangential 3D view, the bordered pits in the DCl5 could only be distinguished at the S-facing slope (Fig. 6), indicating a higher degree of physical cell damage at north exposure.

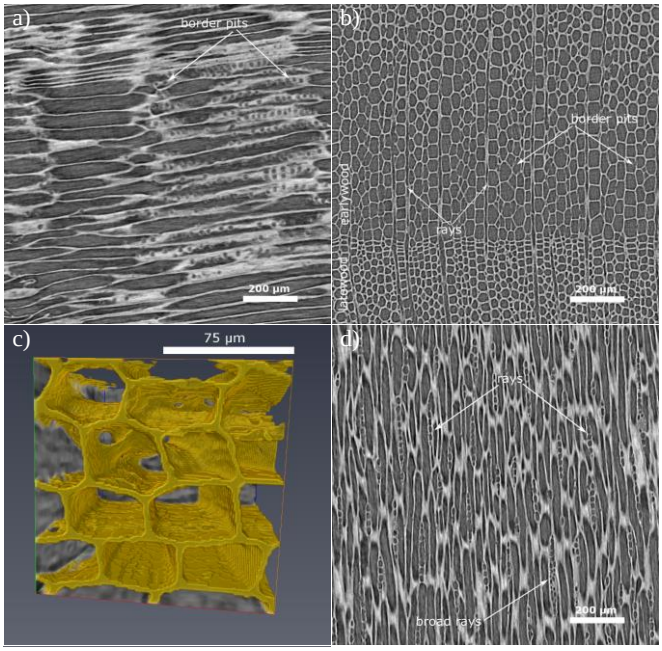

Fig. 3. Structure of the decay class 1, north-facing slope obtained by X-ray tomography analyses: a – tangential view, b – longitudinal view, c – 3D visualization of a 150x150x150 voxels sub-volume, d – radial view.

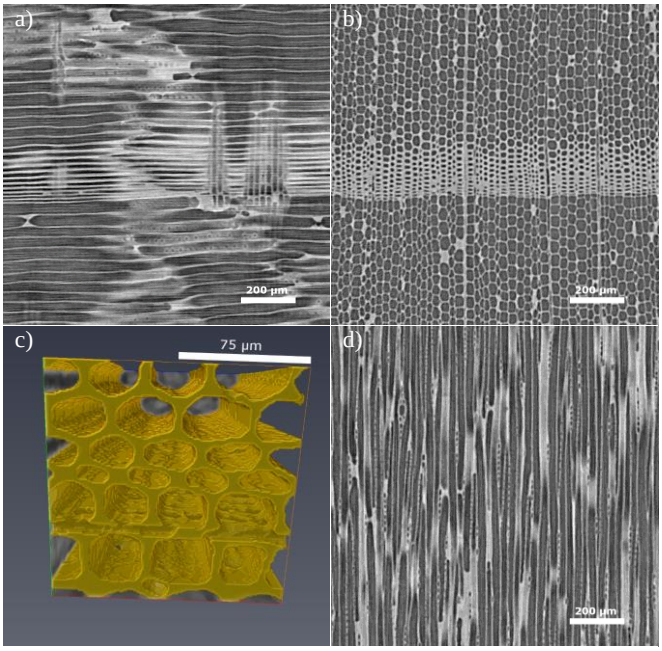

Fig. 4. Structure of the decay class 1, south-facing slope obtained by X-ray tomography analyses: a – tangential view, b – longitudinal view, c – 3D visualization of a 150x150x150 voxels sub-volume, d – radial view.

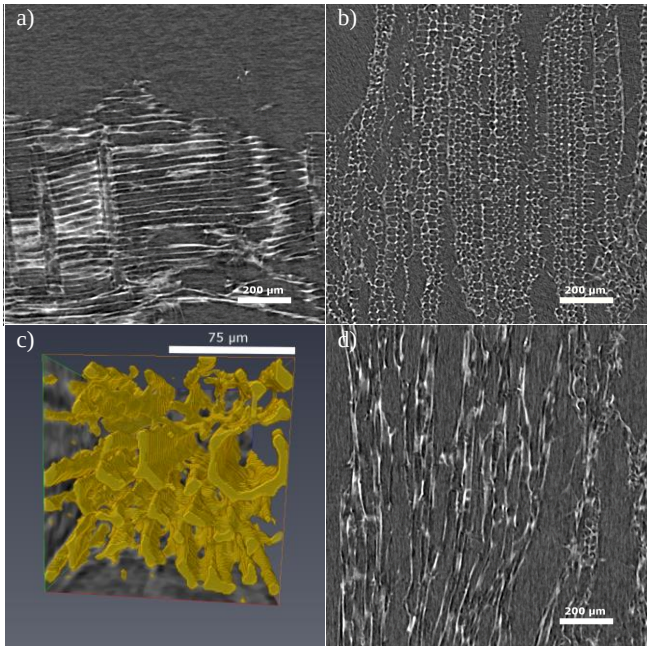

Fig. 5. Structure of the decay class 5, north-facing slope obtained by X-ray tomography analyses: a – tangential view, b – longitudinal view, c – 3D visualization of a 150x150x150 voxels sub-volume, d – radial view.

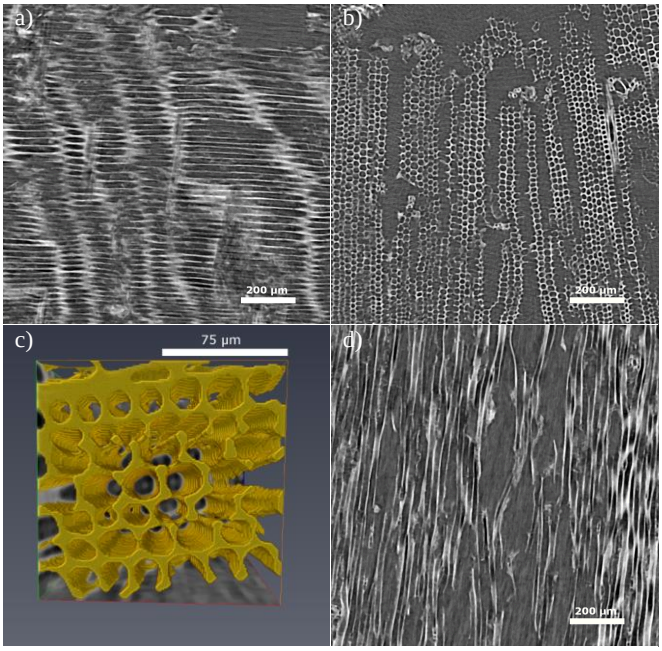

Fig. 6. Structure of the decay class 5, south-facing slope obtained by X-ray tomography analyses: a – tangential view, b – longitudinal view, c – 3D visualization of a 150x150x150 voxels sub-volume, d – radial view.

Discussion

North-facing slopes are generally cooler than comparable south-facing ones (Egli et al., 2006, 2009), but unexpectedly higher microbial abundances were revealed by qPCR in *Picea abies* CWD samples at north exposure irrespective of the decay class and for all of the three microbial domains (bacteria, fungi and archaea). However, in the same study area and for soil microbial communities, Bardelli et al. (2016) observed that the exposure-effect was domain-specific: bacteria (S > N, altitude-independent); fungi (N ~ S); and archaea (N > S, altitude-dependent). Furthermore, in the present study higher abundances of some selected microbial parameters related to the N-cycle (AOB 16S, *Nitrobacter* sp. and nitrogen fixers *nif*H) were recorded at the north- than at the south-facing slope regardless of the decay class. This

thermal signal related to exposure was also evident for the *amo*A gene, as the gene copy numbers for both AOB and AOA were only detected at the north-facing site for the advanced decay stages (DCls 4 and 5). The same trend was observed for the genus *Methanobacterium*. These exposure-effects and, in general, the climate impact on the wood-inhabiting microbiota are of great relevance with regard to the functioning of forest ecosystems because on the one hand, AOA and AOB are responsible for ammonia oxidation, the first and rate limiting step in the process of nitrification (Wessén and Hallin, 2011); and, on the other hand, the detection of methanogenic archaea (*Methanobacterium* and *Methanosaeta*) in the latest decay stages suggests that woody debris might act as a source of biogenic methane, the second most important anthropogenic greenhouse gas after CO_2, as previously reported by Mukhin and Voronin (2007, 2009). These authors proposed a symbiotic association between wood-degrading fungi and methanogenic archaea, where fungi cleave wood carbohydrates and lignin and the products formed are fermented to produce carbon dioxide and hydrogen, the substrates for methane.

In accordance with the qPCR findings, we observed that the content of certain nutrients (Ca, K and Mg) was also greater in the CWD samples from the north- than those from the south-facing sites. This is a consequence of the larger availability of these nutrients in the soil from the north-facing slope (Egli et al., 2006), which could lead to a higher nutrient richness in the *P. abies* tissues and in turn, in the debris at this slope. This is probably related to the higher moisture level and clay content (linked to the higher weathering of the soils) along with the lower pH level at the north-facing sites (Fravolini et al., 2016), which are favourable conditions especially for fungal wood decomposers. Soil moisture controls nutrient availability and oxygen diffusion required for microbial decomposition (Herrmann and Bauhus, 2012) and influences therefore largely the deadwood decomposition

rates.

Furthermore, enzyme-specific exposure effects were recorded for *P. abies* CWD samples even though this thermal signal (N *vs.* S) was strongly dependent on the decay class for most of the enzymes. However, none of the enzymatic activities involved in the P-cycle varied with exposure irrespective of the stage of wood decay. To avoid misinterpretation of environmental changes induced effects a multiple enzyme assay is, therefore, strongly recommended (Bardelli et al., 2016). There is a common acceptance that wood moisture is one of the major factors shaping enzyme activities (Baldrian et al., 2010; van der Wal et al., 2015). We also found that microbial biomass (using dsDNA), together with the yields of intracellular DNA (iDNA; potential living microbiota), positively correlated with most of the enzymes (data not shown) indicating that iDNA makes up the quantitatively dominant portion of the deadwood DNA pool as previously observed in soil (Ascher et al., 2009).

Among the studied wood properties, pH was the most influential driving factor. For soils it has also been shown that even small variations of pH may induce changes in the microbial abundance and diversity, primarily for bacteria (Lauber et al., 2009; Bardelli et al., 2016). Hoppe et al. (2015b) assumed that variations in the abundances of bacterial phyla are rather determined by a combination of wood properties (i.e., C and N concentration, relative wood moisture, density) than by single parameters, such as pH, alone. Baldrian et al. (2016) reported that pH, together with the lignin content, are the best predictors for enzyme activity in coarse deadwood of *P. abies*, *Abies alba* and *Fagus sylvatica* in a mixed natural temperate forest.

The eDNA/iDNA ratio was used as an indicator of microbial activity of the wood decomposing microbiota. As expected, lower ratios, indicative of

higher microbial activity, were found in the CWD samples at the north-facing site. This could be due to a higher degradation of eDNA (due to enzymatic digestion and consumption as microbial nutrient) and/or to higher iDNA yields at the north-facing slope. This suggests a higher occurrence of living wood-inhabiting microbiota at this slope probably due to the more favourable conditions (i.e., higher moisture and higher nutrient contents). These findings are supported by higher microbial abundances (qPCR) registered at the cooler and moister north-facing slope.

As a function of progressing decay, higher eDNA yields were recorded for the latest stages (DCls 4 and 5) at both slopes. The same trend was observed for both the dsDNA and the iDNA yields. As a result, higher microbial abundances prevailed in the last two decay classes. However, the eDNA/iDNA ratio did not show a clear trend with progressing wood decay. The increased amount of eDNA in the last two decay stages is probably due to the release of DNA into the extracellular environment as a consequence of cell death (higher microbial turnover rate). Despite the fact that DNA may act as a source of easily available micronutrients, in our study the higher amounts of micronutrients present at the most advanced stages of decay appear to have been sufficient to satisfy the microbial nutrient demand. However, at the earlier stages of decay where nutrients are more limited, microbes are thought to preferentially feed on eDNA, and consequently lower amounts of eDNA were registered in the first three decay classes.

In comparison to litter, leaves and needles, CWD is a nutrient-poor substrate (Vestin et al., 2013). The elemental nutrient contents usually increase with increasing decay stage (Bütler et al., 2007: *P. abies*, Swiss Jura Montains; Petrillo et al., 2015, 2016: *P. abies*, *Larix decidua*, Trentino; Lombardi et al., 2013: *Abies alba* and *Fagus sylvatica*, Appenines). This could

be due to respiratory C losses (Petrillo et al., 2015) and/or to an active nutrient transfer from the forest floor by mycelial cords of wood-decaying fungi. Accordingly, the highest concentration for most of the nutrients (except for Ca) was detected in the decay class 5. These differences among decay classes were more evident at north exposure, in particular for Fe. In fact, the NM-MDS analysis pointed out Fe as the most important micronutrient together with N and P for grouping the CWD samples according to their stage of decay. Iron is an important structural component of lignin peroxidases (LiP) that are heme-containing glycoproteins present in basidiomycetal white-rot fungi with a central role in the biodegradation of lignin in wood decay processes (Dashtban et al., 2010). Unlike the other peroxidases, LiP enzymes are able to oxidise non-phenolic aromatic substrates and do not require the participation of mediators due to its unusually high redox potential (Dashtban et al., 2010). Nitrogen is a limited nutrient in early wood decay and can be accumulated over time (Baldrian et al., 2016). The importance of nitrogen for fungi relies on the fact that it is required for the chitin cell wall, for proteins, lipids (e.g. sphingolipids) and nucleic acids (Purahong et al., 2016). Through their hyphae, fungi can access nitrogen pools in the surrounding soil and transport it to their deadwood habitat. Merrill and Cowling (1966) along with Larsen et al. (1978) suggested that associations with diazotrophic bacteria might enable fungi to overcome their N deficiencies and they showed that N fixation takes place in living sporocarps. In accordance with these pioneering studies, Hoppe et al. (2014) found positive correlations between fungal sporocarps and the richness of *nif*H (dinitrogen reductase) genes in deadwood logs from *Fagus sylvatica* and *P. abies*. We also observed that *nif*H was strongly correlated with the fungal abundance with respect to the eDNA fraction ($R = 0.90$, $p<0.001$) at the north-facing site. At this slope and concerning the iDNA fraction, the interaction between *nif*H and fungi was close to the significance level ($R =$

0.51, p = 0.05). At south exposure and for iDNA there was also a significant correlation between these two microbial groups (R = 0.69, p = 0.004). All in all, this points to the existence of potential fungal-bacterial interactions in wood, even though, as recently reviewed by Johnston et al. (2016), further research is necessary to unravel the exact identity of such associations (mutualism, commensalism or parasitism), and the major abiotic and biotic factors driving these interactions during wood decay.

Our „decay class - DNA - qPCR approach" confirmed Hunter's five decay-class system of being capable of tracing back the different decay stages of *Picea abies* CWD in subalpine Italian forests. Cellulose concentrations were depleted as a function of progressing decay which is in agreement with previous studies (Bütler et al., 2007; Petrillo et al., 2015, 2016). This can be explained by a preferential degradation of cellulose by brown rot fungi (Lombardi et al., 2013). In contrast, the lignin content increased with progressing decay due to its slower degradation and therefore passive enrichment in the remaining deadwood (Petrillo et al., 2015). Fravolini et al. (2016) observed that almost no time trend was detectable for lignin, while the mass of deadwood and cellulose exhibited a continuous loss during a 2-year mesocosm study on *P. abies*-wood blocks under controlled field conditions in the Trentino area.

The high-resolution X-ray microtomography, capable of non-invasive determination and three-dimensional visualisation of the wood structure as recently reviewed by Brodersen (2013), permitted to trace back the various stages of *P. abies* deadwood decay. Wood is a complex anisotropic biomaterial and its decay induces significant structural changes, modifying its physico-mechanical properties (Sedighi Gilani et al., 2014). In fact, we observed a higher degree of physical cell damage and disruption at the advanced decay stages (DCls 4 and 5), mainly at the cooler and moister

north-facing site characterised by a higher fungal abundance. Fungal deadwood decay involves the initial degradation of the cell wall components through the release of cell penetrating agents that favour the enzymes entrance, which can cause a significant damage to the wood structure (Sedighi Gilani et al., 2014; Thybring, 2013).

Conclusions

The common five decay-class system in combination with the eDNA *vs.* iDNA approach offered the possibility to trace back the decay stages of *Picea abies* CWD under different climatic conditions in mountain forest ecosystems. Our findings underline the importance of a multifactorial approach to understand deadwood decomposition, encompassing both physico-chemical and microbiological methods. In disagreement with our first hypothesis, decomposition of *P. abies* deadwood was enhanced at the cooler, more acidic and moister north-facing slope that offered more favourable conditions especially for fungi. As expected, these exposure-effects (N>S) on microbial abundances were in general more evident for the advanced decay stages (DCls 4 and 5); while for most of the enzymatic activities the impact of exposure was enzyme-specific and strongly dependent on the decay class. Our third hypothesis was partially corroborated since a lower eDNA/iDNA ratio, indicative of a higher microbial activity, was found at the north-exposure, in line with the higher physical wood damage shown by the X-ray microtomography at this slope. In contrast to our expectations, however, this ratio did not show a clear trend with progressing wood decay. Further studies are needed to unravel the taxonomic identities and genomic potential of bacterial wood decomposers and their interactions with wood decaying fungi. To conclude, our findings confirmed that deadwood at the advanced stages of decomposition act as hot spot for microbial life.

Acknowledgments

M. Gómez-Brandón and J. Ascher-Jenull have been funded by the Fonds zur Förderung der wissenschaftlichen Forschung (FWF) Austria (Project I989-B16). J. Ascher-Jenull has also been partially funded by the Ente Cassa di Risparmio di Firenze (Florence, Italy). Tommaso Bardelli has been funded by a PhD grant (DT16364) from the University of Florence (Italy). We would like to thank Marta Petrillo and Rebecca Mayer for their help in the field sampling. We are also indebted to Dr. Fabio Angeli of the Ufficio distrettuale forestale – Malé (Trento, Italy) and his team for their support in the field. We acknowledge Paul Fraiz for his highly valuable help in language editing.

References

Ascher, J., Ceccherini, M.T., Pantani, O.L., Agnelli, A., Borgogni, F., Guerri, G., Nannipieri, P., Pietramellara, G., 2009. Sequential extraction and genetic fingerprinting of a forest soil metagenome. Appl. Soil Ecol. 42, 176–181.

Ascher, J., Sartori, G., Graefe, U., Thornton, B., Ceccherini, M.T., Pietramellara, G., Egli, M., 2012. Are humus forms, mesofauna and microflora in subalpine forest soils sensitive to thermal conditions? Biol. Fertil. Soils 48, 709–725.

Baldrian, P., Merhautová, V., Petránková, M., Cajthaml, T., Šnajdr, J., 2010. Distribution of microbial biomass and activity of extracellular enzymes in a hardwood forest soil reflect soil moisture content. Appl. Soil Ecol. 46, 177–182.

Baldrian, P., Zrustova, P., Tláskal, V., Davidova, A., Merhautová, V., Vrška, 2016. Fungi associated with decomposing deadwood in a natural beech- dominated forest. Fungal Ecol. 23, 109–122.

Bardelli, T., Gómez-Brandón, M., Ascher-Jenull, J., Fornasier, F., Arfaioli, P., Francioli, D., Egli, M., Sartori, G., Insam, H., Pietramellara, G., 2016. Effects of slope exposure on soil physico-chemical and microbiological properties along an altitudinal climosequence in the Italian Alps. Sci. Total Environ.,

http://dx.doi.org/10.1016/j.scitotenv.2016.09.176.

Boettger, T., Haupt, M., Knoller, K., Weise, S.M., Waterhouse, J.S., Rinne, K.T., Loader, N.J., Sonninen, E., Jungner, H., Masson-Delmotte, V., Stievenard, M., Guillemin, M.T., Pierre, M., Pazdur, A., Leuenberger, M., Filot, M., Saurer, M., Reynolds, C.E., Helle, G., Schleser, G.H., 2007. Wood cellulose preparation method and mass spectrometric analysis of delta C-13, delta O-18, and nonexchangeable delta H-2 values in cellulose, sugar and starch: An interlaboratory comparison. Anal. Chem. 79: 4603–4612.

Bradford, M.A., Ii, R.J.W., Baldrian, P., Crowther, T.W., Maynard, D.S., Oldfield, E.E., Wieder, W.R., Wood, S.A., King, J.R., 2014. Climate fails to predict wood decomposition at regional scales. Nat. Clim. Chang. 4, 625–630.

Brodersen, C.R., 2013. Visualizing wood anatomy in three dimensions with high-resolution X-ray micro-tomography (MCT) – a review. IAWA J. 34, 408–424.

Bütler, R., Patty, L., LeBayon, R., Guenat, C, Schlaepfer, R., 2007. Log decay of *Picea abies* in the Swiss Jura Mountains of central Europe. Forest Ecol. Manag. 242, 791–799.

Coolen M.J.L., Hopmans E.C., Rijpstra, W.I.C., Muyzer, G., Schouten, S., Volkman, J.K., Sinninghe Damsté, J.S., 2004. Evolution of the methane cycle in Ace Lake (Antarctica) during the Holocene: response of methanogens and methanotrophs to environmental change. Org. Geochem. 35, 1151–1167.

Dashtban, M., Schraft, H., Syed, T.A., Qin, W., 2010. Fungal biodegradation and enzymatic modification of lignin. Int. J. Biochem. Mol. Biol. 1, 36–50.

De Boer, W., Van der Wal, A., 2008. Interactions between saprotrophic basidiomycetes and bacteria, in Boddy, L., Frankland, J.C., Van West, P. (Eds.), Ecology of saprotrophic basidiomycetes, Academic Press, Amsterdam, pp. 142–151.

Dence, C.W., Lin, S.Y., 1992. Methods in lignin chemistry, Springer, Heidelberg.

Egli, M., Mirabella, A., Sartori, G., Zanelli, R., Bischof, S., 2006. Effect of north and south exposure on weathering rates and clay mineral formation in Alpine soils.

Catena 67, 155–174.

Egli, M., Sartori, G., Mirabella, A., Favilli, F., 2009. Effect of north and south exposure on organic matter in high Alpine soils. Geoderma 149, 124–136.

Ferris, M.J., Muyzer, G., Ward, D.M., 1996. Denaturing gradient gel electrophoresis profiles of 16S rRNA-defined populations inhabiting a hot spring microbial mat community. Appl. Environ. Microbiol. 62, 340–346.

Fischer, A.L., Moncalvo, J.-M., Klironomos, J.N., Malcolm, J.R., 2012. Fruiting body and molecular rDNA sampling of fungi in woody debris from logged and unlogged boreal forests in northeastern Ontario. Ecoscience 19, 374–390.

Floudas, D., Binder, M., Riley, R., Barry, K., Blanchette, R.A., Henrissat, B., Martínez, A.T., Otillar, R., Spatafora, J.W., Yadav, J.S., et al., 2012. The Paleozoic origin of enzymatic lignin decomposition reconstructed from 31 fungal genomes. Science 336, 1715–1719.

Folman, L.B., Gunnewiek, P.J.K., Boddy, L., de Boer, W., 2008. Impact of white-rot fungi on numbers and community composition of bacteria colonizing beech wood from forest soil. FEMS Microbiol. Ecol. 63, 181–191.

Fornasier, F., Margon, A., 2007. Bovine serum albumin and Triton X-100 greatly increase phosphomonoesterases and arylsulphatase extraction yield from soil. Soil Biol. Biochem. 39, 2682–2684.

Fornasier, F., Ascher, J., Ceccherini, M.T., Tomat, E., Pietramellara, G., 2014. A simplified rapid, low-cost and versatile DNA-based assessment of soil microbial biomass. Ecol. Indic. 45, 75–82.

Francis, C. A., Roberts, K. J., Beman, J. M., Santoro, A. E., Oakley, B. B., 2005. Ubiquity and diversity of ammonia - oxidizing archaea in water columns and sediments of the ocean. Proc. Natl. Acad. Sci. U. S. A. 102, 14683–14688.

Franke-Whittle, I. H., M. Goberna, and H. Insam. 2009. Design, testing and application of real-time PCR primers for the detection of *Methanoculleus*, *Methanosarcina*, *Methanothermobacter* and uncultured methanogens. Can. J. Microbiol. 55, 611–616.

Fravolini, G., Egli, M., Derungs, C., Cherubini, P., Ascher-Jenull, J., Gómez Brandón, M., Bardelli, T., Tognetti, R., Lombardi, F., Marchetti, M., 2016. Soil attributes and microclimate are important drivers of initial deadwood decay in sub-alpine Norway spruce forests. Sci. Tot. Environ. 569–570, 1064–1076.

Goberna, M., Gadermaier, M., García, C., Wett, B., Insam, H., 2010. Adaptation of methanogenic communities to the cofermentation of cattle excreta and olive mill wastes at 37 ºC and 55 ºC. Appl. Environ. Microbiol. 76, 6564–6571.

Graham, D.W., Knapp, C.W., Van Vleck, E.S., Bloor, K., Lane, T.B. and Graham, C.E., 2007. Experimental demonstration of chaotic instability in biological nitrification. ISME J. 1, 385–393.

Harmon, M.E., Franklin, J.F., Swanson, F.J., Sollins, P., Gregory, S.V., Lattin, J.D, Anderson, N.H., Cline, S.P., Aumen, N.G., Sedell, J.R., Lienkaemper, G.W., Cromack, K., Cummins, K.W., 1986. Ecology of coarse woody debris in temperate ecosystems, Adv. Ecol. Res. 15, 133–302.

Harmon, M.E., Fasth, B., Woodall, C.W., Sexton, J., 2013. Carbon concentration of standing and downed woody detritus: Effects of tree taxa, decay class, position, and tissue type. Forest Ecol. Manage. 291, 259–267.

Herrmann, S., Bauhus, J., 2012. Effects of moisture, temperature and decomposition stage on respirational carbon loss from coarse woody debris (CWD) of important European tree species. Scand. J. Forest Res. 28, 346–357.

Hermansson, A., Lindgren P.-E., 2001. Quantification of Ammonia-Oxidizing Bacteria in Arable Soil by Real-Time PCR. Appl. Environ. Microbiol. 67, 972–976.

Hervé, V., Ketter, E., Pierrat, J.-C., Gelhaye, E., Frey-Klett, P., 2016. Impact of Phanerochaete chrysosporium on the functional diversity of bacterial communities associated with decaying wood. PLoS ONE e0147100.

Hoppe, B., Kahl, T., Karasch, P., Wubet, T., Bauhus, J., Buscot, F., Krüger, D., 2014. Network analysis reveals ecological links between N-fixing bacteria and wood-decaying fungi. PLoS ONE e88141.

Hoppe, B., Purahong, W., Wubet, T., Kahl, T., Bauhus, J., Arnstadt, T., Hofrichter, M., Buscot, F., Krüger, D., 2015a. Linking molecular deadwood-inhabiting fungal diversity and community dynamics to ecosystem functions and processes in Central European forests. Fungal Divers. 77, 367–379.

Hoppe, B., Krüger, D., Kahl, T., Arnstadt, T., Buscot, F., Bauhus, F., Wubet, T., 2015b. A pyrosequencing insight into sprawling bacterial diversity and community dynamics in decaying deadwood logs of *Fagus sylvatica* and *Picea abies*. Sci. Rep. 5: 9456.

Hunter, M.L., 1990. Wildlife, forests and forestry: principles of managing forests for biological diversity, Prentice Hall, Englewood Cliffs, NJ, USA, pp 370.

Johnston, S.R., Boddy, L., Weightman, A.J., 2016. Bacteria in decomposing wood and their interactions with wood-decay fungi. FEMS Microbiol. Ecol. 92, 1–12.

Kandeler, E., 1993. Bestimmung von Ammonium, in: Schinner, F., Öhlinger, R., Kandeler, E., Margesin, R. (Eds.), Bodenbiologische Arbeitsmethoden. Springer, Berlin, Heidelberg, pp. 366–368.

Klason, P., 1893. Bidrag till kannedomen om sammansattningen af granens ved samt de kemiska processerna vid framstallning af cellulosa darur. Teknisk tidskrift. Afdelningen för kemi och Metallurgi 23, 17–22.

Kowalchuk, G.A., Stephen, J.R., de Boer, W., Prosser, J.I., Embley, T.M., Woldendorp, J.W., 1997. Analysis of ammonia-oxidizing bacteria of the β subdivision of the class Proteobacteria in coastal sand dunes by denaturing gradient gel electrophoresis and sequencing of PCR-amplified 16S ribosomal DNA fragments. Appl. Environ. Microbiol. 63, 1489–1497.

Lauber, C.L., Hamady, M., Knight, R., Fierer, N., 2009. Pyrosequencing-based assessment of soil pH as a predictor of soil bacterial community structure at the continental scale. Appl. Environ. Microbiol. 75, 5111–5120.

Larsen, M.J., Jurgensen, M.F., Harvey, A.E., 1978. Nitrogen fixation associated with wood decayed by some common fungi in western Montana. Can. J. For. Res. 8, 341–345.

Leavitt, S.W., Danzer, S.R., 1993. Method for batch processing small wood samples to holocellulose for stable-carbon isotope analysis. Anal. Chem. 65, 87–89.

Lombardi, F., Cherubini, P., Tognetti, R., Cocozza, C., Lasserre, B., Marchetti, M., 2013. Investigating biochemical processes to assess deadwood decay of beech and silver fir in Mediterranean mountain forests. Ann. For. Sci. 70, 101–111.

Mayo, S.C., Chen, F., Evans, R., 2010. Micron-scale 3D imaging of wood and plant microstructure using high-resolution X-ray phase-contrast microtomography. J. Struct. Biol. 171, 182–188.

Merrill, W., Cowling, E.B., 1966. Role of nitrogen in wood deterioration. IV. Relationship of natural variation in nitrogen content of wood to its susceptibility to decay. Phytopathology 56, 1324–1325.

Mukhin, V.A., Voronin, P. Yu., 2007. Methane emission during wood fungal decomposition. Dokl. Biol. Sci. 413, 159–160.

Mukhin, V.A., Voronin, P. Yu., 2009. Methanogenic activity of woody debris. Russ. J. Ecol. 40, 149–153.

Øvreås, L., Forney, L., Daae, F.L., Torsvik, V., 1997. Distribution of bacterioplankton in meromictic lake Sælenvannet, as determined by denaturing gradient gel electrophoresis of PCR-amplified gene fragments coding for 16S rRNA. Appl. Environ. Microbiol. 63, 3367–3373.

Pan, Y., Birdsey, R.A., Fang, J., Houghton, R., Kauppi, P.E., Kurz, W.A., Phillips, O.L., Shvidenko, A., Lewis, S.L., Canadell, J.G., Ciais, P., Jackson, R.B., Pacala, S.W., McGuire, A.D., Piao, S., Rautiainen, A., Sitch, S., Hayes, D., 2011. A large and persistent carbon sink in the world's forests. Science 333, 988–993.

Petrillo, M., Cherubini, P., Sartori, G., Abiven, S., Ascher, J., Bertoldi, D., Camin, F., Barbero, A., Larcher, R., Egli, M., 2015. Decomposition of Norway spruce and European larch coarse woody debris (CWD) in relation to different elevation and exposure in an Alpine setting. iForest 9, 154–164.

Petrillo, M., Cherubini, P., Fravolini, G., Marchetti, M., Ascher-Jenull, J., Schärer, M., Synal, H.A., Bertoldi, D., Camin, F., Larcher, R., Egli, M., 2016. Time since

death and decay rate constants of Norway spruce and European larch deadwood in subalpine forests determined using dendrochronology and radiocarbon dating. Biogeosciences 13, 1537–1552.

Prévost-Bouré, N.C., Christen, R., Dequiedt, S., Mougel, C., Lelièvre, M., Jolivet, C., Shahbazkia, H.R., Guillou, L., Arrouays, D., Ranjard, L., 2011. Validation and application of a PCR primer set to quantify fungal communities in the soil environment by real-time PCR. Plos One 6, e24166.

Purahong, W., Arnstadt, T., Kahl, T., Bauhus, J., Kellner, H., Hofrichter, M., Krüger, D., Buscot, F., Hoppe, B., 2016. Are correlations between deadwood fungal community structure, wood physico-chemical properties and lignin-modifying enzymes stable across different geographical regions? Fungal Ecol. 22, 98–105.

Rajala, T., Peltoniemi, M., Pennanen, T., Mäkipää, R., 2012. Fungal community dynamics in relation to susbstrate quality of decaying Norway spruce (*Picea abies* [L.] Karst.) logs in boreal forests. FEMS Microbiol. Ecol. 81, 494–505.

Rosch, C., Mergel A., Bothe, H., 2002. Biodiversity of denitrifying and dinitrogen-fixing bacteria in an acid forest soil. Appl. Environ. Microbiol. 68, 3818–3829.

Rotthauwe, J.H., Witzel, K.P., Liesack, W., 1997. The ammonia monooxygenase structural gene *amo*A as a functional marker: molecular fine-scale analysis of natural ammonia-oxidizing populations. Appl. Environ. Microbiol. 63, 4704–4712.

Sedighi Gilani, M., Boone, M.N., Mader, K., Schwarze, F.W.M.R., 2014. Synchrotron X-ray micro-tomography imaging and analysis of wood degraded by *Physisporinus vitreus* and *Xylaria longipes*. J. Struct. Biol.187, 149–157.

Shigematsu, T., Tang, Y., Kawaguchi, H., Ninomiya, K., Kijima, J., Kobayashi, T., Morimura, S., Kida, K., 2003. Effect of dilution rate on structure of a mesophilic acetate-degrading methanogenic community during continuous cultivation. J. Biosci. Bioeng. 96, 547–558.

Thybring, E.E., 2013. The decay resistance of modified wood influenced by

moisture exclusion and swelling reduction. Int. Biodeterior. Biodegradation 82, 87–95.

Töwe, S., Albert, A., Kleineidam, K., Brankatschk, R., Dümig, A., Welzl, G., Munch, J.C., Zeyer, J., Schloter, M., 2010. Abundance of microbes involved in nitrogen transformation in the rhizosphere of *Leucanthemopsis alpina* (L.) heywood grown in soils from different sites of the Damma glacier forefield. Microb. Ecol. 60, 762–770.

Vainio, E.J., Hantula, J., 2000. Direct analysis of wood-inhabiting fungi using denaturing gradient gel electrophoresis of amplified ribosomal DNA. Mycol. Res. 104, 927–936.

van der Wal, A., Ottosson, E., de Boer, W., 2015. Neglected role of fungal community composition in explaining variation in wood decay rates. Ecology 96, 124–133.

Valášková, V., de Boer, W., Gunnewiek, P.J.K., Pospíšek, M., Baldrian, P., 2009. Phylogenetic composition and properties of bacteria coexisting with the fungus in decaying wood. ISME J. 3, 1218–1221.

Vestin, J.L.K., Söderberg, U., Bylund, D., Nambu, K., Hees, P.A.W., Haslinger, E., Ottner, F, Lundström, U.S., 2013. The influence of alkaline and non-alkaline parent material on Norway spruce tree chemical composition and growth rate. Plant Soil 370, 103–113.

Wessén, E., Hallin, S., 2011. Abundance of archaeal and bacterial ammonia oxidizers—Possible bioindicator for soil monitoring. Ecol. Indic. 11, 1696–1698.

Zuo, J., Cornelissen, J.H.C., Hefting, M.M., Sass-Klaassen, U., van Logtestijn, R.S.P., van Hal, J., Goudzwaard, L., Liu, J.C., Berg, M.P., 2016. The (w)hole story: facilitation of dead wood fauna by bark beetles? Soil Biol. Biochem. 95, 70–77.

V. Paper 4

Impact of slope exposure on chemical and microbiological properties of Norway spruce deadwood and underlying soil during early stages of decomposition in the Italian Alps

(photos by J. Ascher-Jenull)

Impact of slope exposure on chemical and microbiological properties of Norway spruce deadwood and underlying soil during early stages of decomposition in the Italian Alps

Tommaso Bardelli[a,b,*], Judith Ascher-Jenull[a,b], Evelyn Burkia Stocker[b], Flavio Fornasier[c], Paola Arfaioli[a], Giulia Fravolini[d], Layzza Roberta Alves Medeiros[e], Markus Egli[f], Giacomo Pietramellara[a], Heribert Insam[b], María Gómez-Brandón[b,g]

[a]Department of Agrifood and Environmental Science, University of Florence, Piazzale delle Cascine 18, 50144 Florence, Italy

[b]Institute of Microbiology, University of Innsbruck, Technikerstraβe 25d, A-6020 Innsbruck, Austria

[c]Consiglio per la Ricerca e la Sperimentazione in Agricoltura, Centro di Ricerca per lo Studio delle Relazioni tra Pianta e Suolo (C.R.A.-R.P.S.), Via Trieste 23, I- 34170 Gorizia, Italy

[d]Department of Bioscience and Territory, University of Molise, 86090 Pesche, Italy

[e]Universidade Federal Rural do Rio de Janeiro, Brazil

[f]Department of Geography, University of Zürich, Winterthurerstrasse 190, 8057 Zürich, Switzerland

[g]Departamento de Ecología y Biología Animal, Universidad de Vigo, Vigo 36310, Spain

*Corresponding autor: tommaso.bardelli@unifi.it;
Tommaso.Bardelli@student.uibk.ac.at

Manuscript submitted to **Catena** on the 24th July 2017

Contribution: T. Bardelli participated in the sampling campaign, in the experimental work including the statistical analyses, and in drafting the manuscript.

Abstract

Mountain forest ecosystems are particularly sensitive to changing environmental conditions that affect the rate of deadwood decay and, thus, also soil carbon turnover and forest productivity. Little is known how slope exposure and climate influence the microbial abundance and activity in general, and the wood-inhabiting bacteria during deadwood decomposition in particular. Therefore, a field experiment using open mesocosms was carried out along an altitudinal gradient (from 1200 to 2000 m above sea level) in the Italian Alps to evaluate the impact of exposure (north- *vs.* south-facing sites) on microbial biomass (double stranded DNA, dsDNA); microbial abundance (real-time PCR-based: fungi; dinitrogen reductase, *nif*H; ammonia-monooxygenase, *amo*A); and several hydrolytic enzyme activities involved in the main nutrient cycles during decomposition of *Picea abies* wood blocks over a 2-year period. In addition, soil properties were determined at each site. Soil microbial biomass was in general higher at the north-facing slope. Exposure, however, affected to a lower extent wood microbial biomass. The cooler, moister and more acidic conditions at north-facing slopes led to an increase in the wood and soil fungal abundance. Furthermore, soil microbial features that are related to the N-cycle gave a different response to exposure with regard to the abundance: *nif*H (N>S); *amo*A gene – ammonia-oxidising bacteria (AOB) (S>N); *amo*A gene – ammonia-oxidising archaea (AOA) (N>S; only at 2000 m a.s.l.). The AOB and AOA abundance, however, was below the detection limit in the wood blocks. Overall, the exposure-effect on the aforementioned parameters as well as for most of the enzymatic activities was altitude- and time-dependent.

Keywords: Fungal abundance; Nitrogen-bacterial functional genes; Enzymatic activities; Climosequence; Topsoil layer; Forest ecosystems

Highlights

- Soil and wood-inhabiting fungi were more abundant on the north-facing slope.
- Complex fungal-bacterial interactions within the *Picea abies* wood blocks.
- Soil microbial biomass was more pronounced at the north-facing slope.
- Higher wood microbial biomass at the end of the monitoring experiment (104 weeks).
- Exposure effects were soil and wood enzyme-specific.

Graphical Abstract

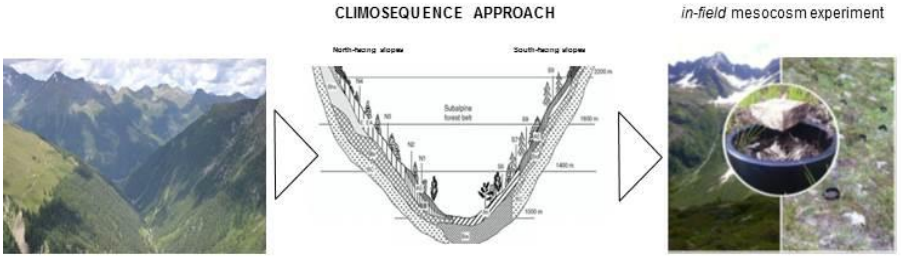

Slope exposure largely influenced the *Picea abies* wood blocks and the underlying soil in terms of microbial abundance and activity

1. Introduction

Deadwood represents one of the most important carbon stocks in forest ecosystems (Pan et al., 2011). Its decay rate is determinant for the soil carbon turnover and forest productivity (Zhou et al., 2007). As woody material decays, its structure and chemical composition gradually change over time which can result in a turnover of the wood-inhabiting microbiota as species are replaced by those better adapted to the substrate according to their biochemical requirements (Rajala et al., 2012). All of these changes can ultimately have consequences on the chemical and biological properties of the forest floor, especially the organic soil surface due to the incorporation

of decaying woody material over the course of decomposition (Strukely et al., 2013; Fravolini et al., 2016).

Fungi are considered the primary wood decomposers thanks to their ability to breakdown complex substrates such as lignin and cellulose, which can comprise 60-75 % of wood dry mass (Meier et al., 2010). In particular, white-rot fungi efficiently degrade lignin via oxidative metalloenzymes such as laccases and manganese peroxidases (Valentín et al., 2014; Kielak et al., 2016). During the decay process the fungal activity may increase the acidic conditions in wood that may result in an adverse environment for the bacterial colonization (Kielak et al., 2016). However, there are indications of both antagonist and beneficial fungal-bacterial interactions occurring in wood as reviewed by Johnston et al. (2016). In line with this, Hoppe et al. (2014) found positive correlations between fungal sporocarps and the richness of *nif*H (dinitrogen reductase) genes in deadwood logs from *Fagus sylvatica* and *Picea abies*. This is in accordance with the pioneering studies from Merrill and Cowling (1966) and Larsen et al. (1978) who suggested that associations with nitrogen-fixing bacteria might enable fungi to overcome their nitrogen deficiencies for vegetative and generative growth. Indeed, nitrogen is a very limited nutrient in early stages of wood decay and can be accumulated over time (Baldrian et al., 2016; Gómez-Brandón et al., 2017; Hu et al., 2017). The role of nitrogen-fixing bacteria is to bind the atmospheric dinitrogen (N_2) into a biologically accessible form (NH_3), being the *nif*H gene the most useful marker to study the distribution of this bacterial group in forest ecosystems (Levy-Booth et al., 2014).

The biological oxidation from ammonia (NH_3) to nitrite (NO_2^-) is also of great relevance in forest soils (Levy-Booth et al., 2014), as it is the rate-limiting step of the nitrification process. This reaction is carried out by both ammonia-oxidising bacteria (AOB) and archaea (AOA), which can be

quantified by the ammonia-monooxygenase (*amo*A) gene (Rotthauwe et al., 1997; Francis et al., 2005; Leininger et al., 2006). Previous studies have suggested that AOB and AOA respond differently to the environmental conditions, with one or the other being more competitive under a given set of conditions, as they belong to separate phylogenetic domains with different cell biochemical and metabolic process (Erguder et al., 2009). However, far less attention has been paid to these bacterial groups in the deadwood environment.

Topographic factors such as slope aspect influence the local climate with consequences on soil properties (Egli et al., 2006, 2009; Ascher et al., 2012; Bardelli et al., 2017) and deadwood decay dynamics (Petrillo et al., 2016; Fravolini et al., 2016; Gómez-Brandón et al., 2017) in mountain ecosystems. However, there is still a paucity of information about how slope exposure and climate, in general, influence the microbial abundance and activity, and in particular, the wood-inhabiting bacteria during deadwood decomposition. We therefore evaluated the impact of exposure (north- *vs.* south-facing sites) on the abundance of N-related bacterial functional genes (*nif*H and *amo*A) assessed by real-time PCR, during decomposition of *Picea abies* deadwood along an altitudinal gradient, reflecting different climate zones, in the Italian Alps. Fungal abundance along with several potential enzymatic activities involved in the main nutrient cycles were also evaluated as a function of exposure in both *P. abies* deadwood and in the uppermost topsoil layer (0-5 cm; in direct contact with the wood blocks).

In the same in-field mesocosm study, Fravolini et al. (2016) found that a higher soil moisture and clay content (related to a higher weathering of the soils) along with a lower pH seemed to accelerate wood decay at the north-facing slopes. We therefore hypothesised that: (1) the microbial biomass and activity will also be more favoured at the north- than at the south-facing

slopes during deadwood decomposition, and such effects on microbial communities will be altitude- and time-dependent; (2) the abundance of *amo*A and *nif*H genes will be affected by the slope exposure over the course of deadwood decomposition.

2. Material and Methods

2.1. Study area and experimental set-up

The study area is located in Val di Rabbi (Trentino) in the Italian Alps (Fig. 1) where a comprehensive database about soils, topographic and environmental settings already exists (Egli et al., 2006; Fravolini et al., 2016; Bardelli et al., 2017). Eight subalpine sites were selected along an altitudinal gradient from 1200 to 2000 m above sea level (a.s.l.), four sites at north- (N_{1-4}) and other four at south-facing (S_{6-9}) slopes, thereby providing a climosequence (Fig 1). The altitudes of the sites were selected to be as similar as possible in order to establish a comparison between both slope exposures. A detailed description of the study sites is shown in Table 1.

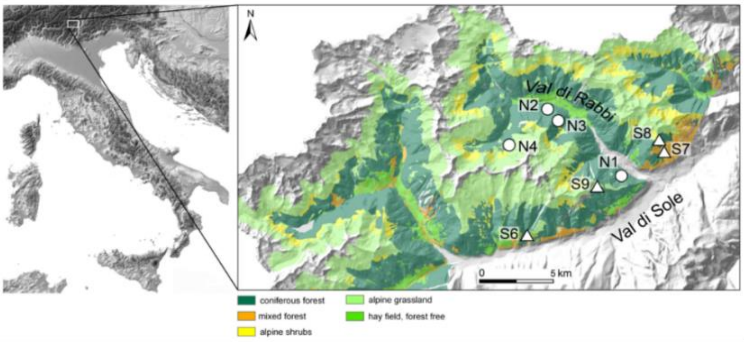

Fig. 1. Overview of the study area (Trentino Alto Adige, Italia) (Egli et al., 2006; Fravolini et al., 2016).

Table 1.

Characteristics of the eight study sites at north-and south-facing slopes (N_{1-4} and S_{6-9}, respectively) in Val di Rabbi (Egli et al., 2006; Petrillo et al., 2015).

Sites	Altitude (m a.s.l.)	Aspect (°N)	Slope (°)	MAP (nmy^{-1})	MAAT (° C)	MAST (° C)	Parent material	Dominating tree species	Land use	Soil classification (WRB)
N_1	1180	340	31	950	5.6	7.3	Paragneiss debris	*Picea abies*	Natural forest (ecological forestry)	Chromi-Episkeletic Cambisol (Dystric)
S_6	1185	160	31	950	7.6	8.1	Paragneiss debris	*Picea abies*	Ex-coppice, natural forest (ecological forestry)	Episkeleti-Endoleptic Cambisol (Chromi-Dystric)
N_2	1390	0	28	1000	4.6	6.3	Paragneiss debris	*Picea abies*	Natural forest (ecological forestry)	Chromi-Episkeletic Cambisol (Dystric)
S_7	1400	145	33	1000	6.6	8.7	Paragneiss debris	*Larix decidua*	Natural forest (ecological forestry)	Dystri-Endoskeletic Cambisol
N_3	1620	0	29	1060	3.5	5.8	Paragneiss debris	*Picea abies*	Natural forest (ecological forestry)	Chromi-Endoskeletic Cambisol (Dystric)
S_8	1660	210	33	1060	5.5	6.0	Paragneiss debris	*Picea abies*	Natural forest (ecological forestry)	Skeletic Umbrisol
N_4	1930	20	12	1180	1.4	5.0	Paragneiss debris, Moraine material	*Larix decidua*	Originally used as pasture	Episkeletic Podzol
S_9	1995	160	25	1180	3.4	6.4	Paragneiss debris	*Larix decidua*	Ex-pasture, natural forest (ecological forestry)	Skeletic Umbrisol

MAP = mean annual precipitation; MAAT = mean annual air temperature (Sboarina and Cescatti, 2004); MAST = mean annual soil temperature.

An in-field mesocosm experiment was set up at each study site of the climosequence as described by Fravolini et al. (2016) in order to monitor the early stage of deadwood decomposition as a function of slope exposure and time in i) wood blocks and ii) the uppermost topsoil layer (0-5 cm). Mesocosms (PVC tubes having diameter = 10.2 cm and height = 25 cm) were installed into the natural soil in August 2012, that is one year prior to the addition of the wood blocks of *Picea abies* (L.) Karst, at a distance of > 1 m from large trees and > 0.5 m from the adjacent mesocosms, leaving at the surface a border of about 1 cm. Considering that the size and geometry of deadwood may have a strong influence on the decay processes (Van der Wal et al., 2007), wood blocks from the same *P. abies* tree and with an uniform size (2 cm × 5 cm × 5 cm) were placed on the soil surface in each of the mesocosm tubes. Three replicate mesocosms for each time point were installed in each of the eight study sites. The wood blocks and the uppermost topsoil layer (0-5 cm) were collected (with lab-gloves) after 12 (t1; August 2013), 25 (t2; October 2013), 52 (t3; July 2014) and 104 (t4; July 2015) weeks, resulting in a total of 96 samples for each substrate (= 8 sites × 4 times × 3 replicates), with three wood blocks kept as controls (t0). Moreover, prior to the placement of the wood blocks into the mesocosms, five soil sub-samples (t0) were collected in the surrounding area of the mesocosm set up at each study site. All the samples were placed in polyethylene bags and transported in cool-boxes to the laboratory. The soil samples were sieved (< 2 mm), and the wood blocks were air-dried at room temperature, cut-milled (4 mm; Retsch mill) and aliquoted into 50-mL sterile conical centrifuge tubes. Samples were then stored at 4 °C and -20 °C for physico-chemical and (micro)biological analyses, respectively.

2.2. Wood and soil physico-chemical analyses

Wood (1 g fresh weight, fw) and soil samples (5 g, fw) were oven-dried (105 °C) for 24 h to determine their dry weight. The volatile solids (VS) content was determined from the weight loss following ignition in a muffle furnace (Carbolite, CWF 1000) at 550 °C for 5 h. Total C and N contents were analysed in dried samples, using a CN analyser (TruSpec CHN; LECO, Michigan, U.S.A.). Electrical conductivity (EC) and pH were measured in water extracts (1:20 and 1:10, w/v for wood and soil, respectively) using a conductivity meter LF 330 WTW (Weilheim, Germany) and a pH meter Metrohm 744, respectively. Cellulose and total lignin contents, along with the determination of mass losses of the wood blocks were assessed as shown in Petrillo et al. (2015) and Fravolini et al. (2016). Soil ammonium (NH_4^+) and nitrate (NO_3^-) contents were measured in 0.0125 M $CaCl_2$ extracts (Kandeler, 1993 a,b). Both the total and available P concentrations in soil samples were determined according to the ascorbic acid method (Kuo, 1996).

2.3. Potential enzyme activities

Seven hydrolytic enzyme activities covering the principal nutrient cycles including: i) C-cycle: β-glucosidase *(gluc*), cellulase (*cell*), xylosidase (*xylo*); ii) N-cycle: chitinase (*chit*), leucine-aminopeptidase (*leu*); and iii) P-cycle: acid and alkaline phosphomonoesterase (*acP* and *alkP*) were determined from wood (0.1 g, fw) and soil (0.2 g, fw) samples by using a heteromolecular exchange procedure as described by Fornasier and Margon (2007). Some modifications were required in order to perform the enzymatic multiple assay for wood extracts as described by Gómez-Brandón et al. (2017). All the measurements were performed in duplicate for each field replicate and the activities were expressed as nanomoles of 4-methyl-umbelliferyl (MUF) min^{-1} g^{-1} dry (wood/soil).

2.4. Molecular analyses

2.4.1. Wood and soil microbial biomass index (dsDNA)

Whole community DNA was extracted from wood (0.1 g, fw) and soil (0.2 g, fw) samples by mechanical cell disruption (bead-beating) in presence of a sodium phosphate buffer (0.12 M, pH 8 Na_2HPO_4), and crude (not purified) double stranded DNA (dsDNA) was directly quantified by using PicoGreen fluorescent dye (Life Technologies) as described in Fornasier et al. (2014).

2.4.2. DNA extraction

Whole community DNA was extracted from wood (0.1 g, fw) and soil (0.2 g, fw) samples and purified by using a commercial kit (FastDNA Kit for Soil, MP-Biomedicals) as described in Ascher et al. (2009) for further downstream analyses. In the case of wood samples, one ceramic sphere (Lysing Matrix E, MP, Biomedicals) was added to the lysing tubes, so as to guarantee for an accurate cell disruption of the woody tissue. DNA was qualitatively and quantitatively characterised as described in Bardelli et al. (2017).

2.4.3. Quantitative real-time PCR

Quantitative real-time PCR (qPCR) analysis was performed to determine the 18S rRNA gene copy number of fungi, and the abundance of certain functional genes involved in the N cycle (*nif*H and *amo*A) in the wood and the soil samples. Real-time PCR was conducted in a Rotorgene 6000 Real Time Thermal Cycler (Corbett Research, Sydney, Australia) in combination with the Rotorgene Series Software 1.7. Standard curves were constructed using the purified PCR products of known concentrations of the following pure cultures used as templates: *Fusarium solani* (DSMZ 10696) – fungi; *Azospirillum irakense* (DSMZ 11586) – *nif*H gene; a plasmid containing an *amo*A sequence – ammonia-oxidising bacteria (AOB) and -archaea (AOA).

The primer pairs used for qPCR were as follows: FF390/FR1 (fungi; Prévost-Bouré et al., 2011); nifHf/nifHr (*nif*H gene; Töwe et al., 2010); amoA1F/amoA2R (*amo*A gene – AOB; Rothauwe et al., 1997); and Arch-amoAF/Arch-amoAR (*amo*A gene – AOA; Francis et al., 2005). Stock concentration [gene copies μL^{-1}] was determined via PicoGreen measurement. Ten-fold dilutions ranging from 10^9 to 10^2 copies μL^{-1} were used for the standard curve construction. The reactions were performed in 20-µL assays containing 1X Sensimix™ SYBR® Hi-rox (Bioline, USA), forward and reverse primers (200 nM each primer), 0.4 mg mL^{-1} BSA, distilled water (RNase/DNase free, Gibco™, UK) and 2 µL of either 1:10 diluted DNA-extract, and ten-fold diluted standard DNA. All the standards and samples were run in duplicate. After an initial denaturation at 95 °C for 10 min, thermal cycling comprised 40 cycles of 15 s at 95 °C, 30 s at 50 °C, 30 s at 72 °C for fungi; 45 s at 95 °C, 45 s at 55 °C, 45 s at 72 °C for *nif*H gene; 25 s at 95 °C, 25 s at 57 °C (AOB) or 53 °C (AOA), followed by 40 s at 72 °C for both AOB and AOA *amo*A gene. To check for product specificity and potential primer dimer formation, runs were completed with a melting analysis starting from 65 °C to 95 °C with temperature increments of 0.25 °C (0.5 °C for *nif*H gene) and a transition rate of 5 s. The purity of the amplified products was checked by the presence of a single band of the expected length on a 1% agarose gel stained with the DNA stain Midori Green (Nippon Genetics, Germany) and visualised by UV-transillumination (Vilber Lourmat Deutschland GmbH).

2.5. Statistical analyses

The exposure (N- *vs.* S-facing slopes) and time (t0, t1, t2, t3, t4) effects on wood and soil physico-chemical and microbiological parameters were evaluated using a factorial analysis of variance (ANOVA). The normality and the variance homogeneity of the data were tested prior to ANOVA

using the Shapiro-Wilks and Levene´s tests, respectively. Prior to analysis, the data were log- or square root-transformed to meet the assumptions for ANOVA (when it was necessary). Paired comparisons were done using the Tukey HSD test. A non-parametric test (Kruskal-Wallis test) was performed when the data did not meet the normality condition. Associations between the potential enzymatic activities and the main chemical and microbiological variables were explored by Pearson's correlation. These analyses were carried out using the software Statistica 9 (StatSoft, USA).

3. Results

3.1. Wood physico-chemical parameters along the studied climosequence

Wood mass loss was significantly higher at the N- than at the S-facing sites after 12 and 104 weeks at 1400 and 2000 m a.s.l., respectively; whereas no exposure- and time-effect was recorded at the remaining altitudes (Tables 2 and 6). Wood moisture was not significantly affected by the slope exposure. However, moisture levels were about 7-times higher after 12 weeks, while no further changes were observed until the end of the monitoring (104 weeks). Slope exposure had a significant impact on the wood pH only at 1600 m a.s.l., being one unit lower at the N- than at the S-facing sites after 52 weeks. Higher wood EC levels were mainly detected at the S-facing sites. This exposure-effect (S>N) was also recorded for the wood C content after 52 weeks at 1200 m a.s.l. and independently of the duration of the monitoring at 1600 m a.s.l. Cellulose and total lignin content were not significantly affected by the slope exposure. The lowest cellulose content was recorded after 104 weeks at both slopes at 1600 and 2000 m a.s.l. However, a significant increase in lignin amount was observed at 2000 m a.s.l. between 25 and 104 weeks. The N content in the wood blocks was below the detection limit.

Table 2.

Physico-chemical properties of wood samples collected in June 2013 (t0; control), in August 2013 (t1; 12 weeks), in October 2013 (t2; 25 weeks); in July 2014 (t3; 52 weeks), in July 2015 (t4; 104 weeks) in the in-field mesocosm experiment along the climosequence scenario. The results are shown pairwise, i.e., the couple of N- and S-facing sites at the same elevation (N_1-S_6; 1200 m a.s.l.; N_2-S_7; 1400 m a.s.l.; N_3-S_8; 1600 m a.s.l.; N_4-S_9; 2000 m a.s.l.). Values are means (n=3) with the standard deviations. Data are expressed on a dry weight basis.

Sites	Time	Wood mass loss (g)	Wood moisture (%)	pH	Electrical Conductivity (µS cm^{-1})	Total C (%)	Cellulose (%)	Total Lignin (%)
	t0	22.5 (0.01)	8.2 (2.0)	5.5 (0.1)	51.7 (6.5)	49.0 (0.3)	44.5 (4.5)	30.7 (1.5)
N_1	t1	22.2 (0.7)	58.9 (0.9)	5.8 (0.03)	16.3 (2.3)	48.8 (0.4)	44.0 (4.7)	31.7 (0.5)
	t2	21.9 (4.0)	54.2 (2.7)	5.7 (0.1)	24.3 (5.2)	48.8 (0.2)	46.5 (1.9)	32.2 (1.3)
	t3	21.7 (1.4)	58.4 (7.99)	5.6 (0.05)	15.8 (1.7)	49.4 (0.3)	40.5 (7.3)	31.3 (0.9)
	t4	21.2 (2.9)	50.6 (15.0)	5.8 (0.4)	46.5 (13.5)	46.7 (1.2)	41.3 (3.9)	33.3 (5.9)
S_6	t1	22.0 (1.8)	55.3 (5.5)	5.9 (0.14)	17.7 (3.5)	48.9 (0.1)	46.4 (0.9)	30.6 (1.3)
	t2	22.2 (0.1)	52.3 (11.3)	5.8 (0.2)	25.5 (4.5)	49.1 (1.5)	44.4 (2.3)	30.3 (0.4)
	t3	21.5 (4.5)	54.5 (3.4)	4.5 (0.7)	80.7 (47.0)	51.6 (0.5)	37.9 (3.1)	31.6 (2.6)
	t4	22.8 (1.9)	39.6 (12.5)	5.5 (0.5)	40.5 (9.7)	46.2 (0.9)	40.5 (2.9)	31.4 (0.8)
N_2	t1	26.0 (0.01)	51.0 (6.9)	5.5 (0.1)	13.8 (1.1)	50.4 (1.0)	43.4 (7.1)	35.1 (3.1)
	t2	21.1 (1.5)	62.6 (1.2)	5.4 (0.1)	13.6 (4.4)	51.8 (0.5)	50.4 (0.9)	33.0 (1.3)
	t3	21.7 (5.5)	58.2 (6.8)	5.0 (0.1)	10.3 (0.8)	50.5 (1.3)	42.2 (5.3)	31.1 (1.9)
	t4	21.3 (2.0)	45.8 (10.5)	4.6 (0.2)	35.0 (25.8)	46.4 (1.4)	39.3 (6.0)	30.4 (1.0)
S_7	t1	17.9 (2.9)	44.7 (1.2)	4.9 (0.9)	55.0 (45.7)	48.7 (0.2)	39.5 (6.9)	34.4 (6.5)
	t2	20.3 (0.9)	50.3 (3.9)	5.8 (0.01)	30.0 (3.3)	51.3 (1.0)	48.4 (3.6)	32.8 (1.7)
	t3	20.0 (1.9)	39.1 (9.8)	5.5 (0.2)	32.9 (1.6)	49.7 (0.5)	37.4 (3.0)	31.8 (1.3)
	t4	23.0 (2.8)	14.0 (6.3)	4.6 (0.4)	99.2 (33.5)	46.9 (2.3)	42.9 (3.7)	34.8 (3.3)

Table 2. Continued

Sites	Time	Wood mass loss (g)	Wood moisture (%)	pH	Electrical Conductivity (µS cm^{-1})	Total C (%)	Cellulose (%)	Total Lignin (%)
N_3	t1	22.6 (2.9)	61.1 (2.7)	5.4 (0.2)	17.7 (8.4)	48.7 (0.3)	46.1 (1.0)	30.9 (1.8)
	t2	23.0 (4.2)	59.8 (6.8)	5.6 (0.01)	9.4 (1.6)	50.1 (0.8)	46.0 (6.3)	34.3 (1.7)
	t3	23.8 (0.01)	48.6 (13.2)	5.2 (0.2)	19.9 (8.5)	49.9 (0.3)	44.5 (3.7)	31.6 (2.1)
	t4	21.0 (3.7)	56.4 (4.5)	5.4 (0.05)	19.2 (3.8)	47.0 (1.2)	37.2 (3.1)	31.3 (0.7)
S_8	t1	21.3 (1.0)	46.7 (11.4)	5.6 (0.01)	17.8 (3.0)	48.6 (0.01)	49.2 (1.9)	35.5 (6.3)
	t2	22.1 (2.8)	55.5 (7.7)	5.7 (0.01)	18.9 (3.2)	51.4 (1.5)	44.3 (1.9)	29.3 (1.9)
	t3	20.5 (1.7)	61.9 (2.5)	5.9 (0.1)	18.2 (2.6)	51.4 (0.5)	41.1 (4.3)	32.0 (1.1)
	t4	23.2 (0.01)	54.5 (3.1)	5.7 (0.3)	40.3 (7.2)	48.6 (1.1)	40.8 (4.5)	32.7 (2.3)
N_4	t1	22.4 (6.2)	54.9 (6.4)	5.5 (0.1)	10.2 (1.2)	48.5 (0.2)	45.3 (2.8)	33.4 (0.9)
	t2	21.6 (1.8)	61.0 (2.1)	5.4 (0.2)	14.3 (6.7)	52.2 (0.5)	46.2 (3.0)	33.6 (3.3)
	t3	16.0 (0.01)	61.0 (2.1)	5.7 (0.3)	22.2 (16.2)	49.1 (0.1)	45.9 (2.2)	33.3 (1.4)
	t4	22.0 (4.6)	44.9 (9.1)	5.4 (0.3)	17.7 (5.9)	48.4 (2.1)	37.7 (3.3)	35.1 (0.9)
S_9	t1	19.1 (3.4)	52.6 (6.4)	5.7 (0.1)	17.3 (6.0)	48.4 (0.4)	45.4 (2.1)	32.4 (2.1)
	t2	20.2 (4.2)	53.8 (6.5)	5.4 (0.2)	32.8 (7.6)	49.5 (0.9)	46.3 (3.2)	28.7 (0.9)
	t3	21.1 (1.1)	53.7 (6.5)	5.4 (0.1)	22.3 (7.2)	48.9 (0.9)	45.5 (2.9)	32.2 (1.2)
	t4	14.9 (1.1)	12.8 (2.7)	4.8 (0.2)	78.6 (25.8)	51.0 (2.6)	31.1 (6.7)	35.8 (2.3)

3.2. Soil physico-chemical parameters along the studied climosequence

An overview of the soil physico-chemical parameters as a function of slope exposure and time along the climosequence is given in Table 3. The statistical results are shown in Table 6.

Along the altitudinal gradient, soil moisture was one to two times higher at the N- than at the S-facing sites and significantly varied with time only at the altitude of 2000 m a.s.l., where the lowest moisture level was found after 104 weeks irrespective of the exposure. The VS content was 2-fold higher at the N- than at the S-facing sites between 1200 and 1600 m a.s.l., whereas no exposure-effect was found at 2000 m a.s.l. The N-facing sites were characterised by higher soil acidity, being soil pH one unit lower than at the comparable S-facing ones. A significant increase in soil pH was found after 12 weeks at both slopes, followed by a decrease until the end of the trial, except for 1200 m a.s.l. The soil EC levels were two to three times higher at the S- than at the N-facing sites after 25 and 52 weeks at 1400 m a.s.l. This exposure-effect (S>N) was also recorded over time at 2000 m a.s.l. Soils at the N-facing sites showed higher total C and N contents than those from the comparable S-facing ones, regardless of the duration of the monitoring. Significant changes in C content over time were observed at 1600 m a.s.l., being 2-times higher after 12 weeks, and remained stable until the end of the trial. At this altitude the soil N content was 2-times higher after 25 weeks, followed by a decrease until 104 weeks at both slopes. This decrease was also observed at 2000 m a.s.l. but only at the N-facing slope. The soil NH_4^+ content was between 5 and 10 times higher at the N- than at the S-facing sites after 12, 25 and 52 weeks along the altitudinal gradient.

Table 3.

Physico-chemical properties of the soil samples collected in June 2013 (t0; control), in August 2013 (t1; 12 weeks), in October 2013 (t2; 25 weeks); in July 2014 (t3; 52 weeks), in July 2015 (t4; 104 weeks) in the in-field mesocosm experiment along the climosequence scenario. The results are shown pairwise, i.e., the couple of N- and S-facing sites at the same elevation (N_1-S_6; 1200 m a.s.l.; N_2-S_7; 1400 m a.s.l.; N_3-S_8; 1600 m a.s.l.; N_4-S_9; 2000 m a.s.l.). Values are means (n=3) with the standard deviations. Data are expressed on a dry weight basis.

Sites	Time	Soil moisture (%)	Volatile solids (%)	pH	Electrical Conductivity (µS cm^{-1})	Total C (%)	Total N (%)	NH_4^+ (mg kg^{-1} dw)	NO_3^- (mg kg^{-1} dw)	Total P (mg kg^{-1} dw)	Available P (mg kg^{-1} dw)
N_1	t0	41.7 (1.6)	30.2 (2.1)	5.8 (0.1)	33.3 (1.5)	22.4 (1.1)	0.9 (0.01)	43.4 (6.4)	6.6 (1.9)	540.4 (13.6)	38.4 (1.8)
	t1	49.8 (7.3)	33.0 (10.7)	5.7 (0.3)	55.5 (11.3)	21.8 (10.5)	0.8 (0.3)	36.3 (4.1)	49.3 (7.6)	569.7 (41.0)	78.3 (36.6)
	t2	43.3 (11.9)	36.9 (20.5)	5.5 (0.1)	45.3 (31.0)	16.9 (7.3)	0.9 (0.4)	16.9 (4.1)	33.2 (12.1)	761.5 (187.0)	75.9 (56.3)
	t3	42.8 (7.8)	22.4 (7.7)	5.3 (0.3)	29.1 (4.6)	11.1 (4.3)	0.3 (0.1)	22.4 (8.1)	59.9 (32.3)	689.4 (542.5)	19.7 (5.3)
	t4	42.5 (16.7)	39.8 (10.4)	5.6 (0.4)	56.7 (27.7)	20.2 (67)	0.8 (0.2)	99.21 (67.8)	13.7 (4.9)	392.7 (169.3)	65.6 (6.6)
S_6	t0	33.6 (0.6)	14.6 (0.1)	5.8 (0.01)	33.5 (1.0)	6.4 (0.2)	0.3 (0.01)	19.2 (1.5)	5.1 (1.1)	363.7 (65.2)	11.5 (2.5)
	t1	45.7 (5.6)	22.7 (4.2)	6.2 (0.4)	68.6 (25.7)	10.9 (3.1)	0.6 (0.2)	2.6 (0.3)	74.2 (2.5)	376.0 (88.4)	39.7 (17.7)
	t2	42.9 (16.6)	22.3 (10.4)	6.1 (0.2)	44.7 (22.8)	5.6 (2.4)	0.6 (0.6)	4.9 (0.8)	30.8 (14.9)	669.2 (193.7)	66.3 (15.3)
	t3	35.2 (7.9)	17.7 (8.5)	5.8 (0.1)	49.2 (20.1)	8.8 (4.8)	0.5 (0.2)	26.1 (8.0)	25.7 (12.7)	359.7 (192.6)	18.8 (9.1)
	t4	23.2(2.2)	20.0 (8.7)	6.4 (0.1)	42.6 (21.2)	9.6 (5.4)	0.5 (0.3)	14.7 (6.5)	6.1 (2.0)	243.5 (51.9)	8.5 (0.7)
N_2	t0	64.1 (1.8)	68.1 (2.3)	4.4 (0.01)	43.0 (1.7)	37.3 (2.7)	1.5 (0.2)	33.7 (2.8)	7.4 (3.2)	506.6 (47.2)	116.9 (20.0)
	t1	73.6 (1.4)	81.6 (5.4)	5.1 (0.2)	51.1 (15.6)	43.9 (1.8)	1.8 (0.2)	161.6 (95.2)	23.2 (7.2)	708.3 (105.3)	184.5 (26.6)
	t2	69.5 (7.8)	72.2 (17.1)	4.8 (0.2)	42.3 (9.0)	36.3 (10.1)	1.9 (0.4)	178.0 (29.1)	37.5 (11.6)	625.0 (43.0)	134.5 (34.4)
	t3	72.9 (1.7)	77.2 (12.5)	4.4 (0.2)	40.8 (10.3)	43.4 (4.4)	1.3 (0.1)	152.4 (32)	30.6 (5.3)	449.6 (68.0)	96.5 (11.8)
	t4	56.8 (13.3)	86.3 (2.6)	4.1 (0.2)	87.0 (25.5)	45.8 (1.3)	1.3 (0.02)	52.0 (31.5)	24.8 (16.0)	534.6 (30.3)	83.3 (22.2)
S_7	t0	38.6 (0.1)	33.4 (0.8)	5.7 (0.08)	78.1 (3.8)	18.8 (0.8)	0.8 (0.01)	28.7 (1.9)	7.5 (0.3)	739.7 (76.7)	91.6 (5.3)
	t1	27.9 (10.9)	24.2 (2.7)	6.2 (0.1)	46.5 (3.1)	14.4 (3.4)	0.7 (0.2)	18.2 (12.6)	25.5 (11.5)	534.4 (84.6)	39.9 (5.2)
	t2	27.4 (7.7)	51.7 (12.9)	6.1 (0.3)	175.7 (8.9)	21.3 (13.4)	1.2 (0.8)	27.2 (8.9)	54.3 (1.0)	773.8 (172.2)	154.1 (94.3)
	t3	44.2 (6.8)	77.2 (12.5)	5.6 (0.1)	94.6 (17.2)	26.9 (8.3)	1.1 (0.3)	49.3 (15.7)	57.9 (13.0)	742.1 (149.3)	90.3 (11.3)
	t4	16.5 (1.3)	52.8 (17.9)	5.8 (0.2)	108.6 (29.7)	26.9 (8.3)	1.2 (0.3)	27.7 (0.6)	35.2 (9.8)	546.6 (43.0)	58.5 (11.8)

Table 3. Continued

Sites	Time	Soil moisture (%)	Volatile solids (%)	pH	Electrical Conductivity (µS cm^{-1})	Total C (%)	Total N (%)	NH_4^+ (mg kg^{-1} dw)	NO_3^- (mg kg^{-1} dw)	Total P (mg kg^{-1} dw)	Available P (mg kg^{-1} dw)
N_3	t0	61.4 (1.0)	59.4 (5.1)	4.6 (0.03)	39.5 (1.9)	33.8 (2.2)	1.2 (0.1)	78.2 (10.7)	6.3 (0.5)	462.6 (99.2)	89.8 (6.4)
	t1	69.0 (2.0)	83.9 (7.5)	5.2 (0.4)	65.5 (15.2)	44.8 (4.5)	1.8 (0.3)	227.4 (118.1)	34.0 (5.4)	453.7 (124.8)	128.0 (33.1)
	t2	72.6 (3.8)	80.7 (7.3)	5.0 (0.2)	39.0 (10.4)	41.1 (3.5)	2.1 (0.1)	171.2 (11.2)	20.8 (6.1)	673.2 (159.6)	87.1 (26.6)
	t3	72.3 (3.2)	84.5 (6.7)	4.8 (0.05)	55.2 (10.8)	44.8 (2.7)	1.4 (0.04)	188.9 (69.8)	56.7 (6.4)	716.8 (80.4)	66.2 (16.4)
	t4	68.5 (6.4)	73.7 (20.4)	4.8 (0.2)	42.4 (4.1)	36.5 (9.1)	1.2 (0.2)	135.6 (38.6)	29.8 (13.0)	459.9 (79.2)	94.6 (38.0)
S_8	t0	33.3 (0.9)	26.5 (0.4)	5.4 (0.2)	30.3 (0.6)	12.8 (1.9)	0.6 (0.1)	10.6 (0.2)	12.6 (0.7)	462.8 (24.7)	13.3 (0.4)
	t1	51.8 (15.5)	48.5 (17.1)	5.6 (0.1)	52.0 (14.6)	30.0 (9.4)	1.3 (0.4)	29.1 (23.3)	60.7 (23.6)	538.9 (141.5)	36.9 (9.2)
	t2	42.1 (4.4)	57.5 (18.0)	5.5 (0.3)	50.7 (22.8)	28.8 (9.7)	1.3 (0.4)	28.9 (16.9)	42.2 (11.2)	655.1 (76.6)	67.6 (27.4)
	t3	55.0 (10.8)	47.6 (15.9)	5.2 (0.1)	150.4 (34.0)	25.2 (8.9)	1.2 (0.2)	7.3 (1.1)	204.5 (81.3)	747.7 (98.9)	26.8 (12.9)
	t4	45.8 (5.5)	47.4 (19.0)	5.4 (0.3)	84.3 (48.1)	24.8 (11.3)	0.9 (0.4)	55.7 (26.1)	53.0 (28.6)	243.9 (25.0)	69.1 (8.3)
N_4	t0	47.7 (0.6)	31.3 (0.7)	5.3 (0.1)	30.3 (1.5)	16.3 (0.6)	1.3 (0.03)	76.1 (1.9)	8.6 (4.3)	1374.7 (56.2)	71.1 (7.9)
	t1	48.7 (5.4)	28.3 (8.5)	5.7 (0.3)	23.3 (6.0)	13.7 (2.9)	1.1 (0.3)	48.9 (24.1)	10.7 (2.2)	1086.6 (185.1)	64.5 (31.1)
	t2	55.1 (1.5)	30.3 (5.2)	6.1 (0.03)	31.7 (5.7)	14.8 (2.9)	1.7 (0.3)	95.4 (32.5)	14.3 (8.2)	1228.2 (61.8)	89.2 (22.7)
	t3	53.2 (4.2)	30.6 (7.3)	5.2 (0.2)	36.8 (18.7)	15.0 (4.0)	1.1 (0.2)	79.3 (20.8)	58.4 (18.3)	1277.3 (279.2)	48.0 (2.2)
	t4	33.4 (2.3)	23.3 (4.1)	4.9 (0.3)	49.5 (30.8)	10.5 (2.0)	0.7 (0.2)	46.5 (5.6)	9.3 (6.7)	311.65 (114.0)	22.9 (3.5)
S_9	t0	28.4 (0.8)	24.3 (0.3)	5.7 (0.1)	28.3 (1.5)	13.3 (0.6)	0.8 (0.1)	31.6 (1.7)	1.8 (1.5)	710.0 (56.2)	25.4 (1.9)
	t1	35.5 (8.6)	24.4 (6.2)	6.1 (0.2)	43.7 (7.2)	12.4 (4.2)	0.8 (0.3)	48.3 (11.0)	24.4 (8.2)	632.4 (74.6)	63.6 (0.4)
	t2	31.9 (10.1)	27.8 (3.3)	5.9 (0.1)	37 (10.5)	10.4 (2.6)	0.7 (0.2)	47.5 (23.5)	8.2 (8.2)	742.3 (141.1)	40.6 (4.5)
	t3	45.8 (3.5)	29.4 (5.2)	5.2 (0.1)	80.1 (15.6)	15.3 (2.7)	1.0 (0.2)	52.2 (13.7)	167.9 (86.0)	839.2 (114.7)	29.6 (15.1)
	t4	23.4 (1.9)	31.5 (3.0)	5.4 (0.2)	61.1 (37.0)	15.5 (3.1)	0.9 (0.1)	62.7 (0.8)	7.6 (2.7)	231.1 (43.5)	22.6 (0.3)

The soil NO_3^- content was also significantly affected by slope exposure at 1400 and 1600 m a.s.l., being 2-fold higher at the S- than at the N-facing sites, irrespective of the duration of the monitoring. The highest NO_3^- level was observed after 52 weeks between 1400 and 2000 m a.s.l, followed by a decrease until the end of the monitoring at both slopes. In addition, a higher total and available P content was found at the N- than at the S-facing slopes along the altitudinal gradient.

3.3. Wood (micro)biological parameters along the studied climosequence

Wood microbial biomass (dsDNA) was 2-times higher at the S- than at the N-facing slopes after 104 weeks at 1400 m a.s.l., whereas no exposure effects were found for the other altitudes (Tables 4 and 6). Moreover, around 15 – 20 times higher dsDNA contents were found after 104 weeks compared to the beginning of the experiment (Table 4). Wood fungal abundance was 2-times higher at the N- than at the S-facing sites at 1400 m a.s.l. irrespective of the time, and after 12 weeks at 1600 m a.s.l. (Table 4). Moreover, at both slopes fungi were 6-fold higher after 25 weeks, followed by a decrease after 52 weeks and a subsequent increase at the end of the trial between 1200 and 1600 m a.s.l. (Table 4). The *nif*H gene abundance in the wood blocks was significantly higher at the N- than at the S-facing sites after 52 and 104 weeks at 2000 m a.s.l. No exposure-effects were recorded for the other altitudes (Table 4). Higher *nif*H gene copy numbers were recorded after 12 weeks at the N- and the S-facing slopes, and remained mostly stable thereafter, except for the S-facing sites at 1400 and 2000 m a.s.l. (Table 4). Both *amo*A bacterial and archaeal abundances were below the detection limit for all of the study sites (data not shown).

Table 4.

Microbiological properties of wood samples collected in June 2013 (t0; control), in August 2013 (t1; 12 weeks), in October 2013 (t2; 25 weeks); in July 2014 (t3; 52 weeks), in July 2015 (t4; 104 weeks) in the in-field mesocosm experiment along the climosequence scenario. The results are shown pairwise, i.e., the couple of N- and S-facing sites at the same elevation (N_1-S_6; 1200 m a.s.l.; N_2-S_7; 1400 m a.s.l.; N_3-S_8; 1600 m a.s.l.; N_4-S_9; 2000 m a.s.l.). Values are means (n=3) with the standard deviations. Data are expressed on a dry weight basis.

Sites	Time	Microbial biomass index (µg dsDNA g^{-1} wood)	Fungi (gene copy number g^{-1} wood)	*nif*H gene (gene copy number g^{-1} wood)
	t0	1.4 (0.2)	3.12×10^9 (1.67×10^9)	8.77×10^6 (1.37×10^6)
N_1	t1	6.5 (2.1)	7.75×10^9 (3.56×10^9)	3.77×10^7 (8.69×10^6)
	t2	12.1 (4.3)	9.39×10^9 (2.56×10^9)	3.90×10^7 (1.85×10^7)
	t3	13.7 (6.6)	1.42×10^9 (1.20×10^8)	8.95×10^7 (7.38×10^7)
	t4	18.8 (1.2)	4.56×10^9 (4.96×10^9)	3.99×10^7 (3.03×10^7)
S_6	t1	10.9 (8.1)	3.03×10^9 (1.51×10^9)	3.70×10^7 (1.27×10^7)
	t2	8.5 (1.2)	7.30×10^9 (5.37×10^9)	7.46×10^7 (3.78×10^7)
	t3	14.6 (1.9)	1.37×10^9 (1.08×10^9)	2.02×10^7 (3.56×10^6)
	t4	16.6 (0.1)	4.09×10^9 (2.86×10^9)	3.18×10^7 (7.21×10^6)
N_2	t1	5.1 (1.3)	1.35×10^{10} (6.21×10^9)	1.97×10^6 (1.76×10^6)
	t2	13.1 (3.4)	2.42×10^{10} (1.38×10^{10})	1.25×10^7 (9.86×10^6)
	t3	10.9 (2.9)	2.15×10^9 (4.72×10^8)	9.76×10^6 (7.10×10^6)
	t4	17.5 (3.5)	1.79×10^{10} (1.00×10^{10})	9.04×10^6 (5.16×10^6)
S_7	t1	6.8 (0.9)	3.86×10^9 (3.00×10^9)	1.55×10^6 (1.77×10^6)
	t2	14.2 (0.9)	4.78×10^9 (2.43×10^9)	7.82×10^6 (5.83×10^6)
	t3	10.0 (1.1)	4.51×10^8 (3.96×10^8)	1.35×10^6 (1.78×10^6)
	t4	27.5 (4.2)	1.22×10^{10} (6.38×10^9)	5.28×10^7 (1.45×10^7)

Table 4. Continued

Sites	Time	Microbial biomass index (µg dsDNA g^{-1} wood)	Fungi (gene copy number g^{-1} wood)	*nif*H gene (gene copy number g^{-1} wood)
N_3	t1	9.5 (4.0)	3.80×10^{10} (2.60×10^{10})	7.58×10^{7} (3.55×10^{7})
	t2	6.1 (1.1)	3.95×10^{10} (1.96×10^{10})	4.07×10^{7} (1.79×10^{7})
	t3	12.1 (0.5)	1.30×10^{9} (1.82×10^{9})	5.32×10^{7} (2.32×10^{7})
	t4	26.1 (2.7)	1.09×10^{11} (1.75×10^{10})	4.03×10^{7} (1.39×10^{7})
S_8	t1	7.0 (1.1)	1.43×10^{9} (1.87×10^{9})	3.75×10^{7} (1.57×10^{7})
	t2	9.6 (0.9)	2.42×10^{10} (1.43×10^{10})	9.10×10^{7} (4.14×10^{7})
	t3	9.2 (1.0)	1.66×10^{9} (6.88×10^{8})	7.67×10^{7} (3.09×10^{7})
	t4	23.0 (4.7)	1.15×10^{11} (1.32×10^{11})	1.29×10^{8} (8.71×10^{7})
N_4	t1	6.4 (0.9)	1.07×10^{11} (6.84×10^{10})	3.91×10^{8} (1.19×10^{8})
	t2	8.2 (1.6)	1.55×10^{11} (3.32×10^{10})	6.68×10^{8} (4.42×10^{8})
	t3	13.0 (2.0)	1.81×10^{11} (1.29×10^{11})	1.03×10^{9} (1.25×10^{9})
	t4	31.6 (15.3)	1.92×10^{11} (8.47×10^{10})	1.28×10^{9} (2.86×10^{8})
S_9	t1	8.1 (0.9)	7.80×10^{10} (4.51×10^{10})	4.59×10^{8} (4.51×10^{8})
	t2	11.4 (3.2)	1.61×10^{11} (3.39×10^{10})	4.10×10^{8} (2.17×10^{8})
	t3	12.7 (2.4)	1.17×10^{11} (1.18×10^{10})	4.27×10^{7} (2.97×10^{7})
	t4	22.8 (13.7)	1.04×10^{11} (1.19×10^{11})	4.60×10^{7} (2.03×10^{7})

The β-glucosidase and xylosidase activities were significantly higher at the S-facing sites at 1600 m a.s.l.; whereas the opposite trend (N>S) was recorded at 1400 and 2000 m a.s.l. after 104 weeks (Figs. 2A & 2C). A pronounced increase in these two enzyme activities was observed after 104 weeks at both slopes at 1200 m a.s.l., and at the N-facing slope at 1400 and 2000 m a.s.l. Overall, the highest cellulase (Fig. 2B) and chitinase (Fig. 3A) activities were generally observed after 104 weeks at both slopes along the climosequence scenario. Leucine-aminopeptidase activity was not significantly affected by the slope exposure; however, it was 11-times higher after 25 weeks, followed by a decrease after 52 weeks and a subsequent increase at the end of the trial between 1200 and 1600 m a.s.l. (Fig. 3B). Acid phosphomonoesterase was significantly higher at the N- than at the S-facing sites after 104 weeks along the altitudinal gradient, except for 1400 m a.s.l. (Fig. 3C). A higher alkaline phosphomonoesterase activity was recorded at the S- than at the N-facing site at 1600 m a.s.l. regardless of the sampling time (Fig. 3D). However, no exposure-effect was observed for the remaining altitudes (Fig. 3D).

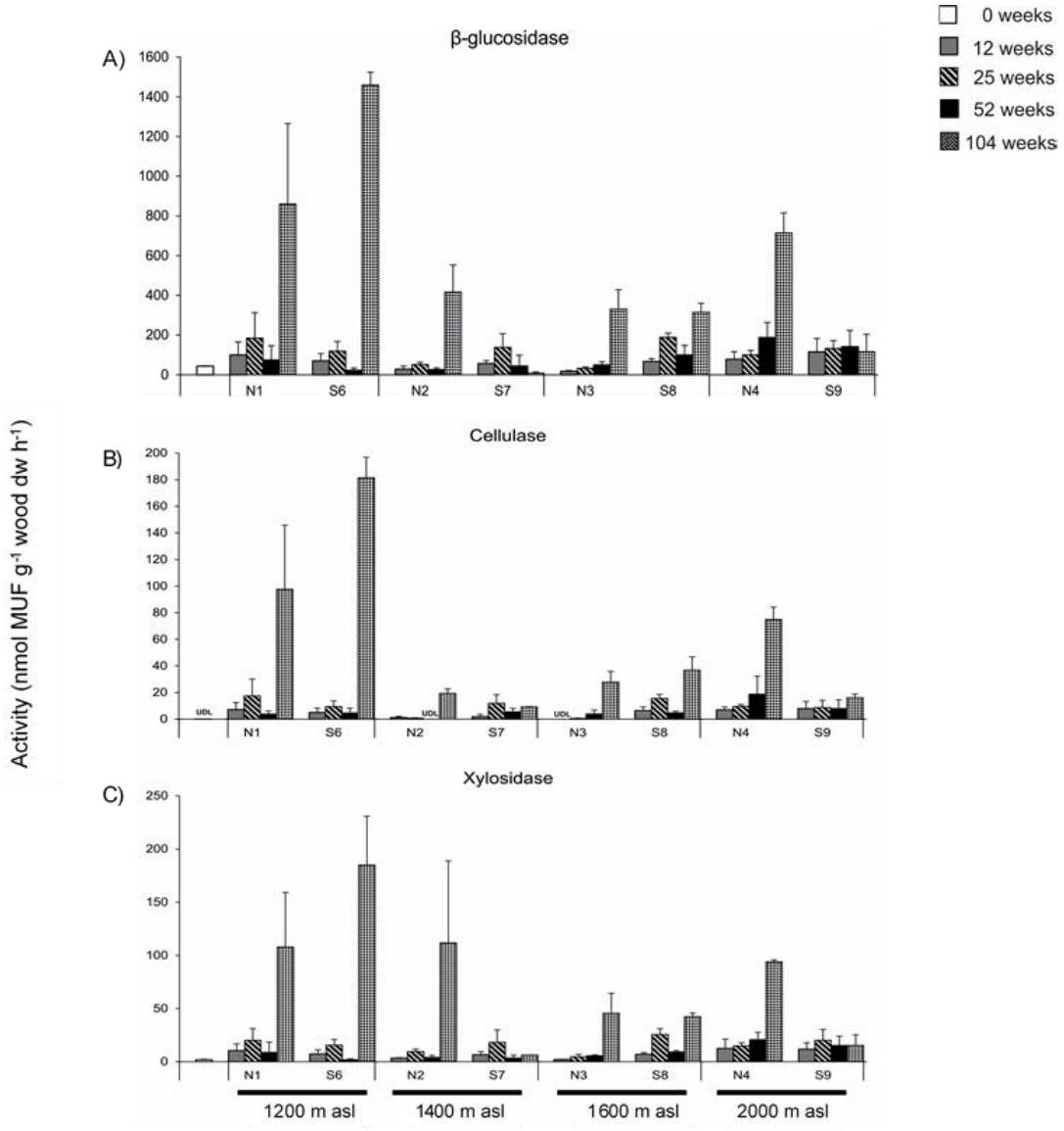

Fig. 2. Potential activities of β-glucosidase (A), cellulase (B), xylosidase (C) of the wood samples collected in June 2013 (0 weeks), in August 2013 (12 weeks), in October 2013 (25 weeks), in July 2014 (52 weeks), and in July 2015 (104 weeks) in the in-field mesocosm experiment within the climosequence scenario. The results are shown pairwise, i.e., the couples of N- and S-facing sites (N_1-S_6; N_2-S_7; N_3-S_8; N_4-S_9) at comparable elevation (1200 m; 1400 m; 1600 m; 2000 m above sea level). Values are means (n = 3) with the standard deviations.

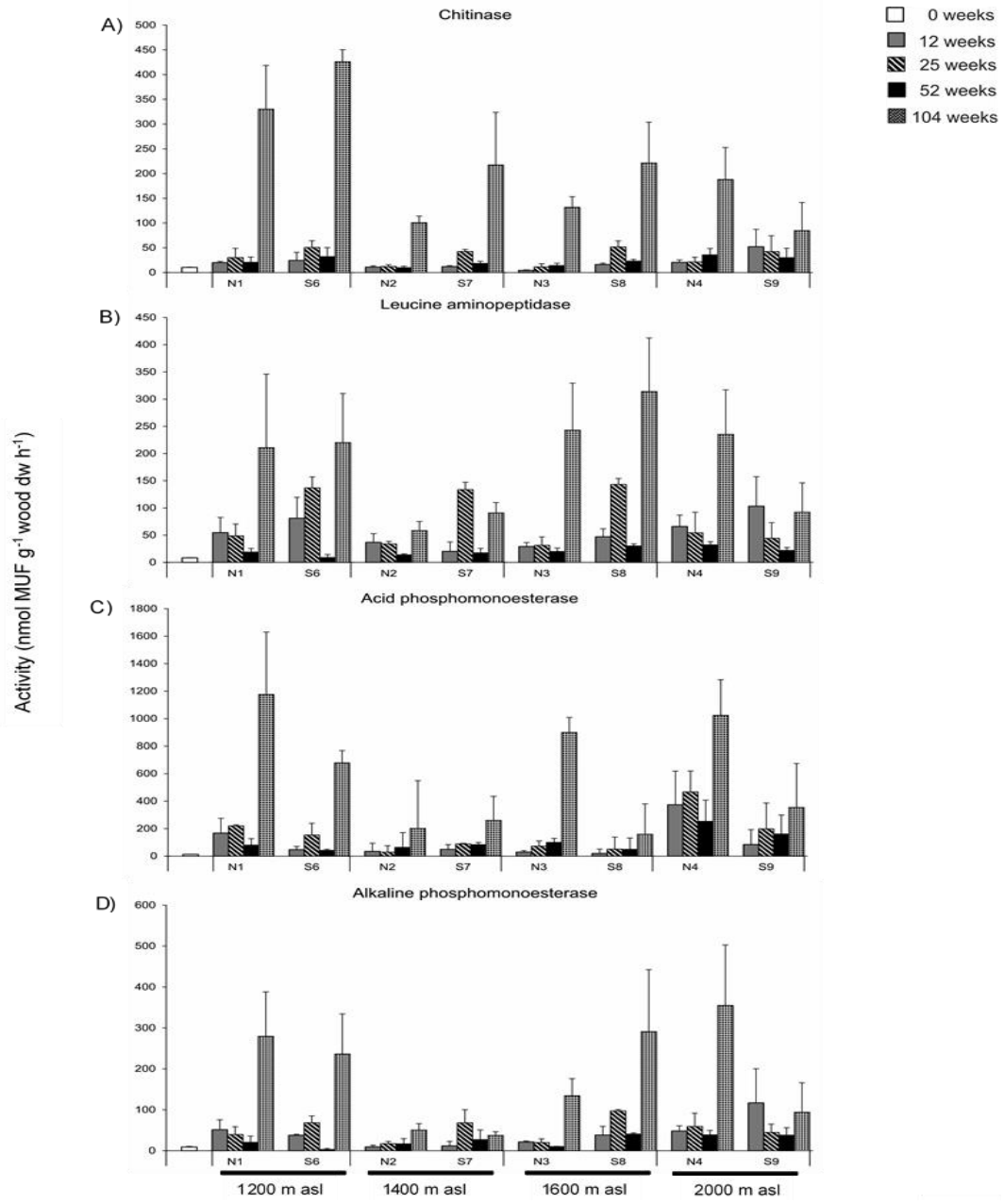

Fig.3. Potential activities of chitinase (A), leucine aminopeptidase (B), acid phosphomonoesterase (C), alkaline phosphomonoesterase (D) of the wood samples collected in June 2013 (0 weeks), in August 2013 (12 weeks), in October 2013 (25 weeks), in July 2014 (52 weeks), and in July 2015 (104 weeks) in the in-field mesocosm experiment within the climosequence scenario. The results are shown pairwise, i.e., the couples of N- and S-facing sites (N_1-S_6; N_2-S_7; N_3-S_8; N_4-S_9) at comparable elevation (1200 m; 1400 m; 1600 m; 2000 m above sea level). Values are means (n = 3) with the standard deviations.

3.4. Soil (micro)biological properties along the studied climosequence

Soil microbial biomass, assessed as double strand DNA (dsDNA), was two to three times higher at the N- than at the S-facing sites after 25 and 104 weeks at 1200 m a.s.l. (Tables 5 and 6). This exposure-effect (N>S) was also observed after 12 and 25 weeks at 1400 m a.s.l.; after 52 weeks at 1600 m a.s.l.; and generally at 2000 m a.s.l. (Table 5). A similar exposure-effect was found for the soil fungal abundance assessed by qPCR (Table 5). The *nif*H gene copy number was 3-times higher at the N- than at the S-facing sites at 1600 m a.s.l. throughout the monitoring. This exposure effect (N>S) was also observed at the beginning of the trial and after 52 weeks at 1400 and 2000 m a.s.l., respectively (Table 5). A higher *amo*A bacterial abundance was recorded at the S- than at the N-facing sites along the altitudinal gradient, except for 1200 m a.s.l. (no exposure-effect; Table 5). The *amo*A archaeal abundance was generally below the detection limit, except at the N-facing site at 2000 m a.s.l. (data not shown).

Table 5.

Microbiological properties of soil samples collected in June 2013 (t0; control), in August 2013 (t1; 12 weeks), in October 2013 (t2; 25 weeks); in July 2014 (t3; 52 weeks), in July 2015 (t4; 104 weeks) in the in-field mesocosm experiment along the climosequence scenario. The results are shown pairwise, i.e., the couple of N- and S-facing sites at the same elevation (N_1-S_6; 1200 m a.s.l.; N_2-S_7; 1400 m a.s.l.; N_3-S_8; 1600 m a.s.l.; N_4-S_9; 2000 m a.s.l.). Values are means (n=3) with the standard deviations. Data are expressed on a dry weight basis.

Sites	Time	Microbial biomass index (μg dsDNA g^{-1} soil)	Fungi (gene copy number g^{-1} soil)	*nif*H gene (gene copy number g^{-1} soil)	*amo*A-AOB gene (gene copy number g^{-1} soil)
N_1	t0	140.0 (12.4)	9.45×10^8 (7.45×10^8)	1.57×10^8 (7.94×10^7)	2.32×10^6 (1.44×10^6)
	t1	101.7 (18.1)	2.03×10^9 (1.10×10^9)	2.73×10^8 (2.49×10^7)	7.43×10^7 (1.70×10^7)
	t2	157.9 (49.9)	1.65×10^9 (5.00×10^8)	1.60×10^8 (8.33×10^7)	4.77×10^7 (3.59×10^7)
	t3	55.8 (21.2)	2.74×10^9 (6.36×10^8)	2.08×10^8 (2.70×10^7)	1.23×10^8 (6.30×10^7)
	t4	160.3 (4.8)	5.51×10^8 (4.74×10^8)	1.64×10^7 (8.74×10^6)	1.90×10^7 (1.32×10^7)
S_6	t0	94.2 (13.4)	5.88×10^8 (1.17×10^8)	1.03×10^8 (7.57×10^6)	1.98×10^6 (7.08×10^5)
	t1	112.2 (25.5)	1.31×10^9 (2.22×10^8)	2.12×10^8 (3.32×10^7)	1.09×10^8 (4.57×10^7)
	t2	70.6 (17.7)	1.11×10^9 (2.98×10^8)	1.61×10^8 (6.15×10^7)	3.11×10^7 (1.34×10^7)
	t3	39.4 (12.5)	1.57×10^9 (6.32×10^8)	1.73×10^8 (2.20×10^7)	4.87×10^7 (3.85×10^7)
	t4	62.2 (29.9)	3.78×10^8 (6.40×10^7)	2.04×10^7 (7.09×10^6)	6.25×10^6 (5.03×10^5)
N_2	t0	229.9 (11.0)	8.33×10^8 (2.95×10^8)	8.46×10^7 (2.33×10^7)	1.48×10^6 (1.26×10^6)
	t1	344.0 (88.1)	1.20×10^9 (3.73×10^8)	5.17×10^7 (4.01×10^7)	2.17×10^6 (2.79×10^6)
	t2	342.4 (55.5)	8.43×10^8 (1.74×10^7)	9.53×10^7 (2.95×10^7)	5.95×10^5 (3.95×10^5)
	t3	185.2 (18.4)	1.53×10^9 (1.55×10^8)	8.32×10^7 (1.02×10^7)	3.99×10^6 (1.10×10^6)
	t4	189.0 (52.4)	5.01×10^8 (2.28×10^8)	3.37×10^7 (1.82×10^7)	5.46×10^6 (2.96×10^6)
S_7	t0	156.5 (23.9)	4.24×10^8 (5.90×10^7)	6.40×10^6 (3.47×10^6)	1.05×10^7 (1.33×10^6)
	t1	83.4 (28.5)	3.55×10^8 (1.02×10^8)	5.09×10^7 (1.63×10^7)	2.73×10^7 (1.34×10^7)
	t2	143.7 (49.5)	4.26×10^8 (1.64×10^8)	1.96×10^7 (1.95×10^7)	3.31×10^7 (6.07×10^6)
	t3	196.1 (12.0)	4.05×10^8 (8.55×10^7)	1.08×10^7 (8.90×10^6)	8.72×10^7 (7.43×10^7)
	t4	186.6 (28.7)	6.56×10^8 (3.93×10^8)	2.23×10^7 (5.20×10^6)	1.09×10^8 (8.24×10^7)

Table 5. Continued

Sites	Time	Microbial biomass index (µg dsDNA g^{-1} soil)	Fungi (gene copy number g^{-1} soil)	*nif*H gene (gene copy number g^{-1} soil)	*amo*A-AOB gene (gene copy number g^{-1} soil)
N_3	t0	242.1 (11.8)	3.11×10^9 (1.16×10^9)	1.52×10^9 (3.07×10^8)	2.56×10^6 (1.12×10^6)
	t1	218.7 (41.0)	3.13×10^9 (8.44×10^8)	1.29×10^9 (2.81×10^8)	6.83×10^7 (7.92×10^7)
	t2	182.0 (79.2)	1.34×10^9 (1.60×10^9)	4.35×10^8 (3.03×10^8)	6.62×10^6 (1.04×10^6)
	t3	381.1 (19.7)	4.53×10^9 (2.89×10^9)	3.47×10^8 (1.80×10^8)	8.05×10^5 (8.23×10^5)
	t4	186.2 (16.7)	7.79×10^8 (1.29×10^8)	5.44×10^7 (1.54×10^7)	4.11×10^7 (3.69×10^7)
S_8	t0	115.8 (5.1)	1.35×10^9 (8.40×10^8)	5.59×10^8 (1.06×10^8)	1.39×10^7 (1.59×10^6)
	t1	201.1 (55.6)	2.36×10^9 (8.72×10^8)	5.11×10^8 (6.43×10^7)	6.82×10^7 (5.00×10^7)
	t2	208.2 (97.6)	1.82×10^9 (4.51×10^8)	1.22×10^8 (2.18×10^7)	2.13×10^7 (3.39×10^6)
	t3	192.3 (29.0)	1.96×10^9 (1.13×10^9)	1.28×10^8 (4.88×10^7)	4.16×10^7 (2.52×10^7)
	t4	71.0 (29.9)	6.63×10^8 (5.85×10^8)	2.20×10^7 (8.51×10^6)	3.66×10^7 (1.83×10^7)
N_4	t0	214.0 (8.8)	1.12×10^9 (3.34×10^8)	5.58×10^8 (4.25×10^8)	3.84×10^6 (2.76×10^6)
	t1	242.8 (30.8)	1.06×10^9 (7.17×10^8)	3.33×10^8 (1.20×10^8)	5.02×10^6 (5.48×10^6)
	t2	235.1 (56.8)	5.58×10^8 (2.18×10^8)	3.58×10^8 (3.47×10^8)	1.00×10^7 (7.38×10^6)
	t3	247.0 (123.6)	1.32×10^9 (7.94×10^8)	7.86×10^8 (4.02×10^8)	2.89×10^7 (3.05×10^7)
	t4	118.5 (14.7)	3.38×10^8 (4.24×10^7)	4.33×10^8 (2.27×10^8)	3.10×10^6 (2.56×10^6)
S_9	t0	135.9 (15.0)	7.62×10^8 (5.79×10^7)	3.83×10^8 (1.45×10^8)	4.89×10^5 (1.30×10^5)
	t1	85.9 (35.9)	1.13×10^9 (1.80×10^8)	6.18×10^8 (3.42×10^8)	4.39×10^7 (3.97×10^7)
	t2	194.6 (43.0)	7.21×10^8 (2.85×10^7)	4.02×10^8 (1.73×10^8)	1.94×10^7 (2.90×10^7)
	t3	209.9 (16.6)	1.41×10^9 (4.53×10^8)	9.12×10^7 (6.96×10^7)	3.52×10^8 (2.24×10^8)
	t4	137.1 (11.5)	1.23×10^9 (1.03×10^9)	5.45×10^7 (5.75×10^7)	3.18×10^7 (1.35×10^7)

The β-glucosidase activity was mostly higher at the S- than at the N-facing slopes (Fig. 4A) and the cellulase activity showed a similar behaviour (Fig. 4B). Xylosidase activity was significantly higher (3 times) at the N- than at the S-facing slopes after 25 and 104 weeks at 1200 m a.s.l., while the opposite trend (S>N) was observed after 52 weeks (Fig. 4C); the same exposure-effect (S>N) was recorded after 12 weeks at 1400 and 1600 m a.s.l. No significant exposure-effect was observed at 2000 m a.s.l. (Fig. 4C). Chitinase showed a higher activity at the S- than at the N-facing sites at 1400 and 1600 m a.s.l. (Fig. 5A). Nonetheless, leucine-aminopeptidase activity was in general higher at the N- than at the S-facing sites over time along the altitudinal gradient, except for the time point of 104 weeks at 1600 and 2000 m a.s.l. (no exposure-effect) (Fig. 5B). Slope exposure also affected significantly the acid phosphomonoesterase activity, recording higher levels at the S- than at the N-facing slopes after 12 and 52 weeks at 1400 m a.s.l. and at the beginning and after 12 weeks at 1600 m a.s.l. (Fig. 5C). Likewise, the alkaline phosphomonoesterase activity was significantly higher at the S-facing sites at the beginning of the experiment, and after 25 and 104 weeks at 1400 m a.s.l. The same exposure effect (S>N) was found at 1600 m a.s.l. throughout the monitoring (Fig. 5D).

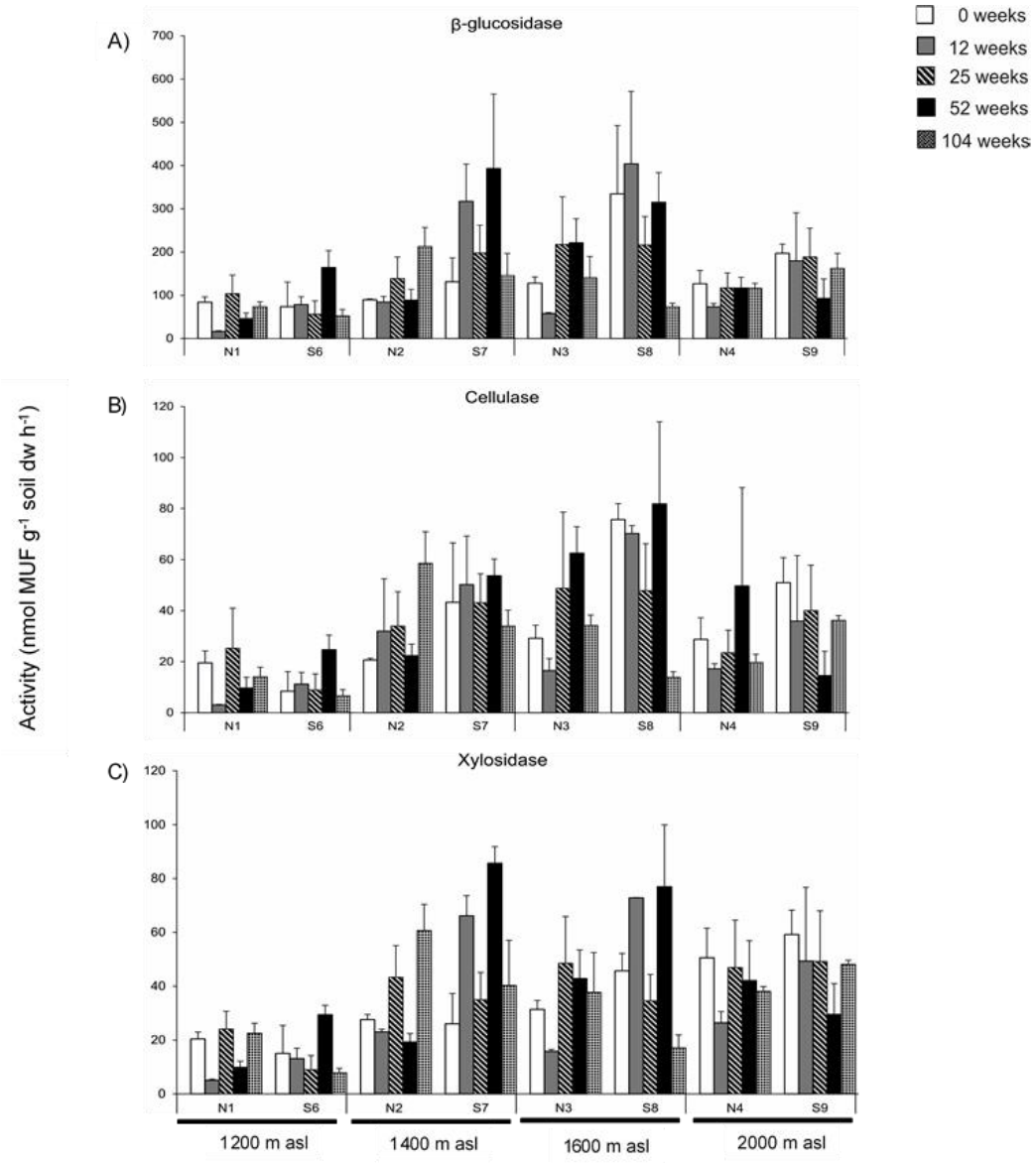

Fig. 4. Potential activities of β-glucosidase (A), cellulase (B), xylosidase (C) of the soil samples collected in June 2013 (0 weeks), in August 2013 (12 weeks), in October 2013 (25 weeks), in July 2014 (52 weeks), and in July 2015 (104 weeks) in the in-field mesocosm experiment within the climosequence scenario. The results are shown pairwise, i.e., the couples of N- and S-facing sites (N_1-S_6; N_2-S_7; N_3-S_8; N_4-S_9) at comparable elevation (1200 m; 1400 m; 1600 m; 2000 m above sea level). Values are means (n = 3) with the standard deviations.

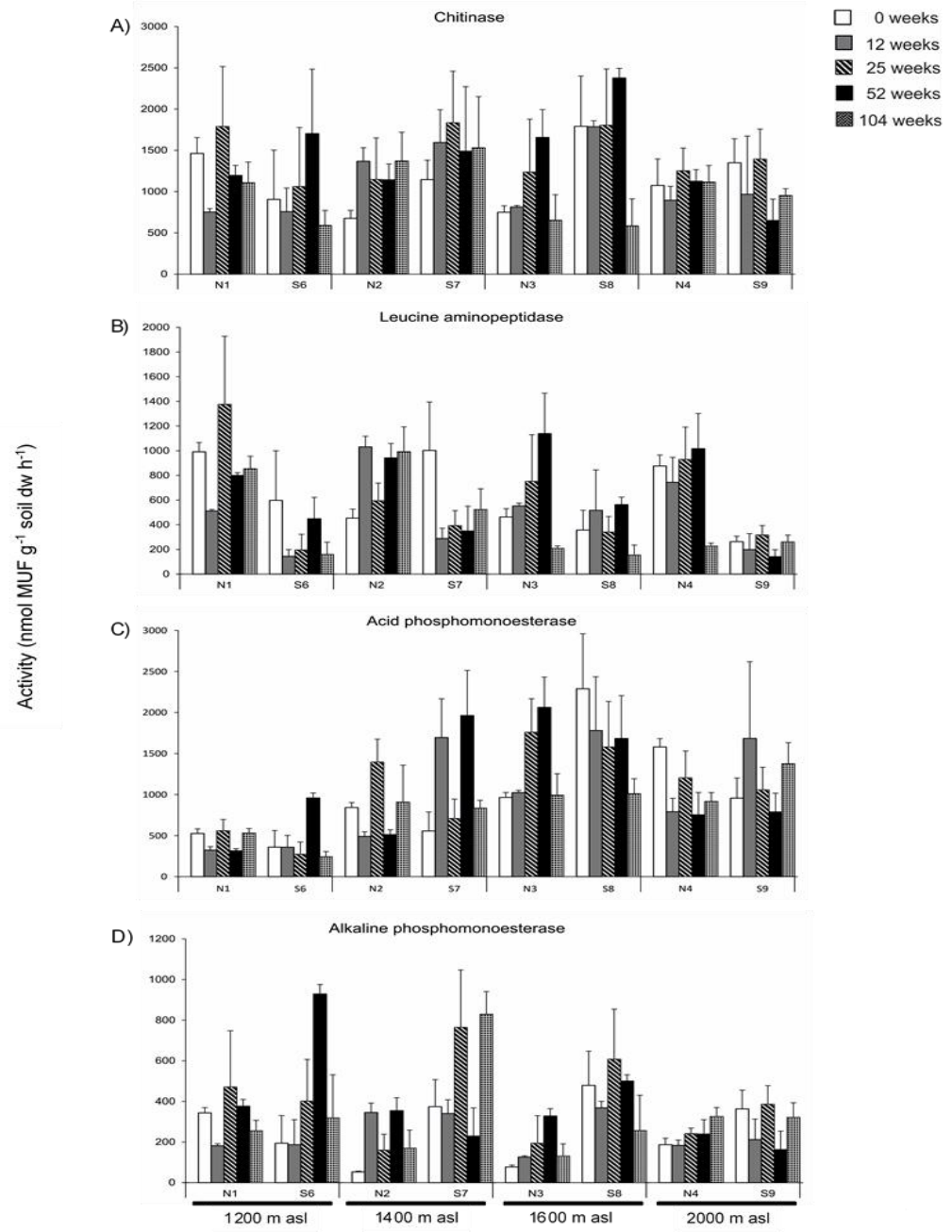

Fig. 5. Potential activities of chitinase (A), leucine aminopeptidase (B), acid phosphomonoesterase (C), alkaline phosphomonoesterase (D) of the soil samples collected in June 2013 (0 weeks), in August 2013 (12 weeks), in October 2013 (25 weeks), in July 2014 (52 weeks), and in July 2015 (104 weeks) in the in-field mesocosm experiment within the climosequence scenario. The results are shown pairwise, i.e., the couples of N- and S-facing sites (N_1-S_6; N_2-S_7; N_3-S_8; N_4-S_9) at comparable elevation (1200 m; 1400 m; 1600 m; 2000 m above sea level). Values are means (n = 3) with the standard deviations.

4. Discussion

Over the decomposition process, deadwood is incorporated into the soil, releasing nutrients and organic C that significantly affect the soil C balance and forest productivity (Spears and Lajtha, 2004; Bradford et al., 2014). Moreover, the wood decay rate can also be accelerated through the activity of the soil microbiota (Garrett et al., 2010). However, to date, few studies have addressed the changes in both deadwood and the forest floor over time from a physico-chemical and microbiological viewpoint (van der Wal et al., 2007; Risch et al., 2013; Gonzalez-Polo et al., 2013). In addition, there exists scarce information of how slope exposure affects the deadwood decay dynamics and the underlying soil.

In agreement with previous studies performed in the same study area (Egli et al., 2006, 2009; Fravolini et al., 2016; Bardelli et al., 2017), the soils located at the N-facing slope were more acidic, moister and richer in OM content compared to those at the S-facing slope. The lower pH values and higher moisture levels recorded at the northern slope led to favourable conditions especially for the fungal deadwood decomposers. Indeed, as revealed by real-time PCR, fungi were more abundant in the wood blocks and in the uppermost topsoil layer at the N-facing slopes, even though this exposure-effect (N>S) was altitude- and time-dependent. This is in line with Fravolini et al. (2016) who observed faster decay rates of *P. abies* deadwood at the N-facing sites under the same experimental conditions.

Furthermore, a significant positive correlation between *nif*H gene and fungal abundances was observed in the *P. abies* wood blocks at the N-facing slopes along the altitudinal gradient (12 weeks: $R = 0.669$, $p < 0.05$; 25 weeks: $R = 0.664$, $p < 0.05$; 52 weeks: $R = 0.943$, $p < 0.001$; 104 weeks: $R = 0.729$, $p < 0.01$). Such a correlation was also found at the S-facing sites after 12 weeks ($R = 0.947$, $p < 0.001$) and 25 weeks ($R = 0.771$, $p < 0.01$). Accordingly,

Gómez-Brandón et al. (2017) also found a strong relationship between these two microbial groups in *P. abies* coarse woody debris at different stages of natural decay in the same Italian Alpine setting (5 decay class study). All in all this underpins the existence of potential fungal-bacterial interactions in wood, even though it is still necessary to unravel the exact identity of such associations as pointed out by Johnston et al. (2016).

Carbon is one of the main energy sources for microorganisms largely influencing their activity, while N is rather a limiting nutrient for microbial growth (Nannipieri et al., 2003). While deadwood, especially in the early decay stages, is N-limited with C/N ratios ranging from about 350 to 800, there is evidence about increasing N contents as wood decay progresses (Rajala et al., 2012; Gómez-Brandón et al., 2017). In our study, the total N content and the abundance of both ammonia-oxidising bacteria and archaea from *P. abies* wood blocks was below the detection limit during the 2-year period observation, which might be ascribed to the duration of the experimental set-up. Indeed, Laiho and Prescott (1999) observed little changes in N concentrations in deadwood logs of *P. glauca* and *P. engelmannii* in a longer-term study (14 years) in the Alberta Rocky Mountains.

Previous studies have reported soil pH and N mineral sources (NH_4^+, NO_3^-) as the major drivers of niche differentiation between AOA *vs.* AOB communities in forest soils (Szukics et al., 2012; Levy-Booth et al., 2014). Generally, higher abundances of archaeal *amo*A genes have been found in acidic environments characterised by low substrate availability and low temperatures (Qin et al., 2013; Stempfhuber et al., 2014). This could explain why this microbial group was more abundant in the soils from the N-facing slopes at the highest altitude (2000 m a.s.l.). In contrast, we found higher soil bacterial *amo*A abundance at the S-facing slopes (except for 1200 m

a.s.l.) that are characterised by lower acidic conditions and a higher NO_3^- content.

Overall, enzyme-specific exposure effects were recorded for *P. abies* wood and soil samples as previously shown in Bardelli et al. (2017) and Gómez-Brandón et al. (2017). The thermal signal (N *vs.* S) was dependent on the altitude and time of decay for most of the enzymatic activities involved in the C-cycle (i.e., β-glucosidase, cellulase and xylosidase). These enzymes are closely linked to fungi which have a relevant role in the degradation of biopolymers such as cellulose and hemicellulose (Makoi and Ndakidemi, 2008; López-Mondéjar et al., 2016). In fact, at both slopes the fungal abundance (qPCR-based) from the *P. abies* wood blocks was positively correlated with the aforementioned enzymes but only after 52 weeks (time-dependent; data not shown). Furthermore, higher levels of wood fungal abundance and, in general, microbial biomass (using dsDNA) were observed at the end of the monitoring, probably due to an increase in the availability of micro- and macronutrients required for the microbial growth as wood decay progresses (Gonzalez-Polo et al., 2013; Gómez-Brandón et al., 2017). This could explain why a decrease in cellulose content was recorded over time at both the N- and the S-facing slopes, which is in agreement with previous studies (Bűtler et al., 2007; Fravolini et al., 2016; Gómez-Brandón et al., 2017). Nevertheless, no time-differences were found for lignin concentration, except at 2000 m a.s.l. Specifically, at this altitude the amount of lignin increased with progressing wood decay probably due to its slower degradation and therefore passive enrichment in deadwood (Petrillo et al., 2015, 2016; Gómez-Brandón et al., 2017).

Moisture and OM levels have been shown as major determinants on the activity of soil enzymes (Makoi and Ndakidemi, 2008; Štursová and Baldrian, 2011). However, in our study the abovementioned enzymes related

to the C-cycle showed a higher activity in soils collected at the S-facing slopes (altitude- and time-dependent), despite a higher soil moisture and OM content along with a higher microbial biomass (using dsDNA) was in general recorded at north exposure. In addition, the N-facing sites were characterised by a higher leucine-aminopeptidase activity regardless of the sampling time. Koch et al. (2007) stated that potential amino-peptidase activities (leucine and tyrosine) had almost constant temperature in the range from 0-30 °C in Alpine areas. This suggests that polypeptide decay can be less sensitive to changes in temperature and even be favoured at lower temperatures as it had occurred in this study. In case of *P. abies* wood blocks, this later enzyme activity was not affected by exposure, probably due to the limited N content in wood throughout the monitoring.

Acid and alkaline phosphomonoesterases have a relevant role in P cycling in forest ecosystems, mainly where P availability may limit plant productivity (Salazar et al., 2011). In the *P. abies* wood blocks, we found higher acid and alkaline phosphomonoesterase activities at the N-and at the S-facing slopes respectively, which is probably related to the differences in acidity between both slopes (Egli et al., 2006). Nonetheless, these two enzymes showed a higher activity in soils from the S-facing slopes than in those from the comparable N-facing sites at 1400 and 1600 m a.s.l. A plausible explanation could rely on the lower P availability found at south exposure, indicating that an increase in P-acquiring enzyme activities would be expected in case of P deficiency (Fraser et al., 2015).

5. Conclusion

Our field experiment provided evidence that climate effects, i.e., different thermal and moisture conditions due to different exposure, largely affected the *P. abies* wood blocks decay and the underlying soil in terms of microbial biomass and activity. It has to be noted that our study was performed in one

specific area of the Alps. Further studies are therefore needed to determine if our findings can be extrapolated to similar regions. Likewise, as we studied only one type of wood, i.e., soft wood, further investigations dealing with different wood types, e.g., soft wood *vs.* hard wood could be a promising approach to assess differences related to wood tissues (tree species). Our first hypothesis is partially corroborated because higher levels of soil microbial biomass were in general recorded at the N-facing slope. However, exposure affected to a less than assumed the wood microbial biomass. Enzyme-specific exposure effects were, however, found in both soil and *P. abies* wood blocks along the climosequence. Furthermore, in the soil the studied microbial groups responded differently to exposure in terms of abundance: fungi and *nif*H (N>S; altitude and time-dependent); AOB (S>N; altitude and time-dependent); AOA (N>S; only at 2000 m a.s.l.). In the wood blocks, however, the AOB and AOA abundance was below the detection limit. Longer-term measurements would, therefore, be advisable to determine the complex deadwood decay process and the involved microbiota. In addition, we found indications of fungal-bacterial interactions within the deadwood environment. The identity and ecology of bacterial communities in decomposing wood still need to be unravelled. In this sense, high-throughput sequencing technologies could offer a comprehensive overview of the microbial diversity patterns and community composition during the deadwood decomposition process.

Acknowledgments

This research is part of the DecAlp D.A.CH. project (Project I989-B16). T. Bardelli has been funded by a PhD grant from the University of Florence (Italy). M. Gómez-Brandón and J. Ascher-Jenull have been funded by the Fonds zur Förderung der wissenschaftlichen Forschung (FWF) Austria (Project I989-B16). María Gómez-Brandón also acknowledges support by

the Programa Ramón y Cajal (RYC-2016-21231; Ministerio de Economía y Competitividad). We would like to thank Sebastian Waldhuber and Ljubica Begovic for their help in the laboratory. We acknowledge Paul Fraiz for his highly valuable help in language editing. We are also indebted to Dr. Fabio Angeli of the Ufficio distrettuale forestale – Malé (Trento, Italy) and his team for their support in the field.

References

Ascher, J., Ceccherini, M.T., Pantani, O.L., Agnelli, A., Borgogni, F., Guerri, G., Nannipieri, P., Pietramellara, G., 2009. Sequential extraction and genetic fingerprinting of a forest soil metagenome. Appl. Soil. Ecol. 42, 176–181.

Ascher, J., Sartori, G., Graefe, U., Thornton, B., Ceccherini, M.T., Pietramellara, G., Egli, M., 2012. Are humus forms, mesofauna and microflora in subalpine forest soils sensitive to thermal conditions? Biol. Fertil. Soils 48, 709–725.

Baldrian, P., Zrustova, P., Tláskal, V., Davidova, A., Merhautová, V., Vrška, T., 2016. Fungi associated with decomposing deadwood in a natural beech-dominated forest. Fungal Ecol. 23, 109–122.

Bardelli, T., Gómez-Brandón, M., Ascher-Jenull, J., Fornasier, F., Arfaioli, P., Francioli, D., Egli, M., Sartori, G., Insam, H., Pietramellara, G., 2017. Effects of slope exposure on soil physico-chemical and microbiological properties along an altitudinal climosequence in the Italian Alps. Sci. Total Environ. 575, 1041–1055.

Bradford, M.A., Ii, R.J.W., Baldrian, P., Crowther, T.W., Maynard, D.S., Oldfield, E.E., Wieder, W.R., Wood, S.A., King, J.R., 2014. Climate fails to predict wood decomposition at regional scales. Nat. Clim. Chang. 4, 625–630.

Bűtler, R., Patty, L., LeBayon, R., Guenat, C., Schlaepfer, R., 2007. Log decay of *Picea abies* in the Swiss Jura Mountains of central Europe. Forest. Ecol. Manage. 242, 791–799.

Egli, M., Mirabella, A., Sartori, G., Zanelli, R., Bischof, S., 2006. Effect of north and south exposure on weathering rates and clay mineral formation in Alpine soils. Catena 67, 155–174.

Egli, M., Sartori, G., Mirabella, A., Favilli, F., 2009. Effect of north and south exposure on organic matter in high Alpine soils. Geoderma 149, 124–136.

Erguder, T.H., Boon, N., Wittebolle, L., Marzorati, M., Verstraete, W., 2009. Environmental factors shaping the ecological niches of ammonia-oxidizing archaea. Fems Microbiol. Rev. 33, 855–869.

Fornasier, F., Margon, A., 2007. Bovine serum albumin and Triton X-100 greatly increase phosphomonoesterases and arylsulphatase extraction yield from soil. Soil Biol. Biochem. 39, 2682–2684.

Fornasier, F., Ascher, J., Ceccherini, M.T., Tomat, E., Pietramellara, G., 2014. A simplified rapid, low-cost and versatile DNA-based assessment of soil microbial biomass. Ecol. Indic. 45, 75–82.

Francis, C.A., Roberts, K.J., Beman, J.M., Santoro, A.E., Oakley, B.B., 2005. Ubiquity and diversity of ammonia-oxidizing archaea in water columns and sediments of the ocean. Proc. Natl. Acad. Sci. U. S. A. 102, 14683–14688.

Fraser, T. D., Lynch, D.H., Bent, E., Entz, M.H., Dunfield, K.E., 2015. Soil bacterial *phoD* gene abundance and expression in response to applied phosphorus and long-term management. Soil Biol. Biochem. 88, 137–147.

Fravolini, G., Egli, M., Derungs, C., Cherubini, P., Ascher-Jenull, J., Gómez Brandón, M., Bardelli, T., Tognetti, R., Lombardi, F., Marchetti, M., 2016. Soil attributes and microclimate are important drivers of initial deadwood decay in sub-alpine Norway spruce forests. Sci. Tot. Environ. 569-570, 1064–1076.

Garrett L.G., Kimberley M.O., Graeme R.O., Pearce S.H., Paul T.S.H., 2010. Decomposition of woody debris in managed Pinus radiata plantations in New Zealand. For Ecol Manag. 260, 1389–1398.

Gómez-Brandón, M., Ascher-Jenull, J., Bardelli, T., Fornasier, F., Fravolini, G., Arfaioli, P., Ceccherini, M.T., Pietramellara, G., Lamorski, K., Sławiński, C.,

Bertoldi, D., Egli, M., Cherubini, P., Insam, H., 2017. Physico-chemical and microbiological evidence of exposure effects on *Picea abies* – Coarse woody debris at different stages of decay. Forest Ecol. Manage. 391, 376–389.

Gonzalez-Polo, M., Fernandez-Souto, A., Austin, A.T., 2013. Coarse woody debris stimulates soil enzymatic activity and litter decomposition in an old-growth temperate forest of Patagonia, Argentina. Ecosys. 16, 1025–1038.

Hoppe, B., Kahl, T., Karasch, P., Wubet, T., Bauhus, J., Buscot, F., Krüger, D., 2014. Network analysis reveals ecological links between N-fixing bacteria and wood-decaying fungi. PLoS ONE e88141.

Hu, Z., Xu, C., McDowell, N.G., Johnson, D.J., Wang, M., Luo, Y., Zhou, X., Huang, Z., 2017. Linking microbial community composition to C loss rates during wood decomposition. Soil Biol. Biochem. 104, 108–116.

Johnston, S.R., Boddy, L., Weightman, A.J., 2016. Bacteria in decomposing wood and their interactions with wood-decay fungi. FEMS Microbiol. Ecol. 92, 1–12.

Kandeler, E., 1993a. Bestimmung von Ammonium. In: Schinner, F., Öhlinger, R., Kandeler, E., Margesin, R. (Eds.), Bodenbiologische Arbeitsmethoden. Springer, Berlin, Heidelberg, 366–368.

Kandeler, E., 1993b. Bestimmung von Nitrat. In: Schinner, F., Öhlinger, R., Kandeler, E., Margesin, R. (Eds.), Bodenbiologische Arbeitsmethoden. Springer, Berlin, Heidelberg, 369–371.

Kielak, A.M., Scheublin, T.R., Mendes, L.W., van Veen, J.A., Kuramae, E.E., 2016. Bacterial community succession in pine-wood decomposition. Front Microbiol. 7, 1–12. http://dx.doi.org/10.3389/fmicb.2016.00231.

Koch, O., Tscherko, D., Kandeler, E., 2007. Temperature sensitivity of microbial respiration, nitrogen mineralization, and potential soil enzyme activities in organic alpine soils. Glob. Biogeochem. Cycles 21, 1–11.

Kuo, S., 1996. Phosphorus. In: In: Sparks, D.L. (Ed.), Methods of Soil Analysis. Part 3. Chemical Methods. SSSA Book Series, vol. 5. Soil Science Society of America Madison, WI, 869–919.

Laiho, R., Prescott, C.E., 1999. The contribution of coarse woody debris to carbon, nitrogen, and phosphorus cycles in three Rocky Mountain coniferous forests. Can. J. For. Res. 29, 1592–1603.

Larsen, M.J., Jurgensen, M.F., Harvey, A.E., 1978. Nitrogen fixation associated with wood decayed by some common fungi in western Montana. Can. J. For. Res. 8, 341–345.

Leininger, S., Urich, T., Schloter, M., Schwark, L., Qi, J., Nicol, G.W., Prosser, J.I., Schuster, S.C., Schleper, C., 2006. Archaea predominate among ammonia-oxidizing prokaryotes in soils. Nature 442, 806–809.

Levy-Booth, D.J., Prescott, C.E., Grayston, S.J., 2014. Microbial functional genes involved in nitrogen fixation, nitrification and denitrification in forest ecosystems. Soil Biol. Biochem. 75, 11–25.

López-Mondéjar, R., Zühlke, D., Becher, D., Riedel, K., Baldrian, P., 2016. Cellulose and hemicellulose decomposition by forest soil bacteria proceeds by the action of structurally variable enzymatic systems. Sci. Rep. 6, 25279.

Makoi, J.H.R., Ndakidemi, P.A., 2008. Selected soil enzymes: examples of their potential roles in the ecosystem. Afr. J. Biotechnol. 7, 181–191.

Meier, C. L., Rapp, J., Bowers, R. M., Silman, M., Fierer, N., 2010. Fungal growth on a common wood substrate across a tropical elevation gradient: temperature sensitivity, community composition, and potential for aboveground decomposition. Soil Biol. Biochem.42, 1083–1090.

Merrill, W., Cowling, E.B., 1966. Role of nitrogen in wood deterioration. IV. Relationship of natural variation in nitrogen content of wood to its susceptibility to decay. Phytopathology 56, 1324–1325.

Nannipieri, P., Ascher, J., Ceccherini, M.T., Landi, L., Pietramellara, G., Renella, G., 2003. Microbial diversity and soil functions. Eur. J. Soil Sci. 54, 655–670.

Pan, Y., Birdsey, R.A., Fang, J., Houghton, R., Kauppi, P.E., Kurz, W.A., Phillips, O.L., Shvidenko, A., Lewis, S.L., Canadell, J.G., Ciais, P., Jackson, R.B., Pacala,

S.W., McGuire, A.D., Piao, S., Rautiainen, A., Sitch, S., Hayes, D., 2011. A large and persistent carbon sink in the world's forests. Science 333, 988–993.

Petrillo, M., Cherubini, P., Sartori, G., Abiven, S., Ascher, J., Bertoldi, D., Camin, F., Barbero, A., Larcher, R., Egli, M., 2015. Decomposition of Norway spruce and European larch coarse woody debris (CWD) in relation to different elevation and exposure in an Alpine setting. iForest 9, 154–164.

Petrillo, M., Cherubini, P., Fravolini, G., Marchetti, M., Ascher-Jenull, J., Schärer, M., Synal, H.A., Bertoldi, D., Camin, F., Larcher, R., Egli, M., 2016. Time since death and decay rate constants of Norway spruce and European larch deadwood in subalpine forests determined using dendrochronology and radiocarbon dating. Biogeosciences 13, 1537–1552.

Prévost-Bouré, N.C., Christen, R., Dequiedt, S., Mougel, C., Lelièvre, M., Jolivet, C., Shahbazkia, H.R., Guillou, L., Arrouays, D., Ranjard, L., 2011. Validation and application of a PCR primer set to quantify fungal communities in the soil environment by real-time PCR. PLoS One 6, e24166.

Rajala, T., Peltoniemi, M., Pennanen, T., Mäkipää, R., 2012. Fungal community dynamics in relation to susbstrate quality of decaying Norway spruce (*Picea abies* [L.] Karst.) logs in boreal forests. FEMS Microbiol. Ecol. 81, 494–505.

Risch, A.C., Jurgensen, M.F., Page-Dumroese, D., Schütz, M., 2013. Initial turnover rates of two standard wood substrates following land-use change in subalpine ecosystems in the Swiss Alps. Can. J. For. Res. 43, 901–910.

Qin, H.L., Yuan, H.Z., Zhang, H., Zhu, Y.J., Yin, C.M., Tan, Z.J., Wu, J.S., Wei, W.X., 2013. Ammonia-oxidizing archaea are more important than ammonia-oxidizing bacteria in nitrification and NO_3-N loss in acidic soil of sloped land. Biol. Fert. Soils 49, 767–776.

Rotthauwe, J.H., Witzel, K.P., Liesack, W., 1997. The ammonia monooxygenase structural gene *amo*A as a functional marker: molecular fine-scale analysis of natural ammonia-oxidizing populations. Appl. Environ. Microbiol. 63, 4704–4712.

Salazar, S., Sánchez, L.E., Alvarez, J., Valverde, A., Galindo, P., Igual, J.M., Peix, A., Santa-Regina, I., 2011. Correlation among soil enzyme activities under different forest ecosystem management practices. Ecol. Eng. 37, 1123–1131.

Sboarina, C., Cescatti, A., 2004. Il clima del Trentino – distribuzione spaziale delle principali variabili climatiche [The climate of Trentino – spatial distribution of the principal climatic variables]. Report 33. Centro di Ecologia Alpina Monte Bondone, Trento, Italy, p. 20.

Spears, J.D.H., Lajtha, K., 2004. The imprint of coarse woody debris on soil chemistry in the Oregon Cascades. Biogeochemistry 71, 163–75.

Stempfhuber, B., Engel, M., Fischer, D., Neskovic-Prit, G., Wubet, T., Schöning, I., Gubry-Rangin, C., Kublik, S., Schloter-Hai, B., Rattei, T., Welzl, G., Nicol, G.W., Schrumpf, M., Buscot, F., Prosser, J.I., Schloter, M., 2014. pH as a driver for ammonia-oxidizing archaea in forest soils. Microb Ecol. 69, 879–883.

Strukelj, M., Brais, S., Quideau, S.A., Angers, V.A., Kebli, H., Drapeau, P., Oh, S.-W., 2013. Chemical transformations in downed logs and snags of mixed boreal species during decomposition. Can. J. For. Res. 43, 785–798.

Štursová, M., Baldrian, P., 2011. Effects of soil properties and management on the activity of soil organic matter transforming enzymes and the quantification of soil-bound and free activity. Plant Soil, 338, 99–110.

Szukics, U., Hackla, E., Zechmeister-Boltenstern, S., Sessitsch, A., 2012. Rapid and dissimilar response of ammonia oxidizing archaea and bacteria to nitrogen and water amendment in two temperate forest soils. Microbiol. Res. 67, 103–109.

Töwe, S., Albert, A., Kleineidam, K., Brankatschk, R., Dümig, A., Welzl, G., Munch, J.C., Zeyer, J., Schloter, M., 2010. Abundance of microbes involved in nitrogen transformation in the rhizosphere of *Leucanthemopsis alpina* (L.) heavy wood grown in soils from different sites of the Damma glacier forefield. Microb. Ecol. 60, 762–770.

Valentín, L., Rajala, T., Peltoniemi, M., Heinonsalo, J., Pennanen, T., Mäkipää, R., 2014. Loss of diversity in wood-inhabiting fungal communities affects

decomposition activity in Norway spruce wood. Front Microbiol. 5, 230. doi:10.3389/fmicb.2014.00230.

Van der Wal, A., de Boer, W., Smant, W., van Veen, J.A., 2007. Initial decay of woody fragments in soil is influenced by size, vertical position, nitrogen availability and soil origin. Plant Soil 301, 189–201.

Zhou, L., Dai, L., Gu, H., Zhong, L., 2007. Review on the decomposition and influence factors of coarse woody debris in forest ecosystem. J. For. Res. 18, 48–54.

VI. Paper 5

Chemical and microbiological changes in Norway spruce deadwood during the early stage of decomposition as a function of exposure in an Alpine setting

(photo by T. Bardelli)

Chemical and microbiological changes in Norway spruce deadwood during the early stage of decomposition as a function of exposure in an Alpine setting

Tommaso Bardelli[a,b,*], María Gómez-Brandón[b,c], Flavio Fornasier[d], Paola Arfaioli[a], Markus Egli[e], Giacomo Pietramellara[a], Maria Teresa Ceccherini[a], Heribert Insam[b], Judith Ascher-Jenull[a,b]

[a]Department of Agrifood and Environmental Science, University of Florence, Piazzale delle Cascine 18, 50144 Florence, Italy

[b]Institute of Microbiology, University of Innsbruck, Technikerstraβe 25d, A-6020 Innsbruck, Austria

[c]Departamento de Ecología y Biología Animal, Universidad de Vigo, Vigo 36310, Spain

[d]Consiglio per la Ricerca e la Sperimentazione in Agricoltura, Centro di Ricerca per lo Studio delle Relazioni tra Pianta e Suolo (C.R.A.-R.P.S.), Via Trieste 23, I- 34170 Gorizia, Italy

[e]Department of Geography, University of Zürich, Winterthurerstrasse 190, 8057 Zürich, Switzerland

*Corresponding autor: tommaso.bardelli@unifi.it;
Tommaso.Bardelli@student.uibk.ac.at

Manuscript under revision in **Arctic, Antarctic, and Alpine Research** since 11th December 2017

Contribution: T. Bardelli participated in the sampling campaign, in the experimental work including the statistical analyses, and in drafting the manuscript.

Abstract

Alpine ecosystems are vulnerable to ever changing environmental conditions, leading to shifts in vegetation distribution and composition with implications on soil functionality and carbon (C) turnover. Although deadwood represents an important global C stock, scarce information is available on how slope exposure influences the wood-inhabiting microbiota over the decomposition process in an alpine setting. We therefore evaluated the impact of slope exposure (north- *vs.* south-facing sites) on physico-chemical and microbiological properties (microbial abundance based on real-time PCR: fungal 18S rRNA, dinitrogen reductase (*nif*H); microbial biomass: double strand DNA; and microbial activity: hydrolytic enzyme activities of the main nutrient cycles) of *Picea abies* wood blocks and the underlying soil in a field experiment in the Italian Alps over a 3-year period. Overall, a higher abundance of fungi and nitrogen-fixing bacteria was recorded in the soil at the north-facing site where cooler and moister conditions were observed. In contrast, no exposure-effects were found for these two microbial groups in the wood blocks, while their abundance increased over time, accompanied by more acidic conditions with progressing wood decay. The impact of exposure was also enzyme-specific and time-dependent for both the *P.abies* wood blocks and the underlying soil.

Keywords: Wood decay, Enzyme activities, Fungal abundance, Nitrogen-fixing bacteria, Topsoil layer

Highlights

- Exposure effects on wood microbiota in the Alpine setting are poorly understood.
- Wood fungal and *nif*H gene abundances increased during the decay process.
- Soil fungal and *nif*H gene abundances were higher at the cooler north-facing site.
- Slope exposure effect was enzyme-specific and dependent on the decay stage.
- Wood-pH is the most important driving factor during the early decay stages.

1. Introduction

Mountain alpine ecosystems have gained increasing attention over the past years because they are particularly sensitive to changing climatic conditions (Egli et al., 2006, 2009). Indeed, an increase of about 2 °C has been recorded in the annual minimum temperature in the European Alps during the 20th century (Beniston et al., 1997). As a consequence, previous studies have reported the occurrence of an upward migration of tree and shrub species in alpine environments owing to rising temperatures (Motta and Nola, 2001; Dullinger et al., 2003). Furthermore, changes in land-use and management also constitute a dominant factor affecting soil biodiversity in Alpine ecosystems (Meyer et al., 2013). Altogether this can ultimately entail changes in the quality and quantity of soil organic matter (SOM), as well as in the vegetation composition and/or activities of soil organisms (Myers et al., 2001; Djukic et al., 2010; Siles et al., 2017), with implications for both carbon (C) dynamics and soil functionality (Theurillat and Guisan, 2001; Allison et al., 2010; A'Bear et al., 2014).

Among the organic C reservoirs, deadwood represents a global C-store estimated to be in the range of 73 ± 6 Pg (Pan et al., 2011). This is mainly due to its high lignin content resulting in a slow C turnover rate making its decomposition dynamics determinant for the soil C balance (Floudas et al., 2012; Moroni et al., 2015). As woody material decays, its physico-chemical properties gradually change over time, which can lead to a succession of microbial communities in wood according to their biochemical requirements and nutrient availability (Rajala et al., 2012). Fungi (brown rot-, soft rot-, and white rot-) are considered the main wood decomposers, having different wood-degradation strategies. In particular, white-rot fungi are capable to degrade all components of the wood cell wall (including lignin) by secreting a plethora of extracellular lignocellulolytic enzymes (van der Wal et al., 2007; Kielak et al., 2016). There exists also evidence of complex fungal-bacterial interactions, both positive and negative, within the deadwood environment as reviewed by Johnston et al. (2016), even though, the identity and ecology of bacterial communities in decomposing wood remained underexplored compared to fungi. For instance, one assumes that fungi might be able to meet the nitrogen requirements for their vegetative and generative growth through the associations with nitrogen-fixing bacteria. Accordingly, Hoppe et al. (2014) found positive correlations between fungal sporocarps and the richness of *nif*H (dinitrogen reductase) genes in deadwood logs from *Fagus sylvatica* and *Picea abies*. This is also in line with recent findings from Gómez-Brandón et al. (2017) who observed that fungal abundance (qPCR-based) was strongly correlated with *nif*H abundance in *P. abies* coarse woody debris at different stages of natural decay.

Several factors were found to act as drivers for the changes in wood-inhabiting microbiota such as the soil type (Sun et al., 2013), wood physico-chemical properties, particularly density, pH, moisture content, total lignin and cellulose (Purahong et al., 2014; Hoppe et al., 2016). The wood decay

stage, with an increase in fungal and bacterial abundance as wood decomposes (Gómez-Brandón et al., 2017) and the host tree species (Hoppe et al., 2016) are also of importance. In addition, topographic features, particularly the slope exposure, may influence the deadwood decay dynamics in subalpine environments (Petrillo et al., 2015; Fravolini et al., 2016). However, there is still a paucity of information about how slope exposure and climate, in general, affect deadwood inhabiting microbiota in alpine environments (Gómez-Brandón et al., 2017).

Therefore, we performed a field mesocosm experiment with equally sized wood blocks of *Picea abies* to evaluate the effect of exposure (north- *vs.* south-facing slope) on the abundance of nitrogen-fixing bacteria (*nif*H gene) and fungi assessed by real-time PCR. In addition, several potential enzymatic activities that are involved in the main nutrient cycles were determined during the early stage of decomposition (0 – 156 weeks) of deadwood in an alpine setting. Furthermore, we assessed which physico-chemical parameters were the most important drivers shaping the microbial communities in wood and in the underlying soil.

We hypothesised that: 1) the microbial biomass and activity will be more favoured at the south- than at the north-facing slope during *P. abies* wood decomposition in a high alpine setting and that such exposure-effects will be time-dependent; 2) the changes in fungal and *nif*H gene abundances as a function of exposure will be more evident at the end of the monitoring owing to an increased nutrient availability as woody decay progresses.

2. Material and Methods

2.1. Experimental set-up

Two study sites were selected at an altitude of 2400 m above sea level (a.s.l.) in Val di Rabbi (Trentino, Italy) on a north- (N_5) and south-facing (S_{10})

slope, respectively. We selected natural grasslands close to the border of the potential tree line in order to minimise the influence of human activities and the grazing by livestock, and to assess how such sites might be affected by the input of wood as trees advance in elevation. Both alpine sites belong to an already well-known climosequence (Egli et al., 2006; Fravolini et al., 2016; Bardelli et al., 2017) and they were located in catchments with acidic paragneiss (Bardelli et al., 2017). The soils were classified as Podzol (north-facing site) and Cambisols (south-facing site; Egli et al., 2006), and are sandy to silty (N_5: sand 53%, silt 28%, clay 19%; S_{10}: sand 51%, silt 27%, clay 21%) according to Bardelli et al. (2017). Mean annual precipitation is around 1300 mm, mean annual air temperature about -1.0 °C (Sboarina and Cescatti, 2004) and mean annual soil temperature ranges from 2.2 °C to 4.5 °C (Egli et al., 2016) at north- and south-exposure, respectively.

A field experiment using open mesocosms was set up at both study sites with the purpose of monitoring the early stage of *P. abies* (L.) Karst deadwood decomposition as a function of slope exposure and time in i) wood blocks and ii) the topsoil layer (0–5 cm) that is in intimate contact with the wood blocks. Mesocosms (PVC tubes, 10.2 cm and 25.0 cm diameter and height, respectively) were installed into the natural soil in summer 2012, prior to the addition of the wood blocks of *P. abies* at a distance of > 0.5 m from the adjacent mesocosms, leaving at the surface a border of about 1 cm. From the mesocosm set-up (August 2012) to the placement of the wood blocks (June 2013) one year passed in order to permit normal conditions to be restored and as such, the decay monitoring study would be performed under undisturbed conditions. Considering that the size and geometry of deadwood may have a strong influence on the decay processes (Van der Wal et al., 2007), equal-sized (5 cm × 5 cm × 2 cm) wood blocks of *P. abies* were directly placed on the soil surface, in each of the mesocosm tubes. Three replicate mesocosms for each time point

were installed in each of the study sites. The wood blocks and the topsoil layer (0–5 cm) were collected (using lab-gloves) in July 2014 (t1; 52 weeks), in July 2015 (t2; 104 weeks) and in July 2016 (t3; 156 weeks); resulting in a total of 18 samples for each substrate (= 2 sites × 3 times × 3 replicates), with three wood blocks kept as controls (t0). Prior to the placement of the wood blocks into the mesocosms, five soil sub-samples (t0) were collected in the surrounding area of the mesocosm. All samples were kept in cooling boxes and transported to the laboratory. The soil samples were sieved (< 2 mm), the wood blocks were air-dried at room temperature, cut-milled (4 mm; Retsch mill) and aliquoted into 50-ml sterile conical centrifuge tubes. The samples were then stored at 4 °C and -20 °C for physico-chemical and (micro)biological analyses, respectively.

2.2. Wood and soil physico-chemical analyses

The fresh and dry weight of the wood blocks were determined to assess the wood mass loss as a function of progressing decay as described in Fravolini et al. (2016) and Petrillo et al. (2016). Wood (1 g fresh weight, fw) and soil (5 g, fw) samples were oven-dried (105 °C) for 24 h to determine their dry weight. The volatile solid (VS) concentration was determined from the weight loss following ignition in a muffle furnace (Carbolite, CWF 1000) at 550 °C for 5 h. Total C and nitrogen contents of the oven-dried samples were analysed using a CN analyser (TruSpec CHN; LECO, Michigan, U.S.A.). Electrical conductivity (EC) and pH were determined in water extracts (1:10 and 1:20, w/v for soil and wood, respectively) using a conductivity Meter LF 330 (WTW,Weilheim, Germany) and a pH meter Metrohm 744, respectively. Inorganic nitrogen (NH_4^+, NO_3^-) was measured in 0.0125 M $CaCl_2$ soil extracts (Kandeler, 1993 a,b). Both the total and available P contents in soil samples were determined according to the ascorbic acid method (Kuo, 1996).

2.3. Potential enzyme activities

A heteromolecular exchange procedure by using a 4% solution of lysozyme as desorbant and a bead-beating agent (Fornasier and Margon, 2007) was performed to assess the following hydrolases in wood (0.1 g, fw) and soil (0.2 g, fw) samples: i) C-cycle: β-glucosidase (*gluc*), xylosidase (*xylo*), cellulase (*cell*); ii) N-cycle: chitinase (*chit*), leucine-aminopeptidase (*leu*); iii) P-cycle: alkaline and acid phosphomonoesterases (*alkP* and *acP*). In order to perform the enzymatic multiple assay for wood extracts, some modifications were required as described by Gómez-Brandón et al. (2017). All measurements were performed in duplicate for each field replicate, and the activities were expressed as nanomoles of 4-methyl-umbelliferyl (MUF) min^{-1} g^{-1} dry (wood/soil).

2.4. Molecular analyses

2.4.1. Wood and soil microbial biomass index (dsDNA)

Direct extraction of total wood (0.1 g, fw) and soil (0.2 g, fw) DNA followed by PicoGreen-based quantification of crude (not purified) double stranded DNA (dsDNA) was performed to estimate wood and soil microbial biomass (Fornasier et al., 2014). Some modifications were required to determine the dsDNA content in wood as described in Gómez-Brandón et al. (2017).

2.4.2. DNA extraction

The whole community DNA was extracted from wood (0.1 g, fw) and soil samples (0.2 g, fw) and purified by using a commercial kit (FastDNA Kit for Soil, MP-Biomedicals) as described in Ascher et al. (2009) for further downstream analyses. For wood samples, one ceramic sphere (Lysing Matrix E, MP, Biomedicals) was added to the lysing tubes, so as to guarantee for an

accurate cell disruption of the woody tissue. DNA extracts were qualitatively and quantitatively characterised as described in Bardelli et al. (2017).

2.4.3. Quantitative real-time PCR

Quantitative real-time PCR (qPCR) was performed to determine the 18S rRNA gene copy number of fungi, the abundance of the functional gene *nif*H in the wood and the soil samples. qPCR was carried out using a Rotorgene 6000 Real Time Thermal Cycler (Corbett Research, Sydney, Australia) in combination with the Rotorgene Series Software 1.7. To build the standard curves we used the purified PCR products of known concentrations of the following pure cultures as templates: *Fusarium solani* (DSMZ 10696) – fungi; *Azospirillum irakense* (DSMZ 11586) – *nif*H gene. The primer pairs were: FF390/FR1 (fungi; Prévost-Bouré et al., 2011); and nifHf/nifHr (*nif*H gene; Töwe et al., 2010). Stock concentration [gene copies μL^{-1}] was determined via PicoGreen measurement and freshly prepared for each run. Ten-fold dilutions ranging from 10^9 to 10^2 copies μL^{-1} were used for the standard curve construction. Quantitative PCR was performed in 20-µL volumes. Each reaction mix contained 1X Sensimix™ SYBR® Hi-rox (Bioline, USA), forward and reverse primers (200 nM each primer), 0.4 mg mL^{-1} BSA, distilled water (RNase/DNase free, Gibco™, UK) and 2 µL of either 1:10 diluted DNA-extract, and ten-fold diluted standard DNA. All the standards and samples were run in duplicate. After an initial denaturation at 95 °C for 10 min, thermal cycling comprised 40 cycles of 15 s at 95 °C, 30 s at 50 °C, 30 s at 72 °C for fungi; and 45 s at 95 ºC, 45 s at 55 ºC, 45 s at 72 ºC for *nif*H gene. To check for product specificity and potential primer dimer formation, runs were completed with a melting analysis starting from 65 °C to 95 °C with temperature increments of 0.25 °C (0.5 °C for *nif*H gene) and a transition rate of 5 s. The purity of the amplicons was checked by the presence of a single band of the expected

length on a 1% agarose gel stained with the DNA stain Midori Green (Nippon Genetics, Germany) and visualised by UV-transillumination (Vilber Lourmat Deutschland GmbH).

2.5. Statistical analyses

A factorial analysis of variance (ANOVA) was done to evaluate the effect of exposure (north *vs.* south exposure) and time (t0, t1, t2, t3) on wood and soil physico-chemical and microbiological parameters. Normality and variance homogeneity of the data were tested prior to ANOVA using the Shapiro-Wilks´ and Levene´s tests, respectively. Prior to analysis, data were log- or square root-transformed to meet the assumptions for ANOVA (when it was necessary). Significant differences ($p \leq 0.05$) were analysed by paired comparisons with the Tukey HSD test. A non-parametric test (Kruskal-Wallis test) was performed when the data did not meet the normality condition. Associations between the potential enzymatic activities and the main chemical and microbiological variables were explored by Pearson's correlation. These analyses were performed using Statistica 9 (StatSoft, USA). Non-metric multidimensional scaling (NMDS) based on Bray-Curtis distance was performed using R 3.1.2 (Open Source Software) to map the wood and soil physico-chemical parameters to the shifts in microbial biomass (dsDNA), microbial abundance (qPCR) and hydrolytic enzyme activities as a function of slope exposure and time. The lengths of the arrows indicate the direction of maximum correlation of the physico-chemical parameters and the significance level was assessed with a permutation test implemented in the envfit function of vegan library (Oksanen et al., 2008).

3. Results

An overview of the wood physico-chemical and (micro)biological parameters as a function of exposure (N- *vs.* S-facing slope) and time (0 –

156 weeks) is given in Tables 1 and 3 and those for the soil in Tables 2 and 3. The statistical results are shown in Table 4.

3.1. Wood physico-chemical parameters

Exposure had a significant impact on the wood moisture content, with higher values at the N- than at the S-facing slope (Tables 1 and 4). Moreover, a 7-fold increase in moisture levels was recorded after 52 weeks compared to the beginning of the experiment at both slopes, followed by a decrease until the end of the monitoring period (156 weeks). The wood VS concentration was not significantly influenced by the slope exposure, and neither exposure nor time significantly affected the wood mass (Tables 1 and 4). In addition, the lowest pH value was measured at the end of the monitoring (156 weeks) at both the N- and the S-facing slopes (Tables 1 and 4). The exposure-effect on EC of the wood was only evident after 156 weeks, with higher values (3 times higher) at the S- than at the N-facing slope. A significant decrease in EC was found after 52 weeks (3 – 5 times lower than at t0), followed by an increase until the end of the monitoring at both slopes (Tables 1 and 4). Exposure did not have a significant impact on the wood total C content (Tables 1 and 4). The nitrogen content in the wood blocks was below the detection limit irrespective of the exposure and time.

Table 1.

Physico-chemical properties of the wood samples collected in August 2013 (t0), July 2014 (t1; 52 weeks), July 2015 (t2; 104 weeks), and in July 2016 (t3; 156 weeks) in the in-field mesocosm experiment at north- and south-facing sites (N_5 and S_{10}, respectively) located at the same elevation (2400 m a.s.l.). Values are means (n=3) with standard deviations in brackets. Data are expressed on a dry weight (dw) basis.

Sites	Time	Moisture (%)	Volatile solids (%)	Wood mass (g)	pH	Electrical Conductivity (µS cm^{-1})	Total C (%)
	t0	8.2 (2.0)	99.2 (0.8)	22.5 (0.0)	5.5 (0.1)	51.7 (6.5)	49.0 (0.3)
N_5	t1	54.2 (2.8)	99.0 (0.5)	21.1 (1.1)	5.4 (0.1)	9.8 (1.4)	50.7 (1.3)
	t2	29.4 (7.9)	99.8 (0.2)	24.3 (2.0)	5.3 (0.1)	32.4 (8.7)	50.5 (1.0)
	t3	39.1 (17.1)	99.6 (0.2)	16.8 (6.2)	5.1 (0.1)	28.5 (6.9)	51.2 (0.9)
S_{10}	t1	56.1 (4.8)	99.0 (0.2)	23.1 (0.9)	5.2 (0.1)	19.1 (10.1)	55.0 (8.0)
	t2	21.1 (7.9)	99.9 (0.2)	19.2 (0.8)	5.1 (0.1)	29.4 (10.2)	51.3 (0.9)
	t3	17.6 (4.5)	99.5 (0.1)	20.4 (3.1)	4.9 (0.1)	77.3 (21.6)	50.4 (0.5)

3.2. Soil physico-chemical parameters

Soil moisture levels were significantly higher at the N- than at the S-facing slope, and the lowest values were found after 104 weeks at both slopes (Tables 2 and 4). The VS concentration was almost twice as high at the N- than at the S-facing site, whereas no significant changes were found over time (Tables 2 and 4).

Slope exposure had a significant impact on the soil pH after 52 weeks, with an average value of 5.0 at the N- and 5.5 at the S-facing site (Tables 2 and 4). A significant decrease in soil pH was recorded after 52 weeks at the N-facing slope, but it remained stable afterwards until the end of the monitoring. No significant differences in soil pH with time were observed at

the S-facing slope (Tables 2 and 4). The soil EC was at the S-facing site twice as high as at the N-facing site at the beginning and at the end of the monitoring (156 weeks); while no exposure-effects were found at the intermediate sampling times. Additionally, the highest EC value was recorded after 156 weeks at both slopes (Tables 2 and 4). In general, the N-facing slope showed higher total C and nitrogen contents compared to the S-facing one, regardless of the duration of the experiment (Tables 2 and 4). There was no a significant exposure-effect on the NH_4^+ and NO_3^- contents. Both parameters, however, significantly varied over time. Indeed, a very distinct increase in NH_4^+ was measured after 52 weeks at both slopes, followed by a continuous increase (2 times) at the end of the monitoring at the N-facing slope (Tables 2 and 4). Concerning the NO_3^- content, the lowest values were generally detected after 104 and 156 weeks at both N- and S-facing slopes (Tables 2 and 4). The total P content was neither influenced by slope exposure nor by time (Tables 2 and 4). Overall, higher available P levels were observed at the S- than at the N-facing slope irrespective of time, except for the last sampling point (no exposure-effect). Moreover, the highest available P levels were recorded after 104 weeks at both slopes, followed by a significant decrease after 156 weeks at the S-facing slope (Tables 2 and 4).

Table 2.

Physico-chemical properties of the soil samples collected in August 2013 (t0), July 2014 (t1; 52 weeks), July 2015 (t2; 104 weeks), and in July 2016 (t3; 156 weeks) in the in-field mesocosm experiment at north- and south-facing sites (N_5 and S_{10}, respectively) located at the same elevation (2400 m a.s.l.). Values are means (n=3) with the standard deviations in brackets. Data are expressed on a dry weight (dw) basis.

Sites	Time	Moisture (%)	Volatile solids (%)	pH	Electrical Conductivity (µS cm^{-1})	Total C (%)	Total N (%)	NH_4^+ (mg kg^{-1} dw)	NO_3^- (mg kg^{-1} dw)	Total P (mg kg^{-1} dw)	Available P (mg kg^{-1} dw)
N_5	t0	54.9 (0.4)	41.1 (1.0)	5.5 (0.1)	15.8 (0.8)	23.5 (1.4)	1.4 (0.1)	4.3 (0.6)	10.2 (3.1)	802.9 (346.3)	4.0 (0.8)
	t1	52.5 (4.0)	40.6 (8.1)	5.0 (0.2)	19.2 (4.1)	20.7 (3.7)	1.1 (0.2)	54.6 (8.0)	15.6 (2.3)	821.6 (552.1)	9.3 (3.1)
	t2	40.1 (6.7)	43.0 (5.1)	5.0 (0.1)	38.9 (4.2)	23.5 (2.0)	1.3 (0.1)	52.0 (15.6)	6.1 (1.9)	891.6 (111.9)	33.0 (7.0)
	t3	51.5 (4.3)	41.8 (7.5)	5.2 (0.01)	39.3 (14.1)	21.9 (5.2)	1.2 (0.3)	117.7 (55.1)	5.6 (2.2)	870.6 (319.6)	25.3 (14.1)
S_{10}	t0	37.5 (4.4)	22.7 (12.0)	5.3 (0.01)	29.4 (0.3)	17.0 (1.4)	1.0 (0.01)	3.3 (0.8)	14.9 (8.9)	931.9 (128.2)	21.3 (8.4)
	t1	49.1 (3.2)	33.0 (4.1)	5.5 (0.1)	26.9 (3.1)	16.3 (2.6)	1.1 (0.2)	97.2 (10.5)	10.4 (1.6)	611.2 (482.9)	46.1 (8.6)
	t2	30.2 (10.2)	26.2 (1.0)	5.3 (0.1)	37.7 (4.5)	13.5 (2.0)	0.9 (0.1)	62.4 (25.7)	6.0 (2.8)	722.9 (312.6)	61.6 (3.1)
	t3	35.4 (1.9)	26.1 (1.7)	5.3 (0.1)	60.5 (10.5)	12.0 (1.5)	0.8 (0.2)	84.3 (16.0)	9.1 (1.3)	450.8 (264.0)	30.0 (3.5)

3.3. Wood (micro)biological parameters

Wood microbial biomass assessed as double stranded DNA yield (dsDNA) was up to 3-times higher at the S- than at the N-facing slope irrespective of time (Tables 3 and 4). Moreover, a significant increase in the dsDNA content was found over time at both slopes (Table 3). Fungal and *nif*H gene abundances in wood were not significantly affected by the slope exposure; however, significant differences were recorded in both microbial groups over time (Tables 3 and 4). The highest *nif*H abundance was recorded after 104 and 156 weeks at the N- and the S-facing slope, respectively. A reduction in the fungal abundance was registered after 52 weeks at both slopes, followed by an increase after 104 weeks reaching similar values to those observed in the initial wood blocks (Table 3).

β-glucosidase, xylosidase and cellulase activities did not vary significantly in terms of exposure (Table 4); however, a sharp increase (around 16-times higher for β-glucosidase and 60-fold higher for xylosidase and cellulase activities) was observed after 104 weeks compared to the beginning of the experiment at both slopes (Figs. 1A–C). Afterwards, a decrease in these three enzyme activities was recorded after 156 weeks at the N-facing slope. The exposure-effect on the chitinase, leucine-aminopeptidase and alkaline phosphomonoesterase activities was time-dependent (Figs. 2A–C; Table 4). Higher activities (between 4- and 6-times higher) were recorded at the S- than at the N-facing slope after 104 and 156 weeks; while no exposure-effect was found after 52 weeks (Figs. 2A–C). Moreover, the highest activity of the three aforementioned enzymes was registered at the end of the monitoring at both slopes. Although the acid phosphomonoesterase activity was not significantly influenced by slope exposure (Table 4), a pronounced increase was found over time compared to the beginning of the monitoring (Fig. 2D).

3.4. Soil (micro)biological properties

Soil microbial biomass (dsDNA) was neither influenced by slope exposure nor by time (Tables 3 and 4). Nonetheless, slope exposure had a significant impact on soil fungal and *nif*H gene abundances (Table 4), being approximately 3-times higher at the N- than at the S-facing slope irrespective of the time (Table 3).

Overall, the β-glucosidase, xylosidase and cellulase activities were 2-times higher at the N- than at the S-facing slope after 104 weeks (Figs. 1D–F); whereas no exposure-effect was observed for the other sampling times, except for the xylosidase activity at the beginning of the monitoring (N>S; Fig. 1E). However, no significant differences over time were recorded for these enzyme activities (Figs. 1D–F; Table 4), except for the β-glucosidase at the S-facing site (52 > 104 weeks; 2-times higher). Chitinase activity significantly varied in terms of exposure only after 156 weeks (S>N; Fig. 2E, Table 4), while no significant differences were detected over time irrespective of the slope exposure (Table 4). The exposure-effect on the leucine-aminopeptidase and alkaline phosphomonoesterase activities was also time-dependent (Table 4). A higher activity was recorded at the S- than at the N-facing slope after 52 weeks; whereas the opposite trend (N>S) was found after 104 weeks (Fig. 2F & G). Furthermore, both enzymes showed higher activities at the last two sampling times (104 and 156 weeks) at the N-facing site; while a higher activity was recorded after 52 weeks at the S-facing one. Nevertheless, acid phosphomonoesterase activity was significantly higher at the N- than at the S-facing slope regardless of the sampling time (Fig. 2H; Table 4).

Table 3.

Microbiological properties of the wood and soil samples collected in August 2013 (t0), July 2014 (t1; 52 weeks), July 2015 (t2; 104 weeks), and in July 2016 (t3; 156 weeks) in the in-field mesocosm experiment at north- and south-facing sites (N_5 and S_{10}, respectively) located at the same elevation (2400 m a.s.l.). Values are means (n=3) with the standard deviations in brackets. Data are expressed on a dry weight (dw) basis.

	Sites	Time	Microbial biomass index (µg dsDNA g^{-1})	Fungi (gene copy number g^{-1})	*nif*H gene (gene copy number g^{-1})
WOOD		t0	1.4 (0.2)	3.12 x 10^9 (1.67 x 10^9)	8.77 x 10^6 (1.37 x 10^6)
	N_5	t1	9.0 (0.9)	1.66 x 10^9 (3.87 x 10^8)	1.46 x 10^7 (3.57 x 10^6)
		t2	10.5 (4.3)	3.20 x 10^9 (1.20 x 10^9)	3.75 x 10^7 (2.44 x 10^7)
		t3	11.6 (4.5)	3.83 x 10^8 (1.88 x 10^8)	2.32 x 10^7 (9.73 x 10^6)
	S_{10}	t1	12.6 (4.3)	9.24 x 10^8 (3.30 x 10^8)	1.51 x 10^7 (1.90 x 10^6)
		t2	30.0 (9.9)	2.98 x 10^9 (4.24 x 10^8)	2.61 x 10^7 (6.58 x 10^6)
		t3	26.5 (17.2)	2.26 x 10^9 (1.29 x 10^9)	4.06 x 10^7 (3.15 x 10^7)
SOIL	N_5	t0	120.7 (11.3)	1.96 x 10^9 (2.91 x 10^8)	1.47 x 10^8 (1.91 x 10^7)
		t1	124.2 (5.4)	1.06 x 10^9 (2.40 x 10^8)	1.74 x 10^8 (7.97 x 10^7)
		t2	128.4 (4.2)	1.88 x 10^9 (5.39 x 10^8)	1.10 x 10^8 (3.13 x 10^7)
		t3	140.1 (19.5)	1.45 x 10^9 (2.06 x 10^8)	1.74 x 10^8 (3.91 x 10^7)
	S_{10}	t0	127.3 (12.4)	4.38 x 10^8 (2.72 x 10^8)	3.57 x 10^7 (5.29 x 10^6)
		t1	128.1 (15.8)	5.83 x 10^8 (2.83 x 10^8)	3.90 x 10^7 (7.68 x 10^6)
		t2	102.1 (3.7)	5.99 x 10^8 (2.56 x 10^8)	5.69 x 10^7 (1.75 x 10^7)
		t3	123.7 (18.1)	5.47 x 10^8 (7.39 x 10^8)	5.04 x 10^7 (2.21 x 10^7)

Table 4.

Factorial ANOVA of the soil and wood physico-chemical and microbiological parameters as a function of slope exposure and time at the N- and S-facing sites (N_5 and S_{10}, respectively) located at the same elevation (2400 m a.s.l.).

	Exposure		Time		Exposure × Time	
SOIL	**F**	**p**	**F**	**p**	**F**	**p**
Moisture	30.34	***	9.60	***	2.31	ns
Volatile solids	32.67	***	0.63	ns	0.88	ns
pH	12.43	**	6.51	**	9.47	***
EC	20.38	***	23.59	***	3.27	*
Total C	46.17	***	1.40	ns	1.44	ns
Total N	17.71	***	1.87	ns	1.99	ns
NH_4^+	0.05	ns	41.68	***	3.12	ns
NO_3^-	0.32	ns	6.26	**	1.77	ns
Total P	1.41	ns	0.43	ns	0.64	ns
Available P	54.24	***	22.83	***	5.53	**
dsDNA	2.38	ns	1.76	ns	2.34	ns
Fungi	42.21	***	1.43	ns	1.99	ns
*nif*H	86.20	***	0.54	ns	1.95	ns
gluc	13.77	**	1.32	ns	8.28	**
xylo	15.34	**	0.11	ns	5.99	**
cell	3.45	ns	1.89	ns	7.18	**
chit	13.64	**	0.80	ns	5.72	**
leu	4.70	*	12.24	***	17.08	***
*ac*P	85.00	***	1.70	ns	4.71	*
*alk*P	0.04	ns	13.50	***	21.05	***
WOOD	F	p	F	p	F	p
Moisture	4.93	*	44.27	***	2.31	ns
Volatile solids	0.04	ns	12.16	**	na	na
Mass	0.01	ns	2.75	ns	na	na
pH	14.20	**	36.57	***	1.87	ns
EC	9.04	**	26.39	***	4.54	*
Total C	0.01	ns	9.60	*	na	na
dsDNA	12.13	**	21.49	***	2.64	ns
Fungi	0.27	ns	5.64	**	1.71	ns
*nif*H	0.13	ns	11.15	***	0.65	ns
gluc	2.30	ns	18.15	***	1.54	ns
xylo	1.09	ns	44.17	***	1.47	ns
cell	1.08	ns	19.92	***	0.42	ns
chit	12.96	**	45.92	***	9.60	***
leu	16.67	***	43.52	***	8.56	**
*ac*P	0.03	ns	19.75	***	0.82	ns
*alk*P	9.07	**	35.74	***	5.99	**

pH (pH H_2O), EC (Electrical conductivity), NH_4^+ (Ammonium content), NO_3^- (Nitrate content), dsDNA (double stranded DNA; soil and wood microbial biomass index), Fungi (18S rRNA gene copy number), *nifH* (Bacterial *nif*H gene copy number), *gluc* (β-glucosidase), *xylo* (xylosidase), *cell* (cellulase), *chit* (chitinase), *leu* (leucine-aminopeptidase), *ac*P (acid phosphomonoesterase), *alk*P (alkaline phosphomonoesterase).

na (not available); ns (not significant); * $p < 0.05$; ** $p < 0.01$; *** $p < 0.001$

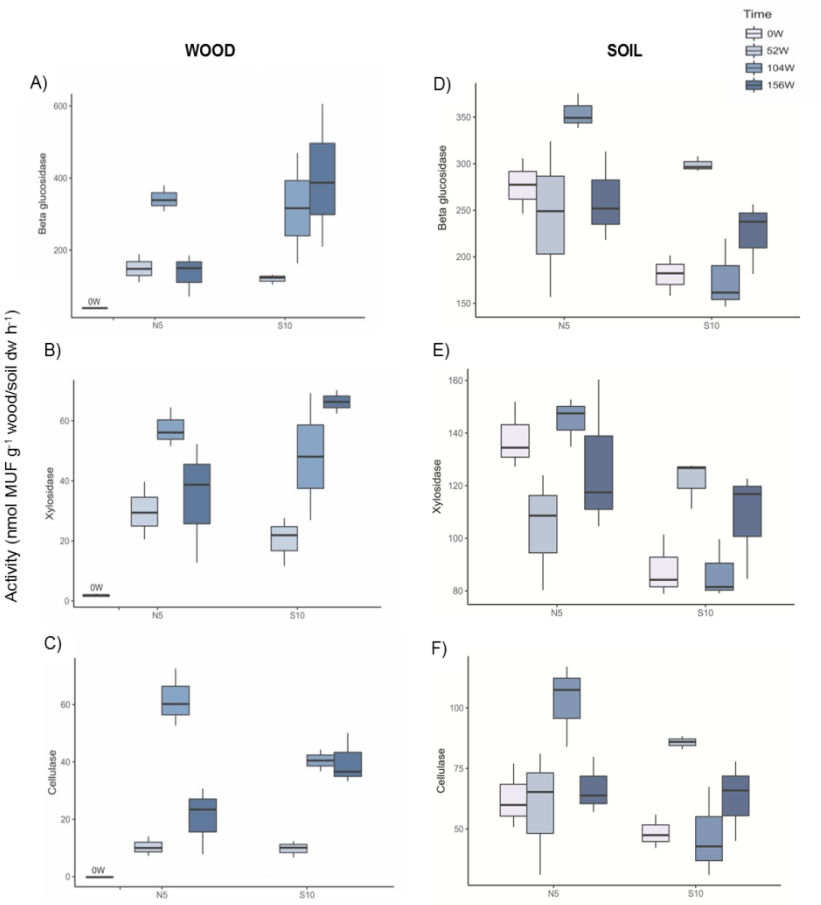

Fig. 1. Potential activities of β-glucosidase (A & D), xylosidase (B & E) and cellulase (C & F) of the wood and soil samples collected in August 2013 (0 weeks), July 2014 (52 weeks), July 2015 (104 weeks), and in July 2016 (156 weeks) at the north- and the south-facing sites (N_5 and S_{10}, respectively). Values are means (n = 3) with standard deviation.

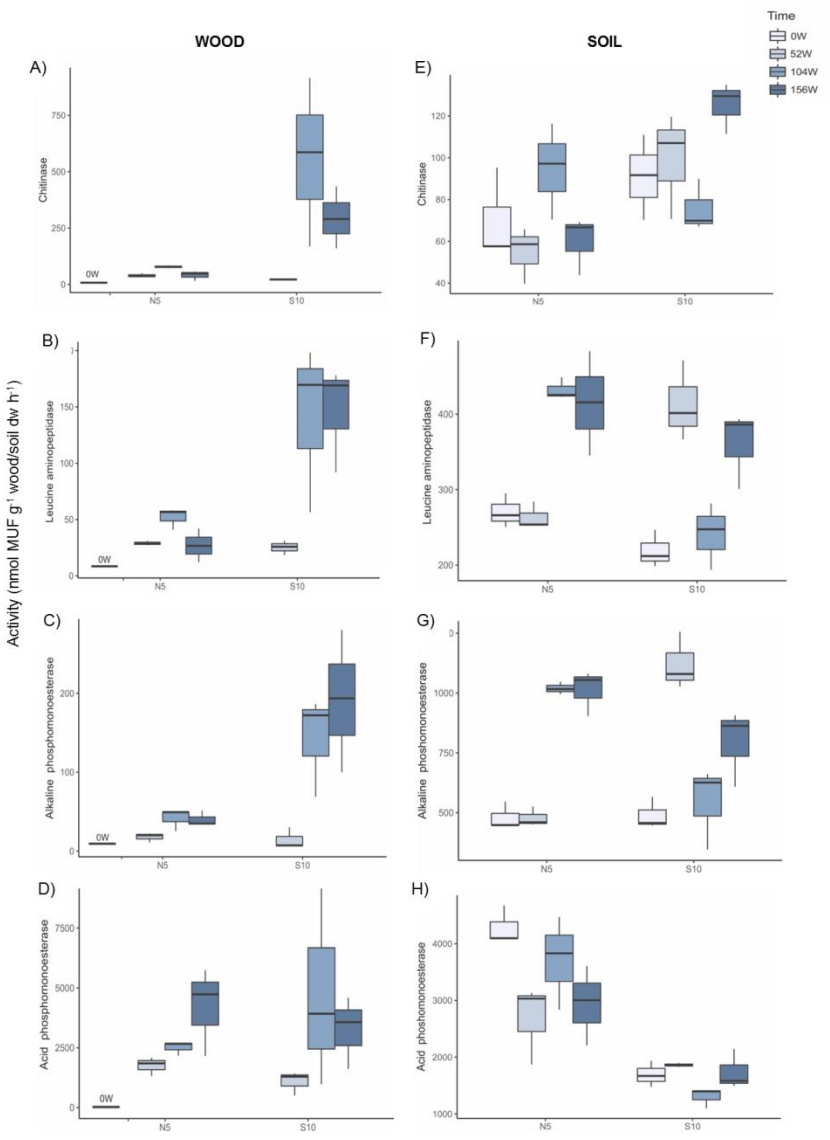

Fig. 2. Potential activities of chitinase (A & E), leucine aminopeptidase (B & F), alkaline phosphomonoesterase (C & G) and acid phosphomonoesterase (D & H) of the wood and soil samples collected in August 2013 (0 weeks), July 2014 (52 weeks), July 2015 (104 weeks), and in July 2016 (156 weeks) at the north- and the south-facing sites (N_5 and S_{10}, respectively). Values are means (n = 3) with standard deviation.

3.5. Non-metric multidimensional scaling (NMDS) analysis

Overall, the *P. abies* wood blocks collected at the beginning of the monitoring (t0) clustered in the negative side of the first ordination axis (Fig. 3A), indicating that they represent a specific microhabitat. All the other wood samples were located in the positive side of the first axis (Fig. 3A), being wood pH (R^2 = 0.45, $p \leq 0.01$) the major determinant for this differentiation. Additionally, along the second axis a separation as a function of exposure was mainly observed for the wood samples collected at the end of the monitoring (i.e., 156 weeks; t3). Wood moisture appeared to be the most determinant factor for this differentiation (R^2 = 0.31, p = 0.06). Furthermore, a clear separation in terms of slope exposure was recorded for the soil samples collected at the N- and the S-facing slopes (negative and positive sides, respectively) along the first ordination axis (Fig. 3B). The major physico-chemical parameters responsible for this differentiation were total C (R^2 = 0.51, $p \leq 0.001$), total nitrogen (R^2 = 0.40, $p \leq 0.01$) and available P (R^2 = 0.40, $p \leq 0.01$), followed by VS (R^2 = 0.38, $p \leq 0.05$) and soil moisture (R^2 = 0.35, $p \leq 0.05$).

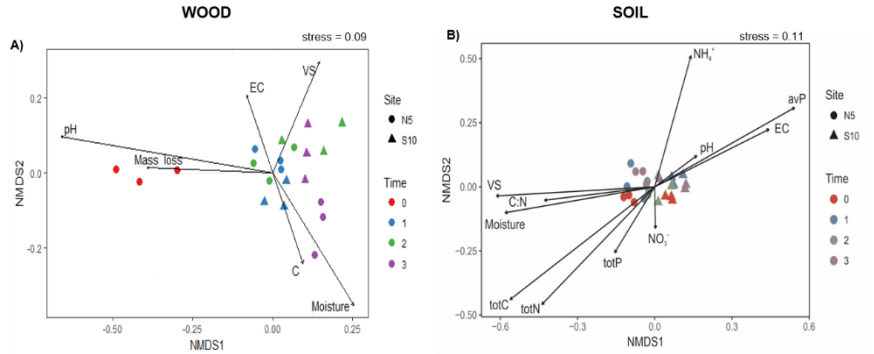

Fig. 3. Non-metric multidimensional scaling (NMDS) ordination was performed to map the physico-chemical parameters to the shifts in wood (A) and soil (B) microbiological properties (microbial abundances and enzyme activities) as a function of time (t0 = control, July 2014; t1 = after 52 weeks, July 2015; t2 = after 104 weeks, July 2016; t3 = after 156 weeks) and slope exposure (N-facing slope = point symbol; S-facing slope = triangle symbol).

4. Discussion

In line with previous studies performed in the Trentino area (Egli et al., 2006, 2009; Fravolini et al., 2016; Bardelli et al., 2017), the soils located at the N-facing slope were moister and richer in total C and nitrogen contents compared to those at the S-facing slope. Along a climosequence, Fravolini et al. (2016) observed faster decay rates of the *Picea abies* wood blocks at N- than at S-facing slopes up to an elevation of 1800 m a.s.l., probably due to the higher soil moisture and clay content along with a lower soil pH. These are favourable conditions especially for fungi which can better develop on N-facing sites. Nevertheless, we did not observe distinct changes in the *P. abies* wood blocks mass loss over the three-year observation period. In general, this fits well with findings of Fravolini et al (2016) and Petrillo et al. (2016) who measured very slow and sometimes almost barely measureable decay rates of Picea abies in alpine environments with wood mass decay rates often between 0.018 to 0.040 y^{-1}. These authors explained the low decay rates to be due to the climatic conditions and the extremely slow decomposition rate of lignin.

In this study, the higher moisture and OM levels recorded at the northern slope were accompanied by higher soil fungal and *nif*H gene abundances in comparison with the southern slope. Bardelli et al. (2017) did not observe an exposure-effect on soil fungal communities (qPCR-based) up to an altitude of 1800 m a.s.l. in the same study area. These discrepancies in terms of exposure might be related to the higher proportion of grassland and a colder climate registered at 2400 m a.s.l. compared to the other study sites surveyed by Bardelli et al. (2017). Indeed, complex interactions between local scale factors, such as soil properties and vegetation composition are known to largely affect soil microbial communities and their spatial distribution in

mountain environments (Ascher et al., 2012; Regan et al., 2017; Siles et al., 2017).

In contrast to soil, exposure did not have a significant impact on the two previously mentioned microbial groups (fungi and *nif*H) in the *Picea abies* wood blocks. This is in disagreement with our second hypothesis. However, a general increase in their microbial abundance was observed over time. This phenomenon could be ascribed to the release of nutrients with progressing wood decay, which provide a source of nutrients for new colonising microorganisms – microbial succession (Hoppe et al., 2015). Moreover, more acidic conditions (lower pH values) were detected in the *P. abies* wood blocks at the end of the monitoring that might lead to favourable conditions for the fungal growth and their activity. In accordance with Baldrian et al. (2016) and Gómez-Brandón et al. (2017), we also found that pH was one of the most influential driving factors shaping the wood microbial abundance and activity during the early stages of decomposition. Hoppe et al. (2015) reported, however, that variations in the abundances of bacterial phyla (using pyrosequencing analysis) are rather determined by a combination of several wood properties (i.e., C and nitrogen contents, wood moisture) than by single parameters such as pH alone.

Although previous studies pointed to an existing association between fungi and diazotrophic bacteria in wood (Hoppe et al., 2014; Johnston et al., 2016; Gómez-Brandón et al., 2017), we did not find a significant interaction between these two microbial groups in terms of abundance. This might be due to the fact that we focused on early stages of decomposition of Norway spruce deadwood. Indeed, Hoppe et al. (2014) found a stronger positive correlation between fungal fructification and *nif*H diversity during the intermediate stage of decay of *P. abies* and *Fagus sylvatica* logs. Another plausible explanation could be related to the moisture content, since it is

known to be one of the limiting factors of the biological nitrogen fixation (Rinne et al., 2017). In fact, a decrease in wood moisture level was found at the end of the monitoring in our study.

Furthermore, enzyme-specific exposure effects were observed for the *P. abies* wood blocks as previously shown by Gómez-Brandón et al. (2017). On the one hand, the C-related enzyme activities were not affected in terms of exposure, while, on the other hand, those activities involved in the N-cycle (leucine-aminopeptidase and chitinase) and P-cycle (alkaline phosphomonoesterase) showed higher activities at the southern slope. This thermal signal (S>N) was time-dependent (i.e., after 104 and 156 weeks), partially corroborating our first hypothesis. This is in line with the fact that the wood samples at the S-facing slope were characterised by a higher microbial biomass (based on dsDNA). Accordingly, the dsDNA yields were positively correlated with most of the previously mentioned enzymes (data not shown) at the end of the monitoring, probably due to more suitable conditions (i.e., higher nutrient availability) for microbial growth as wood decay progresses (Gonzalez-Polo et al., 2013; Petrillo et al., 2015, 2016; Pastorelli et al., 2017). In fact, the increase in fungal abundance after 104 weeks was also accompanied by an increase in the C-related enzyme activities in the *P. abies* wood blocks, suggesting the higher activity of the wood-inhabiting fungi at this stage of decay.

As occurred with wood the exposure-effect on soil enzyme activities related to C- and N-cycles was also time-dependent. Nonetheless, soil microbial biomass (dsDNA) did not vary in terms of exposure which is in agreement with Bardelli et al. (2017). These authors, however, found higher levels of microbial biomass on northern slopes by using the substrate-induced respiration approach. The different effect of exposure on soil microbial biomass could be interpreted in the light of the "method-result effect"

(Nannipieri et al., 2003). Furthermore, we observed a higher soil acid phosphomonoesterase activity at the northern slope over time probably due to the lower soil P availability at this slope than in the comparable S-facing one. Indeed, an increase in P acquiring enzyme activities is expected under conditions of soil P deficiency (Fraser et al., 2015).

5. Conclusion

Our field mesocosm experiment enabled us to observe how different thermal and moisture conditions (due to exposure effects) affected the wood and soil inhabiting microbiota in terms of their abundance and activity in the studied alpine setting. A higher abundance of fungi and nitrogen-fixing bacteria was recorded in the topsoil layer at the N-facing site characterised by cooler and moister conditions. In the *P. abies* wood blocks, however, the abundance of these two microbial groups did not respond to exposure while an increase in their abundance was observed with progressing wood decay along with more acidic conditions. This points wood pH as a crucial driving factor of the deadwood microbiota during the early decay stages. The impact of exposure was also enzyme-specific and time-dependent for both the *P. abies* wood blocks and the underlying soil. Altogether this indicates the importance of performing multiple methods approaches in order to avoid misinterpretation of nutrient cycles in Alpine ecosystems.

Acknowledgments

This research is part of the DecAlp D.A.CH. project (Project I989-B16). T. Bardelli has been funded by a PhD grant from the University of Florence (Italy). M. Gómez-Brandón and J. Ascher-Jenull have been funded by the Fonds zur Förderung der wissenschaftlichen Forschung (FWF) Austria (Project I989-B16). María Gómez-Brandón also acknowledges support by the Programa Ramón y Cajal (RYC-2016-21231; Ministerio de Economía y

Competitividad). We would like to thank Sabina Vrečko, Sebastian Waldhuber and Ljubica Begovic for their help in the laboratory. We acknowledge Paul Fraiz for his highly valuable help in language editing. We are also indebted to Dr. Fabio Angeli of the Ufficio distrettuale forestale – Malé (Trento, Italy) and his team for their support in the field.

References

A'Bear, A.D., Jones, T.H., Kandeler, E., Boddy, L., 2014: Interactive effects of temperature and soil moisture on fungal- mediated wood decomposition and extracellular enzyme activity. Soil Biology and Biochemistry, 70: 151–158.

Allison, S.D., Wallenstein, M.D., Bradford, M.A., 2010: Soil-carbon response to warming dependent on microbial physiology. Nature Geoscience, 3: 336–340.

Ascher, J., Ceccherini, M.T., Pantani, O.L., Agnelli, A., Borgogni, F., Guerri, G., Nannipieri, P., Pietramellara, G., 2009: Sequential extraction and genetic fingerprinting of a forest soil metagenome. Apply Soil Ecology, 42: 176–181.

Ascher, J., Sartori, G., Graefe, U., Thornton, B., Ceccherini, M.T., Pietramellara, G., Egli, M., 2012: Are humus forms, mesofauna and microflora in subalpine forest soils sensitive to thermal conditions? Biology and Fertility of Soils, 48: 709–725.

Baldrian, P., Zrustova, P., Tláskal, V., Davidova, A., Merhautová, V., Vrška, T., 2016: Fungi associated with decomposing deadwood in a natural beech-dominated forest. Fungal Ecology, 23: 109–122.

Bardelli, T., Gómez-Brandón, M., Ascher-Jenull, J., Fornasier, F., Arfaioli, P., Francioli, D., Egli, M., Sartori, G., Insam, H., Pietramellara, G., 2017: Effects of slope exposure on soil physico-chemical and microbiological properties along an altitudinal climosequence in the Italian Alps. Science of the Total Environment, 575: 1041–1055.

Beniston, M., Diaz, H.F., Bradley, R.S., 1997: Climatic change at high elevation sites: an overview. Climatic Change, 36: 233–251.

Djukic, I., Zehetner, F., Mentler, A., Gerzabek, M.H., 2010: Microbial community composition and activity in different Alpine vegetation zones. Soil Biology and Biochemistry, 42: 155–161.

Dullinger, S., Dirnböck, T., Grabherr, G., 2003: Patterns of shrub invasion into high mountain grasslands of the northern calcareous Alps, Austria. Arctic, Antarctic and Alpine Research, 35: 434–441.

Egli, M., Mirabella, A., Sartori, G., Zanelli, R., Bischof, S., 2006: Effect of north and south exposure on weathering rates and clay mineral formation in Alpine soils. Catena, 67: 155–174.

Egli, M., Sartori, G., Mirabella, A., Favilli, F., 2009: Effect of north and south exposure on organic matter in high Alpine soils. Geoderma, 149: 124–136.

Egli, M., Hafner, S., Derungs, C., Ascher-Jenull, J. Camin, F., Sartori, G., Raab, G., Paolini, M., Bontempo, L., Ziller, L., Bardelli, T., Petrillo, M., Abiven, S., 2016: Decomposition and stabilisation of Norway spruce needle-derived material in Alpine soils using a 13C-labelling approach in the field. Biogeochemistry, 13: 321-338.

Floudas, D., Binder, M., Riley, R., Barry, K., Blanchette, R.A., Henrissat, B., Martínez, A. T., Otillar, R., Spatafora, J.W., Yadav, J.S., et al., 2012: The Paleozoic origin of enzymatic lignin decomposition reconstructed from 31 fungal genomes. Science, 336: 1715–1719.

Fornasier, F., Margon, A., 2007: Bovine serum albumin and Triton X-100 greatly increase phosphomonoesterases and arylsulphatase extraction yield from soil. Soil Biology and Biochemistry, 39: 2682–2684.

Fornasier, F., Ascher, J., Ceccherini, M.T., Tomat, E., Pietramellara, G., 2014: A simplified rapid, low-cost and versatile DNA-based assessment of soil microbial biomass. Ecological Indicators, 45: 75–82.

Fraser, T. D., Lynch, D.H., Bent, E., Entz, M.H., Dunfield, K.E., 2015: Soil bacterial *phoD* gene abundance and expression in response to applied

phosphorus and long-term management. Soil Biology and Biochemistry, 88: 137–147.

Fravolini, G., Egli, M., Derungs, C., Cherubini, P., Ascher-Jenull, J., Gómez Brandón, M., Bardelli, T., Tognetti, R., Lombardi, F., Marchetti, M., 2016: Soil attributes and microclimate are important drivers of initial deadwood decay in sub-alpine Norway spruce forests. Science of the Total Environment, 569–570: 1064–1076.

Gómez-Brandón, M., Ascher-Jenull, J., Bardelli, T., Fornasier, F., Fravolini, G., Arfaioli, P., Ceccherini, M.T., Pietramellara, G., Lamorski, K., Sławiński, C., Bertoldi, D., Egli, M., Cherubini, P., Insam, H., 2017: Physico-chemical and microbiological evidence of exposure effects on *Picea abies* – Coarse woody debris at different stages of decay. Forest Ecology and Management, 391: 376–389.

Gonzalez-Polo, M., Fernandez-Souto, A., Austin, A.T., 2013: Coarse woody debris stimulates soil enzymatic activity and litter decomposition in an old-growth temperate forest of Patagonia, Argentina. Ecosystems, 16: 1025–1038.

Hoppe, B., Kahl, T., Karasch, P., Wubet, T., Bauhus, J., Buscot, F., Krüger, D., 2014: Network analysis reveals ecological links between N-fixing bacteria and wood-decaying fungi. PLoS ONE, e88141.

Hoppe, B., Krüger, D., Kahl, T., Arnstadt, T., Buscot, F., Bauhus, F., Wubet, T., 2015: A pyrosequencing insight into sprawling bacterial diversity and community dynamics in decaying deadwood logs of *Fagus sylvatica* and *Picea abies*. Scientific Reports, 5: 9456.

Hoppe, B., Purahong, W., Wubet, T., Kahl, T., Bauhus, J., Arnstadt, T., Hofrichter, M., Buscot, F., Krüger, D., 2016: Linking molecular deadwood-inhabiting fungal diversity and community dynamics to ecosystem functions and processes in Central European forests. Fungal Diversity, 77: 367–379.

Johnston, S.R., Boddy, L., Weightman, A.J., 2016: Bacteria in decomposing wood and their interactions with wood-decay fungi. FEMS Microbiolgy Ecology, 92: 1–12.

Kandeler, E., 1993a: Bestimmung von Ammonium. In Schinner, F., Öhlinger, R., Kandeler, E., Margesin, R. (eds.), Bodenbiologische Arbeitsmethoden. Springer, Berlin: Heidelberg, 366–368.

Kandeler, E., 1993b: Bestimmung von Nitrat. In Schinner, F., Öhlinger, R., Kandeler, E., Margesin, R. (eds.), Bodenbiologische Arbeitsmethoden. Springer, Berlin: Heidelberg, 369–371.

Kielak, A.M., Scheublin, T.R., Mendes, L.W., van Veen, J.A., Kuramae, E.E., 2016: Bacterial community succession in pine-wood decomposition. Frontiers in Microbiology, 7: 1–12, http://dx.doi.org/10.3389/fmicb.2016.00231.

Kuo, S., 1996: Phosphorus. In Sparks, D.L. (eds.), Methods of Soil Analysis. Part 3. Chemical Methods. SSSA Book Series, vol. 5. Soil Science Society of America Madison, WI, 869–919.

Moroni, M.T., Morris, D.M., Shaw, C., Stokland, J.N., Harmon, M.E., Fenton, N.J., Merganičová, K., Merganič, J., Okabe, K., Hagemann, U., 2015: Buried wood: a common yet poorly documented form of deadwood. Ecosystems, 18: 605–628.

Motta, R., Nola, P., 2001: Growth trends and dynamics in sub-alpine forest stands in the Varaita Valley (Piedmont, Italy) and their relationships with human activities and global change. Journal of Vegetation Science, 12: 219–230.

Myers, R.T., Zak, D.R., White, D.C., Peacock, A., 2001: Landscape-level patterns of microbial community composition and substrate use in upland forest ecosystems. Soil Science Society of American Journal, 65: 359–367.

Meyer, A., Focks, A., Radl, V., Keil, D., Welzl, G., Schöning, I., Boch, S., Marhan, S., Kandeler, E., Schloter, M., 2013: Different land use intensities in grassland ecosystems drive ecology of microbial communities involved in nitrogen turnover in soil. PLoS ONE, 8: e73536.

Nannipieri, P., Ascher, J., Ceccherini, M.T., Landi, L., Pietramellara, G., Renella, G., 2003: Microbial diversity and soil functions. European Journal of Soil Science, 54: 655–670.

Oksanen, J., Kindt, R., Legendre, P., Simpson, G., Sólymos, P., Stevens, M. H., et al., 2008: Vegan: Community ecology package - R package version 1.15–2. Available online at: http://cran.r-project.org, accessed 19 December 2013.

Pan, Y., Birdsey, R.A., Fang, J., Houghton, R., Kauppi, P.E., Kurz, W.A., Phillips, O.L., Shvidenko, A., Lewis, S.L., Canadell, J.G., Ciais, P., Jackson, R.B., Pacala, S.W., McGuire, A.D., Piao, S., Rautiainen, A., Sitch, S., Hayes, D., 2011: A large and persistent carbon sink in the world's forests. Science, 333: 988–993.

Pastorelli, R., Agnelli, A.E., De Meo, I., Graziani, A., Paletto, A., Lagomarsino, A., 2017: Analysis of Microbial Diversity and Greenhouse Gas Production of Decaying Pine Logs. Forests, 8: 224, doi:10.3390/f8070224.

Petrillo, M., Cherubini, P., Sartori, G., Abiven, S., Ascher, J., Bertoldi, D., Camin, F., Barbero, A., Larcher, R., Egli, M., 2015: Decomposition of Norway spruce and European larch coarse woody debris (CWD) in relation to different elevation and exposure in an Alpine setting. iForest, 9: 154–164.

Petrillo, M., Cherubini, P., Fravolini, G., Marchetti, M., Ascher-Jenull, J., Schärer, M., Synal, H.A., Bertoldi, D., Camin, F., Larcher, R., Egli, M., 2016: Time since death and decay rate constants of Norway spruce and European larch deadwood in subalpine forests determined using dendrochronology and radiocarbon dating. Biogeosciences, 13: 1537–1552.

Prévost-Bouré, N.C., Christen, R., Dequiedt, S., Mougel, C., Lelièvre, M., Jolivet, C., Shahbazkia, H.R., Guillou, L., Arrouays, D., Ranjard, L., 2011: Validation and application of a PCR primer set to quantify fungal communities in the soil environment by real-time PCR. PLoS One, 6: e24166.

Purahong, W., Hoppe, B., Kahl, T., Schloter, M., Schulze, E.D., Bauhus, J., Buscot, F., Krüger, D., 2014: Changes within a single land-use category alter microbial diversity and community structure: molecular evidence from wood-inhabiting

fungi in forest ecosystems. Journal of Environmental Management, 139: 109–119.

Rajala, T., Peltoniemi, M., Pennanen, T., Mäkipää, R., 2012: Fungal community dynamics in relation to susbstrate quality of decaying Norway spruce (*Picea abies* [L.] Karst.) logs in boreal forests. FEMS Microbiolgy Ecology, 81: 494–505.

Regan, K., Stempfhuber, B., Schloter, M., Rasche, F., Prati, D., Philippot, L., Boeddinghaus, R.S., Kandeler, E., Marhan, S., 2017: Spatial and temporal dynamics of nitrogen fixing, nitrifying and denitrifying microbes in an unfertilized grassland soil. Soil Biology and Biochemistry, 109: 214–226.

Rinne, K.T., Rajala, T., Peltoniemi, K., Chen, J., Smolander, A., Mäkipää, R., 2017: Accumulation rates and sources of external nitrogen in decaying wood in a Norway spruce dominated forest. Functional Ecology, 31: 530–541.

Sboarina, C., Cescatti, A., 2004: Il clima del Trentino – distribuzione spaziale delle principali variabili climatiche [The climate of Trentino – spatial distribution of the principal climatic variables]. Report 33. Centro di Ecologia Alpina Monte Bondone, Trento, Italy, p. 20.

Siles, J.A., Cajthaml, T., Filipová, A., Minerbi, S., Margesin, R., 2017: Altitudinal, seasonal and interannual shifts in microbial communities and chemical composition of soil organic matter in Alpine forest soils. Soil Biology and Biochemistry, 112: 1–13.

Sun, B., Wang, X.Y., Wang, F., Jiang, Y.J., Zhang, X.X., 2013: Assessing the relative effects of geographic location and soil type on microbial communities associated with straw decomposition. Applied and Environmental Microbiology, 79: 3327–3335.

Theurillat, J. P., Guisan, A., 2001: Potential impact of climate change on vegetation in the European Alps: A review. Climatic Change, 50: 77–109.

Töwe, S., Albert, A., Kleineidam, K., Brankatschk, R., Dümig, A., Welzl, G., Munch, J.C., Zeyer, J., Schloter, M., 2010: Abundance of microbes involved in nitrogen transformation in the rhizosphere of *Leucanthemopsis alpina* (L.) heavy

wood grown in soils from different sites of the Damma glacier forefield. Microbial Ecology, 60: 762–770.

Van der Wal, A., de Boer, W., Smant, W., van Veen, J.A., 2007: Initial decay of woody fragments in soil is influenced by size, vertical position, nitrogen availability and soil origin. Plant and Soil, 301: 189–201.

VII. Summary and conclusions

The present thesis is focusing on the impact of climate on soil features and deadwood decomposition dynamics as a function of different thermal conditions due to different slope exposure and altitude in (sub)alpine ecosystems in the Italian Alps. More specifically, *Chapter II* addresses the main changes in composition, activity and diversity of the autochthonous soil microbiota in terms of slope exposure along an altitudinal climosequence in combination with a comprehensive overview of the soil physico-chemical properties. In *Chapter III*, the influence of slope exposure was determined on both the autochthonous soil microbiota and mesofauna, with a special focus on the Enchytraeid community, under different soil ground covers in subalpine forest ecosystems. The main goal of *Chapter IV* was to evaluate the exposure-effects on the abundance and activity of the wood-inhabiting microbiota of *Picea abies* (L.) Karst coarse woody debris at different stages of natural decay. Finally, in the last part of this doctoral thesis (*Chapters V* and *VI*) the main focus was to determine the chemical and microbiological changes in both *P. abies* wood blocks and the underlying soil as a function of slope exposure and time using a field mesocosm experiment along the subalpine and alpine scenarios.

Climate effects on soil properties

The sensitivity of mountain ecosystems to environmental changes (e.g., temperature and precipitation patterns) permitted to evaluate the climate effects on soil properties with a particular emphasis on soil microbiological features. For this purpose, a climosequence approach comprising five pairs of north (N) - and south (S) -facing sites along an altitudinal gradient ranging from 1200 to 2400 m a.s.l., reflecting different climate zones, was set up within the framework of the present thesis. In agreement with previous studies carried out in the Trentino area (Egli et al., 2006, 2009; Ascher et al., 2012), the findings from *Chapter II* show that slope exposure

largely influenced both edaphic properties and soil microbiota in terms of abundance, activity and composition; even though such effects were altitude-dependent for some of the studied parameters. Overall, a higher content of organic matter (OM) was found at the N-facing slopes due to a lower solar irradiation and higher moisture levels in comparison with the drier conditions observed at the S-facing slopes. The cooler and moister conditions resulted in more strongly expressed weathering processes, increased clay mineral formation and consequently, in more acidic conditions at the N-facing slopes (Egli et al., 2006). Soil pH is considered one of the most important drivers of soil microbial communities (Lauber et al., 2009; Siles et al., 2017) and, in general, the bacterial growth is more favored under neutral or slightly alkaline conditions. As such, the S-facing sites were characterised by a higher bacterial abundance (qPCR-based) irrespective of the altitude, despite only small variations in soil pH were recorded between the two slopes. These exposure-effects were not detected for fungi along the studied altitudinal gradient, indicating that they were less sensitive than bacteria to the soil pH changes. Archaea were also considered within the scope of this thesis given the fact that they are known to be well adapted to the harsh environmental conditions of alpine environments (Xu et al., 2015). Although higher archaeal abundance was recorded at the N-facing slopes, these differences in terms of exposure varied depending on the altitude. All in all, this indicates that the three microbial domains respond differently to exposure in terms of abundance. Accordingly, enzyme type-specific reactions to slope exposure and altitude were observed under this scenario, underlining the importance of performing multiple enzyme assays in order to avoid misinterpretation of nutrient cycles (Nannipieri et al., 2012).

In *Chapter III* the discriminatory assessment of the extracellular (eDNA) and intracellular (iDNA) fractions of the total soil DNA pool (soil metagenome)

provided a new perspective on the exposure effects on soil autochthonous microbiota under different ground cover types representative of the studied area. The assessment of both DNA fractions enabled to obtain an index of soil microbial activity as well as information about the vertical distribution of eDNA through the soil layers (structural/functional flexibility; Ceccherini et al., 2007, 2009; Pietramellara et al., 2009). As expected, a higher eDNA/iDNA ratio, indicative of a lower microbial activity, was observed in the deepest topsoil layer (10–12.5 cm) but only under the grass cover at the N-facing slope. This might be related to a lower degradation of eDNA and/or to an accumulation of eDNA in deeper soil layers as a result of leaching (Ascher et al., 2009; Pietramellara et al., 2009). In fact, the eDNA in soil can migrate from the surface to the deeper soil layers (Agnelli et al., 2004) and its persistence and availability in soil is generally related to the properties of humic substances, soil aggregates and organo-mineral complexes. Furthermore, the DNA and in particular the eDNA fraction may act as a potential source of nutrients for soil micro-and mesobiota taking into account that DNA can be present in the gut of the mesofauna as part of the undigested soil and therefore be indirectly used to satisfy their nutrient demands (Poté et al., 2004; Egert et al., 2004). Indeed, a positive correlation between eDNA yields and the abundances of microannelids was found at this specific site-condition (grass plots at north exposure). Overall, microannelids appeared to be sensitive, accurate and reliable biological indicators in the forested subalpine soils, showing a higher abundance at the north-facing slope. There, strong acidity indicator species thrived, owing to the acidity with soil pH being 1 unit lower at this slope compared to the south-facing one. Exposure was therefore found to be more determinative for shaping the composition of microannelid assemblages than the ground cover type.

Climate effects on deadwood decomposition

Understanding the dynamics of deadwood decomposition is essential for understanding the functioning of forest ecosystems (Stokland et al., 2012). Topographic features, particularly the slope exposure, may affect the deadwood decay process as recently shown by Petrillo et al. (2015, 2016) and Fravolini et al. (2016) in the same study area. Nevertheless, to date there is still a gap of knowledge about how slope exposure and, in general, climate affect the wood-inhabiting microbiota in sub(alpine) environments. In this sense, the findings from *Chapter IV* showed higher abundances (qPCR-based) for all of the three microbial domains (bacteria, fungi and archaea) and selected microbial groups related to the nitrogen cycle (AOB and nitrogen fixers *nif*H) in the *Picea abies* wood samples collected at the N- than at the S-facing sites and regardless of the decay stage. Such exposure-effects (N>S) on microbial abundances were in general more expressed for the advanced decay stages, which is in line with the fact that certain nutrients (Ca, K and Mg) become more available to new colonizing microorganisms (Rajala et al., 2012; Hoppe, 2015) as wood decay progresses. Accordingly, a pronounced physical cell wood damage shown by the X-ray microtomography together with a higher microbial activity (lower eDNA/ iDNA ratio) was also more evident at the northern slope. As occurred in soil (*Chapter II*) the impact of exposure was also enzyme-specific for wood and strongly dependent on the decay stage. Moreover, in agreement with studies by Mukhin and Voronin (2007, 2009), methanogenic archaea (*Methanobacterium* and *Methanosaeta*) were detected in the latest wood decay stages suggesting that deadwood might act as a source of biogenic methane. Additionally, it was found that *nifH* and fungi were positively and strongly correlated in terms of abundance, which suggests the existence of complex fungal-bacterial interactions within deadwood, even though this needs to be further explored in future studies.

In the *Chapters V* and *VI* the physico-chemical and microbiological changes in both *P. abies* wood blocks and the underlying forest soil were investigated over time as a function of slope exposure. Although the observation period (2- and 3 years at the subalpine and alpine scenarios, respectively) was rather short, our field mesocosm experiment enabled to observe that different thermal and moisture conditions (due to exposure effects) seemed to affect the wood and soil-inhabiting microbiota (fungi and nitrogen-related bacterial functional genes (*nif*H and *amo*A)) in terms of their abundance and activity. In particular, at the subalpine sites (1200 – 2000 m a.s.l.), a clear exposure-effect (N>S) for the wood and soil microbial abundances (i.e., fungi and *nif*H) was in general recorded; whereas at the alpine sites (> 2000 m a.s.l.) exposure did not have a significant impact on the previously mentioned microbial groups in the *P. abies* wood blocks. However, a general increase in their abundance was observed with progressing wood decay along with more acidic conditions. Overall, wood pH seemed to be the most important driving factor shaping the wood microbial abundance and activity during the early decay stages of decomposition (Baldrian et al., 2016).

Outlook

Overall, the aim of this doctoral thesis was to broaden and deepen our knowledge about the impact of climate (due to differences in slope exposure and altitude) on soil features and deadwood decomposition processes in subalpine and alpine ecosystems. More specifically, it provided insights into the interrelation between soil micro- and mesofauna in this type of ecosystems, as well as into the changes in microbial communities during deadwood decomposition, thus contributing to unravel the complex picture of the forest ecosystem.

Future studies are needed to determine whether the findings from the present thesis can be extrapolated to similar Alpine environments. Furthermore, it would be advisable to further investigate the deadwood decay processes and the involved microbiota using longer-term field measurements. Moreover, as we studied only one type of wood, that is soft wood (*Picea abies*), further investigations comparing soft wood *vs.* hard wood such as *Larix decidua* (Mill.) could be a promising approach to assess distinctions with regard to wood tissue and tree species.

In addition, it would be of great importance to unravel the taxonomic identities of bacterial wood decomposers and their interactions with wood decaying fungi by using high-throughput sequencing technologies. This could offer a more comprehensive picture of the microbial diversity patterns and community composition during the deadwood decomposition processes.

A future challenge would also be to dig deeper into the potential interactions between microbial communities inhabiting wood and soil in (sub)alpine ecosystems, via tracing the wood-derived C into the soil organic matter fraction using ^{13}C isotope labelling as performed by Egli et al. (2016) in order to better understand the dynamics of C stabilization in soil.

References

Agnelli, A., Ascher, J., Corti, G., Ceccherini, M.T., Pietramellara, G., Nannipieri, P., 2007. Purification and isotopic signatures (δ13C, δ15N, Δ14C) of soil extracellular DNA. Biol. Fertil. Soils 44, 353–361.

Ascher, J., Ceccherini, M.T., Guerri, G., Pietramellara, G., 2009. "e-motion" of extracellular DNA (e-DNA) in soil. Fresen. Environ. Bull. 18, 1764–1767.

Ascher, J., Sartori, G., Graefe, U., Thornton, B., Ceccherini, M.T., Pietramellara, G., Egli, M., 2012. Are humus forms, mesofauna and microflora in subalpine forest soils sensitive to thermal conditions? Biol. Fertil. Soils 48, 709–725.

Baldrian, P., Zrustova, P., Tláskal, V., Davidova, A., Merhautová, V., Vrška, T., 2016. Fungi associated with decomposing deadwood in a natural beech-dominated forest. Fungal Ecol. 23, 109–122.

Ceccherini, M.T., Ascher, J., Pietramellara, G., Nannipieri, P., 2007. Vertical advection of extracellular DNA by water capillarity in soil columns. Soil Biol. Biochem. 39, 158–163.

Ceccherini, M.T., Ascher, J., Agnelli, A., Borgogni, F., Pantani, O.L., Pietramellara, G., 2009. Experimental discrimination and molecular characterization of the extracellular soil DNA fraction. Anton Leeuw. Int J. G. 96, 653–657.

Egert, M., Marhan, S., Wagner, B., Scheu, S., Friedrich, M. W., 2004. Molecular profiling of 16S rRNA genes reveals diet-related differences of microbial communities in soil, gut, and casts of *Lumbricus terrestris* L. (Oligochaeta: Lumbricidae). FEMS Microbiol. Ecol. 48, 187–197.

Egli, M., Mirabella, A., Sartori, G., Zanelli, R., Bischof, S., 2006. Effect of north and south exposure on weathering rates and clay mineral formation in Alpine soils. Catena 67, 155–174.

Egli, M., Sartori, G., Mirabella, A., Giaccai, D., Favilli, F., 2009. Effect of north and south exposure on organic matter in high Alpine soils. Geoderma 149, 124–136.

Egli, M., Hafner, S., Derungs, C., Ascher-Jenull, J. Camin, F., Sartori, G., Raab, G., Paolini, M., Bontempo, L., Ziller, L., Bardelli, T., Petrillo, M., Abiven, S., 2016. Decomposition and stabilisation of Norway spruce needle-derived material in Alpine soils using a 13C-labelling approach in the field. Biogeochemistry 13, 321–338.

Fravolini, G., Egli, M., Derungs, C., Cherubini, P., Ascher-Jenull, J., Gómez-Brandón, M., Bardelli, T., Tognetti, R., Lombardi, F., Marchetti, M., 2016. Soil attributes and microclimate are important drivers of initial deadwood decay in sub-alpine Norway spruce forests. Sci. Tot. Env. 569–570, 1064–1076.

Hoppe, B., Krüger, D., Kahl, T., Arnstadt, T., Buscot, F., Bauhus, F., Wubet, T., 2015. A pyrosequencing insight into sprawling bacterial diversity and community dynamics in decaying deadwood logs of *Fagus sylvatica* and *Picea abies*. Sci. Rep. 5, 9456. DOI 10.1038/srep09456

Lauber, C.L., Hamady, M., Knight, R., Fierer, N., 2009. Pyrosequencing-based assessment of soil pH as a predictor of soil bacterial community structure at the continental scale. Appl. Environ. Microbiol. 75, 5111–5120.

Mukhin, V.A., Voronin, P. Yu., 2007. Methane emission during wood fungal decomposition. Dokl. Biol. Sci. 413, 159–160.

Mukhin, V.A., Voronin, P. Yu., 2009. Methanogenic activity of woody debris. Russ. J. Ecol. 40, 149–153.

Nannipieri, P., Giagnoni, L., Renella, G., Puglisi, E., Ceccanti, B., Masciandaro, G., Fornasier, F., Moscatelli, M.C., Marinari, S., 2012. Soil enzymology: classical and molecular approaches. Biol. Fertil. Soils 48, 743–762.

Petrillo, M., Cherubini, P., Sartori, G., Abiven, S., Ascher, J., Bertoldi, D., Camin, F., Barbero, A., Larcher, R., Egli, M., 2015. Decomposition of Norway spruce and European larch coarse woody debris (CWD) in relation to different elevation and exposure in an Alpine setting. iForest 9, 154–164.

Petrillo, M., Cherubini, P., Fravolini, G., Marchetti, M., Ascher-Jenull, J., Schärer, M., Synal, H.A., Bertoldi, D., Camin, F., Larcher, R., Egli, M., 2016. Time since

death and decay rate constants of Norway spruce and European larch deadwood in subalpine forests determined using dendrochronology and radiocarbon dating. Biogeosciences 13, 1537–1552.

Pietramellara, G., Ascher, J., Borgogni, F., Ceccherini, M.T., Guerri, G., Nannipieri, P., 2009. Extracellular DNA in soil and sediment: fate and ecological relevance. Biol. Fertil. Soils 45, 219–235.

Potè, J., Ceccherini, M.T., Tran, V. V., Rosselli, W., Wildi, W., Simonet, P., Vogel, A.M., 2004. Fate and transport of antibiotic resistance genes in saturated soil columns. Eur. J. Soil. Biol. 39, 65–71.

Rajala, T., Peltoniemi, M., Pennanen, T., Mäkipää, R., 2012. Fungal community dynamics in relation to substrate quality of decaying Norway spruce (*Picea abies* [L.] Karst.) logs in boreal forests. FEMS Microbiol. Ecol. 81, 494–505.

Siles, J.A., Cajthaml, T., Filipová, A., Minerbi, S., Margesin, R., 2017. Altitudinal, seasonal and interannual shifts in microbial communities and chemical composition of soil organic matter in Alpine forest soils. Soil Biol. Biochem. 112, 1–13.

Stokland, J., Siitonen, J., Jonsson, B.G., 2012. Biodiversity in deadwood. Cambridge University Press, Cambridge, United Kingdom.

Xu, Z., Yu, G., Zhang, X., Ge, J., He, N., Wang, Q., Wang, D., 2015. The variations in soil microbial communities, enzyme activities and their relationships with soil organic matter decomposition along the northern slope of Changbai Mountain. Appl. Soil Ecol. 86, 19–29.

VIII. Acknowledgements

I would like to express my special appreciation to all people who contributed to this thesis, supporting me during this PhD journey. These three years doing my PhD have been one of the most intensive and interesting times in my life: from each person I met during this trip I learned a lot in Science and Life.

First of all, I owe my deepest gratitude to my Italian PhD advisor Univ. Prof. Giacomo Pietramellara for giving me the chance to achieve this scientific adventure and constantly providing me his advice and support along these years.

Likewise, I am deeply grateful to my Austrian PhD advisor Univ. Prof. Heribert Insam who gave me the opportunity to spend such a great and rewarding time in his working team. With his continuous optimism and enthusiasm concerning Science and Life work, Prof. Insam encouraged my research allowing me to grow as a Research Scientist as well as a human being.

I am also extremely grateful to my co-supervisor Dr. María Gómez Brandón who inspired me both personally and professionally: without her precious support, it would have been very hard for me to conduct my research. Muchas Gracias Turbina!

I want to thank Paul Fraiz for his highly valuable help in language editing and for all the happy moments we spent together.

I will be forever thankful to my other co-supervisor Dr. Judith Ascher-Jenull for teaching me and for her constant support. She is not only a great researcher but also a friendly and familiar figure to me. I will never forget the nice time we spent together "from the field to the lab" and in the other many occasions (lampredotto sandwiches, concerts, the Floating Piers, etc.). Thanks for showing me how to do my very best in Science and Life.

I would like to thank Dr. Paola Arfaioli for the great help in the laboratory and for the amazing moments we shared outside and for our laughers! During these years I learned so much from her attitude towards work and life.

I would like to express my gratitude to Dr. Flavio Fornasier for teaching me and analyzing my samples: his effort in the laboratory was essential to achieve my research.

I want to thank all the D.A.CH.–DecAlp members for the fantastic experience concerning the scientific aspects and personal encounters. At the beginning of my journey I did not expect to meet such a lovely, welcoming and cooperative group of people to work with. Scientists coming from different European countries and field areas but having a unique goal: Passion and Love for Science. I felt and still feel to be part of a big European Family!

Deep and sincere thanks goes to the DISPAA department and in particular to Univ. Prof. Paolo Nannipieri, Dr. Maria Teresa Ceccherini, Univ. Prof. Giancarlo Renella, Univ. Prof. Luca Calamai, Univ. Prof. Giacomo Certini, Dr. Luca Ottorino Pantani, Fabrizio Filindassi for the friendly atmosphere and all the help.

Thanks a lot to Marina Fernández-Delgado Juárez for your support, advice and help especially during the last part of my PhD. I will never forget our talks, laughers in the office and the nice adventures (up to the mountains, in Innsbruck and in Napoli cities). Muchas Gracias! Moreover, a big thanks goes to Franz Tscheikner-Gratl for the great moments we spent together.

Huge thanks goes to all the colleagues at the Institute of Microbiology. It was a great pleasure to work with each of you (Sabine Podmirseg, Magdalena Nagler, Andreas Walter, Sebastian Hupfauf, Sebastian

Waldhuber, Ljubica Begovic, Sonia Tiquia-Arashiro, Maraike Probst, Lidia Nicola, Thomas Klammsteiner, Thomas Mazzier, Deborah Schönegger, Pia Plattner, Anna Winkler, Tajda Bogataj, Ginevra Fabiani, Nadine Präg, Mira Mutschlechner, Andreas Wagner, Nematollah and Mohammad Etemadish). All of them are kind and real FRIENDS.

Further, I would like to thank Evelyn Burkia Stocker and Layzza Roberta Alves Medeiros for the hard work done during the Master thesis and their help within the laboratory analyses.

I wish warmly thank my Austrian family, Heri & Martina, who always made me feel at home.

I would like to thank all the friends who supported me during this experience, especially Giulia Fravolini, Sabina Vrečko, Alessia Bani, Wisarut Tukanghan, TiCha Manning, Katja Kozjek, Lena Nies, Carlos Barutti, Agnes Czingulszki, Shamina Pathan, Divya Baraniya. I want to thank also my PhD fellow travelers: Cristina Marzano, Luisa Leolini, Leonardo Verdi, Gianmarco Mugnai, Riccardo Moretti, Enrico Battiston.

I would like to thank the referees for carefully reading this thesis and taking the time to evaluate.

I will never be thankful enough to my family for all of the sacrifices they have made on my behalf in order to make me chase my dreams.

Finally, I would like to wish all the best to Laura Bardelli for her coming PhD adventure.

GRAZIE MILLE! VIELEN DANK! MUCHAS GRACIAS!

MANY THANKS!

IX. Curriculum Vitae

Tommaso Bardelli, Dott. Mag. (MSc.)

Work adresses:	Department of Agrifood Production and Environmental Science (DISPAA), University of Florence, Piazzale delle Cascine 28, 50144 Florence, Italy Institute für Mikrobiologie, Universität Innsbruck, Technikerstrasse 25, A-6020 Innsbruck, Austria
Email addresses:	tommaso.bardelli@unifi.it Tommaso.Bardelli@student.uibk.ac.at
Current Home address:	Viale Manfredo Fanti 221, 50137 Firenze, Italy
Date and Place of Birth:	2nd October 1987, Bagno a Ripoli (FI), Italy
Nationality:	Italian

Education and training

Since November 1st, 2014

PhD-Student in Joint Agreement (Co-Tutela) between Florence University (Agricultural and Environmental Sciences – XXX Cycle, supervisor: Prof. Giacomo Pietramellara) and Innsbruck University (Doctor of Philosophy Programme Biology (Microbiology), supervisor: Univ. Prof. Dr. Heribert Insam).

April 2014 – September 2011

Master's Degree in Agricultural Science and Technology at the University of Florence (Italy), 110/110 cum laude, after the discussion of the thesis entitled "Climosequence approach to monitor microclima effects (exposure, altitude) on physico-chemical and microbial properties of alpine soils (Trentino Alto Adige)"; supervisors: Prof. Giacomo Pietramellara, Dr. Judith Ascher-Jenull.

November – September 2009

Technical and professional training at the Plant Protection Institute-National Research Council (IPP-CNR), Sesto Fiorentino (FI), Italy; supervisor: Dr. Elena Paoletti.

March 2011 – September 2006

Bacherlor's Degree in Forest and Environmental Science at the University of Florence (Italy), 107/110, after the discussion of the thesis entitled "Effects of Cascine park vegetation on air quality in Florence"; supervisors: Prof. Paolo Grossoni, Dr. Elena Paoletti.

Peer-reviewed publications

- Paoletti, E., **Bardelli, T.**, Giovannini, G., Pecchioli, L. 2011. Air quality impact of an urban park over time. Procedia Environmental Sciences 4:10-16.
- Hoshika, Y., Pecori, F., Conese, I., **Bardelli T.**, Marchi, E., Manning, W.J., Badea, O., Paoletti, E. 2013. Environmental Pollution 180:299-303.
- Fravolini, G., Egli, M., Derungs, C., Cherubini, P., Ascher-Jenull, J., Gómez-Brandón, M., **Bardelli, T.**, Tognetti, R., Lombardi, F., Marchetti, M. 2016. Soil attributes and microclimate are important drivers of initial deadwood decay in sub-alpine Norway spruce forests. Science of the Total Environment 569-570:1064-1076.
- Egli, M., Hafner, S., Derungs, C., Ascher-Jenull, J., Camin, F., Sartori, G., Raab, G., Bontempo, L., Paolini, M., Ziller, L., **Bardelli, T.**, Petrillo, M., Abiven, S. 2016. Decomposition and stabilisation of Norway spruce needle-derived material in Alpine soils using ^{13}C-labelling approach in the field. Biogeochemistry 131:321-338.
- **Bardelli, T**., Gómez-Brandón, M., Ascher-Jenull, J., Fornasier, F., Arfaioli, P., Francioli, D., Egli, M., Sartori, G., Insam, H., Pietramellara, G. 2017. Effects of slope exposure on soil physico-chemical and microbiological properties along an altitudinal climosequence in the Italian Alps. Science of the Total Environment 575:1041-1055.
- Gómez-Brandón, M., Ascher-Jenull, J., **Bardelli, T.**, Fornasier, F., Sartori, G., Pietramellara, G., Arfaioli, P., Egli, M., Beylich, A., Insam, H. 2017. Ground cover and slope exposure effects on micro- and mesobiota in forest soils. Ecological Indicators 80:174-185.
- Gómez-Brandón, M., Ascher-Jenull, J., **Bardelli, T.**, Fornasier, F., Fravolini, G., Arfaioli, P., Ceccherini, M.T., Pietramellara, G., Lamorski,

K., Slawiński, C., Bertoldi, D., Egli, M., Cherubini, P., Insam, H. 2017. Physico-chemical and microbiological evidence of exposure effects on *Picea abies* – coarse woody debris at different stages of decay. Forest Ecology and Management 391:376-389.

- **Bardelli, T.**, Ascher-Jenull, J., Burkia Stocker, E., Fornasier, F., Arfaioli, P., Fravolini, G., Roberta Alves Medeiros, L., Egli, M., Pietramellara, G., Insam, H., Gómez-Brandón, M. Impact of slope exposure on chemical and microbiological properties of Norway spruce deadwood and underlying soil during early stages of decomposition in the Italian Alps. Submitted to Catena.
- **Bardelli, T.**, Gómez-Brandón, M., Fornasier, F., Arfaioli, P., Egli, M., Pietramellara, G., Ceccherini, M.T., Insam, H., Ascher-Jenull, J. Chemical and microbiological changes in Norway spruce deadwood during the early stage of decomposition as a function of exposure in an Alpine setting. Submitted to Arctic, Antarctic, and Alpine Research.
- Longa, C.M.O., Francioli, D., Gómez-Brandón, M., Ascher-Jenull, J., **Bardelli, T.**, Pietramellara, P., Egli, M., Sartori, G., Insam, H. Culturable fungi associated with wood decay of *Picea abies* in subalpine forest soils: a field-mesocosm case study. Submitted to Fungal Ecology.
- Fravolini, G., Tognetti, R., Lombardi, F., Egli, M., Ascher-Jenull, J., Arfaioli, P., **Bardelli, T.**, Cherubini, P., Marchetti, M. 2018. Quantifying decay progression of deadwood in Mediterranean mountain forests. Forest Ecology and Management 408: 228-237.
- Hellwig, N., Gómez-Brandón, M., Ascher-Jenull, J., **Bardelli, T.**, Anschlag, K., Fornasier, F., Pietramellara, P., Insam, H., Broll, G. Humus forms and soil microbiological parameters in a mountain forest: Upscaling to the slope scale. Submitted to Catena.

- Schönegger, D., Gómez-Brandón, M., Mazzier, T., Insam, H., Hermanns, R., Leijenhorst, E., **Bardelli, T.**, Fernández-Delgado Juárez, M. Phosphorus fertilising potential of fly ash and effects on soil microbiota and crop. Submitted to Biology and Fertility of Soils.

Conference participations

Oral presentations

- **Bardelli, T.** Deadwood decomposition along a climosequence scenario in the Italian Alps. International Minisymposium dealing with Deadwood and SOM with the participation of Prof. Cindy Prescott and Prof. Sue Grayston (University of British Columbia, Canada). March 3rd, 2017, University of Innsbruck, Austria.
- **Bardelli, T.**, Gómez-Brandón, M., Ascher-Jenull, J., Fornasier, F., Arfaioli, P., Francioli, D., Egli, M., Sartori, G., Insam, H., Pietramellara G. Effects of slope exposure on soil physico-chemical and microbiological properties along an altitudinal climosequence in the Italian Alps. Florence Symposium: running project focused on C-dynamics in Italian forest soils. September 29th, 2016, Florence, Italy.
- **Bardelli, T.,** Ascher-Jenull, J., Gómez-Brandón, M., Francioli, D., Arfaioli, P., Ceccherini, M.T., Sartori, G., Egli, M., Insam, H., Pietramellara, G., Fornasier, F. Interdisciplinary Characterization Of An Alpine Soil Climosequence By Simple Yet Powerful Techniques. Enzymes in the Environment: Activity, Ecology and Applications, July 24th–27th, 2016, Bangor, Wales (UK).

Poster presentations

- Ascher-Jenull, J., Gómez-Brandón, M., **Bardelli, T.,** Fravolini, G., Arfaioli, P., Ceccherini, M.T., Pietramellara, G., Egli, M., Petrillo, M., Insam, H., , Fornasier, F. Deadwood represents (microbial) *hot spots*: the more advanced the decay the "hotter" the wood. Enzymes in the Environment: Activity, Ecology and Applications, July 24th–27th, 2016, Bangor, Wales (UK).
- **Bardelli, T.**, Gómez-Brandón, M., Ascher-Jenull, J., Fornasier, F., Francioli, D., Arfaioli, P., Egli, M., Sartori, G., Insam, H., Pietramellara, G. Interactive effects of altitude and exposure on microbial communities in (sub)alpine soils. Ecology of Soil Microorganisms, November 29th – December 3rd, 2015, Prague, Czech Republic.
- **Bardelli, T.**, Ascher-Jenull, J., Arfaioli, P., Gómez-Brandón, M., Fornasier, F., Egli, M., Sartori, G., Insam, H., Pietramellara, G. Climosequence approach to monitor the effects of exposure and altitude on physical, chemical and microbial properties of alpine soils. First Global Soil Biodiversity Conference, December 2nd–5th, 2014, Dijon, France.
- Ascher-Jenull, J., Gómez-Brandón, M., Fornasier, F, **Bardelli, T.**, Arfaioli, P., Francioli, D., Egli, M., Sartori, G., Cherubini, P., Petrillo, M., Broll, G., Graefe, U., Gobat, J.M., Pietramellara, G., Insam, H. Fine-tuning DNA approach and multiple enzyme assay to assess soil microbial properties under different forest floors. First Global Soil Biodiversity Conference, December 2nd–5th, 2014, Dijon, France.
- Gómez-Brandón, M., Ascher-Jenull, J., **Bardelli, T.**, Beylich, A., Egli, M., Pietramellara, G., Sartori, G., Insam, H., Graefe, U. Interactive effects of altitude and exposure on soil biota in different Alpine

vegetation zones. First Global Soil Biodiversity Conference, December 2nd–5th, 2014, Dijon, France.

Summer Schools

July 3rd–6th, 2017. Summer school Sostanza Organica e bioagricoltura. LIFE CarbOnFarm, Universita' degli Studi di Napoli Federico II, Portici (Napoli), Italy.

June 26th– July1st, 2017. Summer school I suoli montani, gli humus forestali, l'entomofauna dei suoli. Centro Appenninico del Terminillo "Carlo Iucci", Rieti, Italy.

June 26th–30th, 2016. Joint International Summer School in Advanced methods and new integrated approaches to study soil processes in mountain ecosystems. Società Italiana della Scienza del Suolo, SensFor and COST (European Cooperation in Science and Technology) at the Alpine Study Center in Pieve Tesino, Italy.

Supervised Master students

- Evelyn Burkia Stocker, Master Thesis: Digging deeper into the structure and function of microbial communities invlolved in deadwood decomposition: a mesocosm in filed study. June 19th, 2017.
- Layzza Roberta Alves Medeiros: the Master Thesis is in progress.

Scholarships

November 1st, 2014 – October 31st, 2017

PhD grant from the University of Florence (Italy) (DT16364).

Declaration

I hereby declare that this thesis is my own work and that, to the best of my knowledge and belief, it contains no material previously published or written by another person nor material which to a substantial extent has been accepted for the award of any other degree or diploma of the University or other Institute of higher learning, except where due acknowledgment has been made in the text.